Resting-state EEG functional connectivity analysis in benign childhood epilepsy and neonate

Azeez Ayodeji Adebimpe

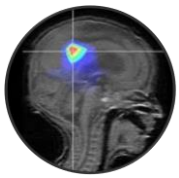

Thèse de Doctorat

Mention BIOLOGIE SANTE
Spécialité NEUROSCIENCES

présentée à ***l'Ecole Doctorale en Sciences Technologie et Santé (ED 585)***

de l'Université de Picardie Jules Verne

par

Azeez Ayodeji ADEBIMPE

pour obtenir le grade de Docteur de l'Université de Picardie Jules Verne

Analyse de connectivité EEG régime reposant dans l'épilepsie bénigne de l'enfance et des nouveau-nés

Soutenue le 14th Juin, 2016 après avis des rapporteurs, devant le jury d'examen :

M^me^ Natasha Maurits, Professeur	**Rapporteur**
M Fabrizio De Vico Fallani, Professeur	**Rapporteur**
M Mario Chavez, Chargée de Recherches	**Examinateur**
M Patrick Berquin, Professeur	**Examinateur**
M Fabrice Wallois, Professeur	**Directeur de Thèse**
M Ardalan Aarabi, Maître de Conférences	**Co-Encadrant**

Abstract

This thesis focuses on two studies investigating the resting-state EEG functional connectivity (i) in patients with benign childhood epilepsy with centrotemporal spikes (BCECTS) and (ii) in preterm and full-term neonates during quite sleep (QS) and active sleep (AS).

In the first part of the thesis, we investigated changes in brain functional connectivity in BECTS patients compared to healthy controls in various frequency bands under the eyes-closed resting condition. The differences in EEG functional and effective connectivity patterns between BCECTS patients and healthy controls were studied in both the sensor and source spaces. The graph theory metrics were also used to characterize functional segregation and integration in BCECTS brain networks in comparison to healthy controls. The first part of the study showed that the EEG resting state network of BCECTS patients was disrupted in the presence and absence of interictal epileptic discharges (IEDs). Patients displayed significantly higher θ power in the scalp EEG across the whole brain regions and lower spectral power in the alpha band especially at the occipital regions in the presence of IEDs. We also observed decreased source activities at the frontal and occipital regions and bilateral increased source activities at the temporal regions in BCECTS patients compared to controls. Our functional connectivity study showed that BCECTS was associated with functionally altered resting state that probably arises from disrupted functional organization of resting-state brain networks on a frequency dependent manner. Our results showed that the BCECTS brain networks were more ordered especially in lower frequency bands in the presence of IEDs and less ordered in the absence of IEDs in comparison to healthy controls. We further investigated the effective connectivity in BCECTS patients to identify major drivers of the epileptic activity. We found that the post and precentral regions with supplementary motor areas were the major drivers in the ipsilateral hemisphere of the epileptic foci. The causal influence from the central to ipsilateral frontal regions and contralateral hemisphere might explain cognitive deficits in children with BCECTS.

In the second part of the thesis, we investigated EEG functional connectivity in preterm babies using high density EEG data and graph metrics during quite sleep. Continuous evolution of cerebral structures during early brain maturation imposes rapid spatial and temporal changes in neonatal EEG patterns. There are different endogenous brain activities such as theta temporal bursts which can serve as biomarkers for neurodevelopment in preterm neonates. We investigated the impact of theta temporal activities on EEG functional connectivity patterns. For normal brain activities with/without theta temporal burst activity, preterm babies presented higher functional connection densities at the frontal and posterior regions compared to other regions. This finding suggests that these regions may functionally develop earlier than other brain regions. The comparison between normal and theta temporal activities revealed higher activity at each of the temporal region. Theta temporal activity in the preterm increased functional connectivity restricted to temporal regions.

In the last part of the thesis, we investigated functional connectivity during QS and AS sleep conditions in full-term neonates. Stronger source activities were observed at the frontal region during AS while the QS condition was characterized with increased source activities at the temporal and posterior regions. Similarly, higher functional connection densities were found at the frontal, temporal and posterior regions during both QS and AS. In both conditions, the clustering coefficient at the central region was lower compared to other regions. The increased source activity at the frontal and posterior regions might support the evidence that these regions develop earlier than other brain regions.

Throughout this thesis, we presented clear and robust approaches for assessing brain functional connectivity patterns in epileptic patients as well as in healthy preterm and full-term neonates. Our findings open new avenues to better understanding complex interactions between brain functional networks involved in epileptic activity. In neonates, our results also demonstrated that the functional connectivity analysis can be efficiently used to study the effect of EEG transients and sleep stages on the functional organization of the brain networks during the early periods of neurodevelopment.

Résumé

Cette thèse porte sur deux aspects de la connectivité fonctionnelle cérébrale en EEG chez l'enfant à l'état de repos : (i) chez les enfants présentant une Epilepsie Bénigne à Pointes Centro-Temporales ou EPCT et (ii) chez les nouveau-nés à terme et prématuré pendant le sommeil.

Dans la première étude, nous avons examiné les modifications de la connectivité fonctionnelle cérébrale liées à l'épilepsie en comparant les résultats chez les patients EPCT par rapport aux témoins sains. Ceci a été réalisé dans différentes bandes de fréquences à l'état de repos, les yeux fermés. Les différences de connectivité fonctionnelle mais aussi effective ont été étudiées dans l'espace capteur et dans l'espace source. La théorie des graphs a été appliquée afin de caractériser la ségrégation et l'intégration fonctionnelle des réseaux cérébraux chez les patients EPCT et les sujets sains.

La première partie de l'étude a montré que les réseaux à l'état de repos des patients EPCT étaient perturbés par la présence de pointes épileptiques intercritiques (IIS). La puissance EEG dans la bande θ était significativement plus élevée sur l'ensemble du scalp lors de la présence des pointes épileptiques alors que la puissance de la bande alpha était diminuée notamment dans les régions occipitales. Dans l'espace source nous avons aussi observé une diminution de l'activité cérébrale dans les régions frontales et occipitales et une augmentation dans les régions temporales bilatérales chez les patients EPCT comparés aux sujets sains.

Notre étude de connectivité fonctionnelle a montré que les patients EPCT présentaient une altération du réseau cérébral au repos qui pouvait être mise en relation avec une perturbation des réseaux dit de repos selon la gamme de fréquence analysée. Nos résultats ont montré que les réseaux cérébraux chez les patients EPCT étaient plus ordonnés en particulier dans les bandes de fréquences basses et notamment en présence des pointes épileptiques intercritiques. Nous avons examiné la connectivité effective chez les patients EPCT afin d'identifier les principaux drivers de l'activité épileptique. Nous avons montré que les régions les plus impliquées dans l'émergence des pointes épileptiques étaient les régions précentrales dont les aires motrices supplémentaires de l'hémisphère ipslatéral au foyer épileptique. L'influence causale de la région centrale vers la région frontale ipsilatérale et controlatérale pourrait être impliquée dans les déficits cognitifs observés chez l'enfant présentant une Epilepsie Bénigne à Pointes Centro-Temporales

Dans la seconde étude, nous avons étudié la connectivité fonctionnelle cérébrale chez les nouveau- nés prématurés, dans le sommeil calme, à l'aide de l'EEG haute densité et en utilisant les outils de la théorie des graphs. L'évolution constante des structures cérébrales au cours de la maturation cérébrale précoce impose des changements rapides spatiaux et temporels des patterns de l'EEG néonatal. Il existe différents types de neurobiomarqueurs développementaux endogènes de l'activité cérébrale néonatale parmi lesquels les activités théta temporales. Nous avons étudié l'impact des activités thêta temporales sur la connectivité fonctionnelle à cette période du développement. Avec ou sans activité théta temporale, la densité de la connectivité fonctionnelle est plus élevée dans les régions frontales et occipitales suggérant l'existence d'un gradient de

maturation. La présence des activités théta temporales induit une augmentation de la connectivité fonctionnelle restreinte aux régions temporales ipsilaterales.

Chez les nouveau-nés nés à terme, nous avons étudié la connectivité fonctionnelle au cours du sommeil calme et du sommeil agité. L'activité de source était plus importante dans les régions frontales au cours du sommeil agité alors qu'elle était plus importante dans les régions temporales et postérieures dans le sommeil calme. De la même manière la densité de connectivité fonctionnelle est plus élevée dans les régions frontales, temporales et postérieures dans le sommeil agité et le sommeil calme. Dans ces deux conditions, le coefficient de clustering était moins important dans la région centrale que dans les autres régions. L'augmentation de l'activité de source dans les régions frontales et postérieures pourrait constituer un autre argument concernant le développement précoce de ces régions.

Publication during candidature

Peer review articles

1. **Adebimpe, A**., Aarabi, A., Bourel-Ponchel, E., Mahmoudzadeh, M., Wallois, F., 2016. EEG Resting State Functional Connectivity Analysis in Children with Benign Epilepsy with Centrotemporal Spikes. Frontiers I 143. doi:10.3389/fnins.2016.00143

2. **Adebimpe, A**., Aarabi, A., Bourel-Ponchel, E., Mahmoudzadeh, M., Wallois, F., 2015a. EEG resting state analysis of cortical sources in patients with benign epilepsy with centrotemporal spikes. NeuroImage Clin. 9, 275–282. doi:10.1016/j.nicl.2015.08.014

3. **Adebimpe, A.,** Aarabi, A., Bourel-Ponchel, E., Mahmoudzadeh, M., Wallois, F., 2015b. Functional Brain Dysfunction in Patients with Benign Childhood Epilepsy as Revealed by Graph Theory. PLoS ONE 10, e0139228. doi:10.1371/journal.pone.0139228

Journals in preparation

1. **Adebimpe, A.,** Aarabi, A., Bourel-Ponchel, E., Mahmoudzadeh, M., Wallois, F., Large-Scale Network Dysfunction in Benign Childhood Epilepsy: A Resting-State Functional Source Connectivity Study.

2. **Adebimpe, A.,** Aarabi, A., Bourel-Ponchel, E., Mahmoudzadeh, M., Wallois, F., Dynamic directed interictal connectivity in benign childhood epilepsy with centrotemporal spikes: A high density EEG study.

3. **Adebimpe, A.,** Aarabi, A., Routier, L., Kongolo, G., Wallois, F., EEG functional connectivity in preterm neonates.

4. **Adebimpe, A.,** Aarabi, A., Héberlé, C., Wallois, F., Functional organisation of fullterm neonates during natural quiet and active sleep

Conference abstracts

Oral Presentations

1. Neonatal Connectome of early preterm babies, 19th Annual meeting of LARC-Neuroscience network, November 13th 2015, CHU SUD, Amiens, France.

2. Influence of temporal theta burst activity on the functional connectivity of the cortical networks in preterm neonates presented at 15th European Congress on Clinical Neurophysiology, Sept 09-13, 2015, Brno, Czech Republic.

3. Theta waves oscillation modulates high frequency signals in premature neonates presented at Annual Conference on Clinical Neurophysiology and NeuroImaging 2015, Sept 30- Oct. 3, 2015, Brno, Munich, Germany

4. Brain networks and functional connectivity in benign childhood epilepsy presented at GDR2904 Multielectrode systems and Signal processing for Neuroscience, October 14-15 in Gif sur Yvette, France

5. Network Modeling of the Brain presented at Young Researchers Network on Complex Systems, Lucca, Italy, 26-30 Sept,2014.

6. The disruption of resting state networks in adolescents with benign childhood epilepsy with centrotemporal spikes presented at Structure Federative de Researche, UPJV, Amiens, France, March 27, 2014.

Poster Presentations

1. Assessing the functional connectome in the preterm brain, 22nd Annual Meeting of the Organization for Human Brain Mapping, June 26 to 30, Geneva, Switzerland.

2. Brain network analysis of EEG functional connectivity in patients with benign childhood epilepsy with centro-temporal spikes 15th European Congress on Clinical Neurophysiology, Sept 30- Oct. 3, 2015, Brno, Czech Republic.

3. Graph theoretical analysis of EEG functional connectivity in children with benign childhood epilepsy. eposter presented at Annual Conference on Clinical Neurophysiology and NeuroImaging 2015, Sept 30- Oct. 3, 2015, Munich, Germany.

4. Investigation of electroencephalographic functional connectivity in term and preterm neonates, Submitted for 12th Congress of Societe de Neurosciences, May 19 - May 22, 2015, Montpellier, France.

5. Altered brain functional connectivity in patients with benign childhood epilepsy, INCF Congress, Aug. 25 - Aug. 27, 2014, Leiden, Netherlands.

6. Resting-state EEG functional connectivity in benign childhood epilepsy, Society for Clinical Neurophysiology and Language(SNCLF), June 25- 27, 2014, Angers, France.

7. The comparison of resting state networks between normal children and adolescents with benign childhood epilepsy with centrotemporal spikes: A high density EEG study, 30th International Congress of Clinical Neurophysiology, March 19-22, 2014, Berlin, Germany, March 19-22, 2014.

"The brain is a world consisting of a number of unexplored continents and great stretches of unknown territory"

Santiago Ramón y Cajal
Spanish neuroscientist and Nobel laureate (1906)

Acknowledgement

I want to thank my supervisor and the Director of the GRAMFC, **Prof. Fabrice Wallois** for giving me opportunity to undertake my PhD thesis in the laboratory. I am immensely grateful for adopting me as one of your PhD students and the opportunity to develop my research skills within the friendly atmosphere of GRAMFC. Your fatherly support in both scientific and nonscientific activities makes it unique experience and I express my gratitude for your guidance and support throughout the period of my study. You have given me strong foundation which will always be reference for my career. I also express my gratitude to my co-supervisor**, Dr Ardalan Aarabi** for all your efforts for the success of my PhD thesis. I am grateful for accepting me as your PhD student and your patience, enthusiasm, throughout the thesis period. Your tireless efforts in proofreading and correcting the drafts of my manuscripts and thesis is greatly appreciated. I gratefully acknowledge financial support from **INSERM** (Institut national de la santé et de la recherche médicale) for my PhD program. I express my sincere appreciation to the staff of INSERM at Lille (L'Inserm en région Nord-Ouest) for your prompt response and speedy processing of all my requests. I also appreciate efforts of administrative staff at Doctoral School of UPJV.

Thank you very much **Dr Emilie Bourel-Ponchel** for sharing your data with me and very grateful for many useful discussions on epilepsy and your assistance with keen interest in my PhD thesis. I sincerely appreciate the effort of Madame **Christine Picard** for your assistance of EEG recording pf young children and neonates. I express my gratitude also to **Drs Viktoriya Osharina, Claire Herbele, Mahdi Mahmoudzadeh** and **Guy Kongolo** for your support, and scientific and nonscientific discussions

To my colleagues in the laboratory, I am sincerely grateful for all your support and assistance. **Hamed Azizollahi** (source localizer), **Lemya Araf** (organizer), **Mina Nourhashemi** ('where is F…'), **Mana Manoochehri**, **Marine Panzani** and **Cristian Arnal** (MUA), thank you all for all your cooperation and fruitful discussion. Thank you Mr. **Romain Palstermans** for all your efforts and assistance. I am sincerely grateful to our secretary **Madame Alexandra Bayle** for all your supportive information, document processing and for making my conferences and workshops went smoothly. I am grateful to nonprofessional football team of CURS for the interesting sporting and social activities.

My warmest regard to my entire family in Nigeria for all their support. My special gratitude to my mother, **Khadijat** for your continuous support and prayer. My warmest appreciation goes to all my friends in Nigeria, Belgium, France, Netherland, Germany and every part of the world. To my colleagues in Erasmus programme, I say thank you all for all your support and stimulating discussion.

Lastly, my warmest appreciation goes to my lovely wife, **Bilikis** for her understanding and dedication and to our little kids **Shamsudeen** and **Abdulrahman**. Thank you all for your love and understanding.

Azeez A. Adebimpe
April, 2016

Table of Contents

List of figures

List of Tables

Chapter 1

Introduction

1.1 Thesis Overview and Problem definitions

Worldwide, about 65 million people are affected by epilepsy, a chronic neurological disease characterized by sudden bursts of abnormal neuronal activities in the brain, manifesting as seizures. Significant progress has been made towards understanding basic mechanisms of epilepsy especially in young children. There are many age-specific clinical and electroencephalographic features of epilepsy that are not clearly understood yet. Functional connectivity analyses can provide fundamental insights into complex interactions and functional organization of the brain networks under normal and pathological conditions. Functional connections between brain networks can occur between spatially close or remote areas to effectively perform information segregation and integration. The functional connectivity analysis in patients with epilepsy helps neurologists to better understand the pathophysiological impact of altered neurophysiology on the brain function especially during critical periods of neurodevelopment.

In adults, the brain neural networks are connected with firmer intricate connections between various brain regions. The infant brain, however, contains less intricate, loose networks with relatively less functional connections between different regions. This suggests that functional brain networks sustaining advanced behavior are immature in infants. During the maturation process, a gradual reorganization of cortical regions between birth and adulthood occurs and large-scale cortical networks develop from a ‘‘local and segregated’’ to a ‘‘distributed and integrated’’ organization.

In neonates, the functional organization of the brain networks is not clearly understood yet. The functional analysis in neonates will expand our understanding of the sequential steps in the brain maturation and may help to investigate disturbances in the maturation process of the brain in preterm and full-term babies.

In this thesis we focus on two studies investigating the resting-state EEG functional connectivity in children with benign childhood epilepsy with centrotemporal spikes (BCECTS) and in preterm and full-term neonates.

1.2 Purpose of the Thesis

The main aim of this thesis is to investigate the functional plasticity in development in neonates and the effect of pathology such as epilepsy in young children during the course of development. Therefore, the thesis was subdivided into two parts

In the first part of the thesis, we investigated changes in brain functional connectivity patterns in BCECTS patients compared to healthy controls in various frequency bands under the eyes-closed resting condition. The differences in EEG functional and effective connectivity patterns between BCECTS patients and healthy controls were studied in both the sensor and source spaces. . The objectives of this study were:

- To investigate the changes in the EEG resting-state spectral power and spatial distribution of EEG cortical sources in different frequency bands in BCECTS patients in comparison to healthy controls.
- To characterize the brain functional connectivity patterns in BCECTS patients with different graph theory metrics commonly used to explore local and global topologies of the brain networks in terms of functional integration and segregation.
- To investigate the impact of interictal epileptic discharges on the functional connectivity patterns in BCECTS patients.
- To identify time-varying changes in functional connectivity as well as the brain regions involved in the generation and propagation of interictal epileptic discharges.

In the second part of the thesis, we assessed functional connectivity patterns of the brain networks in healthy preterm and full-term neonates with high density EEG data during quiet and active sleep periods. The purposes of this study were:

- To investigate the brain functional organization in preterm and full-term neonates.
- To investigate the impact of endogenous brain activities like theta temporal activity on the brain functional connectivity patterns in neonates.
- To characterize the functional connectivity patterns of the neonatal brain networks with different network metrics.
- To investigate the brain functional organization in healthy full-term neonates during quiet and active sleep periods.

1.3 Thesis Outline

Chapter 1 introduces the motivation and purposes of the thesis. The rest of the thesis is organized as follows.

Chapter 2 provides an introduction to the brain anatomy and functional maturation during infancy and adulthood. A short background on the generation and recording of EEG in neonates and adult is also provided. The last part of Chapter 2 presents an overview on epileptic activity with particular attention to the benign childhood epilepsy.

Chapter 3 reports a short review on brain connectivity analyses including structural, functional and effective connectivity. Special attention is paid to the functional connectivity analysis and graph theory metrics with mathematical details.

In chapter 4, we use the approach presented in Chapter 3 to investigate the differences in brain functional connectivity patterns between BCECTS patients and healthy controls under the resting state condition.

Chapter 5 investigates the functional connectivity patterns using the seed-based functional analysis and explores the temporal dynamics of the brain functional connectivity during interictal epileptic discharges in BCECTS patients.

Chapter 6 is devoted to the brain functional connectivity analysis in preterm and full-term neonates using high density EEG. The specific features of neonatal EEG activities such as theta temporal burst activity (TTA) and different sleep stages including quiet and active sleep are taken into considerations.

Chapter 7 gives the concluding remarks and future research directions.

Chapter 2

EEG and Epilepsy

2.1 Introduction

The temporal dynamics of the brain is determined by successions of spatiotemporal transient patterns of activities integrated by the brain's anatomical structure including principally connections with highly adaptable nature. The temporal coherence is achieved by the synchronization of neural networks operating in harmony in distinct frequency bands. The brain functioning can be explained at the level of the neural networks interconnected in an intricate pattern. In this view, the brain can be regarded as an ensemble of connected dynamical systems relating the inputs and outputs of its constituent parts. To capture the temporal evolution of brain activities, one needs a tool to monitor it over time. This chapter describes briefly brain anatomy and functions, EEG genesis and measurement, and basic EEG rhythms during the resting state in adults, young children and neonates. A short overview of epilepsy including pediatric epilepsy is also given, with particular attention to the benign childhood epilepsy.

2.2 Human brain

The brain tissue consists of billions of neurons. It is divided into gray and white matters. Grey matter consists of cell bodies and few myelinated axons, while white matter consists of very few cell bodies and is principally composed of long-range myelinated axon tracts (Stiles and Jernigan, 2010). The brain is protected by the skull and dura matter, arachnoid and pia matter. The space between the pia matter and the arachnoid is filled with cerebrospinal fluid (CSF) (Figure 2.1) (Silverthorn, 2007). The CSF protects the brain against the bone and serves as a medium for the transportation of the brain nutrients and water to the white and gray matters. In large scale, the brain is divided into the cerebellum at the bottom of the brain and the cerebrum at the upper part of the brain usually referred to as the cerebral cortex. The cerebrum is divided into right and left hemispheres including frontal, temporal, parietal and occipital lobes (Figure 2.3).

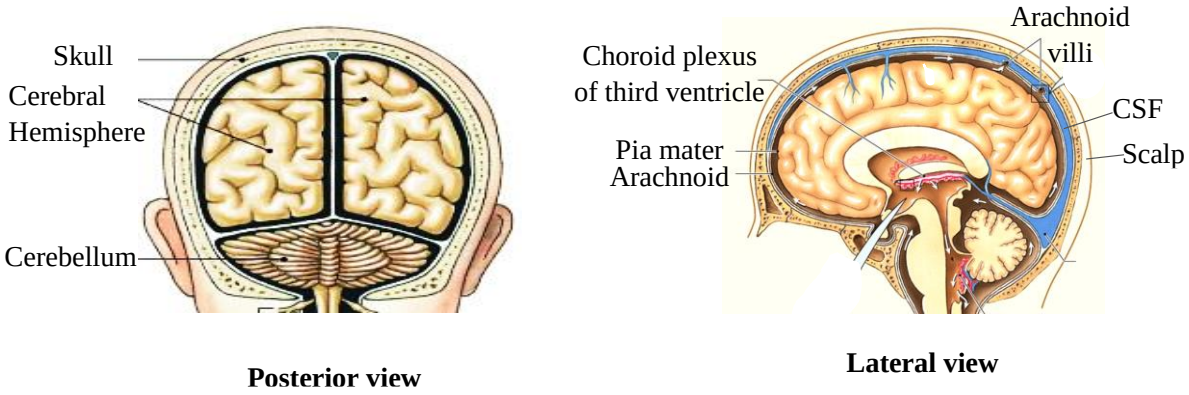

Figure 2.1: Brain structure. Brain is protected by the skull, scalp and CSF with the pia matter and arachnoid membrane (adapted from (Silverthorn, 2007))

Brain structural maturation

The human brain structure matures rapidly form early fetal period within which the brain has a smooth, "lissencephalic" structure and it gradually develops the characteristic mature pattern of gyral and sulcal folding (Figure 2.2). The formation of gyri and sulci follows an orderly sequence as the age increases (Stiles and Jernigan, 2010). Another important characteristic feature of the brain development is the longitudinal fissure that separates the two cerebral hemispheres. Some part of the brain is developed at the early age such as cingulate, parietooccipital and calcarine (14-16 weeks); central and superior temporal regions (20-24 weeks); and superior frontal, precentral, inferior frontal and postcentral regions (25-26 weeks). Secondary sulci emerge between 30-35 weeks. The formation of tertiary sulci begins during 36 weeks and extends into the postnatal period (Figure 2.2) (O'Leary et al., 2007; Stiles and Jernigan, 2010; Van Essen and Dierker, 2007). Although, the development and migration of neurons are largely prenatal events, the proliferation and migration of glial progenitors continues for an extended period after birth, and the differentiation and maturation of these cells continue throughout the childhood period. In the postnatal period, neurogenesis continues to only a very limited degree (O'Leary et al., 2007; Stiles and Jernigan, 2010). However, in some brain region like hippocampus, cortex and striatum, new neurons continue to develop where they migrate from the subgranular layer to the nearby granular layer. These exceptional forms of neurogenesis appear to continue throughout adult life but produce only a small percentage of the neuronal population.

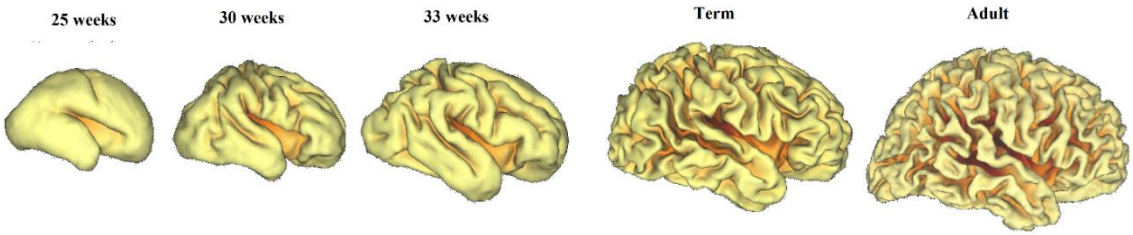

Figure 2.2: Brain structural development. cortical surface in premature infants (shown at several gestational ages), full-term infants, and adults (adapted from (Van Essen and Dierker, 2007))

Functional maturation

The neonatal brain maturation is functionally characterized by specific features which serve as biomarkers for the functional development of the brain (André et al., 2010). Although, most of the primary sensory systems are already functionally established at birth but the long range functional connectivity is limited in infants under the age of 2 years old (Fransson et al., 2007; Stiles and Jernigan, 2010). The functional brain development in neonates is concomitant with the sequential functional maturation of different cortical regions. New cognitive functions during infancy and childhood might be the result of emerging patterns of interactions between different regions (Johnson, 2001). Meanwhile, the mature brain in adults is physically delineated as the cerebral cortex. The cerebral cortex serves as a central processing center integrating sensory information and making decisions for many types of motor output. The cerebral cortex is divided into several brain regions. The functional regions of the cerebral cortex do not necessarily correspond to the anatomical lobes of the brain. However, the frontal lobe (Figure 2.3) is known for thinking, executing functions, planning and behavioral controls (Silverthorn, 2007; Stiles and Jernigan, 2010). The motor cortex is responsible for the motor coordination and movement while the parietal lobe is involved in the perception, sensing, and simple cognitive task. The occipital lobe is involved in visual processing and the temporal lobe in language processing and memoryfunctions . The functional specialization is not symmetrical across the cerebral cortex. For instance, language and verbal skills tend to be concentrated on the left side of the brain, with spatial skills centered on the right side (Knecht et al., 2000; Springer and Deutsch, 1998).

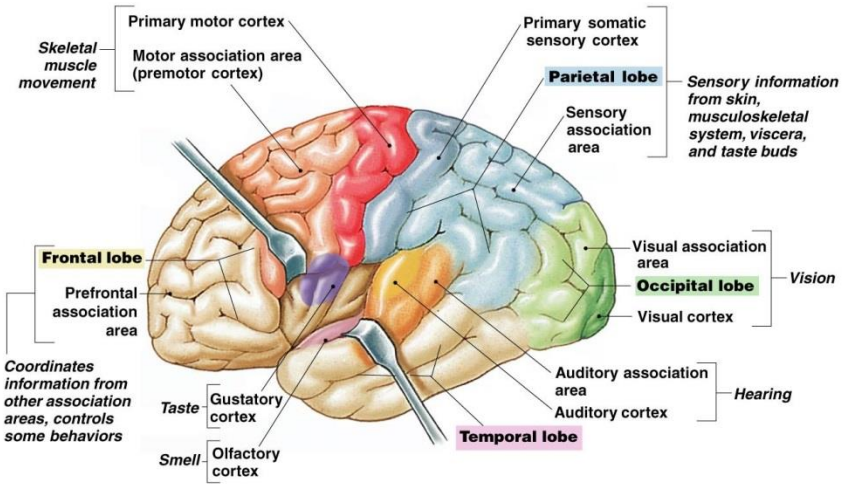

Figure 2.3: The cerebral cortex is specialized into functional areas such as sensory, motor and association areas that integrate information (*adapted from (Silverthorn, 2007)).*

2.3 Electroencephalography

2.3.1 Generators of EEG

EEG is the electrical activity of the brain, most specifically it is the sum of extracellular current flows from large group of neurons (Holmes and Khazipov, 2007). EEG arises from synchronized synaptic activity of populations of cortical neurons called pyramidal cells (Figure 2.4). The pyramidal neurons are organized in such a way that the neighboring dendritic trees are in parallel to each other and almost orthogonal to the cortical surface. The pyramidal neurons are believed to be the main generator of EEG. For more information on the generation of EEG, the readers are referred to the following reviews (Holmes and Khazipov, 2007; Jackson and Bolger, 2014; Silva, 2009). The high temporal resolution of EEG makes it an excellent tool to study the neuronal activity of different brain regions over time.

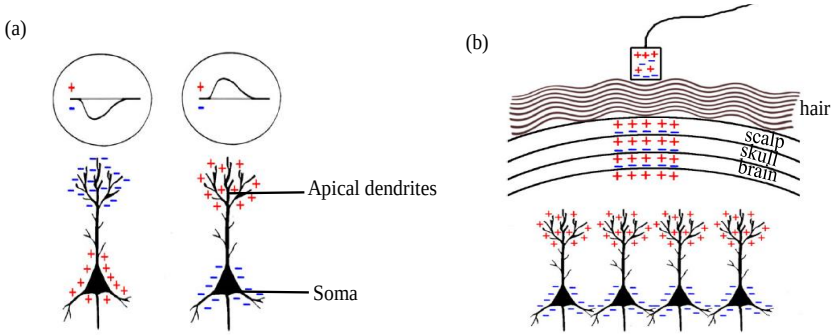

Figure 2.4: The neural source of EEG: (a) parallel pyramidal cells with positive and negative charges at soma and apical dendrites, respectively. A negative deflection of EEG is measured when soma is positive and vice versa. Figure (b) shows that signals are attenuated by the scalp and skull, and the hair on the scalp surface (this figure was modified from (Jackson and Bolger, 2014)).

2.3.2 EEG recordings

EEG recordings are performed by placing electrodes in predefined standard positions on the head. An international standard EEG electrode configuration is shown in Figure 2.5. EEG can be recorded between pairs of active electrodes (bipolar montage) or respective to passive or active reference electrode (monopolar montage). The positions of the electrodes are based on the anatomical landmarks such as *inion* and *nasion.* The number of electrodes and their exact positions depend on the application. In clinical practice, usually 20 to 32 electrodes are used. For research purposes, it is usually required to increase the spatial resolution by increasing the number of electrodes (Lantz et al., 2003; Sohrabpour et al., 2015; Song et al., 2015).

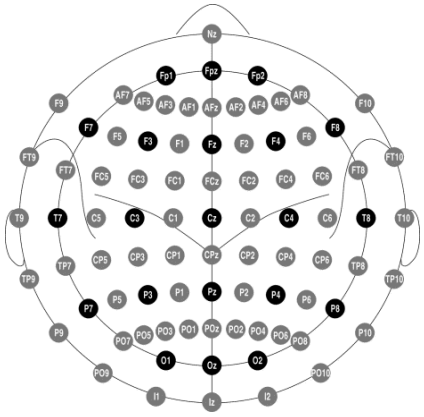

Figure 2.5: International 10-20 Standard EEG electrode configuration, Nz and Iz refer to nasion and inion, respectively.

EEG is mostly recorded on the scalp surface with subjects relaxed or involved in the experimental tasks. One important problem of scalp EEG is the artifact due to head movement, eye blinking, muscle activity and electronic interferences. Due to low amplitude of EEG in the order of 100μV, artifacts can contaminate the recordings and produce false results if not properly minimized or rejected.

Neonatal EEG is usually recorded with 8 surface electrodes positioned according to the international 10/20 system, which is adapted to the newborn head (Figure 2.6). Additional electrodes are also added for monitoring electrocardiography(ECG), respiration and electromyography (EMG). In addition, video-EEG is usually performed to record the activity and response of neonates (Lamblin and de Villepin-Touzery, 2015; Walls-Esquivel et al., 2007). There is growing interest to increase the number of electrodes due to the spatial specificity of the neonatal EEG (Odabaee et al., 2013).

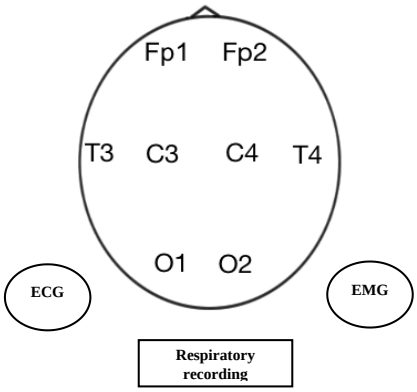

Figure 2.6: Commonly used EEG channels with ECG, EMG and respiratory recording for neonates

2.4 EEG brain activity

2.4.1 Resting state EEG

Resting state is the dynamic substrate of the present momentary state of the brain, and determines the fate of incoming information. At rest, the brain goes through all working modes such as sensory, attention, executive, control and language. Some brain regions are activated or deactivated at rest, usually studied with the functional magnetic resonance imaging (fMRI) (Biswal, 2012).

Resting state EEG is used to monitor brain activity in the absence of task or brain stimulation (Olejniczak, 2006). It can be used to identify abnormalities by comparing different neurological disorders and event related potentials such as visual stimuli or motor responses to resting state activity. The most common way of characterizing resting EEG is by breaking down oscillatory patterns into different frequency bands. Power spectral analysis is the most common method used to quantify the resting state EEG in different frequency bands. The functional connectivity analysis can also be used to assess interaction between brain regions (Coben et al., 2008; Murias et al., 2007; Sponheim et al., 2000).

The mature brain EEG activity is studied based on the different EEG rhythms or brain oscillations according to the frequency contents. The EEG rhythms may be related to the normal brain functions, functional states and pathological conditions (Başar et al., 2013; Başar and Güntekin, 2013; Klimesch, 1999; Michel, 2009). As shown in Figure 2.7, EEG rhythms can be classified into:

Delta rhythm (less than 4Hz): This rhythm is observed in deep sleep stages with large amplitude and its presence in awake adult may indicate brain disorders.

Theta rhythm (4 to 8Hz): Theta rhythm plays an important role in neurodevelopment during childhood, and found in drowsiness and some certain sleep stages. High theta activity in awake young children and adults is related with brain disorders.

Alpha rhythm (8 to 13Hz): It appears spontaneously in relaxed and awake adult with eyes closed and is most pronounced at the occipital regions of the brain. It also relates to cognitive process in normal brain function.

Beta rhythm (13 to 30Hz): It is best defined at the central and frontal brain regions and related to alertness and thinking.

Gamma rhythm (above 30 Hz): With very low amplitude it is related to higher cognitive thinking and information processing in the brain.

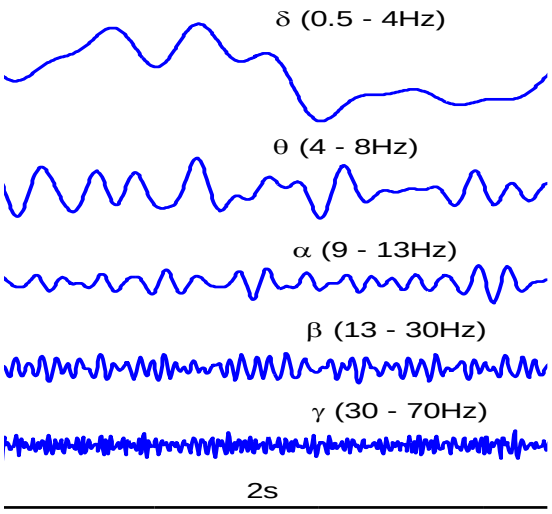

Figure 2.7: Samples of EEG rhythms in different frequency bands

2.4.2 Neonatal resting state EEG

EEG signals in newborns are very different from those in older children and adults due to the explosive maturational changes in the neonatal brain, resulting in rapid changes from 26 40 weeks of gestation age (wGA) (André et al., 2010). The brain changes are resulted fromthe dendritic development, glial proliferations, synaptogenesis and myelination (Zhang et al., 2015). The development underlying rapid sequences of EEG changes are often used to predict and determine the healthy state of newborns. EEG has been proven to be an efficient tool for the assessment of cerebral functions in neonates(Lamblin et al., 1999; Vecchierini et al., 2003).

Preterm neonates born below 32 wGA are characterized by long discontinuity interrupted by bursts of EEG activity (Figure 2.8a). The interburst interval is significantly reduced with increasing with increasing age (Vanhatalo and Kaila, 2006; Wallois, 2010). The EEG bursts are of high amplitude with dominant frequencies in lower frequency bands (δ and θ bands). The amplitude of bursts decreases with increasing age. The duration of interburst is also used to estimate the brain maturity in neonates. In preterm neonates, the theta temporal burst (Figure 2.8b),used as biomarker for the brain maturation, appears at the temporal region. In preterm neonates of 32 to 36 wGA thedelta brushes as another biomarker appear at the occipital and temporal regions(André et al., 2010; Wallois, 2010). The delta brushes are characterized by low amplitude fast activites superimposed on slow waves of high amplitude. Healthy full-term neonates above 37 wGA are characterized with biphasic frontal sharp transients especially during quite sleep (Torres and Anderson, 1985). See Figure 2.9 for the synopsis of maturation in neonates(Wallois, 2010).

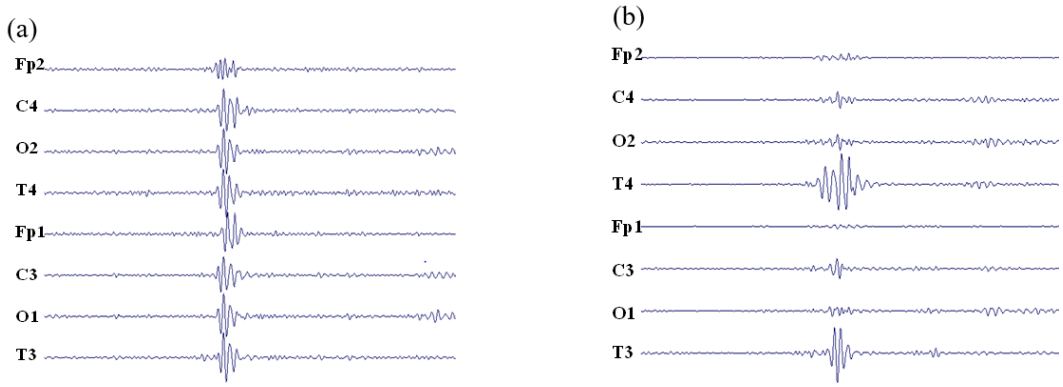

Figure 2.8: EEG Sample from a 28-week Preterm baby: Long discontinuity intertwined with short burst EEG activity (a) and theta temporal activity at both temporal regions (T3 and T4) (b).

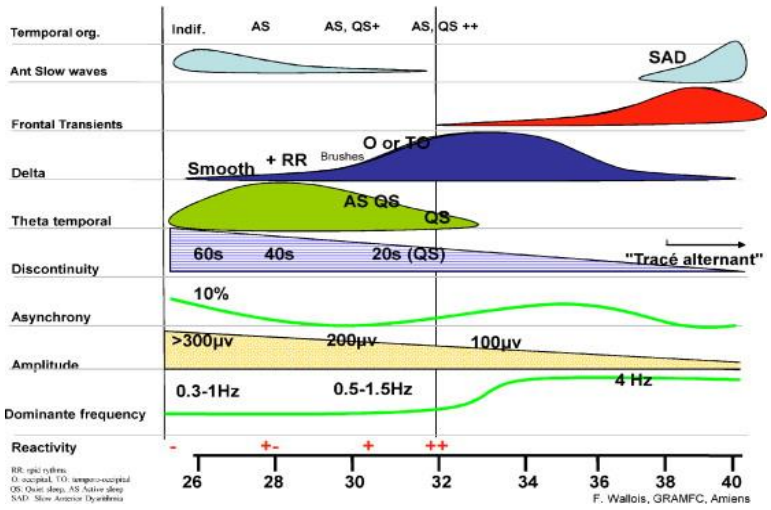

Figure 2.9: Synopsis of maturation of specific features in EEG of premature neonates(adapted from (Wallois, 2010))

EEG recording is rigorous in neonates and mostly recorded during the sleeping period with less artifact. The neonates are mostly asleep during the first few weeks of life. The sleep EEG provides a unique opportunity to observe spontaneous cortical signals and examine brain maturation across the brain regions. The neonatal sleep architecture consists of two periods: active and quite sleep. These periods are intermixed with transitional or intermediate sleep period. Active sleep in neonates are traditionally associated with coalescence of rapid eye movements, increased variability of cardiorespiratory rhythms, low muscle tone, mixed frequency of continuous EEG signals and abundance of body movement. In turn, quite sleep is associated with the absence of rapid eye movement, fewer body movement, higher muscle tones, decreased variability of respiratory rates and high amplitude continuous EEG with less discontinues EEG pattern (André et al., 2010; Mizrahi, 2004; Scher and Loparo, 2009).

2.5 Epilepsy activity in EEG

Epilepsy is a brain disorder that affects about 0.5 to 1% of the world population. It is characterized by the recurrent, excessive and uncontrolled abnormal brain activity. Epilepsy can begin at any age, but is more common in children compared to adults. The prevalence of epilepsy generally depends on the gender, age and geographical population. Many factors are responsible for the epilepsy such as genetic, low oxygen during birth, head injuries that occur during birth or from accidents during youth or adulthood, brain tumors, infections such as meningitis or encephalitis, damage to the brain and abnormal levels of substances (Banerjee et al., 2009; Lars Forsgren et al., 2005; L. Forsgren et al., 2005).

Epileptic seizure is abnormal hypersynchronous neuronal activities of the brain. The clinical manifestation of seizures has many forms depending on which brain regions are involved in epileptic activity. Although the underlying causes of epilepsy are still unknown, certain factors are known to provoke seizures in people with epilepsy. Missing medication doses, heavy alcohol

use, cocaine or other drug, and lack of sleep can provoke seizures in epileptic patients (Bonney et al., 2015; Semah et al., 1998). There are many classifications of epilepsy but depending on the etiology of epilepsy, it can be classified to either partial or generalized epilepsies. Partial epilepsies have focal origin which can be simple without losing consciousness and complex involving losing consciousness. The simple partial epilepsy is characterized by focal motor movements, sensory symptoms or autonomic symptoms (Rheims et al., 2008). This type of epilepsy can be further classified into temporal, frontal, occipital or temporal lobe epilepsy depending on the source of seizure. Different physical sensation and motor automatisms are associated with complex partial epilepsy. The partial epilepsy can evolve to generalized epilepsy if not properly taking care of. The generalized epilepsy involves the whole brain and may last longer in order of 20 seconds. Example of generalized epilepsy is absence epilepsy that consists of sudden lapse of consciousness with the impairment of mental functions(Scheffer and Berkovic, 1997; Singh et al., 1999).

One of the important applications of the EEG is to study epilepsy. The appearance of higher amplitude waves during ictal period compared to interictal periods and several other paroxysms are general landmark of epilepsy. These features help to identify, classify and localize seizures. Epileptic components and waves vary especially in frequency range, duration and topography (Banerjee et al., 2009). Manifestation of epileptic activity can also be obtained during interictal epileptic discharges (IEDs), which are the spike and sharp waves, either of which can occur with or without a subsequent slow wave. IEDs can occur separately in brief burst that look like seizure activity. However, the introduction of video-EEG recording has been an important milestone helping to identify specific movements and behavior of patients during seizures.

2.5.1 Benign childhood epilepsy

Benign childhood epilepsy (BCE) affects 10 to 20% of children with epilepsy (Camfield et al., 2014; Chrysostomos P. Panayiotopoulos, 1999). Characteristically, the seizures begin between 2 and 16 years of age. Benign childhood epilepsy is considered a benign form of childhood epilepsy that occurs in children who show normal mental development. The risk of cognitive impairment has been shown to be higher by comparing the test performance of children with BCE with that of the healthy age-matched children (Danielsson and Petermann, 2009; Datta et al., 2013). Unlike adult epilepsy such as temporal lobe epilepsy, brain imaging has shown that brain structural of BCE patients is usually normal (Fountain, 2008).

The most common BCE is benign childhood epilepsy with central temporal spikes (BCECTS) and often called rolandic epilepsy or *Panayiotopoulos* syndrome (Chrysostomos P. Panayiotopoulos, 1999; C. P. Panayiotopoulos, 1999). The common seizure begins in sleep and is very simple and partial. Secondary generalized type of epilepsy is not that common. The occurrence of BCECTS involves unilateral sensory-motor symptoms, speech arrest and hyper-salivation.

The most useful diagnostic tool for BCE is EEG. The appearance of infrequent seizures or generalized burst in EEG with bi or triphasic spike activity in rolandic areas is highly suggestive of benign childhood epilepsy. It can occur at either left or right hemisphere of the brain region or

at both. With high density EEG (Figure 2.10), it is mainly localized in the high central (C3 and C4) or low central (C5 and C6) supra-sylvian regions. Further analyses including normal neurological examination and spike source imaging showing an anterior-posterior dipole orientation confirm the possibility of BCECTS(Camfield and Camfield, 2002; Panayiotopoulos, 2005). However, brain imaging is not always required except in some difficult cases.

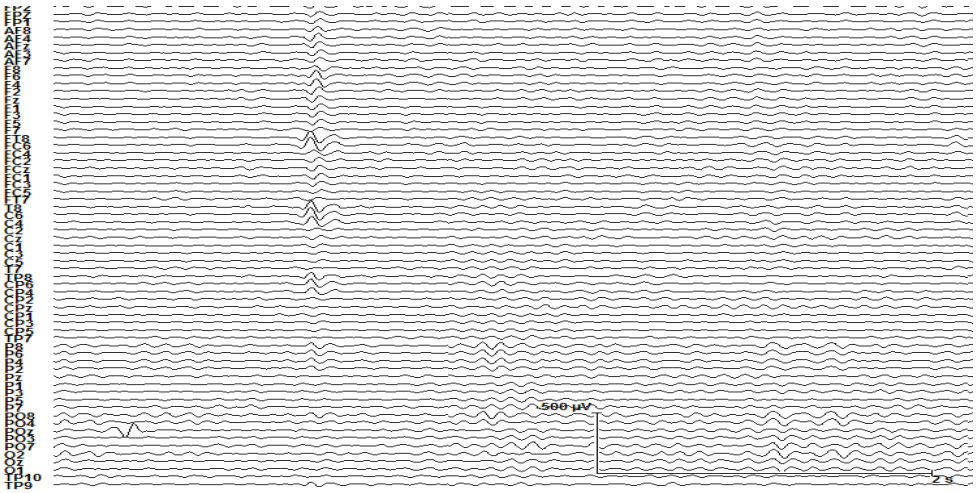

Figure 2.10: EEG sample from a BCECTS patient: EEG spikes are shown at the C2, C4, T8, FC4, and FT8 electrodes, all at the right hemisphere.

Chapter 3

Brain connectivity analysis

3.1 Introduction

The brain is a highly distributed complex system in which a very large number of processes are simultaneously processed in parallel. The brain complexity can be defined based on its neuronal populations, which at a macroscopic scale operate on random and regular regimes. The complex architecture of the brain involves neuronal networks which are highly specialized in multiple parallel operations linked together to give rise to coherent perception and action. The anatomical and functional inter-neuronal connectivity of brain networks can occur between spatially close or remote areas, the former having a relatively high probability of occurrence. The functional connectivity between brain networks are organized for effective information processing including segregation and integration. In particular, both segregation and integration of information have to be dealt within a single architecture of brain networks. At a microscopic scale, the brain consists of electrical circuits formed by the interconnection of billions of elementary processing units (neurons and glia) (Bear et al., 2001).

In adults, the brain neural networks are connected with firmer intricate connections between various brain regions. However, due to higher efficiency the connections in gray matter are significantly reduced. The adult brains have been shown to follow a web-like mesh of many different interconnecting links involving all the regions. In adults, there are brain regions showing a disproportionally high degree of anatomical connectivity (so called ‘‘cortical hubs’’) to control the flow of information (Gong et al., 2008; Hagmann et al., 2008), such as: aspects of self-referential thinking (Gusnard et al., 2001), episodic memory retrieval(Kim et al., 2010), prospective thought (Addis et al., 2007), decision making, and in goal-oriented attentional tasks (Corbetta and Shulman, 2002). These adult hub-related networks largely overlap with the default mode network and the fronto-parietal attention network (task-positive network) (Buckner et al., 2009). Thus, the organization of adult hub-related networks sustains the complexity of the brain functionality (Heuvel and Sporns, 2011).

The infant brain contains less intricate, loose networks with relatively less functional connections between different regions. The functional connectivity associated with cortical hubs in the infant brain largely overlaps with primary sensorimotor, auditory, and visual systems (Fransson et al., 2009, 2007). The information flow through infant cortical hubs is dominated by processes related to rather reflexive (perception-action) behavior. This suggests that functional brain networks sustaining advanced behavior are immature in infants. During the maturation process, a gradual reorganization of hub network connectivity between birth and adulthood occurs and large-scale cortical networks develop from a ‘‘local and segregated’’ to a ‘‘distributed and integrated’’ organization (Fair et al., 2009; Power et al., 2010; Supekar et al., 2009).

At birth, the neural networks are partially developed. In the first 6 years, the networks expand and the brain grows rapidly to allow new skills to be learned. The development of the immature brain is concomitant with certain morphological aspects of the developing brain and EEG results. These aspects are closely associated with the gestational age. Disturbance in the process of maturation for the infant babies of more than 26 weeks is likely to generate structural modification of the brain such as atrophy, gliosis and/or cavitation. Early detection of neurodevelopmental abnormalities would help to diagnose and treat affected babies. Full-term and premature neonates are at high risk of brain damage and life-long cognitive disability. According to different studies(Marlow et al., 2005; Monset-Couchard and de Bethmann, 2000), about 6.2% of new-born infants in France are premature and from 36 to 60% of the premature infants of less than 30 weeks have neurological dysfunctions such as motor, cognitive and sensory deficits and learning disorders.

This chapter describes connectivity methods with particular attention to the functional and effective connectivity measures used in this thesis. The graph theoretical measures are also reviewed. The chapter starts with a short review on analytical signals required for the computation of functional connectivity and EEG source imaging.

3.2 Brain connectivity

Brain networks communicate to execute a particular function or task. The intercommunication phenomenon in the brain is termed brain connectivity. Brain connectivity reveals pathways or how information is exchanged between the brain regions (Breakspear and Jirsa, 2007). Brain connectivity measures are bivariate, i.e., they involve the interactions between two brain regions or scalp electrodes.

There are three modes of brain connectivity- structural, functional and effective (Friston, 2005; Horwitz, 2003). Structural or anatomical connectivity refers to a network of structural (synaptic) connections linking sets of neurons or neuronal elements. Functional connectivity is fundamentally a statistical concept that estimates the temporal correlation between two signals over time. In general, functional connectivity captures deviations from statistical independence between distributed and often spatially remote neuronal units. Effective connectivity investigates the directional effect of one neural element over another. The difference between the three modes of connectivity is shown in Figure 3.1.

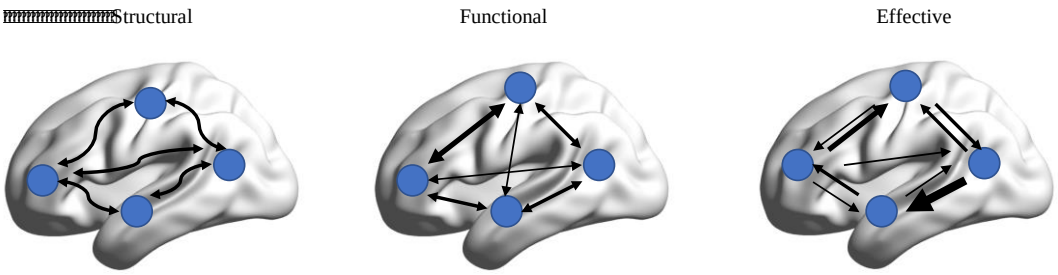

Figure 3.1: Modes of brain connectivity: Structural connectivity shows the white matter connections between the gray matter brain regions. Functional and effective connectivity show the connections between the neuronal activity of the brain regions. Unlike functional connectivity, effective connectivity shows the directionality of the connections.

3.2.1 Structural connectivity

Structural connectivity is the anatomical connections between brain regions. This type of connection includes fiber pathways between the brain regions which can be assessed by the propagation of water molecules. The common imaging technique used is diffusion weighted imaging (DWI) which can be applied in several directions to examine the diffusion of water molecules in the brain (Johansen-Berg and Rushworth, 2009). Diffusion tensor imaging (DTI) (Shenton et al., 2012) is another non-invasive method for characterizing the microstructural organization of the brain tissues in vivo. This method generates maps that visualize different aspects of the tissue microstructure (mean diffusivity, tissue anisotropy and dominant fiber orientation).

3.2.2 Functional connectivity

Functional connectivity is defined as statistical dependencies between brain regions (Friston, 1994). Functional connectivity in neuroimaging is always estimated from fMRI and EEG/MEG time series. Functional connectivity is symmetric, implying that connectivity from x to y is similar to connectivity for y to x. There are many functional connectivity measures and descriptions. In this thesis we will focus on the power-based, phase-based and information-based functional connectivity measures. Before quantifying the functional connectivity between measurement sites or sources, their signals are transformed to the complex-value analytical signals. In addition, the source analysis is required for the transformation of EEG sensors signals to source signals.

Frequency-domain signals

Frequency-domain signal is a complex-valued variable usually obtained from the fast Fourier transform of the signal. The Fourier transform of a time-series, x, is obtained by the dot product of the signal and sine waves of different frequencies:

$$X(f) = \sum_{k=1}^{N} x_k e^{-\frac{i2\pi f(k-1)}{N}} \tag{3.1}$$

where N refers to the number of data points in vector, x, and X(f) is the complex-series signal at frequency f. The number of unique frequencies extracted from a times-series of length N is N/2+1 based on the Nyquist theorem.

The short-time fast Fourier transform (FFT) is an extension of the Fourier transform. The Fourier transform assumes the EEG signal to be stationary and obscures time-frequency changes in EEG data. The short-time FFT is computed by first segmenting (with Hann or Gaussian windows) the data to minimized edge artifacts from contaminating the time-frequency results (Cohen, 2014). However, the disadvantage of this method is that tapering attenuates the signals. The attenuation of signals in the short-time FFT method is corrected by an improved method, called Multitaper method. It is designed to increase the signal to noise ratio of the signal by applying multiple tapers with several different temporal characteristics (Bronez, 1992). The multitaper method introduces some frequency smoothing depending on the number of tapers. This method is beneficial when one deals with noisy or few single trial EEG signals. It is also well suited for high frequency analysis with very good anti-frequency leakage (van Vugt et al., 2007).

Another method usually used to obtain frequency-domain signals is the wavelet analysis like Complex Morlet Wavelet (CMW) which involves many technical details on controlling the frequency smoothing such as number of cycles, minimum and maximum frequencies, and frequency resolution (Tallon-Baudry et al., 1996). The wavelet methods are well suited for localizing frequency information in time. CMW is defined as:

$$w(t,f) = \left(\sigma_t\sqrt{\pi}\right)^{-\frac{1}{2}}\ e^{-\frac{t^2}{2\sigma_t^2}}\ e^{-i2\pi ft} \tag{3.2}$$

where f is the center frequency and σ_t is the temporal standard deviation. The time-frequency analytical signal X (t,f) of a signal $x(t)$ is then computed by convolving $x(t)$ and $w(t,f)$:

$$X(t,f) = x(t) * w(t,f) \tag{3.3}$$

The spectral bandwidth is controlled by the ratio of f to σ_f to obtain desired frequency ranges.

The Hilbert transform is another time-frequency decomposition method which allows more control over frequency characteristics, a major advantage over the wavelet method (Cohen, 2014; Freeman, 2007). The signal is first band-filtered within a desire frequency range. The Hilbert transformation is then applied to extract the frequency-domain signal X (t, f) as:

$$X(t,f) = x(t,f) + ix_H(t,f) \tag{3.4}$$

Where x_H (t, f) is the Hilbert transform of the input signal x (t,f).

These methods are commonly used in EEG data analysis and can give similar results with minimal differences (Akin, 2002; Le Van Quyen et al., 2001; van Vugt et al., 2007). Other time-frequency decomposition methods are S-transform, an adaptation of short-time FFT, matching pursuit, Hilbert-Huang, P-episode and many more.

Power spectral density

Power spectral density function (PSD) is obtained from the analytical signals:

$$\mathrm{PSD(f)} = \frac{\mathrm{X(f)} * \mathrm{X}^*(f)}{N} \qquad (3.5)$$

Where $X^*(f)$ is the complex conjugate of X(f) and N is the number of data points. The power decreases with increasing frequency (Freeman, 2006; Kiebel et al., 2005). Power spectral analysis is used in EEG analysis to evaluate classical EEG frequency bands relevant to physiological rhythms.

Usually, EEG powers are normalized for statistical analysis and comparisons between different conditions. Normalization is done with reference to a baseline or to a maximum value. The common normalization is based on decibel conversion, percentage or unit conversion and z-transform.

The functional connectivity in the source space requires EEG source imaging by transforming EEG signal in the sensor space to source activities in the source space.

EEG source imaging

EEG Source Imaging (ESI) is the modeling of the electrical source distributions associated with the brain activation from noninvasive EEG/MEG recording (He et al., 2011; Michel et al., 2004). ESI comprises forward and inverse problems (Figure 3.2):

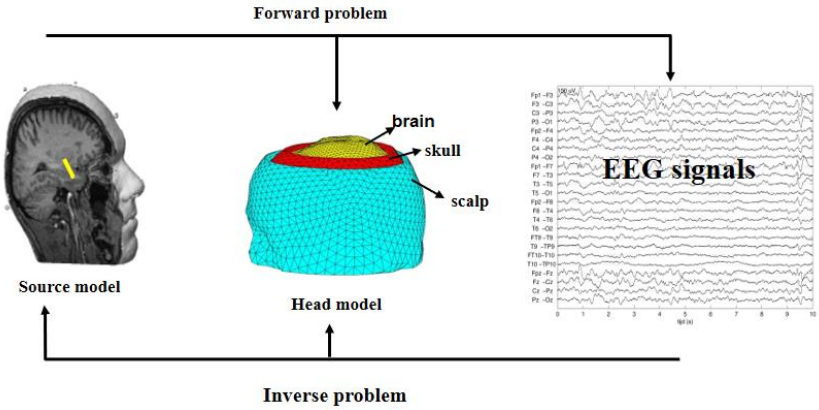

Figure 3.2: EEG source Imaging: Forward and inverse problems.

Forward problem

The forward problem estimates the scalp potentials based on the head volume conductor (Hallez et al., 2007). The accurate modeling of the head volume conductors is very important for accurate imaging of the brain sources. The head model provides the description of the geometry and electrical properties of each tissues type (gray, white matter, CSF, skull and scalp). Simple spherical head model is built from the concentric spheres. The realistic head models are built from the structural MRI and computed tomography (CT) of the brain model by the boundary element method (BEM) (Fuchs et al., 2002), finite difference method (FDM) (Hallez et al., 2005) and finite element method (FEM) (Wolters et al., 2002). BEM usually assumes three homogenous layers (brain, skull and scalp) (Figure 3.2). BEM is computationally efficient unlike FEM and FDM that divide the head into small elements for each of which the geometry and conductivity can be defined separately. FEM and FDM allow incorporation of tissues anisotropy (Hallez, 2008; Wolters et al., 2006) but complexity of the model construction make them computationally very expensive. The scalp potentials, V with the current sources dipole at position r = [x y z] and dipole moment D = [Dx Dy Dz] are related by:

$$V = L(r)D \tag{3.6}$$

where L is the transfer or leadfield matrix that describes the relationship between dipole, D and the scalp potentials, V. The leadfield matrix consists of head geometry and tissues conductivity. Hallez et al. (2007) provide a detailed review on forward modeling.

Inverse problem

The inverse problem estimates the source distribution with the leadfield matrix and scalp potentials measured with electrodes (Grech et al., 2008). The inverse problems are either based on dipoles source model or imaging method. In dipole source modeling, the aim is to estimate one or more

dipole sources while minimizing the relative residual energy (RRE) (Grech et al., 2008; Mosher et al., 1999, 1992). This is done by assuming a predetermined number of dipoles as equivalent to the generator of the EEG. The dipole locations and moments are then estimated through optimization. Dipole source localization has been found to be useful in localizing epileptic activity with a reasonably good source detection rate. RRE is mathematically defined as:

$$RRE = \frac{\|V - LD\|}{\|V\|} \tag{3.7}$$

Where V is scalp potentials, D is the dipole with its orientation and position and L is the leadfield matrix.

The second technique for the inverse problem is the imaging method. Unlike the dipole method, the imaging method is underdetermined, that is, the number of parameters to be estimated is larger than the number of scalp potentials. Imaging methods are based on the distributed source models with a fixed dipole position in each brain voxel. Underdetermined problems in imaging method are solved by the regularization of the parameters. This has led to development of various imaging methods generally based on the equation 3.8 to estimate the current density, D (Grech et al., 2008; Michel, 2009):

$$D = A^{-1}L^T(LA^{-1}L^T + \lambda B^{-1})^{-1}V \tag{3.8}$$

Where L and V are the leadfield matrix and scalp potentials, respectively, λ is the regularization parameter, the choice of A and B determines the type of the method being used such as minimum norm estimate (Gramfort et al., 2012), linear beamfomer (Drongelen et al., 1996; Gross et al., 2001), low resolution electromagnetic tomography (LORETA) (Pascual-Marqui, 2002), and many more.

Time and frequency domain source analysis

The EEG/MEG high temporal resolution is considered as the most important advantage of this type of imaging modality over other techniques like fMRI. In studies on event related potential (ERP) or epilepsy EEG source analysis in the time domain is usually performed on the 'events' selected by searching for electrodes with potential peaks (Michel et al., 2004; Pascual-Marqui, 2002). Alternatively, source localization methods can be applied to each time point and the

temporal dynamics can directly be studied in the source space. This is usually used for the connectivity analysis in the source space.

The EEG high temporal resolution allows studying the behavior of sources in different frequencies by applying frequency transformation algorithms, source localization and connectivity in the frequency domain (Gross et al., 2001; Michel et al., 1992). This is preferable for many researchers that are interested in connectivity analysis and localization of sources for different frequency bands. Source analysis in the frequency domain is preceded by the analysis of analytical signals over a certain time epoch or segment as described earlier.

3.2.2.1 Power-based functional connectivity analysis

The functional connectivity can be evaluated in the time or frequency domain using linear dependence measures such as linear cross-correlation or coherence functions.

The Pearson correlation coefficient is a commonly used correlation method, defined as the covariance of two signals x and y, scaled by their variances:

$$r(x,y) = \frac{\sum_{t=1}^{N}(x_t - \mu_x)(y_t - \mu_y)}{\sqrt{\sum_{t=1}^{N}(x_t - \mu_x)^2 \sum_{t=1}^{N}(y_t - \mu_y)^2}} \tag{3.9}$$

where N is the number of data points, μ_x and μ_y are mean values of the signals x and y, respectively. The resulting correlation value lies between -1 and 1 with 1 implying highest positive correlation.

The spectral coherence is similar to the correlation coefficient but in the frequency domain. The spectral coherence incorporates power information (both amplitude and phase). It is defined as follows:

$$C_{xy}(f) = \frac{\left|S_{xy}(f)\right|^2}{S_{xx}(f)S_{yy}(f)} \tag{3.10}$$

where S_{xy} is the cross-spectral density of analytical signals X and Y, and S_{xx} and S_{yy} are the auto-spectral density of X and Y, respectively. C lies between 0 and 1 with 1 implying highest coherence at frequency f.

The spectral coherence incorporates power information and the results are likely to be influenced by cross-spectral of the two signals. However, it has been suggested to neglect the real

component of the cross-spectrum (Nolte et al., 2004) because it is highly affected by volume-conduction artifacts in EEG.

3.2.2.2 Phase-based functional connectivity analysis

There are several phase-based functional connectivity analyses relying on the distribution of phase differences between different electrodes. A common method to measure the strength of phase synchronization between different brain regions is the phase locking value (PLV) defined as (Lachaux et al., 2000):

$$PLV_{xy}(f) = \frac{1}{N}\left|\sum_{t=1}^{N} e^{i(\emptyset_x - \emptyset_y)}\right| \tag{3.11}$$

Where ϕ_x and ϕ_y are phase angles of the signals x and y, respectively, and N is the number of data points. The phase angles are usually obtained from the frequency-domain signals. The PLV values also range between 0 and 1.

Another method usually used for phase synchronization analysis is the phase lag index (PLI) (Stam et al., 2007). It was introduced to obtain reliable estimates of phase synchronization that are invariant against the presence of common sources (volume conduction and active reference electrodes in the case of EEG sensors). PLI is defined as:

$$PLI_{xy}(f) = \left|\frac{1}{N}\sum_{t=1}^{N} sgn\left(imag\left(S_{xy}\right)\right)\right| \tag{3.12}$$

Where imag(S) is the imaginary part of the cross-spectral density and *sgn* indicates sign (-1 for negative values, +1 for positive values and 0 for zero values). PLI is less sensitive to noise and volume conduction but is hindered by the discontinuity as small perturbations turn phase lags into leads and vice versa. As an extension of PLI, the weighted phase lag index (wPLI) (Vinck et al., 2011) was introduced as :

$$wPLI_{xy}(f) = \frac{\frac{1}{N}\sum_{t=1}^{N}\left|imag\left(S_{xy}\right)\right| sgn(imag\left(S_{xy}\right))}{\frac{1}{N}\sum_{t=1}^{N}\left|imag(S_{xy})\right|} \tag{3.13}$$

3.2.2.3 Information-based functional connectivity analysis

The information-based connectivity analysis involves both linear and non-linear statistical dependencies between two time series (Hurtado et al., 2004; Jeong et al., 2001). This technique is based on the concept of entropy that measures the probability of variable. The Shannon entropy (H_x) of a signal x is defined as:

$$H(X) = -\sum_{i=1}^{N} p(x_i)\log(p(x_i)) \tag{3.14}$$

Where $p(x_i)$ is the probability that signal x has the value of x_i. The probability can be obtained from the histogram of the signal, phase angle or power and N is the number of histogram bins. Interdependence between two signals x and y is obtained from the mutual information based on Equation 3.14:

$$MI_{xy} = H(X) + H(Y) - H(X,Y) \tag{3.15}$$

where H (X, Y) is the joint entropy between signals x and y:

$$H(X,Y) = -\sum_{j=1}^{M}\sum_{i=1}^{N} p(x_i,y_i)\log(p(x_i,y_i)) \tag{3.16}$$

M and N correspond to the number of bins for signals x and y, respectively.

3.2.4 Effective connectivity

The objective of effective connectivity analyses is to estimate causal dependencies between brain regions (Friston, 1994). Unlike functional connectivity measures, effective connectivity indicates the direction of information flow between different brain regions (Friston, 1994). The directional interaction can be estimated by model-based techniques such as dynamic causal modelling (Friston et al., 2003), structural equation modeling (Ullman and Bentler, 2003), or Granger causality (Hesse et al., 2003).

The effective connectivity analysis requires autoregressive modelling and model parameter estimation to estimate effective connections between brain regions.

Autoregressive modeling

Autoregressive (AR) modeling attempts to estimate future values of a signal based on a weighted sum of its past values. For a signal of length n, a multivariate autoregressive (MVAR) (Ding et al., 2000) model is represented by:

$$X(n) = \sum_{m=1}^{p} A(m)X(n-m) \ + E(n) \tag{3.17}$$

where E(n) is the matrix containing uncorrelated white noise at time n, p is the model order, and A(m) is a n by n coefficient matrix for delay m.

Model selection

The most common approach for model order (p) selection involves first setting a set of model orders and then finding one that minimizes one or more information criteria evaluated over the model order range (Lütkepohl, 2005). Two commonly used information criteria are the Akaike Information Criterion (AIC) and Bayesian Information Criterion (BIC).

The AIC and BIC for MVAR are defined as follows:

$$AIC(p) = \ln\left|\sum(p)\right| + \frac{\ln(T)}{T} pK^2 \tag{3.18}$$

$$BIC(p) = \ln\left|\sum(p)\right| + \ \frac{2pK^2}{T} \tag{3.19}$$

Where $\sum$(p) is the covariance matrix of the residuals, T is the number of data points, p is the model number, and k is the number signals. Each of these criteria needs to be minimized to find the optimal model order. Other criteria include the Final Prediction Error (FPE) and Hanna-Quinn Criterion (HQC).

Effective connectivity measures

The power spectral density S of a chosen and validated model is calculated from the coefficients and residuals of MVAR:

$$S(f) = H(f)H^*(f) \tag{3.20}$$

where H(f) (= $A^{-1}(f)$) is the transfer matrix of the MVAR model of dimensions K by K. H_{ij} is the information flow from x_j to x_i at frequency f.

Common effective connectivity measures are:

Partial coherence (Brillinger, 2001)

$$PCOH_{ij} = \frac{\left|S_{ij}(f)\right|^2}{S_{ii}(f)S_{jj}(f)} \tag{3.21}$$

Partial directed coherence (Baccalá and Sameshima, 2001)

$$PDC_{ij} = \frac{\left|A_{ij}(f)\right|^2}{\sum_{j=1}^{k}\left|A_{ij}(f)\right|^2} \tag{3.22}$$

Direct transfer function (Kamiński et al., 2001)

$$DTF_{ij} = \frac{\left|H_{ij}(f)\right|^2}{\sum_{j=1}^{k}\left|H_{ij}(f)\right|^2} \tag{3.23}$$

3.3 Graph network analysis

3.3.1 Introduction

Graph theory is a mathematical framework developed to study physical, biological and information systems. There are increased interests in application of graph theory to study functional and

structural brain networks (He and Evans, 2010; Sporns, 2011), and to expand our knowledge on the human brain diseases, ageing and higher cognitive functions (Bullmore and Bassett, 2011; Deuker et al., 2009; Netoff et al., 2004; Stam, 2014).

All networks consist of two basic components: nodes and pairwise edges (links) between the nodes (Bullmore and Sporns, 2009). Nodes in the brain networks are usually represented by the brain regions or electrodes positions for scalp EEG. Nodes are sometimes determined by the functional activity and parcellation of the surface of the cortex or the entire brain (Figure 3.3). The parcellation is sometime done by using brain atlases constructed with the anatomical features of the brain (Deco and Kringelbach, 2014; Stanley et al., 2013). Functional or effective coupling between electrodes or brain regions indicate edges or links. All networks are represented by their connectivity (adjacency) matrices. Rows and columns in these matrices denote nodes while the entries denote edges.

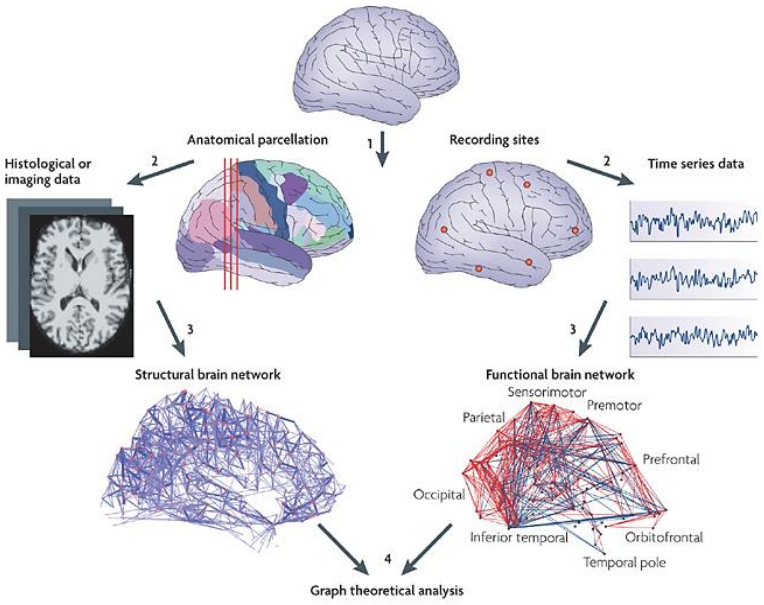

Figure 3.3 Brain Networks: Both structural and functional brain network analyses involve four steps before graph theoretical analysis. The first step is to define the network nodes. The second step involves the estimation of time series signal of each node. The third step is to estimate coupling between the nodes before calculating the network parameters (step 4) (adapted from Bullmore and Sporns (2009)).

3.3.2 Graph theoretical measures

There are many network metrics (Rubinov and Sporns, 2010). Before the computation of networks metrics, the graph is first thresholded (Figure 3.4) and converted to a binary form denoting absence or presence of connections. The network measures can also be applied to the weighted matrices consist of information about the connection strength (Fallani et al., 2014; Rubinov and Sporns, 2010). The threshold is required to increase the signal to noise ratio by pruning out weak and non-significant representing spurious connections.

There are many ways to threshold a graph. The common method is to choose a common arbitrary value for all subjects or conditions in an experiment. Another option is to specify the number of connections (connection density) and keep the strongest connections while setting the rest to zero. Other thresholding methods is by generating surrogate data for the statistical assessment of the functional measures, especially for the short signals (Drakesmith et al., 2015; Langer et al., 2013). Sometimes, thresholds are chosen based on the distribution of the connectivity matrices. Depending on the subject distribution, thresholds will change, this is why it is important to take the topology of the connectivity matrix into consideration (Fallani et al., 2014).

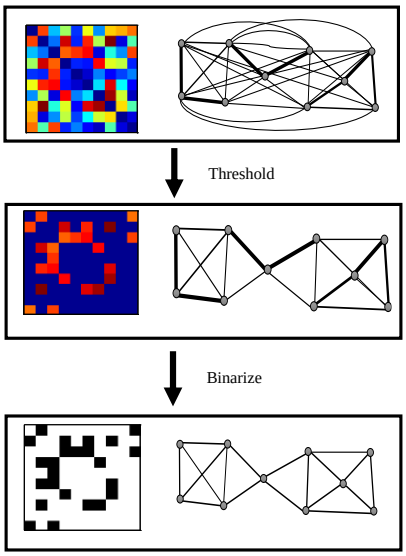

Figure 3.4. Construction of brain networks: Functional networks are commonly represented by their connectivity matrices, with rows and columns representing nodes and matrix entries representing links. Networks are often reduced to a sparse binary undirected form, through thresholding and binarization.

After thresholding, the networks are binarized by setting the suprathreshold values to 1 and the subthreshold values to 0 before the computation of the network metrics. There are many network measures particularly for characterizing the brain functional network topology. The brain network measures are always classified based on the neurobiological interpretations such as network centrality, functional segregation, functional integration, small-world networks, networks motifs and many others. In the following, we pay special attention to the network metrics used throughout the thesis.

Network centrality

Centrality is the most important property of brain networks. It assesses the importance of individual nodes or brain regions by measuring how often a particular node interacts with many other nodes in the network (Figure 3.5). The most common measure of centrality is *degree* which is the number of connections of a node links to the rest of the network. Degree, k of node i, is mathematically defined as:

$$k_i = \sum_{j=1}^{N} a_{ij} \tag{3.24}$$

Where a is the adjacency matrix of dimensions N by N.

Another important centrality measure is the Betweenness Centrality (BC) (Freeman, 1979) which measures the fraction of all shortest paths that pass through a given node. It also detects important anatomical and functional connections, and is defined as:

$$BC_i = \frac{1}{(N-1)(N-2)} \sum_{h,j,h\neq j,h\neq i,j\neq i} \frac{P_{hj}(i)}{P_{hj}} \tag{3.25}$$

P_{hj} is the total number of shortest paths between h and j, and $P_{hj}(i)$ is the number of shortest paths that pass through node i with N total nodes.

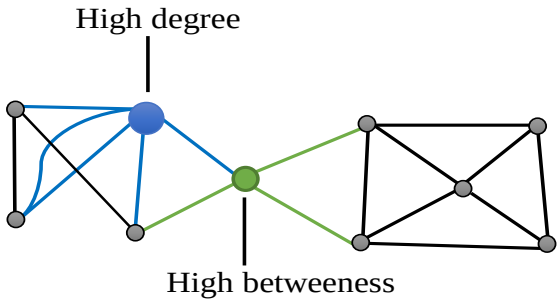

Figure 3.5: Network Centrality: Higher degree at the blue node with higher number of connections and high betweenness at the green node due to the high number of shortest paths.

Other centrality measures include closeness centrality, modularity and participation coefficient (Rubinov and Sporns, 2010).

Functional segregation

Functional segregation of the brain networks reflects the existence of specialized brain regions as modules organized in distinct populations (Tononi et al., 1994). Functional segregation measures the presence of clusters or modules within the network (Figure 3.6). The common functional

segregation measure is the clustering coefficient which measures the fraction of triangles around individual nodes (Watts and Strogatz, 1998). It is defined mathematically as:

$$C_i = \frac{2t_i}{k_i(k_i - 1)} \tag{3.26}$$

Where where k_i and t_i is the degree and number of triangles around ith node, and t is defined as:

$$t_i = \frac{1}{2}\sum_{j,h \in N} a_{ij}a_{ih}a_{jh} \tag{3.27}$$

where a is adjacency matrix.

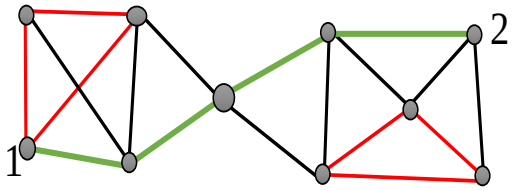

Figure 3.6: Functional Segregation and Integration: The measures of segregation are usually based on triangle counts (red) while the integration is based on shortest path lengths (green) between two nodes (for instance 1 to 2).

An alternative to the clustering coefficient is the local efficiency (LE) which quantify how well information is exchanged between neighboring nodes (Latora and Marchiori, 2001). It is defined mathematically as:

$$LE_i = \frac{\sum_{j,h \in N, j \neq i} a_{ij}a_{ih}\left[d_{jh}(N_i)\right]^{-1}}{k_i(k_i - 1)} \tag{3.28}$$

Where a_{ij} and a_{ih} is the connection status (0 or 1) between the nodes i and j, and i and h, respectively, , and $d_{jh}(N_i)$ is the sum of shortest paths between nodes j and h that contains the neighbors of node i.

Functional integration

Functional integration measures the ease of information transfer or communication between brain regions (Tononi et al., 1994). The communication between brain networks is measured by the paths connecting them (Figure 3.6). The characteristic path length (L) is the most commonly used

measure of functional integration. L is the path between brain regions (Watts and Strogatz, 1998). It is defined mathematically as:

$$L_i = \frac{\sum_{j=1, j\neq i}^{N} d_{ij}}{N-1} \tag{3.29}$$

Where d_{ij} is the shortest absolute distance between the nodes i and j. The inverse of average characteristic path length is known as the global efficiency (E) which is defined as:

$$E = \frac{1}{N}\sum_{i\epsilon N} \frac{\sum_{j\epsilon N, j\neq i} d_{ij}^{-1}}{N-1} \tag{3.30}$$

Small-world networks

The brain is a very complex network that supports spatio-temporal information processing. A normal brain network combines functionally segregated modules with robust functional integrating links. This kind of network is called a *small-world network (SWN)* supporting optimal functional integration and segregation (Bassett and Bullmore, 2006; Sporns and Zwi, 2004). This network structure is highly clustered (high clustering coefficient) with shorter path length (or higher efficiency) (Figure 3.7) between brain regions compared to ordered (high C and long L) or random networks (low C and short L)(Watts and Strogatz, 1998).

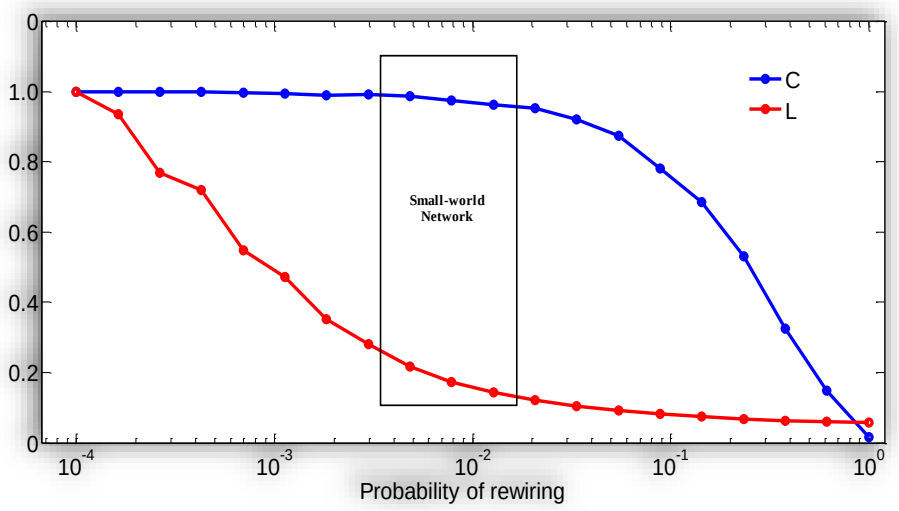

Figure 3.7 Small-world network: Clustering coefficient (C) and path length (L) are plotted as a function of rewiring probability (adapted from Watts and Strogatz (1998)). A small-world network is the network with high C and short L in which nearest neighbours are connected to each other (segregation) and there are short paths to other neighbours (integration). The probability of rewiring indicates the increase in randomness of the network.

A formal test to investigate whether a network behaves like a small-world network is to evaluate the ratio of the normalized clustering coefficient(C) to the characteristic path length (L):

$$SWN = \frac{\left(\frac{C}{C_{rand}}\right)}{\left(\frac{L}{L_{rand}}\right)} \tag{3.31}$$

Where C and C_{rand} are the clustering coefficients, and L and L_{rand} are the characteristic path lengths of the tested network and a random network, respectively. If the SWN value is greater than 1, the network exhibits properties similar to small-world networks. However, the SWN is influenced by several factors such as connectivity methods, the network size (SWN increases with increasing the number of nodes), thresholding and other parameters.

Other network categories include network motifs, network resilience and many others. The readers are referred to these papers (Rubinov and Sporns, 2010; Sporns, 2011; Telesford et al., 2011) for more information.

Chapter 4

EEG resting state functional connectivity analysis in children with benign epilepsy with centrotemporal spikes, Part I

4.1 Introduction

The relationship between epilepsy and cognitive and neuropsychological impairments in children has been observed for a very long time (Datta et al., 2013; Fonseca et al., 2007; Holmes and Lenck-Santini, 2006; Jambaqué et al., 1993). Despite the large number of studies on this topic, the proper effects of epileptic activity on the cognitive functioning and development are not yet clearly defined. Many studies are carried out with patients with different focal sources of epilepsy, age, frequent of seizure and epileptic syndromes. Cognitive and behavioral deficits observed in epileptic children are sometimes regarded as the result of complex interactions between biological, psychological and social factors (Ay et al., 2009; Shields and Snead, 2009).

Benign childhood epilepsy with centrotemporal spike (BCECTS) is one of the most common idiopathic epilepsy with prevalence between 10 to 20% in children with epilepsy under the age of 16 (Panayiotopoulos et al., 2008). BCECTS is characterized by seizures typically originated in the centroptemporal region with autonomic manifestations in the face, mouth and throat (Loiseau, 2001). The majority of seizures occur during sleep or at the sleep onset (Camfield and Camfield, 2014; Shields and Snead, 2009). Unlike other types of epilepsy like temporal lobe epilepsy (Taylor et al., 2015), benign childhood epilepsy is known to be unaffected by the structural abnormality (Hughes, 2010). However, epilepsy activity can cause different malfunctions between subcortical and cortical regions that may lead to changes in resting state EEG activity.

In this chapter we investigate differences in resting-state brain activity between BCECTS patients and healthy controls under the eyes-closed condition in the presence and absence of centrotemporal spike (CTS) or interictal epileptic discharges (IEDs). For this purpose, we studied changes in the EEG spectral power and functional connectivity in both sensor and source spaces. Graph theory metrics were also used to characterize functional connectivity between BCECTS brain networks in comparison to healthy controls.

4.2 EEG spectral power and source analysis

Spectral power analysis is one of the standard methods used for the quantification of EEG. The spectral power density (power spectrum) reflects the distribution of signal power over frequency. Spectral power features in different frequency bands may share different physiological properties (Başar et al., 2013; Klimesch et al., 2007).

There are several studies using spectral power and source analyses of scalp EEG in benign childhood epilepsy (BCE) (Béla et al., 2007; Besenyei et al., 2012; Clemens, 2004; Clemens et al., 2010; Kikumoto et al., 2006). All reported high power spectral mostly at the epileptic region. Most of these studies were done on the diverse groups of patients with different epileptic foci and age group.

In the first study, we recruited twenty-one patients with BCECTS with an average age of 9.84 ± 1.75 years old and twelve healthy controls with the same age range for the EEG resting-state analysis. High density EEG data were recorded under the eye closed condition lasting at least 14 minutes for each subject. A homogenous group of twelve patients was selected based on the source location of interictal epileptic discharges (IEDs). High density EEG data were preprocessed to remove artifacts. The artifact-free segments were then segmented into non-overlapping epochs for each subject. Two conditions were considered for the epileptic patients, EEG segments with and without IEDs. Absolute and relative spectral power and source activities were computed for these conditions in five different frequency bands (δ, θ, α, β_1 and β_2) in both sensor and source spaces. The changes in EEG spectral power were statistically compared between patients and controls with nonparametric statistical tests.

Our results showed that the EEG resting state networks of BCECTS patients were functionally disrupted in the presence and absence of centrotemporal spikes. The major findings were dysfunction at the centrotemporal region, cortical source suppression at the frontal and occipital regions in patients. Patients were also characterized with high θ power in scalp EEG across the brain and lower spectral power in the α band especially at the occipital regions in the presence of IEDs. More details can be found in the following paper[1].

[1] Supplementary information in Appendix

NeuroImage: Clinical 9 (2015) 275–282

Contents lists available at ScienceDirect

NeuroImage: Clinical

journal homepage: www.elsevier.com/locate/ynicl

EEG resting state analysis of cortical sources in patients with benign epilepsy with centrotemporal spikes

Azeez Adebimpe[a], Ardalan Aarabi[a,*], Emilie Bourel-Ponchel[b], Mahdi Mahmoudzadeh[a,b], Fabrice Wallois[a,b]

[a] INSERM U 1105, CURS, CHU sud, Salouël, Av. Laennec, 80054 Amiens Cedex, France
[b] INSERM U 1105, EFSN Pédiatriques, CHU sud, Salouël, Av. Laennec, 80054 Amiens Cedex, France

ARTICLE INFO

Article history:
Received 18 February 2015
Received in revised form 19 August 2015
Accepted 20 August 2015
Available online 3 September 2015

Keywords:
Benign epilepsy
Centrotemporal spikes
Spectral power
Source analysis
EEG

ABSTRACT

Benign epilepsy with centrotemporal spikes (BECTS) is the most common idiopathic childhood epilepsy, which is often associated with developmental disorders in children. In the present study, we analyzed resting state EEG spectral changes in the sensor and source spaces in eight BECTS patients compared with nine age-matched controls. Using high-resolution scalp EEG data, we assessed statistical differences in spatial distributions of EEG power spectra and cortical sources of resting state EEG rhythms in five frequency bands: δ (0.5–3.5 Hz), θ (4–8 Hz), α (8.5–13 Hz), β_1 (13.5–20 Hz) and β_2 (20.5–30 Hz) under the eyes-closed resting state condition. To further investigate the impact of centrotemporal spikes on EEG spectra, we split the EEG data of the patient group into EEG portions with and without spikes. Source localization demonstrated the homogeneity of our population of BECTS patients with a common epileptic zone over the right centrotemporal region. Significant differences in terms of both spectral power and cortical source densities were observed between controls and patients. Patients were characterized by significantly increased relative power in θ, α, β_1 and β_2 bands in the right centrotemporal areas over the spike zone and in the right temporo-parieto-occipital junction. Furthermore, the relative power in all bands significantly decreased in the bilateral frontal and parieto-occipital areas of patients regardless of the presence or absence of spikes in EEG segments. However, the spectral differences between patients and controls were more pronounced in the presence of spikes. This observation emphasized the impact of benign epilepsy on cortical source power, especially in the right centrotemporal regions. Spectral changes in bilateral frontal and parieto-occipital areas may also suggest alterations in the default mode network in BECTS patients.

1. Introduction

Benign epilepsy, also known as Rolandic epilepsy, is the most common idiopathic childhood epilepsy with a prevalence of approximately 15% in children aged 1–15 years (Panayiotopoulos et al., 2008). Rolandic epilepsy is characterized by seizures that typically originate in the centrotemporal area with often the same sensorimotor symptoms and autonomic manifestations in the face, mouth and throat (Loiseau, 2001; Loiseau and Beaussart, 1973). The majority of Rolandic seizures occur during non-REM sleep, at sleep onset or rest (Camfield et al., 2014; Panayiotopoulos et al., 2008; Shields and Snead, 2009). As the hallmark of benign childhood epilepsy, seizures are mostly associated with centrotemporal spikes (CTS) often followed by slow waves, which are typically activated by drowsiness and slow (non-REM) sleep (Blom and Brorson, 1966; Clemens and Majoros, 1987; Smith and Kellaway, 1964). Dipole source localization in patients with BECTS has demonstrated that CTS can be reliably modeled by single tangential dipole sources oriented from central to frontal lobes and localized in the high and low central regions (suprasylvian) (Gregory and Wong, 1992; Jung et al., 2003; Legarda et al., 1994; Panayiotopoulos, 1999b; Tsai and Hung, 1998). Despite the focality of CTS and rolandic seizures in patients with benign epilepsy, there is growing evidence from neuroimaging studies reporting memory, language, attention, auditory and cognitive impairments in BECTS patients that BECTS may functionally and structurally affect a larger portion of the brain at rest (Bocquillon et al., 2009; Cataldi et al., 2013; Lopes et al., 2014; Northcott et al., 2007; Verrotti et al., 2014).

The present study attempted to investigate changes in the spectral power and spatial distribution of cortical sources of eyes-closed resting state EEG rhythms in patients with BECTS compared to healthy subjects under two conditions, in the presence and absence of CTS.

2. Methods

2.1. Subjects

Twenty-one children (9.84 ± 1.75 years) with BECTS and 12 healthy subjects (9.27 ± 1.70 years) used as controls were preselected for resting state analysis. The study was conducted at Amiens University

* Corresponding author.
E-mail address: ardalan.aarabi@u-picardie.fr (A. Aarabi).

http://dx.doi.org/10.1016/j.nicl.2015.08.014

Table 1
Characteristics of the control and patient groups.

Control group			Patient group					
Subject	Age (years)	EEG duration (min)	Patient	Age (years)	EEG duration (min)	Neuropsychological assessment	Description of ictal EEG	Medication
1	6.73	16.21	1	12.63	50.84	Normal	Partial seizure	Sodium valproate
2	11.28	19.59	2	12.64	17.85	Normal	Partial seizure	Sodium valproate
3	10.48	19.75	3	9.25	44.08	Attention deficit	*Generalized tonic–clonic seizure*	Oxcarbezepine
4	10.66	17.44	4	6.03	43.52	–	Brachiofacial nocturnal seizure	Oxcarbezepine
5	7.39	13.54	5	10.47	50.06	Attention deficit	Partial seizure	Sodium valproate
6	7.31	20.30	6	7.16	14.26	–	Brachiofacial nocturnal seizure	Sodium valproate
7	11.92	30.02	7	8.51	30.36	Attention deficit	Nocturnal seizure	–
8	8.44	75.00	8	13.16	20.02	Normal	*Generalized tonic–clonic seizure*	Sodium valproate
9	9.36	28.00	9	9.67	15.63	Language deficit	*Generalized tonic–clonic seizure*	Lamotrigine
10	9.48	45.09	10	7.79	23.12	Normal	*Generalized tonic–clonic seizure*	Micropakine
11	10.32	18.97	11	8.91	16.78	Normal	*Generalized tonic–clonic seizure*	Trileptal
12	7.98							
Mean ± SD	9.27 ± 1.70			9.65 ± 2.36				

Hospital (France) and was approved by the hospital's ethics committee (CPP Nord-Ouest No: 2011-A00782-39). Written informed consent was obtained from each subject's caregivers. Healthy subjects had no history of neurological disorders. Patients showed no structural brain abnormalities on MRI.

2.2. Data acquisition and preprocessing

An EEG lasting at least 14 min was recorded in each individual at a sampling rate of 256 Hz with a high-resolution EEG recording system (ANT, Netherlands) using 64 electrodes placed on the scalp according to the international 10–10 system. Forehead ground and linked-ear reference electrodes were used for data collection. During the recordings, the subjects were asked to rest comfortably in a supine position in a quiet dark room and were instructed to stay fully relaxed and motionless. We made sure that they were fully awake during data collection. Since the reference electrode could be contaminated by ocular artifacts, EEG data were offline re-referenced to common average reference and filtered between 0.5 to 30 Hz to remove possible high frequency noise. Two experienced neurophysiologists visually inspected the EEG data to identify centrotemporal spikes.

To define a homogeneous group of patients, we first identified the location of interictal sources for each patient using the spatiotemporal dipole modeling method (Advanced Source Analysis Software, Enschede, The Netherlands) (Scherg and Von Cramon, 1985). To define a homogeneous sample of patients for both single subject and group analyses, eleven of the twenty-one patients (9.65 ± 2.36 years) with right centrotemporal spikes were selected to form the epileptic group. Table 1 lists the characteristics of patients and controls and a summary of their EEG records. Three of the eight patients were diagnosed with attention deficit hyperactivity disorder. Fig. 1 shows the EEG dipole source localization results projected onto the MRI template and sample EEG of one of the patients.

To identify EEG portions with ocular and movement artifacts, the EEG recordings were first normalized by the Z-score transformation and then processed semi-automatically using a threshold method as it was implemented in Fieldtrip software[1] (Oostenveld et al., 2011). For each channel, EEG portions that exceeded a predefined threshold were marked and visually inspected by the experts. The threshold was set to the mean plus one standard deviation of the z-score amplitude distribution for each channel. The artifact-free eyes-closed portions of the EEG recordings were then segmented into non-overlapping 2-s epochs. In this study, all statistical comparisons were performed between controls and patients under the eyes-closed (EC) condition. To study the effect of interictal spikes on the dynamics of EEG and cortical sources during the resting state, patients were compared with controls under two conditions, EC_{NS} (eyes-closed without spike) and EC_{WS} (eyes-closed with spike). Five segments were randomly selected for each subject and condition for further analysis. The EC_{WS} EEG segments contained an average of 7 spikes as a requirement to ensure homogeneity across the patients.

[1] http://www.fieldtriptoolbox.org/tutorial/visual_artifact_rejection.

2.3. EEG spectral analysis

The absolute power spectral density for each channel and EEG segment was computed by using the multi-taper method with Slepian sequences (Jarvis and Mitra, 2001; Mitra and Pesaran, 1999) with a frequency resolution of 0.5 Hz. Multi-taper frequency method is similar to the classical Fourier transform but it is frequency specific with very good anti-frequency leakage properties (van Vugt et al., 2007). Power spectral analysis was performed using the Fieldtrip toolbox (http://www.ru.nl/donders/fieldtrip) (Oostenveld et al., 2011). To investigate homogeneity across patients and controls, we computed individual alpha frequency (IAF) as described by Klimesch (1999) and Klimesch et al. (1993). IAF was calculated as the sum of the product of the spectral power estimates and the frequency divided by the total sum of spectral power estimates within α band. This method has shown to be more robust and adequate particularly if there are multiple peaks in the α range (Klimesch, 1999).

For statistical analysis, the whole frequency range (0.5–30 Hz) was reduced into five frequency bands: δ (0.5–3.5 Hz), θ (4.0–8.0 Hz), α (8.5–13.0 Hz), β_1 (13.5–20.0 Hz) and β_2 (20.5–30 Hz), corresponding to the most common frequency bands in all epileptic patients and healthy subjects.

For each channel and each subject, the power spectrum was then averaged over all five segments. The relative power spectrum was then obtained by normalizing the power spectral density of each channel to its total power.

To reduce the spatial dimensionality of the data, we first grouped the 63 channels into 13 brain regions as shown in Fig. 2. For each region and frequency band, we reported absolute and relative spectral power. We then compared regional relative spectral powers within each frequency band between groups by computing across-subject grand average Scalp Topographic Patterns (STPs) of relative EEG spectral power (STP, ± standard deviation) for each frequency band and group. The statistical analysis was performed in each region including four electrodes on average. The group comparison was performed by the standard nonparametric paired two-way ANOVA with 5000 permutations and $p < 0.01$ (Maris and Oostenveld, 2007).

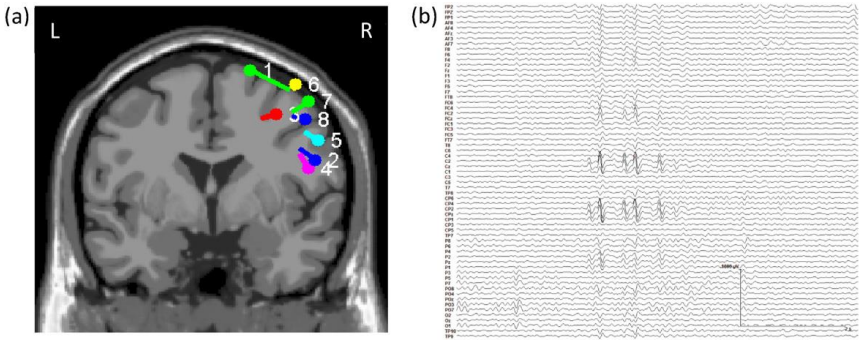

Fig. 1. (a) Dipole locations of the averaged spikes for patients, and (b) a sample EEG recording from patient 1.

2.4. EEG source distribution analysis using eLORETA

EEG cortical source analysis was performed by the functional brain imaging method known as eLORETA (exact Low-Resolution Electromagnetic Tomography), which models 3D distributions of EEG cortical sources (Grech et al., 2008; Pascual-Marqui, 2002, 1999) in the frequency domain. This method does not require a priori knowledge of dipole positions and has been successfully used in recent studies on resting state EEG analysis (Babiloni et al., 2010; Li, 2010). eLORETA is a discrete, linear, weighted minimum norm inverse solution and provides better accurate localization of highly correlated point sources with low signal to noise ratio data (Pascual-Marqui, 2007; Pascual-Marqui et al., 2011). We first used eLORETA to localize interictal spike sources for each patient to investigate the spatial extent of spike sources.

3D source localization in the frequency domain was then performed by computing the cross-spectra of EEG segments for each subject. The eLORETA algorithm was used to compute the current density (Intensity of the current/area, measured in A/m^2) for each voxel within different frequency bands. The eLORETA solution space was restricted to the cortical gray matter of a realistic head model (MNI152) coregistered to the Talairach brain atlas and digitized at the Montreal Neurologic Institute (MNI) brain imaging center (Mazziotta et al., 2001). The brain compartment included 6239 voxels (5 mm spatial resolution). Before any statistical analysis, the eLORETA solutions were normalized for each voxel at each frequency band as implemented in the eLORETA software (Pascual-Marqui, 2002). The normalization was done by normalizing the eLORETA current density at each voxel to the eLORETA current density averaged across all frequencies (0.5–30 Hz) (Babiloni et al., 2010).

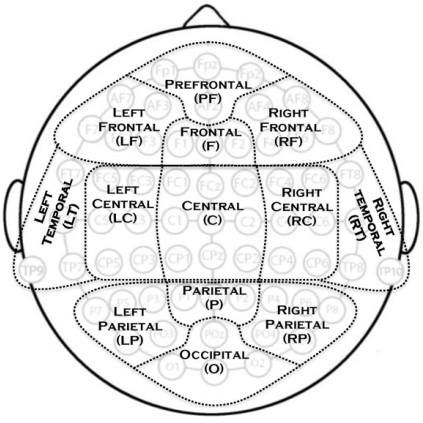

Fig. 2. Thirteen brain regions defined for statistical comparisons.

2.5. Statistical analysis of the eLORETA solutions

Statistical comparisons of cortical sources between the two groups were performed on the eLORETA current density of the voxels in all five frequency bands using the statistical nonparametric mapping approach (SnPM) via randomizations (Nichols and Holmes, 2002). The randomization determined the critical threshold values for the observed t-values with correction ($p < 0.05$) for multiple comparisons across all voxels and all frequency bands. A total of 5000 permutations were used to determine the significance level for each test. The log of F-ratios were then color-coded and projected onto the MNI152 MRI and the cortical layer of the realistic head model. The color-coded Topographic Significance Maps (TSMs) represented statistical differences in estimated cortical sources between the groups.

3. Results

For illustrative purposes, we only present STP (sensor space) and TSM (source space) with statistically distinct spatial patterns. The remaining results can be found in Supplementary Materials. The absolute power for all the conditions is shown in Table 2.

3.1. Scalp topographic patterns (STP)

Fig. 3 shows the STPs for controls and patients in the δ, θ and α bands.

Compared to controls, the patient group presented significantly higher relative EEG power values in the θ band (Fig. 3, left STP map) in right centrotemporal and bilateral frontal and parieto-occipital areas under EC_{NS} and EC_{WS} conditions. The θ power increases in all cortical regions were more pronounced when spikes were included in the EEG segments analyzed (EC_{WS} condition). In contrast, the relative α, β_1 and β_2 powers tended to decrease in homologous areas especially under the EC_{NS} condition (Figs. 3 and S1). Furthermore, relative δ power significantly decreased in right centrotemporal and bilateral frontal areas, but only in the presence of CTS. The results obtained in the sensor space are summarized in Table 2. Table 3 lists the mean and standard deviation of absolute power values for each region, frequency band and condition. As shown, patients displayed increased absolute θ power and decreased absolute α power at the parietal and

Table 2
Observed patterns of changes in relative EEG spectral power in patients compared to controls in the five frequency bands.

Frequency band	EC_{NS} condition (eyes-closed without spike)	EC_{WS} condition (eyes-closed with spike)
	Brain regions exhibiting significant changes in scalp EEG relative power	Brain regions exhibiting significant changes in scalp EEG relative power
δ (0-3.5Hz)	–	LF, RF ↓ C, RC, RT↓
θ (4-8Hz)	C, RC, RT ↑ LP, P, RP ↑	All cortical regions ↑
α (8.5-13Hz)	PF, LF, RF ↓ LT, RC↑ LP, P, RP, O↓	LP, P, RP, O↓
β_1 (13.5-20Hz)	PF↓ C, RC↓ LP, P, RP, O↓	C, RP↓
β_2 (20.5-30Hz)	PF↓ RC, C, LC↓ LP, P, RP, O↓	PF, LF, F↓ C, RC↓ LP, P, RP, O↓

The significant increase (↑) or decrease (↓) in EEG relative power was identified by statistical comparisons ($p < 0.01$) between controls and patients. See Fig. 1 for the abbreviations used for brain regions.

occipital regions especially under the EC_{WS} conditions in comparison to EC_{CT}.

The group IAF values are shown in Fig. 4. The IAF values of EC_{CT} were significantly higher than those found for both the epileptic conditions in all regions excluding the right frontal region. EC_{NS} showed was lower IAF values in comparison to EC_{WS} in almost all cortical regions.

3.1.1. Statistical comparisons of EEG cortical sources

To further investigate the impact of BECTS on the cortical sources of resting state EEG rhythms, we computed TSMs in the five frequency bands under the EC_{NS} and EC_{WS} conditions (Figs 5–7, S2–4). Fig. S5 shows the spatial extent of the distributed sources of interictal spikes localized using eLORETA and averaged across all patients. As shown, only the right centro-temporal regions are highly involved in the generation of the spikes.

Compared to controls, patients exhibited increased θ, α and β_2 activity under both conditions in the right centrotemporal regions, which are involved in the generation and propagation of the spikes. However, the spectral power increases of cortical sources were more pronounced in the presence of CTS, and were also observed in β_1 in the right centrotemporal region and its immediately surrounding regions.

In patients, the right temporo-parieto-occipital junction also showed increased θ and α activities under the EC_{NS} condition (Fig. 5). However, the presence of CTS within EEG segments increased power in higher frequencies (β_1 and β_2) in the right temporo-parieto-occipital junction (Fig. S4). Furthermore, in patients, the bilateral temporal poles displayed increased cortical activities in all five-frequency bands under both conditions. To a lesser degree, the left centrotemporal area including the insula also exhibited increased power in all bands.

Compared to controls, patients were characterized by significantly decreased power in all bands in bilateral frontal and occipital lobes, especially in the presence of CTS. Other spurious increases/decreases in the power of various bands were also observed in deeper structures (see supplementary figures).

4. Discussion

This study was the first attempt to investigate differences in the topographic distribution of EEG relative and absolute spectral power and EEG cortical sources between healthy control subjects and patients with BECTS under the eyes-closed resting state condition in five frequency bands. Our findings demonstrated that BECTS has a profound effect on the spectral power of resting state EEG activities and cortical sources by activating/deactivating cortical regions.

In the sensor space, we found significant increases in relative and absolute θ power in all brain regions especially in the epileptogenic zone in the right centrotemporal region in comparison to healthy controls. Meanwhile, the θ power decreased in frontal and occipital regions in comparison to central region of epileptic patients. This observation is consistent with results from other studies conducted on Temporal Lobe Epileptic patients (TLE) (Quraan et al., 2013). Several studies (Clemens, 2004; Clemens et al., 2000; Douw et al., 2010; Schneebaum-Sender et al., 2012) have reported enhanced θ power in children with epilepsy with and without medication in comparison to controls (Clemens et al., 2010). However, it has been shown that the increased theta power in some cerebral regions is more pronounced in epileptic patients taking anti-epileptic drugs (Béla et al., 2007; Clemens, 2008; Clemens et al., 2006; Kikumoto et al., 2006). Nevertheless, in our study the drug effect can be ruled out to explain the spectral differences between the EC_{NS} (eyes-closed without spike) and EC_{WS} (eyes-closed with spike) conditions.

Significant increases in θ, α, and β cortical sources were observed in the source space of the right centrotemporal area, the region of CTS generation, under the EC_{WS} condition. Centrotemporal spikes are known to be highly reproducible sharp waves with similar morphological characteristics, high amplitudes and durations of more than 70 ms corresponding to frequencies above the θ band (Panayiotopoulos, 1999a,b. Therefore, in our analysis, the increased relative power in frequencies

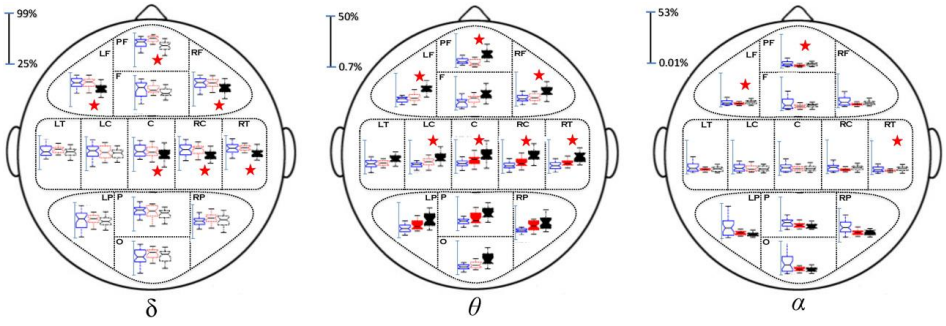

Fig. 3. Average normalized spectral power maps (±standard deviation) in the sensor space under the eyes-closed condition for the control group (ECCT, left boxplots), patient group (ECNS, no spike condition, middle boxplots) and patient group (ECWS, with spike condition, right boxplots) in δ, θ and α bands. Significant differences between ECCT and ECNS/ECWS are shown in solid boxplots. Asterisks indicate statistically significant differences ($p < 0.01$) between ECNS and ECWS.

Table 3
Absolute power (μV^2/Hz) computed for each region, frequency band and all the conditions.

Region	Freq. Band	δ mean±std	Θ mean±std	α mean±std	β_1 mean±std	β_2 mean±std
PF	EC_{CT}	0.0504±0.0013	0.0076±0.0003	0.0049±0.0008	0.0013±0.0001	0.0005±0.0000
	EC_{WS}	0.0444±0.0009	0.0135±0.0018	0.0035±0.0002	0.0001±0.0000	0.0003±0.0001
	EC_{NS}	0.0604±0.0007	0.0073± 0.0007	0.0018±0.0025	0.0008±0.0009	0.0004±0.0035
L	EC_{CT}	0.0495±0.0014	0.0072±0.0003	0.0052±0.0009	0.0016±0.0001	0.0008±0.0001
	EC_{WS}	0.04010±0.005	0.0146±0.0011	0.0040±0.0004	0.0012±0.0002	0.0004±0.0003
	EC_{NS}	0.0535±0.0074	0.0082±0.0068	0.0026±0.0028	0.0012±0.0009	0.0007±0.0005
F	EC_{CT}	0.0465±0.0022	0.0089±0.0006	0.0068±0.0011	0.0019±0.0002	0.0007±0.0001
	EC_{WS}	0.0481±0.0048	0.0167±0.0009	0.0056±0.0009	0.0022±0.0002	0.0007±0.0002
	EC_{NS}	0.0483±0.0032	0.0130±0.0010	0.0049±0.003	0.0027±0.0001	0.0012±0.0009
RF	EC_{CT}	0.0473±0.0018	0.0074±0.0004	0.0051±0.0008	0.0016±0.0001	0.0007±0.0001
	EC_{WS}	0.0425±0.0041	0.0123±0.0015	0.0044±0.0004	0.0015±0.0002	0.0006±0.0001
	EC_{NS}	0.0557±0.0021	0.0083±0.0077	0.0029±0.0034	0.0015±0.0013	0.0007±0.0001
LC	EC_{CT}	0.0390±0.0017	0.0088±0.0006	0.0088±0.0007	0.0019±0.0002	0.0007±0.0001
	EC_{WS}	0.0369±0.0051	0.0128±0.0012	0.0044±0.0007	0.0015±0.0003	0.0004±0.0001
	EC_{NS}	0.0403±0.0062	0.0102±0.0006	0.0048±0.0042	0.0015±0.0015	0.0005±0.0002
C	EC_{CT}	0.0411±0.0020	0.0097±0.0004	0.0080±0.0010	0.0017±0.0002	0.0005±0.0001
	EC_{WS}	0.0367±0.0041	0.0157±0.0011	0.0047±0.0008	0.0012±0.0002	0.0003±0.0001
	EC_{NS}	0.0382±0.0021	0.0118±0.0074	0.0039±0.0030	0.0011±0.00105	0.0003±0.0002
RC	EC_{NS}	0.0422±0.0017	0.0076±0.0004	0.0081±0.0007	0.0017±0.0002	0.0007±0.0001
	EC_{WS}	0.0381±0.0046	0.0157±0.0014	0.0055±0.0011	0.0015±0.0002	0.0003±0.0001
	EC_{NS}	0.0420±0.0037	0.0103±0.0063	0.0035±0.0031	0.0014±0.0012	0.0005±0.0004
LT	EC_{CT}	0.0460±0.0009	0.0094±0.0006	0.0079±0.0007	0.0018±0.0001	0.0007±0.0001
	EC_{WS}	0.0405±0.0033	0.0126±0.0020	0.0041±0.0005	0.0016±0.0002	0.0007±0.0001
	EC_{NS}	0.0432±0.0052	0.0111±0.0051	0.0036±0.0037	0.0018±0.0017	0.0009±0.0010
RT	EC_{CT}	0.0456±0.0016	0.0085±0.0004	0.0063±0.0006	0.0020±0.0002	0.0007±0.0001
	EC_{WS}	0.0429±0.0029	0.0149±0.0014	0.0054±0.0004	0.0016±0.0001	0.0005±0.0001
	EC_{NS}	0.0467±0.0032	0.0104±0.0082	0.0031±0.0038	0.0015±0.0011	0.0007±0.0000
LP	EC_{CT}	0.0434±0.0021	0.0101±0.0005	0.0197±0.0014	0.0023±0.0003	0.0005±0.0000
	EC_{WS}	0.0385±0.0043	0.0155±0.0016	0.0053±0.0010	0.0013±0.0003	0.0003±0.0001
	EC_{NS}	0.0422±0.0056	0.0116±0.0087	0.0048±0.0064	0.0013±0.0013	0.0003±0.0008
P	EC_{CT}	0.0370±0.0020	0.0079±0.0006	0.0109±0.0014	0.0016±0.0002	0.0004±0.0001
	EC_{WS}	0.0346±0.0023	0.0149±0.0023	0.0041±0.0008	0.0011±0.0002	0.0003±0.0000
	EC_{NS}	0.0401±0.0034	0.0129±0.0093	0.0041±0.0036	0.0011±0.0012	0.0002±0.0013
RP	EC_{CT}	0.0394±0.0015	0.0089±0.0004	0.00173±0.0017	0.0024±0.0017	0.0003±0.0003
	EC_{WS}	0.0428±0.0051	0.0153±0.0002	0.00059±0.0008	0.0014±0.0002	0.0003±0.0000
	EC_{NS}	0.0443±0.0076	0.0125±0.0028	0.00043±0.0044	0.0011±0.0012	0.0003±0.0001
O	EC_{CT}	0.0426±0.0018	0.0092±0.0007	0.0173±0.0004	0.0024±0.0005	0.0006±0.0000
	EC_{WS}	0.0435±0.0045	0.0136±0.0024	0.0064±0.0008	0.0013±0.0002	0.0003±0.0000
	EC_{NS}	0.0482±0.0056	0.0108±0.0020	0.0051±0.0008	0.0011±0.0002	0.0002±0.0000

above the θ band can be simply explained by the presence of CTS in EEG segments.

The increase in relative power of higher frequencies especially several hundred milliseconds around CTS (Bourel-Ponchel, 2013; Gotman et al., 2005) resulted in a less significant increase in the power of low frequencies (δ band). Under both conditions, in most frequency bands, similar trends of spectral changes were observed in BECTS patients, which may reflect the modulatory effect of epileptic networks on the spectral power of cortical sources regardless of the presence of CTS in the scalp EEG segments analyzed. These findings indicate that, even in the absence of CTS in the scalp EEG, the activity of epileptic networks in BECTS has a profound impact on the EEG resting activity. This finding is consistent with those reported in other resting state studies (Ciumas et al., 2014; Kim et al., 2014; Pardoe et al., 2013). However, the presence of CTS clarified spectral differences between patients and controls with a wider spatial impact within the β_1 band.

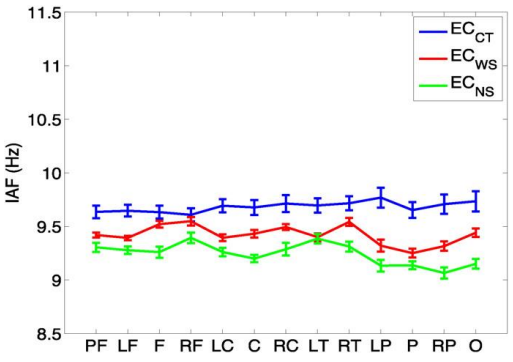

Fig. 4. Individual alpha frequency (IAF) for all the 13 regions (see Fig. 2 for abbreviations).

IAF differences between the groups may reflect decreased cognitive performances in patients as suggested in several studies (Angelakis et al., 2004; Khader et al., 2010; Klimesch et al., 1993). The lower IAF was correlated with lower power at parietal and occipital region especially under the EC_{WS} condition. This finding might explain cognitive and attention impairment in BCECTS patients (Holmes and Lenck-Santini, 2006; Metz-Lutz et al., 1999).

Another major finding of this study was the increased relative θ and α power under the EC_{NS} condition, and the increased relative α, β_1 and β_2 power under the EC_{WS} condition consistently in the right temporo-parieto-occipital (TPO) junction. This finding may suggest that the epileptic zone in BECTS impairs the right temporo-parieto-occipital region. The temporo-parieto-occipital region is believed to be involved in high level neurological functions (De Benedictis et al., 2014), especially auditory, visual, somatosensory and memory processes. Impairment of the TPO in children with epilepsy has been shown to be associated with higher activity in this region (Barba et al., 2007; Besseling et al., 2013; Hewett et al., 2011; Tang et al., 2014), which is likely to have neurobiological relevance determined by anatomical development and neurocognitive factors (Jiang et al., 2015; Tang et al., 2014). The

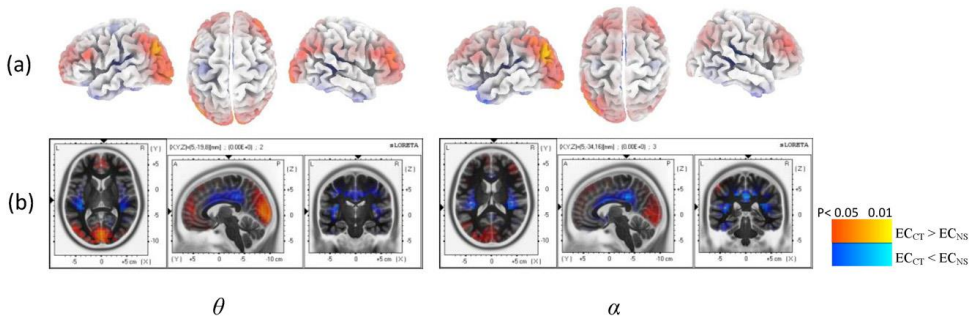

Fig. 5. Statistical maps of differences between cortical sources computed under the eyes-closed condition for the control group (EC_{CT}, left boxplots) and the patient group (EC_{NS}, no spike condition, right boxplots) in θ and α bands. The results have been projected onto the cortical layer of the realistic head model (a) and the MNI152 MRI (b). Color bars indicate significant differences between EC_{CT} and EC_{NS}, red ($EC_{CT} > EC_{NS}$) and blue ($EC_{CT} < EC_{NS}$).

disconnection or resection of TPO in children with epilepsy has been shown to increase the likelihood of alternative epilepsy treatment (Ansari et al., 2010; Mohamed et al., 2011), which may indicate the involvement of the TPO region in epileptic networks.

The bilateral increases in all bands under both conditions in the poles of the temporal lobes, known to be the regions responsible for language and speech processing, suggest possible interhemispheric synchronization in temporal regions due to CTS. Several studies (Ay et al., 2009; Baglietto et al., 2001; Kossoff et al., 2007; Liasis et al., 2006; Metz-Lutz et al., 1999; Northcott et al., 2007) have discussed the impaired visual and auditory networks and alternation of source activities at the bilateral poles of the temporal lobes in BECTS patients.

A compelling finding of the present study was the decreased activities of cortical sources in the frontal and occipital lobes in BECTS patients compared to healthy subjects in all frequency bands and conditions, notably under the EC_{WS} condition. The frontal and occipital cortical depression in BECTS patients is likely to be associated with decreased activity of the default mode network (Archer et al., 2003; Blumenfeld et al., 2004; Fahoum et al., 2013; Gotman et al., 2005; Ibrahim et al., 2014; Laufs et al., 2007; Ligot et al., 2014; Yang et al., 2014). This finding is also in line with the frontal decrease in the relative power of lower frequencies observed in the time–frequency domain several hundred milliseconds before and after centrotemporal spikes in BECTS patients (Bourel-Ponchel, 2013). The reduced activity of the prefrontal and frontal lobes might also explain some of the cognitive impairments and other brain malfunctions related to benign epilepsy (Holmes and Lenck-Santini, 2006; Weglage et al., 1997), as it has been shown that any dysfunction in this region in childhood is likely to affect cognitive development (Badre et al., 2009; Stuss and Alexander, 2000).

Certain discrepancies between the topographic distribution of scalp EEG relative spectral power (in the sensor space) and the spatial distribution of cortical sources (in the source space) in different frequency bands were observed in this study. In our study, the increased or decreased cortical activities in various frequency bands estimated by means of the eLORETA approach were not expected to exactly follow the same spatial pattern of the spectral changes obtained using power spectrum analysis in the sensor space. The discrepancies can be explained by methodological differences between the approaches. Our STP maps were obtained by averaging the relative power values over groups of electrodes in each of 13 regions, while eLORETA maps were t-maps generated from statistical analysis of all 6234 voxels, whose source activities were estimated using all electrodes. *Frequency-domain eLORETA* generally provides better results for EEG resting analysis because the estimated neuronal generator distribution, when using this approach, does not depend on the polarity of the scalp EEG maps (Pascual-Marqui, 2014).

A potential limitation of our study is the sample size. For the thirteen cerebral regions, we computed the minimum sample size (Freedman et al., 2001) with the statistical power of 80%. The average sample size required for performing statistical comparisons between the groups was about 7 which was less than the sample sizes (eleven patients and twelve controls) set in our study.

Our overall findings indicate that, in addition to the dysfunction of the right centrotemporal region, which is the epileptic focus, cortical depression of frontal and occipital regions may show resting network

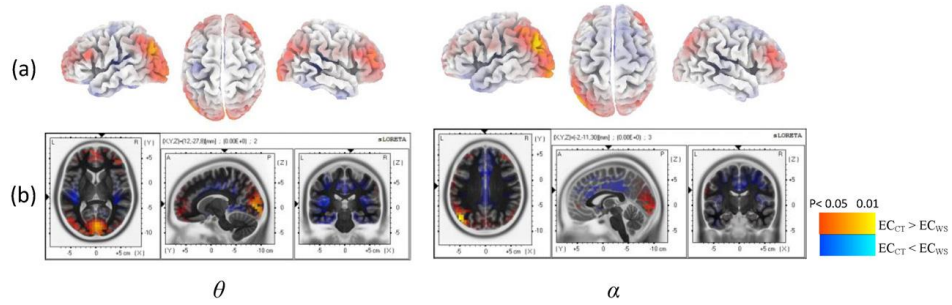

Fig. 6. Statistical maps of differences between cortical sources computed under the eyes-closed condition for the control group (EC_{CT}, left boxplots) and patient group (EC_{WS}, with spike condition, right boxplots) in θ and α bands. The results have been projected onto the cortical layer of the realistic head model (a) and the MNI152 MRI (b). Color bars indicate significant differences between EC_{CT} and EC_{WS}, red ($EC_{CT} > EC_{WS}$) and blue ($EC_{CT} < EC_{WS}$).

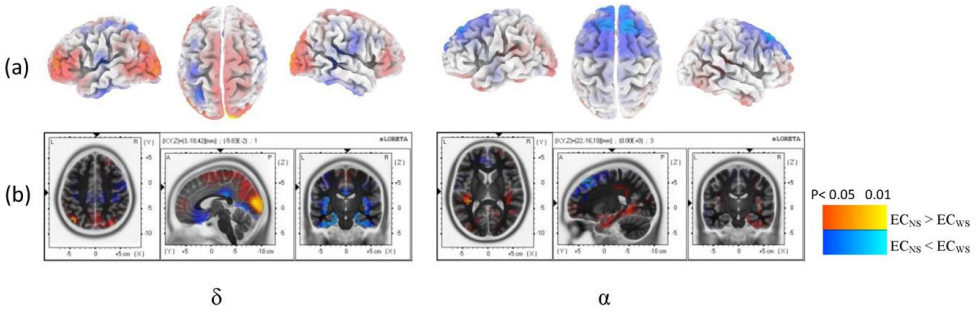

Fig. 7. Statistical maps of differences between cortical sources computed under the no-spike (EC_{NS}, left boxplots) and with-spike (EC_{WS}, right boxplots) eyes-closed conditions in δ and α bands for the epileptic group. The results have been projected onto the cortical layer of the realistic head model (a) and the MNI152 MRI (b). Color bars indicate significant differences between EC_{NS} and EC_{WS}, red ($EC_{ns} > EC_{WS}$) and blue ($EC_{NS} > EC_{WS}$).

disruption in benign childhood epilepsy with centrotemporal spikes. These findings encourage further investigation into the impact of BECTS on the resting state networks.

Appendix A. Supplementary data

Supplementary data associated with this article can be found online at http://dx.doi.org/10.1016/j.nicl.2015.08.014.

References

Angelakis, E., Lubar, J.F., Stathopoulou, S., Kounios, J., 2004. Peak alpha frequency: an electroencephalographic measure of cognitive preparedness. Clin. Neurophysiol. Off. J. Int. Fed. Clin. Neurophysiol. 115 (4), 887–897. http://dx.doi.org/10.1016/j.clinph.2003.11.03415003770.

Ansari, S.F., Maher, C.O., Tubbs, R.S., Terry, C.L., Cohen-Gadol, A.A., 2010. Surgery for extratemporal nonlesional epilepsy in children: a meta-analysis. Childs Nerv. Syst. ChNS Off. J. Int. Soc. Pediatr. Neurosurg. 26 (7), 945–951. http://dx.doi.org/10.1007/s00381-009-1056-720013124.

Archer, J.S., Abbott, D.F., Waites, A.B., Jackson, G.D., 2003. fMRI "deactivation" of the posterior cingulate during generalized spike and wave. NeuroImage 20 (4), 1915–1922. http://dx.doi.org/10.1016/S1053-8119(03)00294-514683697.

Ay, Y., Gokben, S., Serdaroglu, G., Polat, M., Tosun, A., Tekgul, H., Solak, U., Kesikci, H., 2009. Neuropsychologic impairment in children with rolandic epilepsy. Pediatr. Neurol. 41 (5), 359–363. http://dx.doi.org/10.1016/j.pediatrneurol.2009.05.01319818938.

Babiloni, C., Pistoia, F., Sarà, M., Vecchio, F., Buffo, P., Conson, M., Onorati, P., Albertini, G., Rossini, P.M., 2010. Resting state eyes-closed cortical rhythms in patients with locked-in-syndrome: an EEG Study. Clin. Neurophysiol. Off. J. Int. Fed. Clin. Neurophysiol. 121 (11), 1816–1824. http://dx.doi.org/10.1016/j.clinph.2010.04.02720541461.

Badre, D., Hoffman, J., Cooney, J.W., D'Esposito, M., 2009. Hierarchical cognitive control deficits following damage to the human frontal lobe. Nat. Neurosci. 12 (4), 515–522. http://dx.doi.org/10.1038/nn.227719252496.

Baglietto, M.G., Battaglia, F.M., Nobili, L., Tortorelli, S., De Negri, E., Calevo, M.G., Veneselli, E., De Negri, M., 2001. Neuropsychological disorders related to interictal epileptic discharges during sleep in benign epilepsy of childhood with centrotemporal or rolandic spikes. Dev. Med. Child Neurol. 43 (6), 407–412. http://dx.doi.org/10.1017/S0012162201000755114098330.

Barba, C., Barbati, G., Minotti, L., Hoffmann, D., Kahane, P., 2007. Ictal clinical and scalp-EEG findings differentiating temporal lobe epilepsies from temporal "plus" epilepsies. Brain J. Neurol. 130 (7), 1957–1967. http://dx.doi.org/10.1093/brain/awm10817535836.

Béla, C., Mónika, B., Márton, T., István, K., 2007. Valproate selectively reduces EEG activity in anterior parts of the cortex in patients with idiopathic generalized epilepsy. A low resolution electromagnetic tomography (LORETA) study. Epilepsy Res. 75 (2–3), 186–191. http://dx.doi.org/10.1016/j.eplepsyres.2007.06.00917624734.

Besseling, R.M.H., Jansen, J.F.A., Overvliet, G.M., van der Kruijs, S.J.M., Vles, J.S.H., Ebus, S.C.M., Hofman, P.A.M., de Louw, A., Aldenkamp, A.P., Backes, W.H., 2013. Reduced functional integration of the sensorimotor and language network in rolandic epilepsy. Neuroimage Clin. 2, 239–246. http://dx.doi.org/10.1016/j.nicl.2013.01.00424179777.

Blom, S., Brorson, L.O., 1966. Central spikes or Sharp waves (Rolandic spikes) in children's EEG and their clinical significance. Acta Paediatr Scand 55 (4), 385–393. http://dx.doi.org/10.1111/j.1651-2227.1966.tb08809.x5966338.

Blumenfeld, H., McNally, K.A., Vanderhill, S.D., Paige, A.L., Chung, R., Davis, K., Norden, A.D., Stokking, R., Studholme, C., Novotny, E.J., Zubal, I.G., Spencer, S.S., 2004. Positive and negative network correlations in temporal lobe epilepsy. Cereb. Cortex 14 (8), 892–902. http://dx.doi.org/10.1093/cercor/bhh04815084494.

Bocquillon, P., Dujardin, K., Betrouni, N., Phalempin, V., Houdayer, E., Bourriez, J.-L., Derambure, P., Szurhaj, W., 2009. Attention impairment in temporal lobe epilepsy: a neurophysiological approach via analysis of the P300 wave. Hum. Brain Mapp. 30 (7), 2267–2277. http://dx.doi.org/10.1002/hbm.2066619034898.

Bourel-Ponchel, E., 2013. Exploration de l'unité neurovasculaire dans l'épilepsie de l'enfant: approche multimodale haute densité couplant l'EEG à l'imagerie optique fonctionnelle. Amiens.

Camfield, C.S., Berg, A., Stephani, U., Wirrell, E.C., 2014. Transition issues for benign epilepsy with centrotemporal spikes, nonlesional focal epilepsy in otherwise normal children, childhood absence epilepsy, and juvenile myoclonic epilepsy. Epilepsia 55 (Suppl. 3), 16–20. http://dx.doi.org/10.1111/epi.1270625209080.

Cataldi, M., Avoli, M., de Villers-Sidani, E., 2013. Resting state networks in temporal lobe epilepsy. Epilepsia 54 (12), 2048–2059. http://dx.doi.org/10.1111/epi.1240024117098.

Ciumas, C., Saignavongs, M., Ilski, F., Herbillon, V., Laurent, A., Lothe, A., Heckemann, R.A., de Bellescize, J., Panagiotakaki, E., Hannoun, S., Marinier, D.S., Montavont, A., Ostrowsky-Coste, K., Bedoin, N., Ryvlin, P., 2014. White matter development in children with benign childhood epilepsy with centro-temporal spikes. Brain J. Neurol. 137 (4), 1095–1106. http://dx.doi.org/10.1093/brain/awu03924598359.

Clemens, B., 2004. Pathological theta oscillations in idiopathic generalised epilepsy. Clin. Neurophysiol. 115 (6), 1436–1441. http://dx.doi.org/10.1016/j.clinph.2004.01.01815134712.

Clemens, B., 2008. Valproate decreases EEG synchronization in a use-dependent manner in idiopathic generalized epilepsy. Seizure 17 (3), 224–233. http://dx.doi.org/10.1016/j.seizure.2007.07.00517697790.

Clemens, B., Bessenyei, M., Fekete, I., Puskás, S., Kondákor, I., Tóth, M., Hollódy, K., 2010. Theta EEG source localization using LORETA in partial epilepsy patients with and without medication. Clin. Neurophysiol. Off. J. Int. Fed. Clin. Neurophysiol. 121 (6), 848–858. http://dx.doi.org/10.1016/j.clinph.2010.01.02020181513.

Clemens, B., Majoros, E., 1987. Sleep studies in benign epilepsy of childhood with rolandic spikes. II. Analysis of discharge frequency and its relation to sleep dynamics. Epilepsia 28 (1), 24–27.

Clemens, B., Ménes, A., Piros, P., Bessenyei, M., Altmann, A., Jerney, J., Kollár, K., Rosdy, B., Rózsavölgyi, M., Steinecker, K., Hollódy, K., 2006. Quantitative EEG effects of carbamazepine, oxcarbazepine, valproate, lamotrigine, and possible clinical relevance of the findings. Epilepsy Res. 70 (2–3), 190–199. http://dx.doi.org/10.1016/j.eplepsyres.2006.05.00316765028.

Clemens, B., Szigeti, G., Barta, Z., 2000. EEG frequency profiles of idiopathic generalised epilepsy syndromes. Epilepsy Res. 42 (2–3), 105–115. http://dx.doi.org/10.1016/S0920-1211(00)00167-411074183.

De Benedictis, A., Duffau, H., Paradiso, B., Grandi, E., Balbi, S., Granieri, E., Colarusso, E., Chioffi, F., Marras, C.E., Sarubbo, S., 2014. Anatomo-functional study of the temporo-parieto-occipital region: dissection, tractographic and brain mapping evidence from a neurosurgical perspective. J. Anat. 225 (2), 132–151. http://dx.doi.org/10.1111/joa.122042497542 1.

Douw, L., van Dellen, E., de Groot, M., Heimans, J.J., Klein, M., Stam, C.J., Reijneveld, J.C., 2010. Epilepsy is related to theta band brain connectivity and network topology in brain tumor patients. B.M.C. Neurosci. 11, 103. http://dx.doi.org/10.1186/1471-2202-11-10320731854.

Fahoum, F., Zelmann, R., Tyvaert, L., Dubeau, F., Gotman, J., 2013. Epileptic discharges affect the default mode network – fMRI and intracerebral EEG evidence. PLOS One 8 (6), e68038. http://dx.doi.org/10.1371/journal.pone.0068038.

Freedman, K.B., Back, S., Bernstein, J., 2001. Sample size and statistical power of randomised, controlled trials in orthopaedics. J. Bone Joint Surg. Br. 83 (3), 397–402. http://dx.doi.org/10.1302/0301-620X.83B3.1058211341427.

Gotman, J., Grova, C., Bagshaw, A., Kobayashi, E., Aghakhani, Y., Dubeau, F., 2005. Generalized epileptic discharges show thalamocortical activation and suspension of the default state of the brain. Proc. Natl. Acad. Sci. U. S. A. 102 (42), 15236–15240. http://dx.doi.org/10.1073/pnas.05049351021621704 2.

Grech, R., Cassar, T., Muscat, J., Camilleri, K.P., Fabri, S.G., Zervakis, M., Xanthopoulos, P., Sakkalis, V., Vanrumste, B., 2008. Review on solving the inverse problem in EEG source analysis. J. Neuroengineering Rehabil. 5, 25. http://dx.doi.org/10.1186/1743-0003-5-2518990257.

Gregory, D.L., Wong, P.K., 1992. Clinical relevance of a dipole field in rolandic spikes. Epilepsia 33 (1), 36–44. http://dx.doi.org/10.1111/j.1528-1157.1992.tb02280.x1370800.
Hewett, R., Guye, M., Gavaret, M., Bartolomei, F., 2011. Benign temporo-parieto-occipital junction epilepsy with vestibular disturbance: an underrecognized form of epilepsy? Epilepsy Behav. E B 21 (4), 412–416. http://dx.doi.org/10.1016/j.yebeh.2011.05.01721704564.
Holmes, G.L., Lenck-Santini, P.-P., 2006. Role of interictal epileptiform abnormalities in cognitive impairment. Epilepsy Behav. E B 8 (3), 504–515. http://dx.doi.org/10.1016/j.yebeh.2005.11.01416540376.
Ibrahim, G.M., Morgan, B.R., Lee, W., Smith, M.L., Donner, E.J., Wang, F., Beers, C.A., Federico, P., Taylor, M.J., Doesburg, S.M., Rutka, J.T., Snead, O.C., 2014. Impaired development of intrinsic connectivity networks in children with medically intractable localization-related epilepsy. Hum. Brain Mapp. 35 (11), 5686–5700. http://dx.doi.org/10.1002/hbm.2258024976288.
Jarvis, M.R., Mitra, P.P., 2001. Sampling properties of the spectrum and coherency of sequences of action potentials. Neural Comput. 13 (4), 717–749. http://dx.doi.org/10.1162/089976601300014312115555666.
Jiang, L., Xu, T., He, Y., Hou, X.-H., Wang, J., Cao, X.-Y., Wei, G.-X., Yang, Z., He, Y., Zuo, X.-N., 2015. Toward neurobiological characterization of functional homogeneity in the human cortex: regional variation, morphological association and functional covariance network organization. Brain Struct. Funct. 220 (5), 2485–2507. http://dx.doi.org/10.1007/s00429-014-0795-824903825.
Jung, K.-Y., Kim, J.-M., Kim, D.W., 2003. Patterns of interictal spike propagation across the central sulcus in benign rolandic epilepsy. Clin. E.E.G. Electroencephalogr. 34 (3), 153–15714521277.
Khader, P.H., Jost, K., Ranganath, C., Rösler, F., 2010. Theta and alpha oscillations during working-memory maintenance predict successful long-term memory encoding. Neurosci. Lett. 468 (3), 339–343. http://dx.doi.org/10.1016/j.neulet.2009.11.02819922772.
Kikumoto, K., Yoshinaga, H., Oka, M., Ito, M., Endoh, F., Akiyama, T., Ohtsuka, Y., 2006. EEG and seizure exacerbation induced by carbamazepine in Panayiotopoulos syndrome. Epileptic Disord. Int. Epilepsy J. Videotape 8 (1), 53–5616567326.
Kim, S.E., Lee, J.H., Chung, H.K., Lim, S.M., Lee, H.W., 2014. Alterations in white matter microstructures and cognitive dysfunctions in benign childhood epilepsy with centrotemporal spikes. Eur. J. Neurol. 21 (5), 708–717. http://dx.doi.org/10.1111/ene.1230124330132.
Klimesch, W., 1999. EEG alpha and theta oscillations reflect cognitive and memory performance: a review and analysis. Brain Res. Brain Res. Rev. 29 (2–3), 169–195. http://dx.doi.org/10.1016/S0165-0173(98)00056-310209231.
Klimesch, W., Schimke, H., Pfurtscheller, G., 1993. Alpha frequency, cognitive load and memory performance. Brain Topogr. 5 (3), 241–251. http://dx.doi.org/10.1007/BF011289918507550.
Kossoff, E.H., Los, J.G., Boatman, D.F., 2007. A pilot study transitioning children onto levetiracetam monotherapy to improve language dysfunction associated with benign rolandic epilepsy. Epilepsy Behav. E B 11 (4), 514–517. http://dx.doi.org/10.1016/j.yebeh.2007.07.01117936689.
Laufs, H., Hamandi, K., Salek-Haddadi, A., Kleinschmidt, A.K., Duncan, J.S., Lemieux, L., 2007. Temporal lobe interictal epileptic discharges affect cerebral activity in "default mode" brain regions. Hum. Brain Mapp. 28 (10), 1023–1032. http://dx.doi.org/10.1002/hbm.2032317133385.
Legarda, S., Jayakar, P., Duchowny, M., Alvarez, L., Resnick, T., 1994. Benign rolandic epilepsy: high central and low central subgroups. Epilepsia 35 (6), 1125–1129. http://dx.doi.org/10.1111/j.1528-1157.1994.tb01777.x7988499.
Li, L., 2010. The differences among eyes-closed, eyes-open and attention States: an EEG study. 6th International Conference on Wireless Communications Networking and Mobile Computing (WiCOM), 23–25 September, 2010, pp. 1–4 http://dx.doi.org/10.1109/WICOM.2010.5600726.
Liasis, A., Bamiou, D.E., Boyd, S., Towell, A., 2006. Evidence for a neurophysiologic auditory deficit in children with benign epilepsy with centro-temporal spikes. J Neural Transm 113 (7), 939–949. http://dx.doi.org/10.1007/s00702-005-0357-616252074.
Ligot, N., Archambaud, F., Trotta, N., Goldman, S., Van Bogaert, P., Chiron, C., De Tiège, X., 2014. Default mode network hypometabolism in epileptic encephalopathies with CSWS. Epilepsy Res. 108 (5), 861–871. http://dx.doi.org/10.1016/j.eplepsyres.2014.03.01424746674.
Loiseau, P., 2001. Benign childhood partial seizures and related epileptic syndromes. J. R. Soc. Med. 94, 651.
Loiseau, P., Beaussart, M., 1973. The seizures of benign childhood epilepsy with rolandic paroxysmal discharges. Epilepsia 14 (4), 381–389. http://dx.doi.org/10.1111/j.1528-1157.1973.tb03977.x4521094.
Lopes, A.F., Monteiro, J.P., Fonseca, M.J., Robalo, C., Simões, M.R., 2014. Memory functioning in children with epilepsy: frontal lobe epilepsy, childhood absence epilepsy, and benign epilepsy with centrotemporal spikes. Behav. Neurol. 2014, 218637. http://dx.doi.org/10.1155/2014/21863725157201.
Maris, E., Oostenveld, R., 2007. Nonparametric statistical testing of EEG- and MEG-data. J. Neurosci. Methods 164 (1), 177–190. http://dx.doi.org/10.1016/j.jneumeth.2007.03.02417517438.
Mazziotta, J., Toga, A., Evans, A., Fox, P., Lancaster, J., Zilles, K., Woods, R., Paus, T., Simpson, G., Pike, B., Holmes, C., Collins, L., Thompson, P., MacDonald, D., Iacoboni, M., Schormann, T., Amunts, K., Palomero-Gallagher, N., Geyer, S., Parsons, L., Narr, K., Kabani, N., Le Goualher, G., Feidler, J., Smith, K., Boomsma, D., Hulshoff Pol, H., Cannon, T., Kawashima, R., Mazoyer, B., 2001. A four-dimensional probabilistic atlas of the human brain. J. Am. Med. Inform. Assoc. 8 (5), 401–430. http://dx.doi.org/10.1136/jamia.2001.008040111522763.
Metz-Lutz, M.N., Kleitz, C., de Saint Martin, A., Massa, R., Hirsch, E., Marescaux, C., 1999. Cognitive development in benign focal epilepsies of childhood. Dev. Neurosci. 21 (3–5), 182–19010575241.
Mitra, P.P., Pesaran, B., 1999. Analysis of dynamic brain imaging data. Biophys. J. 76 (2), 691–708. http://dx.doi.org/10.1016/S0006-3495(99)77236-X9929474.
Mohamed, A.R., Freeman, J.L., Maixner, W., Bailey, C.A., Wrennall, J.A., Harvey, A.S., 2011. Temporoparietooccipital disconnection in children with intractable epilepsy. J. Neurosurg. Pediatr. 7 (6), 660–670. http://dx.doi.org/10.3171/2011.4.PEDS1045421631206.
Nichols, T.E., Holmes, A.P., 2002. Nonparametric permutation tests for functional neuroimaging: a primer with examples. Hum. Brain Mapp. 15 (1), 1–25. http://dx.doi.org/10.1002/hbm.105811747097.
Northcott, E., Connolly, A.M., Berroya, A., McIntyre, J., Christie, J., Taylor, A., Bleasel, A.F., Lawson, J.A., Bye, A.M.E., 2007. Memory and phonological awareness in children with benign rolandic epilepsy compared to a matched control group. Epilepsy Res. 75 (1), 57–62. http://dx.doi.org/10.1016/j.eplepsyres.2007.04.00417531444.
Oostenveld, R., Fries, P., Maris, E., Schoffelen, J.-M., 2011. FieldTrip: open source software for advanced analysis of MEG, EEG, and invasive electrophysiological data. Comput. Intell. Neurosci. 2011, e156869. http://dx.doi.org/10.1155/2011/15686921253357.
Panayiotopoulos, C.P., 1999a. Early-onset benign childhood occipital seizure susceptibility syndrome: a syndrome to recognize. Epilepsia 40 (5), 621–630. http://dx.doi.org/10.1111/j.1528-1157.1999.tb05565.x10386532.
Panayiotopoulos, C.P., 1999b. Benign Childhood Partial Seizures and Related Epileptic Syndromes. John Libbey Eurotext.
Panayiotopoulos, C.P., Michael, M., Sanders, S., Valeta, T., Koutroumanidis, M., 2008. Benign childhood focal epilepsies: assessment of established and newly recognized syndromes. Brain 131 (9), 2264–2286. http://dx.doi.org/10.1093/brain/awn16218718967.
Pardoe, H.R., Berg, A.T., Archer, J.S., Fulbright, R.K., Jackson, G.D., 2013. A neurodevelopmental basis for BECTS: evidence from structural MRI. Epilepsy Res. 105 (1–2), 133–139. http://dx.doi.org/10.1016/j.eplepsyres.2012.11.00823375559.
Pascual-Marqui, R.D., 1999. Review of methods for solving the EEG inverse problem. Int. J Bioelectromagn 1, pp. 75–86.
Pascual-Marqui, R.D., 2002. Standardized low-resolution brain electromagnetic tomography (sLORETA): technical details. Methods Find. Exp. Clin. Pharmacol. 24 (Suppl. D), 5–12125575463.
Pascual-Marqui, R.D., 2007. Discrete, 3D distributed, linear imaging methods of electric neuronal activity. Part 1: exact, zero error localization ArXiv07103341 (Math-Ph) Physics) Q-Bio.
Pascual-Marqui, R.D., Lehmann, D., Koukkou, M., Kochi, K., Anderer, P., Saletu, B., Tanaka, H., Hirata, K., John, E.R., Prichep, L., Biscay-Lirio, R., Kinoshita, T., 2011. Assessing interactions in the brain with exact low-resolution electromagnetic tomography. Philos. Transactions A Math. Phys. Eng. Sci. 369 (1952), 3768–3784. http://dx.doi.org/10.1098/rsta.2011.00812189352 7.
Pascual-Marqui, R.D., 2014. The Resting Microstate Networks (RMN): Cortical Distributions, Dynamics, and Frequency Specific Information Flow [arXiv:1411.1949v2].
Quraan, M.A., McCormick, C., Cohn, M., Valiante, T.A., McAndrews, M.P., 2013. Altered resting state brain dynamics in temporal lobe epilepsy can be observed in spectral power, functional connectivity and graph theory metrics. PLOS One 8 (7), e68609. http://dx.doi.org/10.1371/journal.pone.006860923922658.
Scherg, M., Von Cramon, D., 1985. Two bilateral sources of the late AEP as identified by a spatio-temporal dipole model. Electroencephalogr Clin Neurophysiol 62 (1), 32–44. http://dx.doi.org/10.1016/0168-5597(85)90033-42578376.
Schneebaum-Sender, N., Goldberg-Stern, H., Fattal-Valevski, A., Kramer, U., 2012. Does a normalizing electroencephalogram in benign childhood epilepsy with centrotemporal spikes abort attention deficit hyperactivity disorder? Pediatr. Neurol. 47 (4), 279–283. http://dx.doi.org/10.1016/j.pediatrneurol.2012.06.00922964442.
Shields, W.D., Snead, O.C., 2009. Benign epilepsy with centrotemporal spikes. Epilepsia 50 (Suppl. 8), 10–15. http://dx.doi.org/10.1111/j.1528-1167.2009.02229.x19702727.
Smith, J., Kellaway, P., 1964. Central (rolandic) foci in children: an analysis of 200 cases. Electroencephalogr. Clin. Neurophysiol. 17, 460–461.
Stuss, D.T., Alexander, M.P., 2000. Executive functions and the frontal lobes: a conceptual view. Psychol. Res. 63 (3–4), 289–298. http://dx.doi.org/10.1007/s004269900007 11004882.
Tang, Y.-L., Ji, G.-J., Yu, Y., Wang, J., Wang, Z.-J., Zang, Y.-F., Liao, W., Ding, M.-P., 2014. Altered regional homogeneity in rolandic epilepsy: a resting-state fMRI study. BioMed Res. Int. 2014, e960395. http://dx.doi.org/10.1155/2014/96039525247197.
Tsai, M.L., Hung, K.L., 1998. Topographic mapping and clinical analysis of benign childhood epilepsy with centrotemporal spikes. Brain Dev. 20 (1), 27–32. http://dx.doi.org/10.1016/S0387-7604(97)00089-29533557.
van Vugt, M.K., Sederberg, P.B., Kahana, M.J., 2007. Comparison of spectral analysis methods for characterizing brain oscillations. J. Neurosci. Methods 162 (1–2), 49–63. http://dx.doi.org/10.1016/j.jneumeth.2006.12.00417292478.
Verrotti, A., Filippini, M., Matricardi, S., Agostinelli, M.F., Gobbi, G., 2014. Memory impairment and benign epilepsy with centrotemporal spike (BECTS): a growing suspicion. Brain Cogn. 84 (1), 123–131. http://dx.doi.org/10.1016/j.bandc.2013.11.01424362071.
Weglage, J., Demsky, A., Pietsch, M., Kurlemann, G., 1997. Neuropsychological, intellectual, and behavioral findings in patients with centrotemporal spikes with and without seizures. Dev. Med. Child Neurol. 39 (10), 646–651. http://dx.doi.org/10.1111/j.1469-8749.1997.tb07357.x9352724.
Yang, T., Fang, Z., Ren, J., Xiao, F., Li, Q., Liu, L., Lei, D., Gong, Q., Zhou, D., 2014. Altered spontaneous activity in treatment-naive childhood absence epilepsy revealed by regional homogeneity. J. Neurol. Sci. 340 (1–2), 58–62. http://dx.doi.org/10.1016/j.jns.2014.02.02524746024.

One of the major problems with the EEG spectral power analysis in the sensor space was the volume conduction effect. Also, scalp EEG reference may introduce spurious synchrony (Nunez et al., 1997) making the sensor-space analysis and interpretation more difficult. This problem still persists in the source space (van den Broek et al., 1998). On the other hand, spectral power analysis in the source and sensor spaces are univariate analyses that only show changes in brain activity at the single-channel or voxel level.

The interaction between brain regions are analyzed by bivariate and multivariate functional connectivity analyses. Functional connectivity refers to the functional relationship between spatially separated brain regions and has been applied to several studies including epilepsy (Centeno and Carmichael, 2014). The characterization of the dynamics of cortical networks in EEG and Electrocorticography (ECoG) in epileptic patients during the resting state has demonstrated disruptions in global and regional brain networks (Douw et al., 2010a, 2010b; Quraan et al., 2013). The functional connectivity of human brain networks is often characterized with the graph theory (Rubinov and Sporns, 2010). A large number of graph theory metrics has been used in epilepsy studies such as degree, or other metrics used for characterizing functional segregation, integration and modularity of the brain networks (Fallani et al., 2014; Stam, 2014).

4.3 EEG functional connectivity and graph theory

Introduction

In the previous studies, the functional connectivity analysis was performed to explore functional alteration of the brain networks in BCECTS patients in comparison to healthy controls. This was done using EEG segments with/without interictal discharges in the sensor and source spaces to investigate the impact of interictal epileptic discharges on functional interactions between brain networks in BCECTS patients. In the first study, phase locking value (PLV) (Lachaux et al., 1999) was applied to the scalp EEG to estimate functional connectivity. The functional connectivity in the second study was estimated by the lagged phase synchronization (Pascual-Marqui, 2007) in the source space with 84 brain regions defined by the Brodmann atlas (Brodmann, 1909). LPS has been shown to be less sensitive to non-physiological signals and volume conduction artifacts (Pascual-Marqui et al., 2011).

Both PLV and LPS measured phase synchronization by computing relative phase difference between two electrodes or brain regions. However, PLV like spectral coherence measure zero-lag connectivity and are developed based on scalp electrodes and therefore sensitive to volume conduction. PLV is one of the common functional connectivity measures used extensively for the correlation between EEG electrodes. Unlike PLV, LPS is non-zero lag connectivity and was developed and implemented in eLORETA(Pascual-Marqui et al., 2011)

academic software that was used for this study. LPS removes confounding effect of instantaneous dependencies by removing zero-lag contribution due to volume conduction and low spatial resolution which makes LPS adequate measure of electrophysiological connectivity.

The functional connectivity in both sensor and source spaces were characterized with graph metrics. The network centrality was measured by the degree, functional segregation by clustering coefficient and functional integration by characteristic path length or global efficiency. The was aimed to investigate both local and global connectivity in epileptic patients in comparison to healthy controls.

In the sensor space, patients were characterized with higher connection density at the epileptic zone in all frequency bands. Lower connection density was also observed at the frontal and posterior region with or without IEDs. The BCECTS brain network showed deviations from small-word features in comparison to the healthy controls in a frequency dependent manner. The BCECTS brain networks were more functionally ordered in the presence of IEDs compared to healthy controls. However, in the absence of IEDs, BCECTS brain networks were less ordered compared to the healthy controls in all frequency bands (see the following paper for more details)[2].

[2] Supplementary information in Appendix A

PLOS ONE

RESEARCH ARTICLE

Functional Brain Dysfunction in Patients with Benign Childhood Epilepsy as Revealed by Graph Theory

Azeez Adebimpe[1], Ardalan Aarabi[1]*, Emilie Bourel-Ponchel[1,2], Mahdi Mahmoudzadeh[1,2], Fabrice Wallois[1,2]

1 Institut National de la Santé et de la Recherche Médicale (INSERM U1105), Centre Universitaire de Recheche en Santé (CURS), University Hospital, Amiens, France, **2** Explorations Fonctionnelles du Système Nerveux (EFSN) pédiatrique, University Hospital, Amiens, France

* ardalan.aarabi@u-picardie.fr

Citation: Adebimpe A, Aarabi A, Bourel-Ponchel E, Mahmoudzadeh M, Wallois F (2015) Functional Brain Dysfunction in Patients with Benign Childhood Epilepsy as Revealed by Graph Theory. PLoS ONE 10(10): e0139228. doi:10.1371/journal.pone.0139228

Editor: Bin He, University of Minnesota, UNITED STATES

Received: June 8, 2015

Accepted: September 10, 2015

Published: October 2, 2015

Data Availability Statement: Patient data (EEG recordings) used for this publication contain confidential information and therefore cannot be shared. Essential analysis subroutines written in Matlab can be obtained from the first authors on request, ardalan.aarabi@u-picardie.fr.

Funding: The fund is from INSERM (Institut national de la santé et de la recherche médicale, www.inserm.fr). The funders had no role in study design, data collection and analysis, decision to publish, or preparation of the manuscript.

Abstract

There is growing evidence that brain networks are altered in epileptic subjects. In this study, we investigated the functional connectivity and brain network properties of benign childhood epilepsy with centrotemporal spikes using graph theory. Benign childhood epilepsy with centrotemporal spikes is the most common form of idiopathic epilepsy in young children under the age of 16 years. High-density EEG data were recorded from patients and controls in resting state with eyes closed. Data were preprocessed and spike and spike-free segments were selected for analysis. Phase locking value was calculated for all paired combinations of channels and for five frequency bands (δ, θ, α, β_1 and β_2). We computed the degree and small-world parameters—clustering coefficient (C) and path length (L)—and compared the two patient conditions to controls. A higher degree at epileptic zones during interictal epileptic spikes (IES) was observed in all frequency bands. Both patient conditions reduced connection at the occipital and right frontal regions close to the epileptic zone in the α band. The "small-world" features (high C and short L) were deviated in patients compared to controls. A changed from an ordered network in the δ band to a more randomly organized network in the α band was observed in patients compared to healthy controls. These findings show that the benign epileptic brain network is disrupted not only at the epileptic zone, but also in other brain regions especially frontal regions.

Introduction

Benign childhood epilepsy with centrotemporal spikes (BCECTS) is the most common childhood epilepsy syndrome, usually affecting the children under the age of 16 years [1,2]. Several studies have demonstrated different cognitive impairments [3] including frontal dysfunction [4] in patients with benign epilepsy with no evidence of large structural changes compared to other forms of epilepsy [5,6]. However, all forms of epilepsy are associated with abnormal brain activity and impaired neural processing as a result of unstable brain dynamics and

Competing Interests: The authors have declared that no competing interests exist.

networks [7]. Dynamic changes of epileptic brain networks are believed to be caused by dysregulation of neurotransmitters leading to abnormal electrical activity [8].

Abnormal synchronization of neurons, probably due to changes in the spatial organization of the neural networks, is also thought to contribute to the generation and propagation of epileptic seizures [9]. Graph theory is a promising mathematical approach to study topological characteristics of both local and long distance brain functional connectivity using fMRI, EEG and MEG [10–12]. Graph analysis of brain connectivity has revealed reconfiguration of both structural and functional connections between different neural networks in several brain disorders [13]. Few studies have compared the resting state of healthy controls to that of epileptic patients at network level [14]. The characterization of the dynamics of the cortical networks in scalp EEG and electrocorticography (ECoG) in epileptic patients during the resting state has demonstrated disruptions in global and regional brain networks [15–17].

A large number of graph metrics have been proposed, two of which, clustering coefficient and path length [18], have been mostly used to characterize the functional connectivity of human brain networks [13,19]. The clustering coefficient (C) is a measure of functional segregation quantifying the presence of locally connected groups known as clusters or modules, which indicate segregated neural processing [18]. Path length (L), however, measures network integration by estimating the effective communications between different brain regions [18]. A graph comprising numerous local and few long-distance connections (high C and short L) most closely corresponds to the optimal network, called the 'small-world network (SWN)', which is intermediate between ordered (high C and long L) and random networks (low C and short L) [20,21]. However, various types of neurological diseases, including epilepsy, have been reported to deviate from SWN properties [22–24].

In this study, we investigated changes in brain functional connectivity in BCECTS patients compared to healthy controls in various frequency bands using high-density resting EEG data under the eyes-closed condition. For this purpose, we quantified the topological properties of the BCECTS brain networks at rest during periods with and without interictal epileptic spikes (IES) by estimating the clustering coefficient (C) and path length (L) from the functional connectivity matrices reconstructed with phase locking value (PLV). We also estimated the degree of centrality that measures the number of connections between a particular node (a specific brain region) to other nodes [18]. In summary, this study was designed to investigate whether BCECTS functional brain networks in the presence or absence of interictal spikes exhibited characteristic changes in small-world network features.

Materials and Methods

Subjects

Our study was conducted at Amiens University Hospital (Amiens, France) and approved by the hospital's ethics committee (CPP Nord-Ouest 2, approval No. 2011-A00782-39). Written consent approved by the ethics committee was obtained from parents/caregivers. Eight healthy adolescents (9 ± 0.21 years old) and nine young patients (9 ± 0.24 years old) with BCECTS were included in this study. All patients presented right centrotemporal spikes (see S1 Fig) and were free of any other neurological disorder at the time of the study.

EEG recording and preprocessing

On average, thirteen-minute high-resolution EEG data were recorded from each subject resting comfortably in a supine position in a quiet room. EEG data were recorded with 64 channels based on the international 10–10 system and a sampling rate of 256 Hz. An average reference montage was used for all of the analysis. Data were filtered offline between 0.5 to 30 Hz to

exclude high-frequency noise including muscle activities. To identify EEG portions with ocular and movement artifacts, which were excluded from the analysis, the EEG recordings were first normalized by the Z-score transformation and then processed semi-automatically (with visual inspection) using a simple threshold method (threshold set to the mean of the z-score distribution for each channel) as it was implemented in Fieldtrip software (http://www.fieldtriptoolbox.org/tutorial/visual_artifact_rejection) [25]. Two neurophysiologists visually inspected the filtered data in order to identify spikes segment and artifacts.

Artifact-free portions of the EEG data were partitioned into two-second non-overlapping segments. Five segments were randomly selected for each of the control subjects (CON). Two conditions were defined for the epileptic group: 5 segments with interictal spikes (With Spike Condition—WSC) and 5 spike-free segments (No Spike Condition—NSC), all randomly selected. On average, the WSC EEG segments contained 7 spikes considered as a requirement to ensure homogeneity across the patients.

Functional Connectivity

Pairwise correlations between all EEG channels were computed with the Phase Locking Value (PLV) [26,27]. Briefly, the PLV belongs to the family of phase synchronization values that are used to estimate functional connectivity between two signals based on their relative phase differences. To calculate the PLV, we first filtered the data into frequency bands (δ (0.5–3.5 Hz), θ (4–8 Hz), α (8.5–13 Hz), β_1 (13.5–20 Hz) and β_2 (20.5–30 Hz) using zero-phase forward and reverse digital filtering. The analytical signals were obtained by Hilbert transformation of the filtered signals. The Hilbert transformed signals consisted of the instantaneous amplitude and phase of the signals. The phase angle (φ) was used to compute the PLV. The PLV ranged from 0 to 1, with 0 and 1 indicating no connection and maximum connection between any given pair of signals, respectively. The end-result of computing the PLV for all paired combinations of channels was a square matrix of size 63 (number of EEG channels), in which each entry $N_{x,y}$ (= $N_{y,x}$) contained the PLV for channels x and y (see Supporting information for more details).

Computation of graph theory parameters

A graph is a basic topographical representation of a network consisting of nodes or vertices (in this case brain regions or electrodes) and edges (correlation between nodes). In this study, the network consisted of 63 vertices (electrodes) connected by edge weights (or elements) between all pairs of channels. The first step in applying graph theoretical analysis to functional connectivity matrices consists of converting the matrix into a binary graph, in which the edges either exist (1) or do not exist (0), i.e, with no graded values. Functional connectivity matrices were converted to binary graphs by applying an optimal threshold, τ above/below which connectivity values were set to 1/0. This operation transformed functional connectivity matrices to binary adjacency matrices, which was then followed by computation of graph metrics.

For each subject and frequency band, we determined the optimal threshold using an iterative method to make sure that the proportion and global spatial distribution of connections between brain regions were similar across subjects. We did not, however, choose a single threshold for all frequency bands mainly because it could lead to false positives in some frequency bands resulted from highly disconnected or over-densely networks [28]. Our threshold optimization procedure was based on the computation of the degree, which is defined for each node as the number of links connected to the node. The degree is used to measure the importance of individual nodes (nodes with a high degree of interaction with other nodes). The optimal thresholds were iteratively determined by means of the following procedure. First, for each functional connectivity matrix, we set the threshold to one standard deviation above the

median connectivity value. We then calculated the mean degree for the whole brain network. The optimal threshold was determined under two conditions, (i) the mean degree must not be less than 2ln(N), and (ii) at least 95% of nodes must be connected to one or more nodes [28,29] (see SI for more information). These conditions were then used to optimize the connection strength, which was used to increase the signal-to-noise ratio and to reduce false-positive edges in the graph [29].

To investigate the global topology of large-scale brain functional networks in patients and controls, the optimal threshold for each subject and frequency band was applied to the functional connectivity matrix for computation of degree of the whole brain network. We then investigated whether the occurrence of interictal spikes could change the small-world network features (C and L) in BCECTS brain networks. The clustering coefficient of a node is the ratio of the number of actual edges to the total number of potential edges adjacent to the node. The clustering coefficient was computed for all nodes and averaged (mean clustering coefficient, C). The path length is the mean shortest path connecting any two nodes of the graph and indicates how well the nodes are interconnected or integrated [18,20]. Similarly, we computed the mean path length (L) of the whole brain network (see SI for mathematical description). C and L were computed as a function of network density defined as the ratio of the actual number of edges in the graph to the total number of possible edges. In order to detect significant differences in network organization between the groups and to minimize the number of false (or noisy) edges in the networks, we only investigated strong connections by changing the network density from 30% to 60% in steps of 5% based on previous studies [30,31].

Statistical analysis

Nonparametric permutation testing was used for all graph parameters with correction for multiple comparisons including *post hoc* tests with a p-value ≤ 0.05. A total of 1,000 permutations were used to determine the significance level for each test [32]

All computations and statistical analyses were performed in Matlab with custom scripts and open source toolboxes: Fieldtrip (http://fieldtrip.fcdonders.nl/), EEGLAB (for 3D topological plots, http://sccn.ucsd.edu/eeglab/), and the brain connectivity toolbox (for graph parameter computations, https://sites.google.com/site/bctnet/).

Results

Synchronization and degree

The mean PLV was analysed under the three conditions in order to investigate differences in synchronization between patients and controls (Fig 1). As shown, the mean PLV under the with-spike condition exhibited significantly higher values in the θ band compared to the other two conditions (CON and NSC). No significant differences in synchronization were observed between the groups in the other frequency bands.

Compared to controls, BCECTS patients were characterized by significantly lower mean degree values in the δ band (under both WSC and NSC) and in the β_1 band (only under NSC).

We also investigated whether our results were affected by the precise choice of the thresholds. As shown in Table 1, within each group the variations in PLV and K due to changes in the optimal thresholds were very small for each particular frequency band.

We further investigated the regional differences in the degree (K) distribution between the groups (Fig 2). In the presence of IES (WSC vs. CON), K significantly increased in the right centrotemporal region (IES generator region), and decreased in the occipital region in almost all frequency bands. Right frontocentral areas exhibited lower K values in mid-range

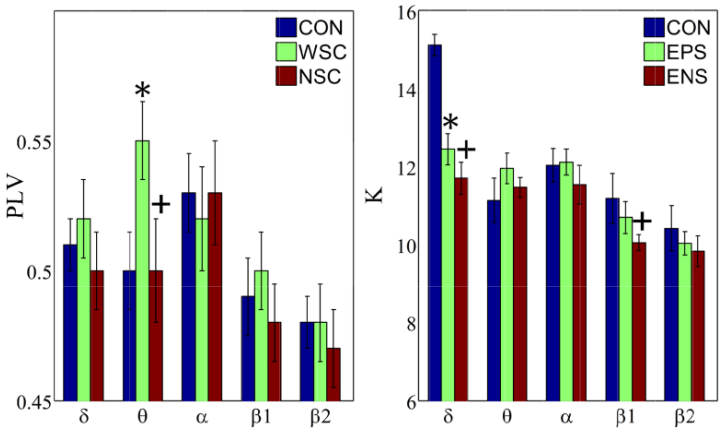

Fig 1. Group mean Phase Locking Value (PLV) and group mean degree (K). Error bars show standard errors with 95% confidence intervals. CON, WSC and NSC indicate the control, with spike and no spike conditions, respectively. Statistical significance is denoted by * (WSC vs CON) and + (NSC vs CON) with $p<0.05$.

doi:10.1371/journal.pone.0139228.g001

frequencies (θ and α). On the contralateral side, however, the degree significantly increased in the left frontal and frontotemporal regions in the θ band.

In the absence of IES (NSC vs. CON), K increased in the left frontal region in the θ band and in right centrotemporal areas in high frequencies (β_1 and β_2). In the mid- and high-range frequencies, patients exhibited relatively lower values of degree in occipital areas.

Compared to NSC, WSC was characterized with significant increases of K in the right centrotemporal regions in the δ and α band, and in the right parietotemporal regions in the β_1

Table 1. Mean and range of changes (at 95% confidence interval) of phase locking value (PLV), threshold (τ) and degree (K) computed for each group and frequency band.

	Frequency band	PLV	τ	K
CON	δ	0.51±0.02	0.59±0.01	15.12±1.40
	θ	0.50±0.03	0.60±0.01	11.14±1.13
	α	0.53±0.03	0.63±0.02	12.04±0.86
	β_1	0.49±0.03	0.57±0.01	11.19±1.28
	β_2	0.48±0.02	0.54±0.01	10.42±1.16
WSC	δ	0.52±0.03	0.63±0.02	12.45±0.80
	θ	0.55±0.03	0.64±0.01	11.96±0.79
	α	0.52±0.04	0.62±0.03	12.12±0.66
	β_1	0.50±0.03	0.58±0.01	10.70±0.81
	β_2	0.48±0.03	0.55±0.00	10.04±0.59
NSC	δ	0.50±0.03	0.60±0.03	11.71±0.82
	θ	0.50±0.04	0.60±0.02	11.47±0.50
	α	0.53±0.04	0.62±0.04	11.54±1.00
	β_1	0.48±0.03	0.55±0.01	10.06±0.41
	β_2	0.47±0.03	0.53±0.01	9.83±0.79

doi:10.1371/journal.pone.0139228.t001

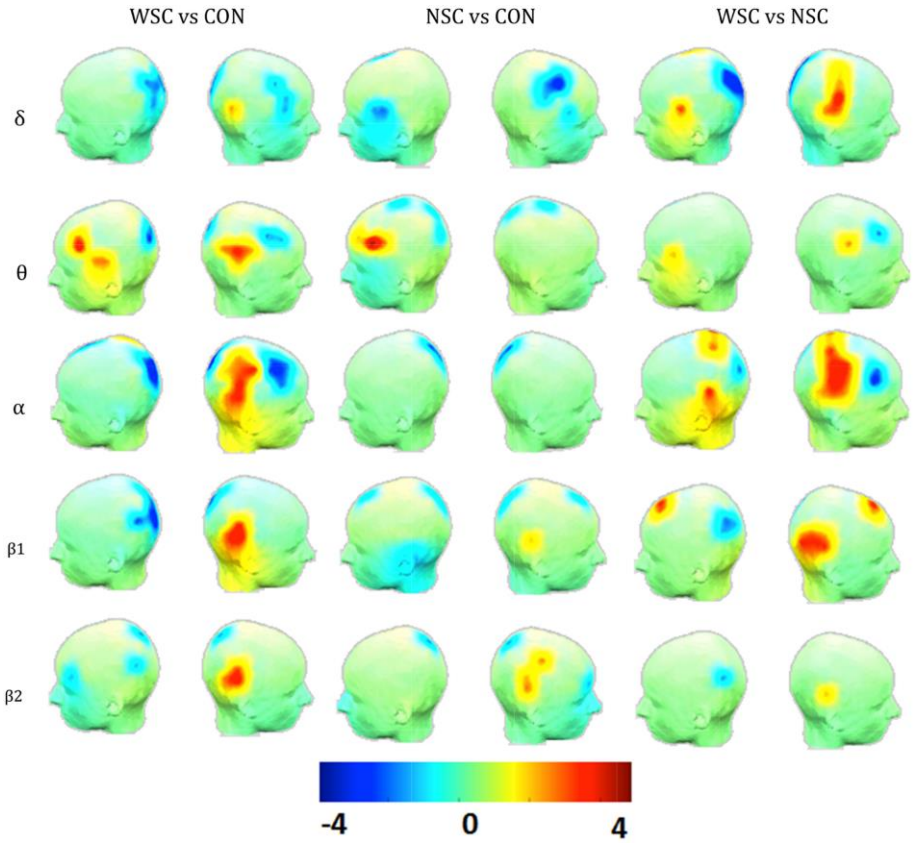

Fig 2. Statistical difference (t-value) maps of degree between the control (CON) and the epileptic groups (WSC and NSC). The color bar indicates the t values projected onto a standardized head shape. The significant increase (indicated by red) and decrease (indicated by blue) in degree have been represented, respectively, by positive and negative t values resulted from statistical comparisons between (WSC and CON), (NSC and CON), and (WSC and NSC).

doi:10.1371/journal.pone.0139228.g002

band. The degree decreased significantly in occipital areas in all frequencies except in the θ band, in the right frontocentral region close to the spike generation zone in mid-range frequencies (θ and α), and in the left posterior region in the β_1 band.

Clustering coefficient and path length

Fig 3 shows the mean clustering coefficient (C) and mean path length (L) computed for each condition.

In low frequencies (δ), the presence of IES (WSC) in the EEG segments significantly increased C at low connection densities (<50%) in comparison to the other two conditions.

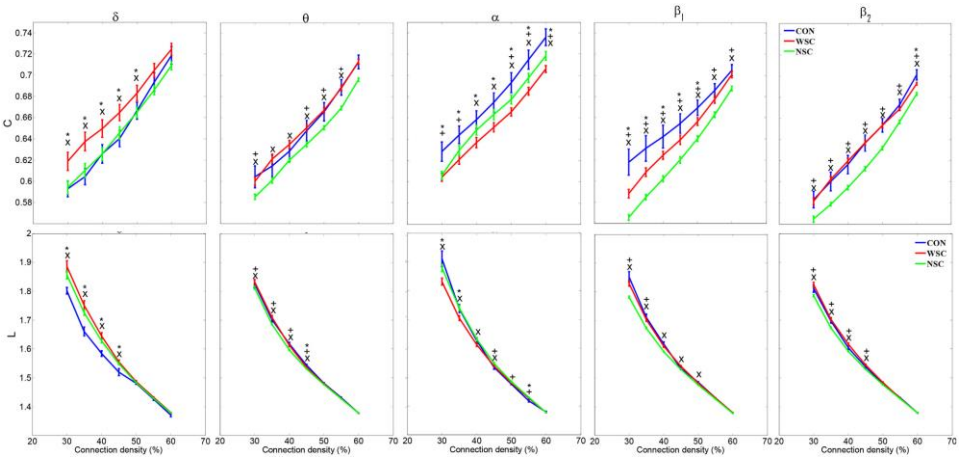

Fig 3. Mean clustering coefficient (C) and mean path length (L) as a function of network density for each frequency band. The error bars represent standard error with 95% confidence intervals. CON, WSC and NSC indicate the control, with spike and no spike conditions, respectively. Statistical significance is denoted by * (WSC vs. CON), + (NSC vs. CON) and × (WSC vs. NSC) with $p<0.05$.

doi:10.1371/journal.pone.0139228.g003

Compared to CON, both epileptic conditions exhibited shorter path length at connection densities up to 45%.

In the θ band, compared to NSC, WSC and CON showed significantly higher C (for all connection densities) and longer L (for connection densities less than 40%). No significant differences in clustering coefficients were observed between WSC and CON at almost all connection densities.

In the α band, both NSC and WSC compared to CON, and WSC compared to NSC exhibited significantly lower C values for almost all connection densities. Similar differences in L were found between the groups on a less significant level. The only exception was shorter path lengths found for WSC compared to CON and NSC at connection densities up to 45%.

In higher frequencies (β_1 and β_2), lower C (over all connection densities) and shorter L (for connection densities less than 45%) were found under NSC (vs. WSC and CON). In the β_1 band, compared to CON, WSC was characterized by significantly lower clustering coefficients. Table 2 roughly summarizes overall significant differences between the conditions.

Table 2. Summary of differences in mean clustering coefficient (C) and mean path length (L) between the three conditions as shown in Fig 3.

	C					L				
	δ	θ	α	β_1	β_2	δ	θ	α	β_1	β_2
WSC vs. NSC	↑	↑	↓	↑	↑	NS	↑	↓	↑	↑
WSC vs. CON	↑	NS	↓	↓	NS	↑	NS	↓	NS	NS
NSC vs. CON	NS	↓	↓	↓	↓	↑	↓	↓	↓	↓

↑ and ↓ indicate significant increase and decrease in C and L between conditions, respectively. NS represents non-significant differences.

doi:10.1371/journal.pone.0139228.t002

Discussion

This study investigated differences in the brain functional connectivity between BCECTS patients and healthy controls. Statistical dependencies between EEG time-series recorded from different brain regions were investigated by computing functional interactions using PLV as a measure of phase synchronization as well as graph metrics. The brain functional connectivity of BCECTS patients was found to be disrupted in terms of synchronization and degree of connectivity not only in the IES zone but also in frontal and temporal areas. Deviations from small-world features and network parameters were also observed in various frequency bands in BCECTS patients regardless of the presence or absence of spikes in EEG segments.

Many studies have shown that neurological diseases in children [33,34] are associated with differences in the level of synchronization compared to healthy controls. Compared to the other frequency bands, we found higher synchronization values in the α band in healthy subjects (Fig 1). The increased α synchronization is generally accepted to be due to the increased alpha activation under the eyes-closed resting state of the brain [35]. However, compared to controls, BCECTS patients exhibited significantly increased θ and decreased α synchronization under the with-spike condition. Our observations are consistent with those reported in patients with temporal lobe epilepsy [30], who presented significantly increased synchronization in the θ band, but non-significantly decreased synchronization in the α band. The increase of θ synchronization is commonly observed, not only in epilepsy [36,37] but also in other neurological diseases such as Parkinson's disease [38] and Alzheimer's disease [39].

Interictal spikes disrupt the global topology of brain functional connectivity

The disruption of brain dynamics in BCECTS patients probably results in higher levels of synchronization in some regions of the brain (especially in the epileptogenic zone) and lower levels of synchronization in other regions due to epileptic spikes. Although there is little evidence to suggest that BCECTS is associated with structural brain abnormalities [40], we found strong frequency-dependent changes in the degree as a measure of centrality or information coordination implying disrupted functional connectivity in the epileptic zone in BCECTS patients.

However, increased and decreased degrees in other regions, notably frontal and occipital, support the idea that disruption of brain functional connectivity in BCECTS patients is unlikely to be restricted to the epileptogenic zone. This finding may reflect the functional reorganization of the BCECTS brain network topology.

Functional disruption of BCECTS frontal networks

Our results revealed functional dysfunction of frontal brain networks in the presence/absence of interictal epileptic spikes. Compared to controls, BCECTS patients were characterized by a reduced degree in the right frontal region in the α band and an increased degree in the left frontal region in the θ band. These observations suggest functional network reorganization in the frontal regions regardless of the presence or absence of spikes in EEG segments. This frontal functional dysfunction may confirm the results of longitudinal MRI studies [41], which suggested that learning and memory difficulties in BCECTS patients may be associated with serial changes in the frontal and prefrontal lobes [42–44].

The alteration of brain functional connectivity in the absence of IES does not exclusively affect the frontal regions; it also involves the occipital region. This spatial pattern of changes

was also observed in the presence of IES, especially in the α band. The decreased degree in the α band in the posterior region under the epileptic conditions may support the disruption of functional brain connectivity in BCECTS patients even though the differences in global synchronization did not reach statistical significance. Since in healthy controls the functional connectivity has been shown to increase in frontal and posterior regions under the eyes-closed condition in the α band [45], in BCECTS patients the reduced α degree at the occipital region may support their poor visual spatial memory [46].

Deviation from small-world network features

There has been a growing interest in small-world analysis of brain networks in various neurological diseases [13]. The small-world network features of healthy controls have been compared to different brain diseases, such as schizophrenia [47], depression [48], Alzheimer's disease [24] and various types of epilepsy [14]. Most of these neurological diseases are associated with lower clustering coefficients and shorter path lengths compared to healthy controls.

The present study demonstrated frequency-dependent alterations of small-world features and network parameters in BCECTS patients in the presence and in the absence of IES. In the δ band, patients under the WSC condition exhibited higher C and long L compared to controls, implying that, at very low frequencies, BCECTS brain networks exhibit more functionally ordered organization in the presence of IES. This observation is consistent with the findings observed in other types of epilepsy [49]. In higher frequency bands (α and β_1), patients showed lower C values under both WSC and NSC compared to controls. The simultaneous decrease in C and L in the β_1 band may indicate loss of global processing and stronger integration between long-distance brain regions, which can be interpreted as increased functional interaction between long-range brain connections in BCECTS patients.

Interestingly, a switch in the brain network functional organization in the θ and α bands was observed when comparing WSC and NSC conditions. BCECTS patients' brain networks tended to change from a more randomly organized network (low C, short L) in the α band to a functionally ordered network (high C, long L) in the θ and β bands due to IES. The global increase in C in the presence of IES (excluding the α band) reflects orderly connection of IES brain networks. This finding is in agreement with studies on the other types of epilepsies using intracranial EEG and ECoG [16,50]. Small-world networks allow more rapid information processing and learning than either random or regular networks [51] and the results may suggest that the cognitive impairments observed in BCECTS may be associated with rapid changes in the functional reconfiguration of BCECTS brain networks. Although the shorter path length in higher frequency bands (in the α band for WSC and the β band for NSC has been shown to support effective interactions between and across brain regions [21], BCECTS brain networks may more closely resemble randomly organized networks.

In the absence of IES, C was lower in all frequency bands and L was lower in the θ and β bands in BCECTS patients compared to controls, indicating that, in the absence of IES, the BCECTS brain network is less ordered regardless of the frequency band except for the α band. It is generally believed that random networks ensure even better synchronization than small-world networks [52], as pathological random networks present rapid phase transition that could lead to the onset of interictal epileptic discharges. In agreement with our observations, temporal lobe epilepsy [30] has been characterized by lower C and shorter L in the α band compared to controls. These discrepancies between TLE and BCECTS are clinically relevant and may constitute a specific biomarker of the type of epilepsy. However, to confirm our findings, further study with a larger population of patients will be needed.

Limitations and future directions

A potential limitation of our study is the use of scalp EEG for the functional connectivity analysis. In studies on epilepsy, scalp EEG is usually used for EEG source imaging and/or functional connectivity analysis [53], are employed for localizing the epileptogenic foci and investigating the functional organization of the epileptic cortical networks, respectively. In our study, we used PLV as a measure of undirected functional connectivity between electrodes to explore the global topology and dynamics of the interactions between large-scale brain regions during the interictal state over a range of frequencies. The functional connectivity analysis in the sensor space might provide inaccurate information on the overall organization of the cortical region mainly because EEG electrodes detect spatially averaged overlapping EEG signals from several brain sources or the signal generated by a focal cerebral source can be detected by nearby electrodes [54].

Our main direction of future work will be to use the EEG source space connectivity tools such as the directed transfer function (DTF)[55] or the Phase-Slope Index (PSI) [56] for the identification and characterization of the cortical networks involved in the interictal states.

In patients with epilepsy, the functional connectivity analysis using DTF has provided promising results using scalp EEG [57] and ECoG [58] for exploring the directed functional connectivity between cortical regions and the propagation of activation [58,59]. In general, the EEG functional connectivity analysis between neighbouring voxels might lead to spurious and over-represented results [60] because of the volume conduction effect which highly affects the accuracy of the functional connectivity tools [61]. However, DTF has been shown to be insensitive to volume conduction and less sensitive to noise [62]. We will also increase the number of electrodes to improve the accuracy of the functional connectivity analysis in the source space [63,64].

Conclusion

This study investigated functional alterations in small-world characteristics in patients with benign epilepsy with centrotemporal spikes and showed that the functional organization of BCECTS brain networks changed from an ordered structure in low frequency bands (δ and θ bands) to a less randomly ordered network in higher frequency bands (α band).

This study provides further evidence that the BCECTS brain network is altered. The degree spatial distribution showed that alteration of the functional connectivity in the BCECTS brain was not limited to the epileptogenic zone, but also involved other regions, especially the frontal and occipital regions. The decreased connection density in the occipital and right frontal regions supports functional impairment of these regions. The BCECTS brain with IES, which does not present the features of a small-world network, showed topological characteristics of an ordered network in the δ band and a less ordered network in the α band. A more randomly organized network was also observed in the absence of IES compared to healthy controls.

Supporting Information

S1 Fig. Dipole locations of the averaged spikes for patients.
(DOCX)

S2 Fig. A sample interictal EEG recording from patient 1. The spikes have been outlined in blue.
(DOCX)

S3 Fig. (A) Example of the functional connectivity matrix obtained for Subject 1. (B) The distribution of the PLV values of the functional connectivity matrix; the vertical line shows the

optimal threshold. (C) The binarized functional connectivity matrix obtained after applying the optimal threshold.
(DOCX)

S1 Materials.
(DOCX)

Author Contributions

Conceived and designed the experiments: A. Adebimpe A. Aarabi EB MM FW. Performed the experiments: EB MM. Analyzed the data: A. Adebimpe A. Aarabi. Contributed reagents/materials/analysis tools: A. Adebimpe A. Aarabi EB MM FW. Wrote the paper: A. Adebimpe A. Aarabi FW. Read and accepted the manuscript: A. Adebimpe A. Aarabi EB MM FW.

References

1. Shields WD, Snead OC. Benign epilepsy with centrotemporal spikes. Epilepsia. 2009; 50 Suppl 8: 10–15. doi: 10.1111/j.1528-1167.2009.02229.x PMID: 19702727
2. Camfield CS, Berg A, Stephani U, Wirrell EC. Transition issues for benign epilepsy with centrotemporal spikes, nonlesional focal epilepsy in otherwise normal children, childhood absence epilepsy, and juvenile myoclonic epilepsy. Epilepsia. 2014; 55 Suppl 3: 16–20. doi: 10.1111/epi.12706 PMID: 25209080
3. Datta AN, Oser N, Bauder F, Maier O, Martin F, Ramelli GP, et al. Cognitive impairment and cortical reorganization in children with benign epilepsy with centrotemporal spikes. Epilepsia. 2013; 54: 487–494. doi: 10.1111/epi.12067 PMID: 23297860
4. Kanemura H, Aihara M. Growth disturbance of frontal lobe in BCECTS presenting with frontal dysfunction. Brain Dev. 2009; 31: 771–774. doi: 10.1016/j.braindev.2008.12.007 PMID: 19168301
5. Coan AC, Campos BM, Yasuda CL, Kubota BY, Bergo FP, Guerreiro CA, et al. Frequent seizures are associated with a network of gray matter atrophy in temporal lobe epilepsy with or without hippocampal sclerosis. PloS One. 2014; 9: e85843. doi: 10.1371/journal.pone.0085843 PMID: 24475055
6. Huang W, Lu G, Zhang Z, Zhong Y, Wang Z, Yuan C, et al. Gray-matter volume reduction in the thalamus and frontal lobe in epileptic patients with generalized tonic-clonic seizures. J Neuroradiol J Neuroradiol. 2011; 38: 298–303. doi: 10.1016/j.neurad.2010.12.007 PMID: 21354624
7. Cressman JR, Ullah G, Ziburkus J, Schiff SJ, Barreto E. The influence of sodium and potassium dynamics on excitability, seizures, and the stability of persistent states: I. Single neuron dynamics. J Comput Neurosci. 2009; 26: 159–170. doi: 10.1007/s10827-008-0132-4 PMID: 19169801
8. Werner F-M, Coveñas R. Classical neurotransmitters and neuropeptides involved in generalized epilepsy: a focus on antiepileptic drugs. Curr Med Chem. 2011; 18: 4933–4948. PMID: 22050744
9. Baumgartner C, Graf M, Doppelbauer A, Serles W, Lindinger G, Olbrich A, et al. The Functional Organization of the Interictal Spike Complex in Benign Rolandic Epilepsy. Epilepsia. 1996; 37: 1164–1174. doi: 10.1111/j.1528-1157.1996.tb00548.x PMID: 8956847
10. Zhang ZJ, Valiante TA, Carlen PL. Transition to seizure: from "macro"- to "micro"-mysteries. Epilepsy Res. 2011; 97: 290–299. doi: 10.1016/j.eplepsyres.2011.09.025 PMID: 22075227
11. Shen X, Papademetris X, Constable RT. Graph-theory based parcellation of functional subunits in the brain from resting-state fMRI data. NeuroImage. 2010; 50: 1027–1035. doi: 10.1016/j.neuroimage.2009.12.119 PMID: 20060479
12. Huberfeld G, Menendez de la Prida L, Pallud J, Cohen I, Le Van Quyen M, Adam C, et al. Glutamatergic pre-ictal discharges emerge at the transition to seizure in human epilepsy. Nat Neurosci. 2011; 14: 627–634. doi: 10.1038/nn.2790 PMID: 21460834
13. Stam CJ. Modern network science of neurological disorders. Nat Rev Neurosci. 2014; 15: 683–695. doi: 10.1038/nrn3801 PMID: 25186238
14. Netoff TI, Clewley R, Arno S, Keck T, White JA. Epilepsy in small-world networks. J Neurosci Off J Soc Neurosci. 2004; 24: 8075–8083. doi: 10.1523/JNEUROSCI.1509-04.2004
15. Ponten SC, Bartolomei F, Stam CJ. Small-world networks and epilepsy: Graph theoretical analysis of intracerebrally recorded mesial temporal lobe seizures. Clin Neurophysiol. 2007; 118: 918–927. doi: 10.1016/j.clinph.2006.12.002 PMID: 17314065
16. Wilke C, Worrell G, He B. Graph analysis of epileptogenic networks in human partial epilepsy. Epilepsia. 2011; 52: 84–93. doi: 10.1111/j.1528-1167.2010.02785.x PMID: 21126244

17. Kramer MA, Kolaczyk ED, Kirsch HE. Emergent network topology at seizure onset in humans. Epilepsy Res. 2008; 79: 173–186. doi: 10.1016/j.eplepsyres.2008.02.002 PMID: 18359200

18. Rubinov M, Sporns O. Complex network measures of brain connectivity: uses and interpretations. NeuroImage. 2010; 52: 1059–1069. doi: 10.1016/j.neuroimage.2009.10.003 PMID: 19819337

19. Bullmore E, Sporns O. Complex brain networks: graph theoretical analysis of structural and functional systems. Nat Rev Neurosci. 2009; 10: 186–198. doi: 10.1038/nrn2575 PMID: 19190637

20. Bassett DS, Bullmore E. Small-world brain networks. Neurosci Rev J Bringing Neurobiol Neurol Psychiatry. 2006; 12: 512–523. doi: 10.1177/1073858406293182

21. Sporns O, Zwi JD. The small world of the cerebral cortex. Neuroinformatics. 2004; 2: 145–162. doi: 10.1385/NI:2:2:145 PMID: 15319512

22. Zhang Z, Liao W, Chen H, Mantini D, Ding J-R, Xu Q, et al. Altered functional-structural coupling of large-scale brain networks in idiopathic generalized epilepsy. Brain J Neurol. 2011; 134: 2912–2928. doi: 10.1093/brain/awr223

23. Wang L, Zhu C, He Y, Zang Y, Cao Q, Zhang H, et al. Altered small-world brain functional networks in children with attention-deficit/hyperactivity disorder. Hum Brain Mapp. 2009; 30: 638–649. doi: 10.1002/hbm.20530 PMID: 18219621

24. Stam CJ, de Haan W, Daffertshofer A, Jones BF, Manshanden I, van Walsum AM van C, et al. Graph theoretical analysis of magnetoencephalographic functional connectivity in Alzheimer's disease. Brain. 2009; 132: 213–224. doi: 10.1093/brain/awn262 PMID: 18952674

25. Oostenveld R, Fries P, Maris E, Schoffelen J-M. FieldTrip: Open Source Software for Advanced Analysis of MEG, EEG, and Invasive Electrophysiological Data. Comput Intell Neurosci. 2010; 2011: e156869. doi: 10.1155/2011/156869

26. Lachaux J-P, Rodriguez E, Le Van Quyen M, Lutz A, Martinerie J, Varela FJ. Studying single-trials of phase synchronous activity in the brain. Int J Bifurc Chaos. 2000; 10: 2429–2439. doi: 10.1142/S0218127400001560

27. Mormann F, Lehnertz K, David P, Elger C E. Mean phase coherence as a measure for phase synchronization and its application to the EEG of epilepsy patients. Phys Nonlinear Phenom. 2000; 144: 358–369. doi: 10.1016/S0167-2789(00)00087-7

28. Bassett DS, Meyer-Lindenberg A, Achard S, Duke T, Bullmore E. Adaptive reconfiguration of fractal small-world human brain functional networks. Proc Natl Acad Sci. 2006; 103: 19518–19523. doi: 10.1073/pnas.0606005103 PMID: 17159150

29. Humphries MD, Gurney K. Network "Small-World-Ness": A Quantitative Method for Determining Canonical Network Equivalence. PLoS ONE. 2008; 3. doi: 10.1371/journal.pone.0002051

30. Quraan MA, McCormick C, Cohn M, Valiante TA, McAndrews MP. Altered Resting State Brain Dynamics in Temporal Lobe Epilepsy Can Be Observed in Spectral Power, Functional Connectivity and Graph Theory Metrics. PLoS ONE. 2013; 8: e68609. doi: 10.1371/journal.pone.0068609 PMID: 23922658

31. He H, Sui J, Yu Q, Turner JA, Ho B-C, Sponheim SR, et al. Altered Small-World Brain Networks in Schizophrenia Patients during Working Memory Performance. PLoS ONE. 2012; 7: e38195. doi: 10.1371/journal.pone.0038195 PMID: 22701611

32. Maris E, Oostenveld R. Nonparametric statistical testing of EEG- and MEG-data. J Neurosci Methods. 2007; 164: 177–190. doi: 10.1016/j.jneumeth.2007.03.024 PMID: 17517438

33. Liu T, Lin P, Chen Y, Wang J. Electroencephalogram synchronization analysis for attention deficit hyperactivity disorder children. Biomed Mater Eng. 2014; 24: 1035–1039. doi: 10.3233/BME-130901 PMID: 24211994

34. Doesburg SM, Ribary U, Herdman AT, Cheung T, Moiseev A, Weinberg H, et al. Altered Long-Range Phase Synchronization and Cortical Activation in Children Born Very Preterm. IFMBE Proc. 2010; 29: 250–253. doi: 10.1007/978-3-642-12197-5_57 PMID: 21331353

35. Pfurtscheller G, Stancák A Jr., Neuper C. Event-related synchronization (ERS) in the alpha band—an electrophysiological correlate of cortical idling: A review. Int J Psychophysiol. 1996; 24: 39–46. doi: 10.1016/S0167-8760(96)00066-9 PMID: 8978434

36. Douw L, de Groot M, van Dellen E, Heimans JJ, Ronner HE, Stam CJ, et al. "Functional connectivity" is a sensitive predictor of epilepsy diagnosis after the first seizure. PloS One. 2010; 5: e10839. doi: 10.1371/journal.pone.0010839 PMID: 20520774

37. Douw L, van Dellen E, de Groot M, Heimans JJ, Klein M, Stam CJ, et al. Epilepsy is related to theta band brain connectivity and network topology in brain tumor patients. BMC Neurosci. 2010; 11: 103. doi: 10.1186/1471-2202-11-103 PMID: 20731854

38. Stoffers D, Bosboom JLW, Deijen JB, Wolters EC, Stam CJ, Berendse HW. Increased cortico-cortical functional connectivity in early-stage Parkinson's disease: an MEG study. NeuroImage. 2008; 41: 212–222. doi: 10.1016/j.neuroimage.2008.02.027 PMID: 18395468

39. Stam CJ, Jones BF, Manshanden I, van Cappellen van Walsum AM, Montez T, Verbunt JPA, et al. Magnetoencephalographic evaluation of resting-state functional connectivity in Alzheimer's disease. NeuroImage. 2006; 32: 1335–1344. doi: 10.1016/j.neuroimage.2006.05.033 PMID: 16815039

40. Xiao F, Chen Q, Yu X, Tang Y, Luo C, Fang J, et al. Hemispheric lateralization of microstructural white matter abnormalities in children with active benign childhood epilepsy with centrotemporal spikes (BECTS): A preliminary DTI study. J Neurol Sci. 2014; 336: 171–179. doi: 10.1016/j.jns.2013.10.033 PMID: 24210075

41. Kanemura H, Hata S, Aoyagi K, Sugita K, Aihara M. Serial changes of prefrontal lobe growth in the patients with benign childhood epilepsy with centrotemporal spikes presenting with cognitive impairments/behavioral problems. Brain Dev. 2011; 33: 106–113. doi: 10.1016/j.braindev.2010.03.005 PMID: 20381984

42. Kwon S, Seo H-E, Hwang SK. Cognitive and other neuropsychological profiles in children with newly diagnosed benign rolandic epilepsy. Korean J Pediatr. 2012; 55: 383–387. doi: 10.3345/kjp.2012.55.10.383 PMID: 23133485

43. Danielsson J, Petermann F. Cognitive deficits in children with benign rolandic epilepsy of childhood or rolandic discharges: a study of children between 4 and 7 years of age with and without seizures compared with healthy controls. Epilepsy Behav EB. 2009; 16: 646–651. doi: 10.1016/j.yebeh.2009.08.012

44. Verrotti A, Filippini M, Matricardi S, Agostinelli MF, Gobbi G. Memory impairment and Benign Epilepsy with centrotemporal spike (BECTS): a growing suspicion. Brain Cogn. 2014; 84: 123–131. doi: 10.1016/j.bandc.2013.11.014 PMID: 24362071

45. Tan B, Kong X, Yang P, Jin Z, Li L. The Difference of Brain Functional Connectivity between Eyes-Closed and Eyes-Open Using Graph Theoretical Analysis. Comput Math Methods Med. 2013; 2013. doi: 10.1155/2013/976365

46. Cohen M. Auditory/verbal and visual/spatial memory in children with complex partial epilepsy of temporal lobe origin. Brain Cogn. 1992; 20: 315–326. doi: 10.1016/0278-2626(92)90024-G PMID: 1449761

47. Liu Y, Liang M, Zhou Y, He Y, Hao Y, Song M, et al. Disrupted small-world networks in schizophrenia. Brain. 2008; 131: 945–961. doi: 10.1093/brain/awn018 PMID: 18299296

48. Li W, Douglas Ward B, Liu X, Chen G, Jones JL, Antuono PG, et al. Disrupted small world topology and modular organisation of functional networks in late-life depression with and without amnestic mild cognitive impairment. J Neurol Neurosurg Psychiatry. 2014; doi: 10.1136/jnnp-2014-309180

49. Ponten SC, Douw L, Bartolomei F, Reijneveld JC, Stam CJ. Indications for network regularization during absence seizures: Weighted and unweighted graph theoretical analyses. Exp Neurol. 2009; 217: 197–204. doi: 10.1016/j.expneurol.2009.02.001 PMID: 19232346

50. Wu H, Li X, Guan X. Networking Property During Epileptic Seizure with Multi-channel EEG Recordings. In: Wang J, Yi Z, Zurada JM, Lu B-L, Yin H, editors. Advances in Neural Networks—ISNN 2006. Springer Berlin Heidelberg; 2006. pp. 573–578. Available: http://link.springer.com/chapter/10.1007/11760191_84

51. Simard D, Nadeau L, Kröger H. Fastest learning in small-world neural networks. Phys Lett A. 2005; 336: 8–15. doi: 10.1016/j.physleta.2004.12.078

52. Percha B, Dzakpasu R, Żochowski M, Parent J. Transition from local to global phase synchrony in small world neural network and its possible implications for epilepsy. Phys Rev E. 2005; 72: 031909. doi: 10.1103/PhysRevE.72.031909

53. Barkley GL, Baumgartner C. MEG and EEG in epilepsy. J Clin Neurophysiol Off Publ Am Electroencephalogr Soc. 2003; 20: 163–178.

54. Ioannides AA. Dynamic functional connectivity. Curr Opin Neurobiol. 2007; 17: 161–170. doi: 10.1016/j.conb.2007.03.008 PMID: 17379500

55. He B, Dai Y, Astolfi L, Babiloni F, Yuan H, Yang L. eConnectome: A MATLAB Toolbox for Mapping and Imaging of Brain Functional Connectivity. J Neurosci Methods. 2011; 195: 261–269. doi: 10.1016/j.jneumeth.2010.11.015 PMID: 21130115

56. Nolte G, Ziehe A, Nikulin VV, Schlögl A, Krämer N, Brismar T, et al. Robustly Estimating the Flow Direction of Information in Complex Physical Systems. Phys Rev Lett. 2008; 100: 234101. doi: 10.1103/PhysRevLett.100.234101 PMID: 18643502

57. Li W, Wu N, Hou W, Zhang J, Xu W, Wu G, et al. Lateralization of epileptic foci through causal analysis of scalp-EEG interictal spike activity. J Clin Neurophysiol Off Publ Am Electroencephalogr Soc. 2015; 32: 57–65.

58. Wilke C, Ding L, He B. Estimation of time-varying connectivity patterns through the use of an adaptive directed transfer function. IEEE Trans Biomed Eng. 2008; 55: 2557–2564. doi: 10.1109/TBME.2008.919885 PMID: 18990625

59. Wilke C, van Drongelen W, Kohrman M, He B. Neocortical seizure foci localization by means of a directed transfer function method. Epilepsia. 2010; 51: 564–572. doi: 10.1111/j.1528-1167.2009.02329.x PMID: 19817817

60. Stanley ML, Moussa MN, Paolini BM, Lyday RG, Burdette JH, Laurienti PJ. Defining nodes in complex brain networks. Front Comput Neurosci. 2013; 7: 169. doi: 10.3389/fncom.2013.00169 PMID: 24319426

61. Nunez PL, Srinivasan R, Westdorp AF, Wijesinghe RS, Tucker DM, Silberstein RB, et al. EEG coherency: I: statistics, reference electrode, volume conduction, Laplacians, cortical imaging, and interpretation at multiple scales. Electroencephalogr Clin Neurophysiol. 1997; 103: 499–515. doi: 10.1016/S0013-4694(97)00066-7 PMID: 9402881

62. Blinowska KJ. Review of the methods of determination of directed connectivity from multichannel data. Med Biol Eng Comput. 2011; 49: 521–529. doi: 10.1007/s11517-011-0739-x PMID: 21298355

63. Sohrabpour A, Lu Y, Kankirawatana P, Blount J, Kim H, He B. Effect of EEG electrode number on epileptic source localization in pediatric patients. Clin Neurophysiol Off J Int Fed Clin Neurophysiol. 2015; 126: 472–480. doi: 10.1016/j.clinph.2014.05.038

64. Hassan M, Dufor O, Merlet I, Berrou C, Wendling F. EEG source connectivity analysis: from dense array recordings to brain networks. PloS One. 2014; 9: e105041. doi: 10.1371/journal.pone.0105041 PMID: 25115932

Volume conduction artifacts may confound the results of EEG functional connectivity in sensor space. In source space, we used the Lagged Phase Synchronization (LPS) which is generally believed to be less sensitive to volume conduction compared to other zero-lagged functional connectivity metric like the classical coherence and PLV. LPS was computed between 84 Region of Interests (ROIs) defined by the Brodmann atlas as implemented in eLORETA software. Compared to controls, patients (without IEDs) showed higher θ- α and lower β LPS. Patients also displayed higher integration and lower segregation in the θ and α bands compared to healthy controls. They also exhibited higher local functional connectivity at the epileptogenic network including motor areas, central region and temporal regions of the ipsilateral hemisphere to the epileptic zone. The contralateral frontal region in patients was also found to exhibit lower local connectivity. All of these findings support the evidence of alteration of resting state functional connectivity in BCECTS patients in different frequency bands. More information can be found in the following article.

frontiers in Neuroscience

ORIGINAL RESEARCH
published: 31 March 2016
doi: 10.3389/fnins.2016.00143

EEG Resting State Functional Connectivity Analysis in Children with Benign Epilepsy with Centrotemporal Spikes

Azeez Adebimpe[1], *Ardalan Aarabi*[1]*, *Emilie Bourel-Ponchel*[2], *Mahdi Mahmoudzadeh*[2] *and Fabrice Wallois*[1,2]

[1] *INSERM U 1105, CURS, Centre Hospitalier Universitaire Amiens-Picardie, Amiens, France,* [2] *INSERM U 1105, EFSN Pédiatriques, Centre Hospitalier Universitaire Amiens-Picardie, Amiens, France*

In this study, we investigated changes in functional connectivity (FC) of the brain networks in patients with benign epilepsy with centrotemporal spikes (BECTS) compared to healthy controls using high-density EEG data collected under eyes-closed resting state condition. EEG source reconstruction was performed with exact Low Resolution Electromagnetic Tomography (eLORETA). We investigated FC between 84 Brodmann areas using lagged phase synchronization (LPS) in four frequency bands (δ, θ, α, and β). We further computed the network degree, clustering coefficient and efficiency. Compared to controls, patients displayed higher θ and α and lower β LPS values. In these frequency bands, patients were also characterized by less well ordered brain networks exhibiting higher global degrees and efficiencies and lower clustering coefficients. In the β band, patients exhibited reduced functional segregation and integration due to loss of both local and long-distance functional connections. These findings suggest that benign epileptic brain networks might be functionally disrupted due to their altered functional organization especially in the α and β frequency bands.

Keywords: children epilepsy, centrotemporal spikes, resting sate, functional connectivity, phase synchronization, graph theory

OPEN ACCESS

Edited by:
Pedro Antonio Valdes-Sosa, Centro de Neurociencias de Cuba, Cuba

Reviewed by:
Koichi Sameshima, Universidade de São Paulo, Brazil
Theodore J. Huppert, University of Pittsburgh Medical Center, USA
Amir Omidvarnia, Florey Institute of Neuroscience and Mental Health, Australia

***Correspondence:**
Ardalan Aarabi
ardalan.aarabi@u-picardie.fr

Specialty section:
This article was submitted to Brain Imaging Methods, a section of the journal Frontiers in Neuroscience

Received: *30 December 2015*
Accepted: *21 March 2016*
Published: *31 March 2016*

Citation:
Adebimpe A, Aarabi A, Bourel-Ponchel E, Mahmoudzadeh M and Wallois F (2016) EEG Resting State Functional Connectivity Analysis in Children with Benign Epilepsy with Centrotemporal Spikes. Front. Neurosci. 10:143. doi: 10.3389/fnins.2016.00143

INTRODUCTION

Benign epilepsy with centrotemporal spikes (BECTS) is the most common idiopathic epileptic syndrome with a prevalence of 8–20% of pediatric patients with epilepsy (Holmes, 1993; Wirrell, 1998; Panayiotopoulos, 1999). In BECTS, although interictal spikes arise primarily within centrotemporal regions, there is growing evidence that abnormal functional networks in BECTS patients, like other types of focal epilepsy, are not restricted to the epileptogenic region as revealed by the functional connectivity (FC) analysis of the brain networks (Kramer and Cash, 2012; Laufs, 2012; Adebimpe et al., 2015b). Moreover, our previous studies have shown that functional organization of the brain networks in BECTS patients largely differs from normal brain in presence or absence of interictal epileptic discharges (IES) (Adebimpe et al., 2015b, 2016).

Over the past decade, graph-theoretical analysis of resting state FC in EEG and MEG data have gained attention in healthy subjects (Deco and Kringelbach, 2014), and in patients suffering from various diseases (Prinz, 2008; Stam et al., 2009; Zhang et al., 2014). In our previous study using graph metrics we found that the brain networks in BECTS patients show functionally disrupted

connectivity patterns (Adebimpe et al., 2015b). However, the main shortcoming of that study was that the FC analysis and graph metrics were estimated in the sensor space that might not provide information on the overall functional organization of the cortical regions mainly because scalp EEG electrodes detect spatially averaged overlapping EEG signals from several brain sources. Moreover, our previous study focused on global clustering coefficient and path length.

In the present study, we investigated changes in brain FC including local and regional graph metrics in BECTS patients compared to healthy controls in various frequency bands under the eyes-closed resting condition. Abnormal patterns of resting-state EEG source FC in patients were determined by using lagged phase synchronization (LPS), a non-linear connectivity measure implemented in the eLORETA software (http://www.uzh.ch/keyinst/eLORETA/). Graph theory was also used to characterize FC by estimating network centrality, functional segregation and integration. We further investigated whether functional brain networks in BECTS patients displayed altered network efficiency and disrupted local neural processing (segregation and integration) in comparison to healthy controls.

MATERIALS AND METHODS

Subjects

This study was performed on 11 young patients (9.65 ± 2.36 years) with benign childhood epilepsy with right centrotemporal spikes (see **Table 1** and Adebimpe et al., 2015a, for more information). None of the patients presented any other neurological disorders at the time of the study, which was conducted at Amiens University Hospital (Amiens, France) and approved by the hospital's ethics committee (CPP Nord-Ouest 2, approval No. 2011-A00782-39). We also recruited 12 healthy subjects in the same age range (9.27 ± 1.70 years) as controls. Written consent approved by the ethics committee was obtained from parents/caregivers.

EEG Recording and Pre-Processing

EEG data were recorded with a high density recording system (ANT, Netherlands) based on the international 10–10 system at a sampling rate of 256 Hz under the eyes-closed resting condition. EEG data were first digitally re-referenced to an average reference, z-scored, and band-pass filtered between 0.5 and 40 Hz to exclude high-frequency noise including muscle activities. EEG portions with occular and movement artifacts were identified automatically using a thresholding method (threshold was set to the mean of the z-score distribution for each channel) as implemented in Fieldtrip software (Oostenveld et al., 2010; tutorial:visual_artifact_rejection – FieldTrip[1]) and rejected by visual inspection. No ECG artifacts were visually observed in any of the EEG recordings. The artifact-free portions of the EEG data were partitioned into 2-s quasi-stationary segments required for spectral analysis with a frequency resolution of 0.5 Hz. Five EEG segments of 2 s were randomly selected for each patient (PAT) and healthy control (CON). The EEG segments selected for patients included no centrotemporal spikes.

[1]tutorial:visual_artifact_rejection – FieldTrip Available at: http://www.fieldtriptoolbox.org/tutorial/visual_artifact_rejection [Accessed May 15, 2015].

EEG Source Connectivity Analysis

We first used the exact Low Resolution Electromagnetic Tomography (eLORETA) method (Pascual-Marqui, 2007a) to identify the average location of interictal spike sources in patients. EEG source connectivity analysis was then performed using eLORETA by restricting the source space within the gray matter including 6239 voxels with a 5-mm spatial resolution. The Montreal Neurologic Institute average MRI brain (MNI152) (Fonov et al., 2011) with anatomical labels corresponding to Brodmann areas was used as the realistic head model to compute the lead field. The 84 commonly used Brodmann areas were chosen as regions of interests (ROIs) for connectivity analysis between the centroids of the ROIs.

To analyze the FC we computed LPS (Pascual-Marqui, 2007b) between ROIs. This measure has been shown to be less sensitive than other techniques to non-physiological signals including artifacts and the volume conduction effect (Pascual-Marqui et al., 2011). For each subject, four FC matrices were computed in four frequency bands, δ (0.5–3.5 Hz), θ (4–8 Hz), α (8.5–13 Hz), and β (14–30 Hz). For each subject and each frequency band, an average FC matrix was obtained over the five EEG segments selected for the subject and was used to compute graph metrics.

Graph Theoretical Analysis

From each FC matrix, we extracted three graph measures to investigate functional integration and segregation between brain networks in patients compared to controls (for mathematical definitions see (Rubinov and Sporns, 2010): network degree (K), a measure of node centrality, global efficiency (E) and clustering coefficient (C), measures of functional integration and segregation in large-scale brain networks, respectively.

The graph measures were calculated using the brain connectivity toolbox (Rubinov and Sporns, 2010). To make connectivity matrices comparable across subjects, an individual optimal threshold was needed to convert each FC matrix to a binary adjacency matrix. This step was necessary to ensure that all graphs had equal connection densities within the small world network range (Bassett et al., 2006). Moreover, the optimal thresholds have been shown to reduce the number of false-positive edges and minimize the noise (Drakesmith et al., 2015). To obtain an optimal threshold for each subject and frequency band, we first set the threshold to one standard deviation above the median connectivity value. The threshold was iteratively adjusted to satisfy two conditions: (i) the mean network degree had to be less than 2log(N), where N was the total number of nodes, and (ii) at least 95% of nodes must be connected to one or more nodes (Bassett et al., 2006; Erdős and Rényi, 2013). Using the optimal thresholds, the FC matrices were thresholded and binarized to calculate the network degree (K), clustering coefficient (C), and global efficiency (E). The global value for each graph metric was calculated by the average over the whole nodes for a wide range of thresholds from 0.2 to 0.7 with 0.05 increments to investigate differences between the two groups.

TABLE 1 | Characteristics of the control and patient groups.

Control group			Patient group					
Subject	Age (years)	EEG duration (min)	Patient	Age (years)	EEG duration (min)	Neuropsychological assessment	Description of ictal EEG	Medication
1	6.73	16	1	12.63	50	Normal	Partial seizure	Sodium valproate
2	11.28	19	2	12.64	17	Normal	Partial seizure	Sodium valproate
3	10.48	19	3	9.25	44	Attention deficit	Generalized tonic-clonic seizure	Oxcarbezepine
4	10.66	17	4	6.03	43	–	Brachiofacial nocturnal seizure	Oxcarbezepine
5	7.39	13	5	10.47	50	Attention deficit	Partial seizure	Sodium valproate
6	7.31	20	6	7.16	14	–	Brachiofacial nocturnal seizure	Sodium valproate
7	11.92	30	7	8.51	30	Attention deficit	Nocturnal seizure	–
8	8.44	75	8	13.16	20	Normal	Generalized tonic-clonic seizure	Sodium valproate
9	9.36	28	9	9.67	15	Language deficit	Generalized tonic-clonic seizure	Lamotrigine
10	9.48	45	10	7.79	23	Normal	Generalized tonic-clonic seizure	Micropakine
11	10.32	18	11	8.91	16	Normal	Generalized tonic-clonic seizure	Trileptal
12	7.98	20		–	–	-	–	–
Mean ± SD	9.3 ± 1.7	27 ± 17		9.6 ± 2.4	29.7 ± 14			

Statistical Analysis

Group differences in FC and global network metrics were statistically evaluated. Statistical comparisons between patients and controls were performed using non-parametric permutation *t*-tests with $p < 0.05$ (Bonferroni corrected for multiple comparisons). We further used *Post-hoc t*-tests to explore the directionality of effects over conditions with $p < 0.05$. A total of 1000 permutations were used to determine the significance level for each test (Maris and Oostenveld, 2007). The results were then projected onto a 3D surface using BrainNet (Xia et al., 2013).

RESULTS

EEG Source Functional Connectivity

Figure 1 shows the average localization of interictal spikes in patients. As shown, all the patients exhibited an epileptic focus at the right hemisphere with a spatial extent restricted to the right central areas. Results of lagged connectivity differences between patients and healthy controls in all frequency bands are summarized in **Figure 2**. The major differences between the two groups were observed in the α and β bands. Compared to healthy controls, patients showed significantly increased α LPS over most cortical regions. There was also significantly reduced α LPS in the temporal and right centrotemporal areas. In contrast with the α band, significantly lower LPS values were observed in the β band in almost all brain regions of patients. In patients compared to controls, δ LPS values were significantly higher between the right anterior and posterior areas along the midline and lower between the temporal and posterocentral areas. In the θ band, patients displayed higher LPS values between temporal and central areas, mostly over the left hemisphere.

Global Network Measures

Figure 3 shows the global metric values over thresholds between 0.2 and 0.7. Patients presented higher global network degree and efficiency and lower clustering coefficients in the θ and α bands.

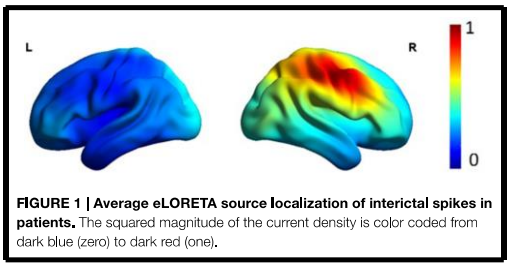

FIGURE 1 | Average eLORETA source localization of interictal spikes in patients. The squared magnitude of the current density is color coded from dark blue (zero) to dark red (one).

At higher frequencies (β), patients were characterized by lower values for all three measures over thresholds up to 0.4. At very low frequency (δ), no significant differences were observed over all of the threshold range between patients and healthy controls. **Table 2** presents the optimal thresholds used to compute the global network degree (K), global clustering coefficient (C), and global efficiency (E) for both groups.

Nodal Network Degree and Clustering Coefficient

Figure 4 illustrates the regions presenting statistically significant differences between patients and healthy controls for nodal network degree (K) and clustering coefficient (C) computed using optimal thresholds.

Network Degree (K)

In the δ band, patients, compared to controls displayed higher network degree values at the right somatosensory cortex, left motor cortex and right occipital lobe and decreased K at the right anterior frontal cortex and opercula frontal regions. In the θ band, patients showed significantly higher K values at the right inferior temporal and left primary auditory cortex. In the α band, patients displayed a higher K at the right posterior cingulate

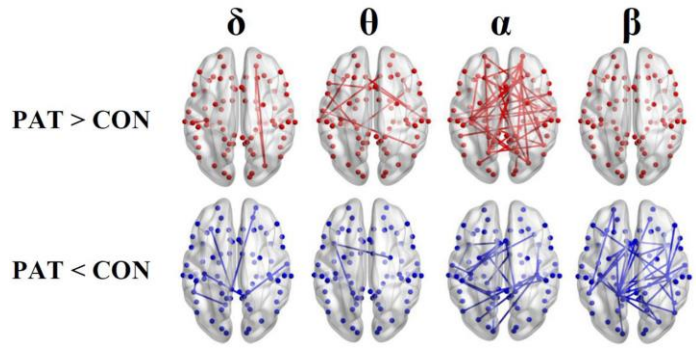

FIGURE 2 | Results of the functional resting-state source connectivity analysis with the seeds located at the Brodmann area centroids. The upper and lower rows indicate significantly higher (red lines) and lower (blue lines) connectivity values in patients (PAT) compared to controls (CON), respectively.

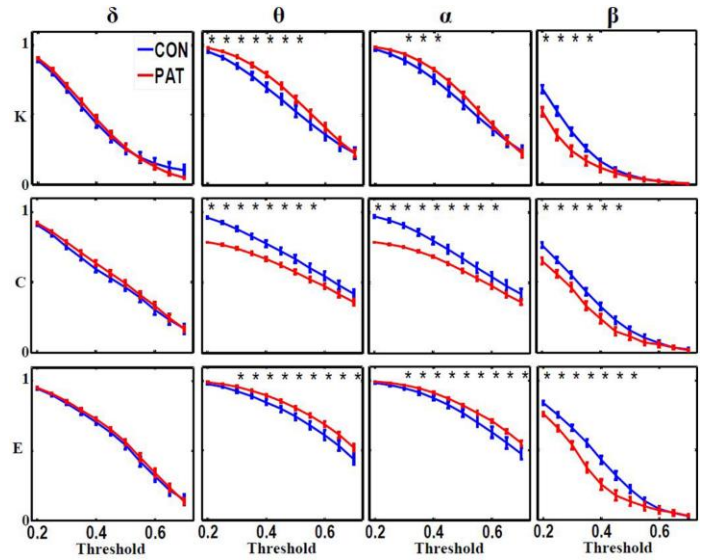

FIGURE 3 | Global network degree (K), clustering coefficient (C) and efficiency (L) as a function of threshold values for each frequency band. The error bars represent the standard error of the mean with 95% confidence intervals and * indicate significant differences between PAT and CON.

cortex, right temporal and left isthmus of the cingulate cortex. In both the α and β bands, patients displayed lower K values at the left frontal cortex. In the β band, patients displayed higher K values at the right superior parietal and left prefrontal cortex.

Clustering Coefficient (C)

In the δ band, patients displayed higher clustering coefficient (C) at the right primary motor and visual cortex, right cingulate gyrus, and lower C values at the left primary auditory cortex. In the θ band, patients displayed higher C values at the right postcentral, right angular gyrus and left dorsal cingulate gyrus and lower C in the left intermediate frontal region. In the α band, patients displayed higher C values at the right primary motor and right posterior cingulate cortices, and, in the β band, displayed a decreased C at the right orbital frontal with higher C values in the frontal regions.

DISCUSSION

In this study, we investigated abnormal patterns of resting-state EEG FC in BECTS patients using graph metrics in various frequency bands. Our results suggest that the functionality of brain networks in BECTS patients is altered, particularly in the α and β bands. Compared to healthy subjects, BECTS patients were characterized by widespread higher and lower phase synchronization values in the α and β bands, respectively.

In the θ and α bands, significantly lower global clustering coefficient and higher network degree and efficiency were observed in patients. In contrast, compared to controls, patients displayed significant lower global metrics in the β band. In the δ band, no significant differences in global graph metrics were observed between patients and controls.

TABLE 2 | Mean values (with range at 95% confidence interval) of threshold (T), degree (K), clustering coefficient (C), and global efficiency (E) computed for each group and frequency band.

	Frequency band	T	K	C	E
Controls (CON)	δ	0.54 ± 0.05	0.16 ± 0.05	0.42 ± 0.03	0.48 ± 0.04
	θ	0.70 ± 0.05	0.14 ± 0.05	0.44 ± 0.04	0.47 ± 0.05
	α	0.71 ± 0.05	0.15 ± 0.05	0.45 ± 0.03	0.46 ± 0.04
	β	0.38 ± 0.02	0.18 ± 0.01	0.46 ± 0.00	0.53 ± 0.01
Patients (PAT)	δ	0.54 ± 0.02	0.17 ± 0.00	0.43 ±0.01	0.51 ± 0.01
	θ	0.72 ± 0.03	0.16 ± 0.01	0.43 ± 0.01	0.50 ± 0.01
	α	0.73 ± 0.02	0.15 ± 0.01	0.41 ± 0.02	0.49 ± 0.00
	β	0.32 ± 0.03	0.17 ± 0.00	0.42 ± 0.02	0.44 ± 0.01

Global Functional Integration and Segregation

The human brain is very complex, comprising inhibitory and excitatory circuits that interact by integrating information at local and global levels. The functional segregation and integration of brain networks is expected to be balanced in healthy subjects. It has been shown that the normal brain has a small world functional topology, which can efficiently combine functionally specialized (segregated) modules with intermodular (integrating) links (Bassett and Bullmore, 2006). This type of organization reflects an optimal balance between functional integration and integration (Bassett and Bullmore, 2006; Ponten et al., 2007).

In BECTS patients, however, we found that the functional organization of brain networks was altered in a frequency dependent manner. Our results indicate that the interictal state in BECTS patients is less well ordered, displaying lower segregation (lower global clustering coefficient) and higher integration (higher global efficiency and network degree) in the θ and α bands. This finding is in line with the results reported in our previous study (Adebimpe et al., 2015b) and other related studies (Clemens, 2004; Boor et al., 2007; Quraan et al., 2013). As a characteristic feature of BECTS, the alteration in brain functional organization might be explained by the abnormal significant increase in the power of θ oscillations (Clemens, 2004; Clemens et al., 2010; Douw et al., 2010; Adebimpe et al., 2014, 2015a).

In the α band, the lower clustering coefficient and the higher network degree might be due to the loss of local connectivity between neighbor nodes in comparison to increased long distance connections in BECTS patients, as shown in **Figure 2**. The less ordered network configuration in patients with BECTS has also been reported in previous studies on epilepsy (Ponten

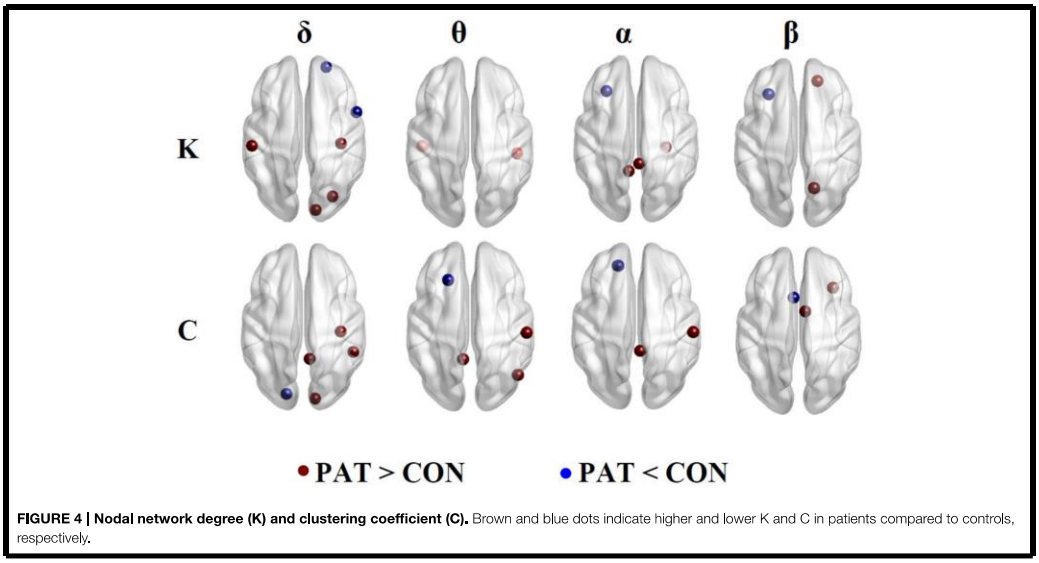

FIGURE 4 | Nodal network degree (K) and clustering coefficient (C). Brown and blue dots indicate higher and lower K and C in patients compared to controls, respectively.

et al., 2007; Quraan et al., 2013; Adebimpe et al., 2015b) and other neurological diseases (Liu et al., 2008; Stam et al., 2009; Wang et al., 2009; Zhang et al., 2011) compared to healthy controls. Our findings are consistent with a recent fMRI study (Song et al., 2015) reporting low local efficiency (an alternative to the clustering coefficient) and high global efficiency in BECTS patients. Our findings are also in agreement with those of Quraan et al. (2013), who reported low C and short L (high E) in patients with temporal lobe epilepsy (TLE) in the α band. In patients with focal epilepsy, however, higher clustering coefficients and longer path lengths have been reported in comparison to healthy subjects (Bernasconi et al., 2003; van Diessen et al., 2014; Taylor et al., 2015). Both TLE and focal epilepsy are known to be associated with abnormal structural brain alterations. In BECTS, there is no evidence of alterations in the brain structure.

In the β band, we observed a significant pruning of long- and short-distance functional connections in BECTS patients, who exhibited reduced clustering coefficient (representing functional segregation) and lower global efficiency and network degree (representing functional integration) compared to healthy controls. The frequency-dependent alterations in the brain functional organization in BECTS patients may constitute specific biomarkers of the benign epilepsy.

In healthy subjects, studies of large-scale brain FC have also shown that interactions between spatially distinct brain regions are frequency dependent. Delta, theta and alpha FC have been shown to be related to attention, learning, memory, and emotion processing (Knyazev, 2007; Bekkedal et al., 2011; Calmels et al., 2012). Alpha FC is also shown to be associated to motor performance in adults (Sauseng et al., 2005; Klimesch et al., 2007; Palva and Palva, 2007). Based on these findings, we postulate that in BECTS patients alterations in brain FC in different frequency bands may cause cognitive, mental, memory and attention impairment (Baglietto et al., 2001; Datta et al., 2013; Kim et al., 2014; Verrotti et al., 2014).

Local Changes in Functional Connectivity

Our FC analysis at Brodmann areas revealed higher network degree and clustering coefficient in epileptogenic areas, including centrotemporal, premotor, and somatosensory regions in the θ and α bands in BECTS patients. We also found higher degree in the posterior cingulate cortex in patients in the θ and α bands. This finding is consistent with the results of previous studies (Boor et al., 2007; Besseling et al., 2013; Tang et al., 2014) indicating higher activity in the supplementary motor region in epileptic patients. Our results also confirmed the higher phase synchronization values in the regions with increased local segregation neural processing (high clustering coefficient), especially in the primary motor, postcentral and posterior cingulate regions. Significantly, higher phase synchronization values were also observed in the central regions, including somatosensory cortex and motor cortex (Avanzini et al., 2012). However, a decreased network degree was observed in the right frontal cortex in the α and β bands, and a low clustering coefficient was also observed in the intermediate frontal region in the θ band. The frontal lobe is known to play a major role in the processing and execution of higher cognitive skills and behaviors (Stuss, 2011) and children with benign epilepsy have been found to present cognitive deficits and impaired mental activity (Ay et al., 2009; Datta et al., 2013; Verrotti et al., 2014). Furthermore, the right auditory network, including right temporal, parietal and left auditory cortex (in θ band), also showed altered (higher) functional integration (network degree) in patients, which could affect auditory processing in both hemispheres, resulting in language processing deficits in BECTS patients (Naganuma et al., 1994; Tomé et al., 2014; Filippini et al., 2015).

Several fMRI studies have reported impairments in different brain networks in BECTS patients (Kim et al., 2014; Yang et al., 2015; Xiao et al., 2015a,b). We also found differences in brain functional organization between BECTS patients and healthy controls. Although some studies reported associations between EEG rhythms and fMRI maps but there are some inconsistencies (Laufs et al., 2003; Mantini et al., 2007; Bridwell et al., 2013) due to underlying differences between these modalities as EEG measures direct neuronal activity while fMRI records indirectly brain activity.

In our previous work (Adebimpe et al., 2015b), we compared patients and controls using three graph metrics, degree, clustering coefficient and path length computed using sensor-level EEG data. In that study, we used the Phase Locking Value (PLV) as a measure of FC between electrodes to explore the global topology and dynamics of functional interactions between large-scale brain regions during the resting state over a range of frequencies. The results obtained using the sensor- and source-level connectivity analyses were consistent. In the present study, we also found higher clustering coefficients and shorter path lengths in the theta and alpha bands in BECTS patients compared to controls. However, the FC analysis in the sensor space is more sensitive to artifacts of volume conduction especially using zero-lag connectivity measures like PLV. Moreover, statistical comparisons at the group level are less reliable at the sensor space because of variability in EEG electrode positions across subjects. Instead, FC estimated at the source level reflects actual interactions between brain areas.

Methodological Consideration and Limitations

In this study, we used eLORETA, an improved version of LORETA, for source imaging. It has been reported that this technique has no localization bias even in the presence of structured noise (Pascual-Marqui, 2007a). However, this technique like other EEG localization method is vulnerable to artifacts of volume conduction, head-modeling errors and EEG noise (Grech et al., 2008). Moreover, since the results of LORETA are model dependent, it may not accurately represent the neuronal origins of the brain activity (Hata et al., 2016).

Another major challenge is the choice of source FC analysis. The majority of zero-lag connectivity measures such as correlation, coherence, and PLV are developed based on scalp sensors and thus sensitive to volume conduction effect (Gross et al., 2001). In a MEG study, Ghuman et al. (2011) have shown that artifacts of volume conduction can result in increased false-positive PLVs. To reduce the effect of volume conduction on

the results of the source connectivity analysis, we used the LPS to investigate FC in the source space (Pascual-Marqui, 2007b). This method has been successfully used to explore EEG source FC in epilepsy studies (Canuet et al., 2011; Vecchio et al., 2015; Hata et al., 2016). This connectivity measure is resistant to artifacts of volume conduction by excluding the instantaneous zero-lag contribution (Canuet et al., 2011; Vinck et al., 2011). However, like phase lag index, LPS's sensitivity to uncorrelated perturbation, which can turn phase lags into leads, has to be investigated especially when EEG noise is strong (Nolte et al., 2004; Stam et al., 2007; Vinck et al., 2011).

We further used a ROI-based approach, which is a common practice in neuroimaging studies to reduce variability in brain size and shape between individuals which might affect estimation of source FC (Schoffelen and Gross, 2009). This approach is based on the BA regions cytoarchitectonically defined in the Talairach atlas. The ROI for each of 84 BA regions was defined as a single centroid voxel (the closest to the center of each region). The ROI-approach is more efficient in reducing volume conduction artifacts than the voxel-by-voxel connectivity analysis as it has been shown that the spatial correlation between sources decays with increasing distance between them (Mehrkanoon et al., 2014).

Our results should be interpreted with caution because of the low sample size, limited number of EEG segments, and short EEG data lengths. Apart from technical limitations, collecting long EEG recordings from children under age 16 is difficult because they cannot adequately follow instructions. We further had to exclude artifactual EEG portions and segments with interictal spikes from our analysis. Therefore, for each subject only five segments were randomly selected for FC analysis. Further studies with larger samples and longer EEG recordings are required to confirm our findings.

CONCLUSION

In this study, we investigated functional alterations in BECTS patients with BECTS. Compared to controls, patients were characterized by higher θ and α and lower β phase synchronization values. Our observations support previously reported evidence that alteration in BECTS brain networks is frequency-dependent, as patients showed lower clustering coefficients in the three frequency bands. Our findings suggest that benign focal epilepsy is associated with altered resting state FC that probably arises from disrupted topological organization of resting-state functional brain networks.

AUTHOR CONTRIBUTIONS

Conceived and designed the experiments: AA, AA, FW. Performed the experiments: EB, MM. Analyzed the data: AA, AA. Contributed reagents/materials/analysis tools: AA, AA, EB, MM, FW. Wrote the paper: AA, AA, FW. Read and accepted the manuscript: AA, AA, EB, MM, FW.

REFERENCES

Adebimpe, A., Aarabi, A., Bourel-Ponchel, E., Mahmoudzadeh, M., and Wallois, F. (2015a). EEG resting state analysis of cortical sources in patients with benign epilepsy with centrotemporal spikes. *Neuroimage Clin.* 9, 275–282. doi: 10.1016/j.nicl.2015.08.014

Adebimpe, A., Aarabi, A., Bourel-Ponchel, E., Mahmoudzadeh, M., and Wallois, F. (2015b). Functional brain dysfunction in patients with benign childhood epilepsy as revealed by graph theory. *PLoS ONE* 10:e0139228. doi: 10.1371/journal.pone.0139228

Adebimpe, A. A., Aarabi, A., Bourel, E., Mahmoudzadeh, M., and Wallois, F. (2016). ID 234 – brain network analysis of EEG functional connectivity in patients with benign childhood epilepsy with centro-temporal spikes. *Clin. Neurophysiol.* 127:e60. doi: 10.1016/j.clinph.2015.11.198

Adebimpe, A. A., Aarabi, A., Mahmoudzadeh, M., Bourel-Ponchel, E., and Wallois, F. (2014). LP7: the comparison of resting state networks between normal children and adolescents with benign childhood epilepsy with centrotemporal spikes: a high density EEG study. *Clin. Neurophysiol.* 125, S80–S81. doi: 10.1016/s1388-2457(14)50268-4

Avanzini, G., Manganotti, P., Meletti, S., Moshé, S. L., Panzica, F., Wolf, P., et al. (2012). The system epilepsies: a pathophysiological hypothesis. *Epilepsia* 53, 771–778. doi: 10.1111/j.1528-1167.2012.03462.x

Ay, Y., Gokben, S., Serdaroglu, G., Polat, M., Tosun, A., Tekgul, H., et al. (2009). Neuropsychologic impairment in children with rolandic epilepsy. *Pediatr. Neurol.* 41, 359–363. doi: 10.1016/j.pediatrneurol.2009.05.013

Baglietto, M. G., Battaglia, F. M., Nobili, L., Tortorelli, S., De Negri, E., Calevo, M. G., et al. (2001). Neuropsychological disorders related to interictal epileptic discharges during sleep in benign epilepsy of childhood with centrotemporal or Rolandic spikes. *Dev. Med. Child Neurol.* 43, 407–412. doi: 10.1017/S0012162201000755

Bassett, D. S., and Bullmore, E. (2006). Small-world brain networks. *Neurosci. Rev. J. Bringing Neurobiol. Neurol. Psychiatry* 12, 512–523. doi: 10.1177/1073858406293182

Bassett, D. S., Meyer-Lindenberg, A., Achard, S., Duke, T., and Bullmore, E. (2006). Adaptive reconfiguration of fractal small-world human brain functional networks. *Proc. Natl. Acad. Sci. U.S.A.* 103, 19518–19523. doi: 10.1073/pnas.0606005103

Bekkedal, M. Y. V., Rossi, J., and Panksepp, J. (2011). Human brain EEG indices of emotions: delineating responses to affective vocalizations by measuring frontal theta event-related synchronization. *Neurosci. Biobehav. Rev.* 35, 1959–1970. doi: 10.1016/j.neubiorev.2011.05.001

Bernasconi, N., Bernasconi, A., Caramanos, Z., Antel, S. B., Andermann, F., and Arnold, D. L. (2003). Mesial temporal damage in temporal lobe epilepsy: a volumetric MRI study of the hippocampus, amygdala and parahippocampal region. *Brain J. Neurol.* 126, 462–469. doi: 10.1093/brain/awg034

Besseling, R. M. H., Jansen, J. F. A., Overvliet, G. M., van der Kruijs, S. J. M., Vles, J. S. H., Ebus, S. C. M., et al. (2013). Reduced functional integration of the sensorimotor and language network in rolandic epilepsy. *Neuroimage Clin.* 2, 239–246. doi: 10.1016/j.nicl.2013.01.004

Boor, R., Jacobs, J., Hinzmann, A., Bauermann, T., Scherg, M., Boor, S., et al. (2007). Combined spike-related functional MRI and multiple source analysis in the non-invasive spike localization of benign rolandic epilepsy. *Clin. Neurophysiol.* 118, 901–909. doi: 10.1016/j.clinph.2006.11.272

Bridwell, D. A., Wu, L., Eichele, T., and Calhoun, V. D. (2013). The spatiospectral characterization of brain networks: fusing concurrent EEG spectra and fMRI maps. *Neuroimage* 69, 101–111. doi: 10.1016/j.neuroimage.2012.12.024

Calmels, C., Foutren, M., and Stam, C. J. (2012). Beta functional connectivity modulation during the maintenance of motion information in working memory: importance of the familiarity of the visual context. *Neuroscience* 212, 49–58. doi: 10.1016/j.neuroscience.2012.03.045

Canuet, L., Ishii, R., Pascual-Marqui, R. D., Iwase, M., Kurimoto, R., Aoki, Y., et al. (2011). Resting-state EEG source localization and functional

connectivity in schizophrenia-like psychosis of epilepsy. *PLoS ONE* 6:e27863. doi: 10.1371/journal.pone.0027863

Clemens, B. (2004). Pathological theta oscillations in idiopathic generalised epilepsy. *Clin. Neurophysiol.* 115, 1436–1441. doi: 10.1016/j.clinph.2004.01.018

Clemens, B., Bessenyei, M., Fekete, I., Puskás, S., Kondákor, I., Tóth, M., et al. (2010). Theta EEG source localization using LORETA in partial epilepsy patients with and without medication. *Clin. Neurophysiol.* 121, 848–858. doi: 10.1016/j.clinph.2010.01.020

Datta, A. N., Oser, N., Bauder, F., Maier, O., Martin, F., Ramelli, G. P., et al. (2013). Cognitive impairment and cortical reorganization in children with benign epilepsy with centrotemporal spikes. *Epilepsia* 54, 487–494. doi: 10.1111/epi.12067

Deco, G., and Kringelbach, M. L. (2014). Great expectations: using whole-brain computational connectomics for understanding neuropsychiatric disorders. *Neuron* 84, 892–905. doi: 10.1016/j.neuron.2014.08.034

Douw, L., van Dellen, E., de Groot, M., Heimans, J. J., Klein, M., Stam, C. J., et al. (2010). Epilepsy is related to theta band brain connectivity and network topology in brain tumor patients. *BMC Neurosci.* 11:103. doi: 10.1186/1471-2202-11-103

Drakesmith, M., Caeyenberghs, K., Dutt, A., Lewis, G., David, A. S., and Jones, D. K. (2015). Overcoming the effects of false positives and threshold bias in graph theoretical analyses of neuroimaging data. *Neuroimage* 118, 313–333. doi: 10.1016/j.neuroimage.2015.05.011

Erdős, P., and Rényi, A. (2013). On the strength of connectedness of a random graph. *Acta Math. Acad. Sci. Hung.* 12, 261–267. doi: 10.1007/BF02066689

Filippini, M., Boni, A., Giannotta, M., Pini, A., Russo, A., Musti, M. A., et al. (2015). Comparing cortical auditory processing in children with typical and atypical benign epilepsy with centrotemporal spikes: electrophysiologic evidence of the role of non–rapid eye movement sleep abnormalities. *Epilepsia* 56, 726–734. doi: 10.1111/epi.12959

Fonov, V., Evans, A. C., Botteron, K., Almli, C. R., McKinstry, R. C., and Collins, D. L. (2011). Unbiased average age-appropriate atlases for pediatric studies. *Neuroimage* 54, 313–327. doi: 10.1016/j.neuroimage.2010.07.033

Ghuman, A. S., McDaniel, J. R., and Martin, A. (2011). A wavelet-based method for measuring the oscillatory dynamics of resting-state functional connectivity in MEG. *Neuroimage* 56, 69–77. doi: 10.1016/j.neuroimage.2011.01.046

Grech, R., Cassar, T., Muscat, J., Camilleri, K. P., Fabri, S. G., Zervakis, M., et al. (2008). Review on solving the inverse problem in EEG source analysis. *J. Neuroengineering Rehabil.* 5:25. doi: 10.1186/1743-0003-5-25

Gross, J., Kujala, J., Hamalainen, M., Timmermann, L., Schnitzler, A., and Salmelin, R. (2001). Dynamic imaging of coherent sources: studying neural interactions in the human brain. *Proc. Natl. Acad. Sci. U.S.A.* 98, 694–699. doi: 10.1073/pnas.98.2.694

Hata, M., Kazui, H., Tanaka, T., Ishii, R., Canuet, L., Pascual-Marqui, R. D., et al. (2016). Functional connectivity assessed by resting state EEG correlates with cognitive decline of Alzheimer's disease – an eLORETA study. *Clin. Neurophysiol.* 127, 1269–1278. doi: 10.1016/j.clinph.2015.10.030

Holmes, G. L. (1993). Benign focal epilepsies of childhood. *Epilepsia* 34, S49–S61. doi: 10.1111/j.1528-1167.1993.tb06259.x

Kim, E.-H., Yum, M.-S., Kim, H.-W., and Ko, T.-S. (2014). Attention-deficit/hyperactivity disorder and attention impairment in children with benign childhood epilepsy with centrotemporal spikes. *Epilepsy Behav.* 37, 54–58. doi: 10.1016/j.yebeh.2014.05.030

Klimesch, W., Sauseng, P., and Hanslmayr, S. (2007). EEG alpha oscillations: the inhibition-timing hypothesis. *Brain Res. Rev.* 53, 63–88. doi: 10.1016/j.brainresrev.2006.06.003

Knyazev, G. G. (2007). Motivation, emotion, and their inhibitory control mirrored in brain oscillations. *Neurosci. Biobehav. Rev.* 31, 377–395. doi: 10.1016/j.neubiorev.2006.10.004

Kramer, M. A., and Cash, S. S. (2012). Epilepsy as a disorder of cortical network organization. *Neurosci. Rev. J. Bringing Neurobiol. Neurol. Psychiatry* 18, 360–372. doi: 10.1177/1073858411422754

Laufs, H. (2012). Functional imaging of seizures and epilepsy: evolution from zones to networks. *Curr. Opin. Neurol.* 25, 194–200. doi: 10.1097/WCO.0b013e3283515db9

Laufs, H., Kleinschmidt, A., Beyerle, A., Eger, E., Salek-Haddadi, A., Preibisch, C., et al. (2003). EEG-correlated fMRI of human alpha activity. *Neuroimage* 19, 1463–1476. doi: 10.1016/S1053-8119(03)00286-6

Liu, Y., Liang, M., Zhou, Y., He, Y., Hao, Y., Song, M., et al. (2008). Disrupted small-world networks in schizophrenia. *Brain* 131, 945–961. doi: 10.1093/brain/awn018

Mantini, D., Perrucci, M. G., Del Gratta, C., Romani, G. L., and Corbetta, M. (2007). Electrophysiological signatures of resting state networks in the human brain. *Proc. Natl. Acad. Sci. U.S.A.* 104, 13170–13175. doi: 10.1073/pnas.0700668104

Maris, E., and Oostenveld, R. (2007). Nonparametric statistical testing of EEG- and MEG-data. *J. Neurosci. Methods* 164, 177–190. doi: 10.1016/j.jneumeth.2007.03.024

Mehrkanoon, S., Breakspear, M., Britz, J., and Boonstra, T. W. (2014). Intrinsic coupling modes in source-reconstructed electroencephalography. *Brain Connect.* 4, 812–825. doi: 10.1089/brain.2014.0280

Naganuma, Y., Konishi, T., Hongou, K., Murakami, M., Yamatani, M., Yagi, S., et al. (1994). Auditory event-related potentials in benign childhood epilepsy with centrotemporal spike: the effects of carbamazepine. *Clin. EEG Electroencephalogr.* 25, 8–12. doi: 10.1177/155005949402500105

Nolte, G., Bai, O., Wheaton, L., Mari, Z., Vorbach, S., and Hallett, M. (2004). Identifying true brain interaction from EEG data using the imaginary part of coherency. *Clin. Neurophysiol.* 115, 2292–2307. doi: 10.1016/j.clinph.2004.04.029

Oostenveld, R., Fries, P., Maris, E., and Schoffelen, J.-M. (2010). FieldTrip: open source software for advanced analysis of MEG, EEG, and invasive electrophysiological data. *Comput. Intell. Neurosci.* 2011:e156869. doi: 10.1155/2011/156869

Palva, S., and Palva, J. M. (2007). New vistas for alpha-frequency band oscillations. *Trends Neurosci.* 30, 150–158. doi: 10.1016/j.tins.2007.02.001

Panayiotopoulos, C. P. (1999). *Benign Childhood Partial Seizures and Related Epileptic Syndromes.* Lodon: John Libbey Eurotext.

Pascual-Marqui, R. D. (2007a). Discrete, 3D distributed, linear imaging methods of electric neuronal activity. Part 1: exact, zero error localization. *ArXiv07103341 Math Phys. Q-Bio*. Available online at: http://arxiv.org/abs/0710.3341 [Accessed January 21, 2015].

Pascual-Marqui, R. D. (2007b). Instantaneous and lagged measurements of linear and nonlinear dependence between groups of multivariate time series: frequency decomposition. *ArXiv07111455 Stat*. Available online at: http://arxiv.org/abs/0711.1455 [Accessed October 29, 2015].

Pascual-Marqui, R. D., Lehmann, D., Koukkou, M., Kochi, K., Anderer, P., Saletu, B., et al. (2011). Assessing interactions in the brain with exact low-resolution electromagnetic tomography. *Philos. Transact. A Math. Phys. Eng. Sci.* 369, 3768–3784. doi: 10.1098/rsta.2011.0081

Ponten, S. C., Bartolomei, F., and Stam, C. J. (2007). Small-world networks and epilepsy: graph theoretical analysis of intracerebrally recorded mesial temporal lobe seizures. *Clin. Neurophysiol.* 118, 918–927. doi: 10.1016/j.clinph.2006.12.002

Prinz, A. A. (2008). Understanding epilepsy through network modeling. *Proc. Natl. Acad. Sci. U.S.A.* 105, 5953–5954. doi: 10.1073/pnas.0802299105

Quraan, M. A., McCormick, C., Cohn, M., Valiante, T. A., and McAndrews, M. P. (2013). Altered resting state brain dynamics in temporal lobe epilepsy can be observed in spectral power, functional connectivity and graph theory metrics. *PLoS ONE* 8:e68609. doi: 10.1371/journal.pone.0068609

Rubinov, M., and Sporns, O. (2010). Complex network measures of brain connectivity: uses and interpretations. *Neuroimage* 52, 1059–1069. doi: 10.1016/j.neuroimage.2009.10.003

Sauseng, P., Klimesch, W., Stadler, W., Schabus, M., Doppelmayr, M., Hanslmayr, S., et al. (2005). A shift of visual spatial attention is selectively associated with human EEG alpha activity. *Eur. J. Neurosci.* 22, 2917–2926. doi: 10.1111/j.1460-9568.2005.04482.x

Schoffelen, J.-M., and Gross, J. (2009). Source connectivity analysis with MEG and EEG. *Hum. Brain Mapp.* 30, 1857–1865. doi: 10.1002/hbm.20745

Song, J., Nair, V. A., Gaggl, W., and Prabhakaran, V. (2015). Disrupted brain functional organization in epilepsy revealed by graph theory analysis. *Brain Connect.* 5, 276–283. doi: 10.1089/brain.2014.0308

Stam, C. J., de Haan, W., Daffertshofer, A., Jones, B. F., Manshanden, I., van Cappellen van Walsum, A. M., et al. (2009). Graph theoretical analysis of magnetoencephalographic functional connectivity in Alzheimer's disease. *Brain* 132, 213–224. doi: 10.1093/brain/awn262

Stam, C. J., Nolte, G., and Daffertshofer, A. (2007). Phase lag index: assessment of functional connectivity from multi channel EEG and MEG with diminished bias from common sources. *Hum. Brain Mapp.* 28, 1178–1193. doi: 10.1002/hbm.20346

Stuss, D. T. (2011). Functions of the frontal lobes: relation to executive functions. *J. Int. Neuropsychol. Soc.* 17, 759–765. doi: 10.1017/S1355617711000695

Tang, Y.-L., Ji, G.-J., Yu, Y., Wang, J., Wang, Z.-J., Zang, Y.-F., et al. (2014). Altered regional homogeneity in rolandic epilepsy: a resting-state fMRI study. *Biomed. Res. Int.* 2014:e960395. doi: 10.1155/2014/960395

Taylor, P. N., Han, C. E., Schoene-Bake, J.-C., Weber, B., and Kaiser, M. (2015). Structural connectivity changes in temporal lobe epilepsy: spatial features contribute more than topological measures. *Neuroimage Clin.* 8, 322–328. doi: 10.1016/j.nicl.2015.02.004

Tomé, D., Sampaio, M., Mendes-Ribeiro, J., Barbosa, F., and Marques-Teixeira, J. (2014). Auditory event-related potentials in children with benign epilepsy with centro-temporal spikes. *Epilepsy Res.* 108, 1945–1949. doi: 10.1016/j.eplepsyres.2014.09.021

van Diessen, E., Zweiphenning, W. J. E. M., Jansen, F. E., Stam, C. J., Braun, K. P. J., and Otte, W. M. (2014). Brain network organization in focal epilepsy: a systematic review and meta-analysis. *PLoS ONE* 9:e114606. doi: 10.1371/journal.pone.0114606

Vecchio, F., Miraglia, F., Curcio, G., Della Marca, G., Vollono, C., Mazzucchi, E., et al. (2015). Cortical connectivity in fronto-temporal focal epilepsy from EEG analysis: a study via graph theory. *Clin. Neurophysiol.* 126, 1108–1116. doi: 10.1016/j.clinph.2014.09.019

Verrotti, A., Filippini, M., Matricardi, S., Agostinelli, M. F., and Gobbi, G. (2014). Memory impairment and Benign Epilepsy with centrotemporal spike (BECTS): a growing suspicion. *Brain Cogn.* 84, 123–131. doi: 10.1016/j.bandc.2013.11.014

Vinck, M., Oostenveld, R., van Wingerden, M., Battaglia, F., and Pennartz, C. M. A. (2011). An improved index of phase-synchronization for electrophysiological data in the presence of volume-conduction, noise and sample-size bias. *Neuroimage* 55, 1548–1565. doi: 10.1016/j.neuroimage.2011.01.055

Wang, L., Zhu, C., He, Y., Zang, Y., Cao, Q., Zhang, H., et al. (2009). Altered small-world brain functional networks in children with attention-deficit/hyperactivity disorder. *Hum. Brain Mapp.* 30, 638–649. doi: 10.1002/hbm.20530

Wirrell, E. C. (1998). Benign epilepsy of childhood with centrotemporal spikes. *Epilepsia* 39, S32–S41. doi: 10.1111/j.1528-1157.1998.tb05123.x

Xia, M., Wang, J., and He, Y. (2013). BrainNet viewer: a network visualization tool for human brain connectomics. *PLoS ONE* 8:e68910. doi: 10.1371/journal.pone.0068910

Xiao, F., Lei, D., An, D., Li, L., Chen, S., Chen, F., et al. (2015a). Functional brain connectome and sensorimotor networks in rolandic epilepsy. *Epilepsy Res.* 113, 113–125. doi: 10.1016/j.eplepsyres.2015.03.015

Xiao, F., Li, L., An, D., Lei, D., Tang, Y., Yang, T., et al. (2015b). Altered attention networks in benign childhood epilepsy with centrotemporal spikes (BECTS): a resting-state fMRI study. *Epilepsy Behav.* 45, 234–241. doi: 10.1016/j.yebeh.2015.01.016

Yang, B., Wang, X., Shen, L., Ye, X., Yang, G.-E., Fan, J., et al. (2015). The attentional networks in benign epilepsy with centrotemporal spikes. *Epilepsy Behav. EB* 53, 78–82. doi: 10.1016/j.yebeh.2015.09.034

Zhang, Z., Liao, W., Chen, H., Mantini, D., Ding, J.-R., Xu, Q., et al. (2011). Altered functional-structural coupling of large-scale brain networks in idiopathic generalized epilepsy. *Brain J. Neurol.* 134, 2912–2928. doi: 10.1093/brain/awr223

Zhang, Z., Liao, W., Wang, Z., Xu, Q., Yang, F., Mantini, D., et al. (2014). Epileptic discharges specifically affect intrinsic connectivity networks during absence seizures. *J. Neurol. Sci.* 336, 138–145. doi: 10.1016/j.jns.2013.10.024

Conflict of Interest Statement: The authors declare that the research was conducted in the absence of any commercial or financial relationships that could be construed as a potential conflict of interest.

All of these studies further supported the evidence that EEG resting-state functional connectivity in BCECTS patients was altered in a frequency dependent manner. In the next chapter, we focus on the direction of information flow between different brain regions in BCECTS patients.

Chapter 5

EEG resting state functional connectivity analysis in children with benign epilepsy with centrotemporal spikes, Part II

5.1 Introduction

In the previous chapter, we investigated frequency-dependent alterations in BCECTS functional brain network topology in BCECTS patients. Some regions especially the epileptic zone showed activation in the presence or absence of interictal epileptic discharges (IEDs). Despite the fact that BCECTS is focal, we found that epileptic brain reorganized because of lower activity at other regions especially frontal and posterior regions due to presence of IEDs at the centrotemporal region.

The lower activity at the frontal and posterior regions can be categorized as the primary effect of IEDs. However, in order to investigate the secondary effect of IEDs, we computed functional connectivity from the epileptic zone and its primary effect regions (frontal and posterior) to all other regions. This was done with the seed-based functional connectivity analysis. The BCECTS patients with and without IEDS functional connectivity patterns were compared to the healthy controls. The seed points were selected based on the results of our previous studies. In the second part of this chapter, the dynamic of directed interictal connectivity associated with IEDs was studied. This was done to investigate major drivers in BCECTS brain networks and effective connective pattern during IEDs.

5.2 Resting-state Functional Source connectivity

Large-Scale Network Dysfunction in Benign Childhood Epilepsy: A Resting-State Functional Source Connectivity Study

In the first part of this chapter, we investigated the impact of IEDs on the resting-state source functional connectivity (FC) pattern in BCECTS patients in comparison to the healthy controls. The FC in large-scale source space was computed by the Imaginary Coherence (IC) which has been demonstrated to be insensitive to the volume conduction (Nolte et al., 2004) and reflected true measure for studying brain connectivity in resting state EEG data. Some regions of interests (ROIs) were selected as seed points including the epileptic zone (right central), left central, prefrontal cortex and occipital regions. These regions were found to be activated/deactivated in our previous studies. The FC patterns from these regions to other regions were studied under three

conditions (controls, with and without IEDs in patients). The functional connectivity topology was characterized with two main graph metrics, betweenness and local efficiency. These two graph metrics were selected in order to investigated regions that involve as a central communicator between regions and as well as efficiency of the local between neighbor brain regions.

Through the resting-state source functional connectivity analysis, we found that the central regions including supplementary motor areas showed activation in the presence of IEDs. Higher FC patterns were also observed in the ipsilateral superior frontal region of the epileptic zone in these patients (see the following study for more details).

5.2.1 Introduction

Benign childhood epilepsy with centrotemporal spikes (BCECTS) is an idiopathic epilepsy syndrome usually affecting the young children under the age of 16 (Panayiotopoulos et al., 2008). BCECTS is characterized by the occurrence of biphasic sharp waves discharges arising from the precentral and postcentral gryi in the suprasylvian region with motor, sensory and autonomic manifestations in the face, mouth and throat (Bourel-Ponchel, 2013). Though the benign epilepsy is not associated with large structural changes(Camfield and Camfield, 2002), there are several reports of cognitive disturbances in BCECTS (Camfield and Camfield, 2014) such as memory, language, attention and auditory impairments in BCECTS children.

In BCECTS patients, beside microstructural changes within and around the epileptic zone (Ciumas et al., 2014) studies using EEG (Adebimpe et al., 2015a; Yeom et al., 2014) have reported abnormal distribution of spectral power and current source density especially within the epileptogenic zone but also in more distant areas including the language and speech networks(Besenyei et al., 2012). Over the past decade, the fMRI and EEG studies on the brain resting-state functional connectivity have reported altered functional interactions between brain networks in BCECTS and other types of epilepsy(Centeno and Carmichael, 2014; Tracy and Doucet, 2015). In BCECTS patients the functional alterations and reorganization of the brain networks have been observed not only in the epileptic zone but also in other distant neuronal networks areas(Adebimpe et al., 2015b) . However, little is known about the alteration of resting state brain networks in BCECTS.

In recent years, large scale functional connectivity analysis using high-density EEG data have gained attention in healthy subjects (Deco and Kringelbach, 2014) and in patients suffering from various diseases(Prinz, 2008; Stam et al., 2009; Zhang et al., 2014). In the present study, we performed seed-based functional connectivity analysis in BCECTS patients using high-density EEG data with or without interictal spikes in comparison to healthy controls. To assess spatial functional network interactions in different frequency bands, we reconstructed cortical source activities from high-density EEG recordings using a linear spatial filter(Gross et al., 2001)(Travis et al., 2010). Functional connectivity was computed by the imaginary coherence which has been shown to be insensitive to volume conduction artifacts(Nolte et al., 2004). We investigated voxel-wise whole-brain functional connectivity with a priori restriction to specific regions of interests (sROIs) based on our previous results obtained using the EEG power spectral analysis and functional connectivity in sensor and source spaces(Adebimpe et al., 2016, 2015a, 2015b). We also used the network metrics from the graph theory to measure the flow of information and local

efficiency in the brain networks. Our study was designed to investigate: (i) the functional connections from the origin of the epileptic zone to other brain regions, and (ii) the impact of interictal discharges on the BCECTS functional connectivity topology.

5.2.2 Materials and methods

Subjects

The EEG data were collected from twelve healthy controls (9.13 ± 1.50 years) and twenty-one children (9.73 ± 0.95 years) with BCECTS. The study was conducted in accordance with *Amiens University* Hospital's ethics committee (CPP Nord-Ouest No: 2011-A00782-39) and informed consent was obtained from each subject's parents. Healthy subjects had no history of neurological disorders. All patients showed no structural brain abnormalities on MRI.

High resolution EEG recording

EEG was recorded with an EEG system (ANT, Netherlands) using 64 electrodes placed on the scalp according to the international 10-10 systems. The EEG signals were recorded with a sampling frequency of 1024Hz. Linked-ear reference electrodes were used for data collection. All the subjects were fully awake with eyes closed. On average, 13 minutes of EEG were recorded for each subject.

Patient group

To better define the homogeneity of the patients, we first identified the location of interictal sources for each patient, using the spatiotemporal dipole modeling method (Advanced Source Analysis Software, Enschede, The Netherlands) (Scherg and Von Cramon, 1985) and the eLORETA (Pascual-Marqui, 2002) source localization method as implemented in the Fieldtrip (Oostenveld et al., 2011). Eleven of the twenty-one patients (9.25 ± 2.43 years) with only right centrotemporal spikes (CTS) were included in the epileptic group. Table 5.1 lists the characteristics of patients and controls and a summary of their EEG

Table 5.1: Characteristics of the control and patient groups

Control Group			Patient Group					
Subject	Age (years)	EEG duration (min)	Patient	Age (years)	EEG duration (min)	Neuropsychological assessment	Description of ictal EEG	Medication
1	6.73	16	1	12.63	50	Normal	Partial seizure	Sodium valproate
2	11.28	19	2	12.64	17	Normal	Partial seizure	Sodium valproate
3	10.48	19	3	9.25	44	Attention deficit	Generalized tonic-clonic seizure	Oxcarbezepine
4	10.66	17	4	6.03	43	-	Brachiofacial nocturnal seizure	Oxcarbezepine
5	7.39	13	5	10.47	50	Attention deficit	Partial seizure	Sodium valproate
6	7.31	20	6	7.16	14	-	Brachiofacial nocturnal seizure	Sodium valproate
7	11.92	30	7	8.51	30	Attention deficit	Nocturnal seizure	-
8	8.44	75	8	13.16	20	Normal	Generalized tonic-clonic seizure	Sodium valproate
9	9.36	28	9	9.67	15	Language deficit	Generalized tonic-clonic seizure	Lamotrigine
10	9.48	45	10	7.79	23	Normal	Generalized tonic-clonic seizure	Micropakine
11	10.32	18	11	8.91	16	Normal	Generalized tonic-clonic seizure	Trileptal
12	7.98	20		-	-	-	-	-
Mean±sd	9.3±1.7	27±17		9.6±2.4	29.7±14			

Pre-processing and artefa ct rejection

The EEG data were band-pass filtered between 0.5-40 Hz with a 4th order Butterworth filter and re-referenced to an average reference. The EEG recordings were then normalized by the Z-score transformation and thresholded using a threshold set to the mean of the z-score amplitude distribution for each channel, as implemented in Fieldtrip software[3] (Oostenveld et al., 2011), to identify and reject ocular, movement and muscular artifacts.

The artifact-free EEG portions of the recordings were then segmented into 2-second non-overlapping epochs. Five segments were randomly selected for each of the control subjects (CON). Two conditions were defined for the epileptic group: 5 segments with interictal spikes (with spikes condition - WSC) and 5 spike-free segments (with no spikes condition - NSC), all randomly selected. On average, WSC segments contained 7 interictal spikes.

Forward model

We used the Montreal Neurological Institute (MNI) brain MRI template for the construction of head model for lead field calculation using the Boundary Element Method (BEM) (Oostendorp and van Oosterom, 1989). The MNI template was segmented by SPM8(Ashburner et al., 2012, p. 8) into scalp, skull and brain compartments with conductivity values of 0.33 S/m, 0.0041 S/m and 0.33 S/m, respectively. The lead fields were calculated using FieldTrip (Oostenveld et al., 2011)

[3] http://www.fieldtriptoolbox.org/tutorial/visual_artifact_rejection

for 2726 source locations inside the brain. The electrodes were aligned to the head geometry using the fiducial points. The lead field, L(k), at each source location, k, was a 63 x 3 matrix, describing the contribution of source k to the sensors in 3 directions in the Cartesian space where 63 was the number of sensors in our study.

Source analysis

We used the beamforming method (Gross et al., 2001) to create spatial filters in order to estimate the spectral amplitude and phase of neuronal signals at source level. The three orthogonal (one for each direction) spatial filters, A, were computed for each source location k:

$$A(k,p) = [L^T(k) * C(p,p)^{-1} * L(k)]^{-1} * L^T(k) * C(p,p)^{-1} \quad (5.1)$$

Where L(k) is the lead field matrix at each source location with three orthogonal dipoles of all the sensors, C is the covariance matrix obtained from the sensor data, and p is the number of EEG channel. T indicates matrix transpose.

The eigenvalue decomposition method (Sekihara et al., 2004) was used to determine the dominant dipole orientation and to obtain high SNR for reconstructed source activities. This is done by weightening the filters with the first eigenvectors v (i.e, the eigenvector with the largest eigenvalue of the real part of the covariance matrix at source location, k):

$$v(k,p) = [v1, v2, v3] = svd(A(k,p) * C * A(k,p)^{*T}) \quad (5.2)$$

Where v1, v2 and v3 are spatial filters in x, y and z directions respectively. We linearly combined the three filters to a single filter pointing in the dominant dipole orientation:

$$F(k,p) = [v1, v2, v3] * [A_1(k,p)A_2(k,f) \; A_3(k,p)] \quad (5.3)$$

Finally, the source signal was obtained by multiplying the spatial filter with the raw EEG data in the sensors space:

$$S_{source}(k,t) = F(k,p) * S_{sensor}(p,t) \quad (5.4)$$

Functional connectivity analysis

We computed the spectral estimates of source signals by using the multi-taper Fourier transform (Mitra and Pesaran, 1999) with a frequency resolution of 0.5Hz for five frequency bands - δ (0.5–3.5 Hz), θ (4–8 Hz), α (8.5–13 Hz), β_1 (13.5–20 Hz) and β_2 (20.5–30 Hz). The multi-taper frequency method is similar to the classical Fourier transform but with a very good anti-frequency leakage property (van Vugt et al., 2007).

Functional interaction between sources was quantified by the imaginary coherence (IC).

The computation of IC is straightforward and computationally inexpensive even for analyzing large number of connections among numerous voxels. The IC is calculated as follows:

$$X = X_1 * X_2^* \tag{5.5}$$

$$IC = imag\left\{\frac{E\{X\}}{\sqrt{E\{|X_1|^2\}E\{|X_2|^2\}}}\right\} \tag{5.6}$$

Where X is the cross-spectrum of sources X_1 and X_2, and X_2^* is the complex conjugate of X_2. The results were 2726 by 2726 adjacent functional connectivity matrices.

We defined three regions of interest (ROIs) based on our previous studies, the epileptic zone (right central region area), the left frontal region and the right occipital region(Adebimpe et al., 2015b, 2015c) . The ROIs were defined based on the automated anatomical labeling (AAL) (Tzourio-Mazoyer et al., 2002). We computed the mean absolute IC between the sources in each ROI and all other voxels.

Graph theoretical analysis

To further quantify basic properties of local connectivity, we computed betweenness and efficiency(Bullmore and Sporns, 2009) for each subject and frequency band. Before computation of these metrics, we set the threshold of functional connectivity matrix to one standard deviation above median connectivity values to obtain networks with fully connected nodes.

The betweenness centrality measures the fraction of shortest paths in the network that pass through a given node and is defined as:

$$B_i = \frac{1}{(N-1)(N-2)} \sum_{h,j,h\neq j,h\neq i,j\neq i} \frac{P_{hj}(i)}{P_{hj}} \quad (5.7)$$

Where B_i is the betweenness of node i, P_{hj} is the total number of shortest paths between h and j and $P_{hj}(i)$ is the number of shortest paths that pass through node i.

The local efficiency of a particular node is similar to clustering coefficient that measure functional segregation:

$$LE_i = \frac{\sum_{j,h\in N,j\neq i} a_{ij}a_{ih}\left[d_{jh}(N_i)\right]^{-1}}{k_i(k_i-1)} \quad (5.8)$$

Where LE_i is the local efficiency at node i, a_{ij} and a_{ih} are the connection status (0 or 1) between nodes i and j, and between i and h, respectively, and $d_{jh}(N_i)$ is the sum of shortest paths between nodes j and h that contain the neighbors of node i.

Statistical analyses

We compared the voxel-by-voxel IC values between the three groups for all the frequency bands. This was done by nonparametric paired t-tests with multiple comparisons (Maris and Oostenveld, 2007) by randomly permuting source locations across the subjects (1000 resamples). The statistically significant ($p<0.01$) t-values were projected onto the MNI template surface with the BrainNet Viewer (Xia et al., 2013).

5.2.3 Results

Interictal spikes induced high activity at the centrotemporal region

We assessed the whole-brain source connectivity with the seed point located at the right central region (epileptogenic source) as shown in Figure 5.1. Both patients group showed increased functional connectivity from the right central to the left central region especially in the θ band. Meanwhile, patients with spike (WSC) exhibited stronger functional connectivity at the right central, parietal, supplementary motor area (SMA), bilateral rolandic region in the δ and β bands. Both epileptic conditions (with and without spikes) displayed significantly stronger functional connections from right central zone to the right frontal region in the δ band.

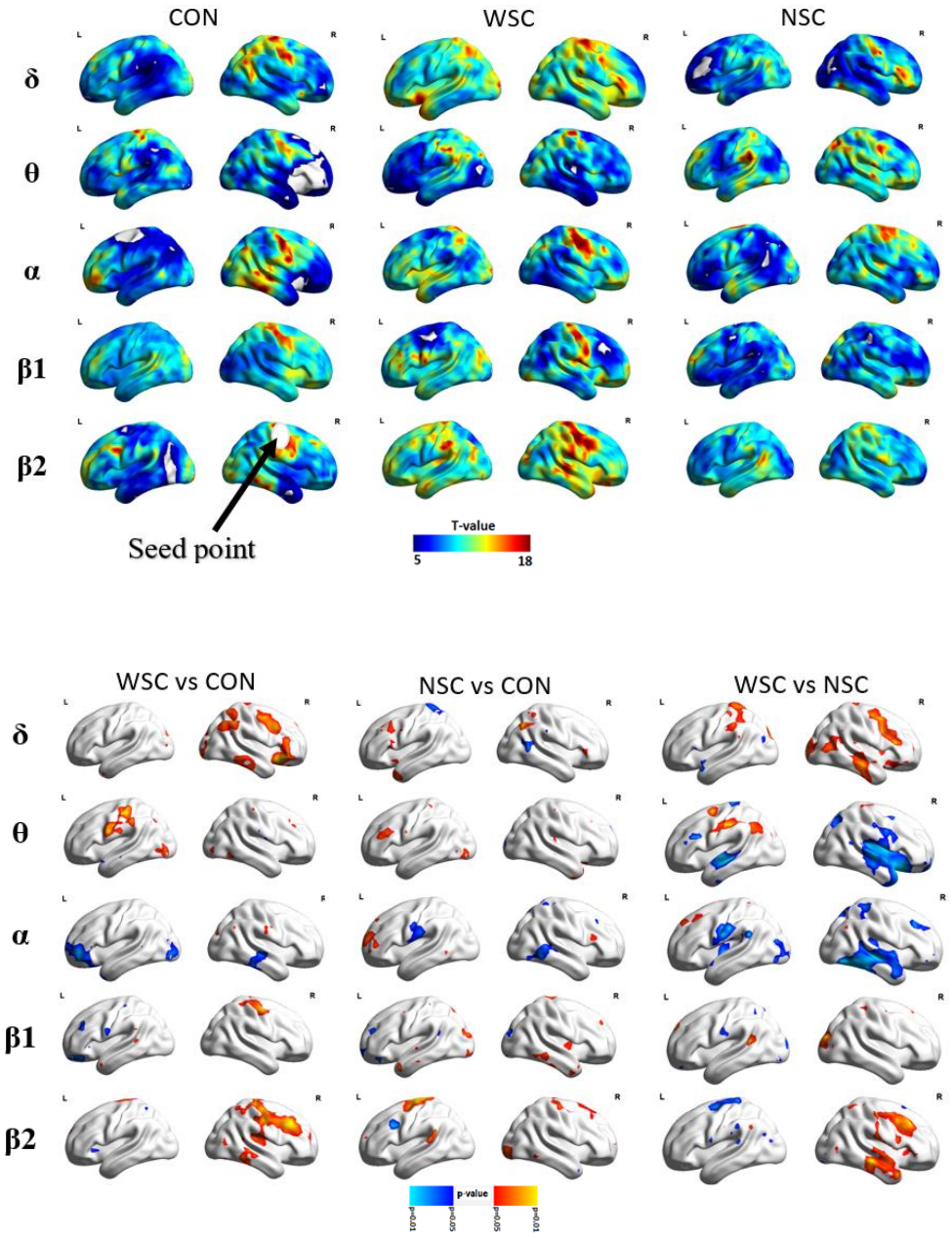

Figure 5.1: Right central seed region: Functional connection from the right central to other regions for each of the group; control (CON), patients group with the spike segments (WSC) and non-spike segments(NSC) and, comparison between the three conditions (WSC vs CON, NSC vs CON and WSC vs NSC).

We exploited the difference between the three groups for all the frequency bands. For each pair of groups as shown in Figure 5.1 WSC, compared to the other two conditions, had higher IC values at the epileptic region, right temporal, right frontal, parietal, occipital, frontal superior and prefrontal cortex in the δ band. In the presence of IEDs (WSC), higher IC values were observed at the left central region in the θ band. Meanwhile, decreased functional connectivity was observed in the prefrontal cortex in WSC compared to CON; and in the left central and right temporal

regions compared to NSC in the α band. In the β band, WSC showed higher IC values at the right central, right rolandic, right temporal, and SMA regions, in comparison to the other conditions. Compared to controls, patients under NSC showed stronger functional connections at the supplementary motor area in the β2 band.

Decreased functional connections in patients in the left central regions

Figure 5.2 shows lower functional connectivity in patients with the seed points at the left central regions. In all the group, there were direct functional connections between the left and right central regions especially in the δ and θ bands. Higher functional connectivity in healthy controls was found in the β1 band between the left and right central regions. Patients with IEDs exhibited higher functional connectivity from the left central to left temporal and rolandic regions in the δ, θ, α and β1 bands.

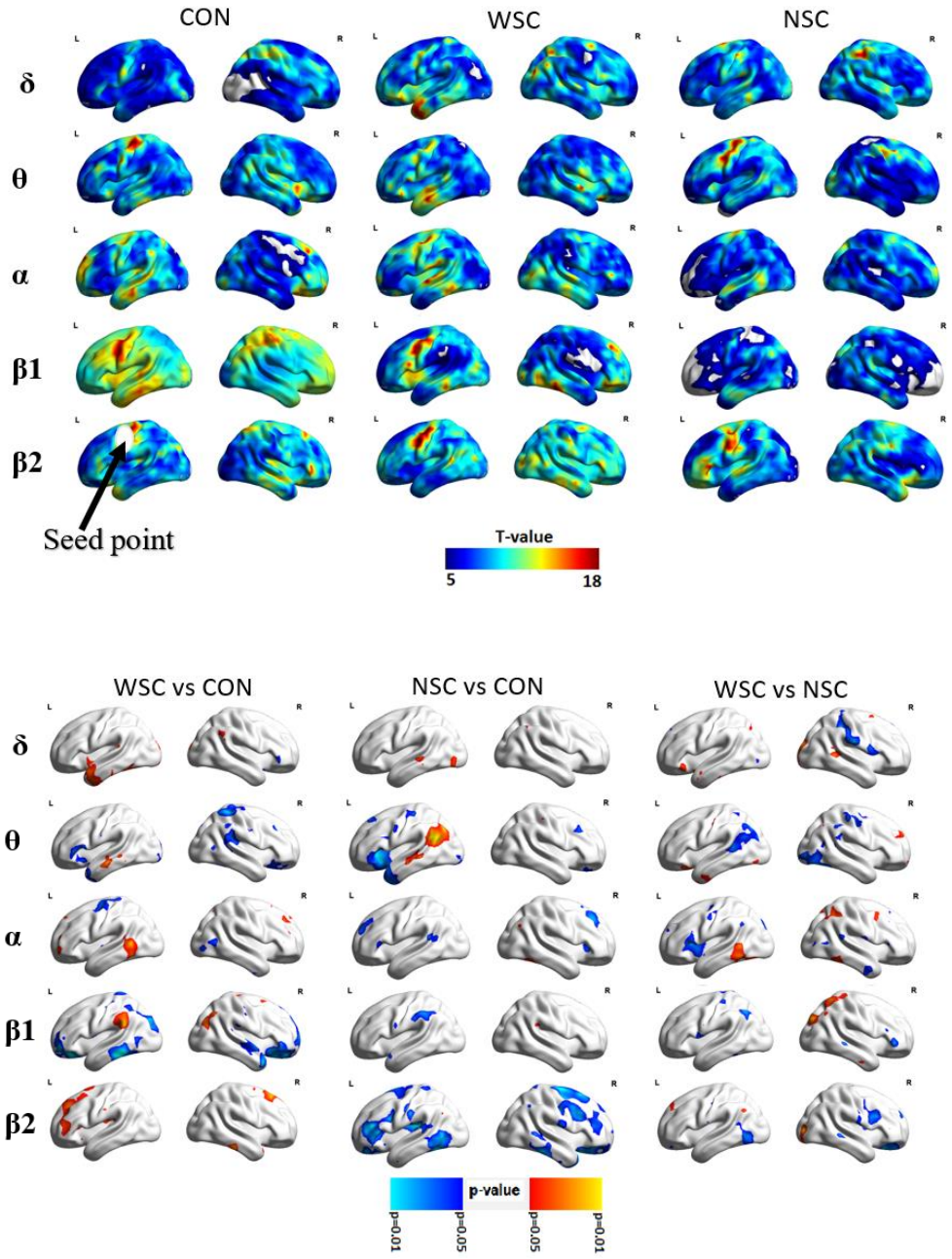

Figure 5.2: Left central seed region: Functional connections from the left central to other regions for each of the group; control (CON), patients group with the spike segments (WSC) and non-spike segments(NSC) and, comparison between the three conditions (WSC vs CON, NSC vs CON and WSC vs NSC).

Comparison between epileptic patients under WSC and controls revealed significantly stronger functional connections at the left temporal region in the δ, θ and α bands. Also, higher functional connectivity was observed at the frontal superior and SMA regions in WSC compared to CON in the β2 bands. Comparison between WSC and CON showed weaker functional connectivity at the right parietal and bilateral prefrontal cortex in the θ band; in the left parietal region in the α band;

and in the bilateral prefrontal cortex, left temporal and left occipital regions in the β1 band. In the absence of spike (NSC compared to CON), there was reduced functional connectivity in the left prefrontal cortex in the θ band; in SMA, bilateral temporal regions, bilateral central regions, the bilateral prefrontal cortices and the right frontal superior region in the β2 bands.

Disrupted functional connectivity in patients' frontal region

With the seed points at the left prefrontal cortex as shown in Figure 5.3, patients showed higher FC under WSC in the α band. Higher FC at the bilateral prefrontal cortex, occipital, parietal and frontal superior regions in β1 band was observed in CON. In the absence of IEDS in epileptic patients, we observed higher FC from left to right prefrontal cortex in δ, and β bands.

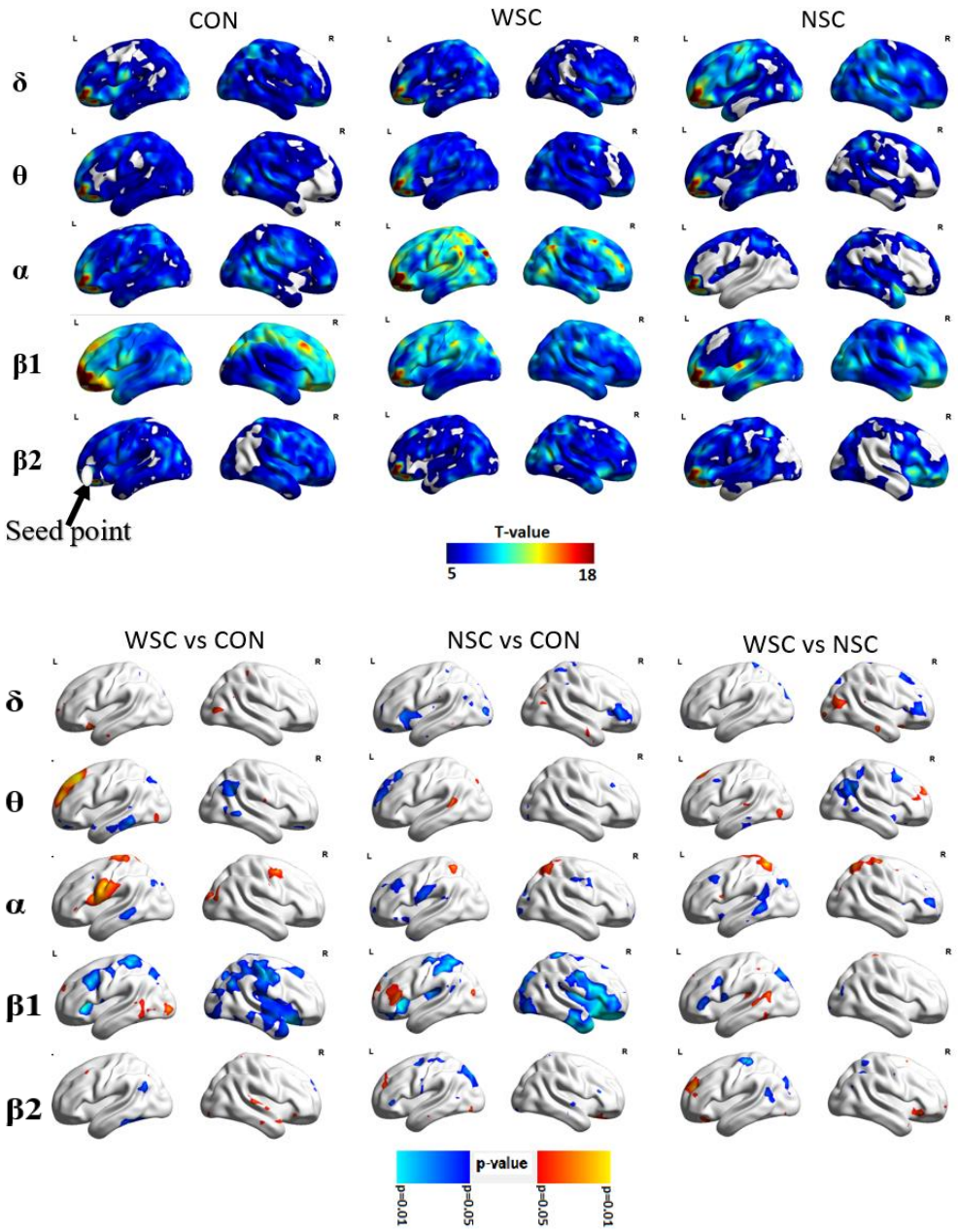

Figure 5.3. Left Frontal seed region: Functional connectivity from the left frontal to other region for each of the group; control (CON), patients group with the spike segments (WSC) and non-spike segments(NSC) and, comparison between the three conditions (WSC vs CON, NSC vs CON and WSC vs NSC).

Comparison of WSC to control shows higher FC at the left superior frontal region in θ band; bilateral central regions, SMA and occipital in α band but lower FC in bilateral parietal, bilateral frontal superior, right rolandic and right temporal regions in β 1 bands. Reduced FC was also observed in patients without spike in comparison to CON at the parietal, bilateral rolandic regions, prefrontal cortex and occipital regions in β1 band. Comparison between both epileptic conditions

shows higher FC at the parietals in α band of WSC and lower FC at the occipital region of the WSC compared to NSC in β 1 band.

Interictal spike reduced functional connectivity from occipital to other regions

We observed lower FC in patients with IEDS condition (WSC) compared to other groups as shown in Figure 5.4. In healthy controls, group statistical significance showed increased FC from the occipital to the right frontal and central regions in θ band and β2 bands. WSC revealed high FC at the right temporal in δ band; right central and temporal regions in θ, α and β1 bands.

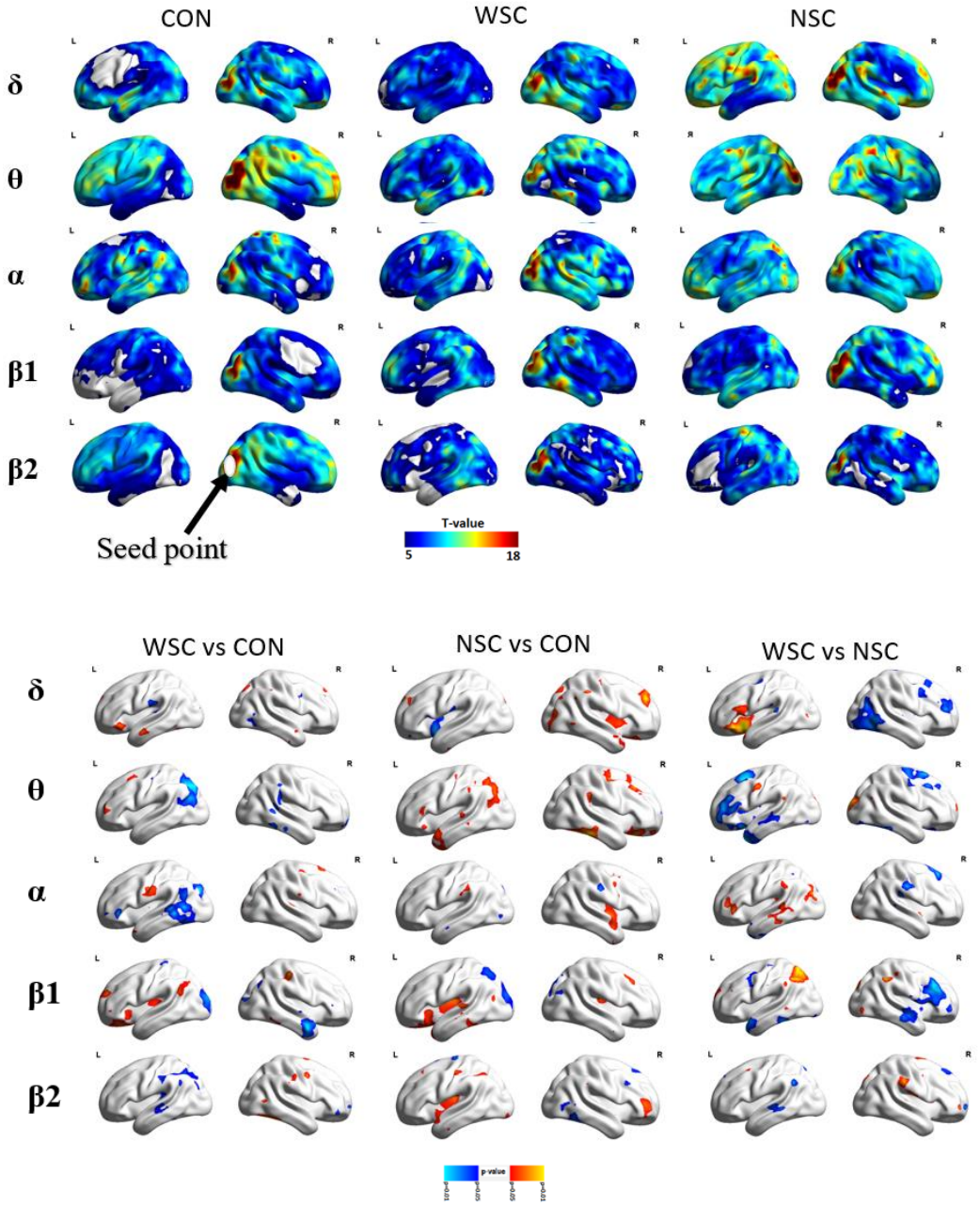

Figure 5.4: Right Occipital seed region: Functional connectivity from the right occipital to other region for each of the group; control (CON), patients group with the spike segments (WSC) and non-spike segments(NSC) and, comparison between the three conditions (WSC vs CON, NSC vs CON and WSC vs NSC).

Comparison of WSC to CON revealed lower FC from the occipital to the left parietal regions in θ, α and β2 band; left occipital regions in α and β1 bands. There was higher FC in the absence of spike at the right frontal superior and rolandic regions in δ band; right rolandic and temporal region in α band. Meanwhile, lower FC at the parietal and occipital regions in β1 band in NSC compared to CON was observed. Comparison between epileptic patient conditions shows lower FC in δ band at the right occipital and temporal and frontal regions in WSC and bilateral central region and left prefrontal cortex in θ band. In β1 band, there was lower FC at the right frontal superior region, closer to the epileptic zone, of WSC compare to NSC.

Graph measures indicate disrupted connectivity pattern in patients

The spatial differences of betweenness and local efficiency between patients and control revealed different patterns of connectivity as a function of frequency bands as shown in Figures 5.5 and 5.6 respectively. Betweenness shows the how the brain region functionally interacts with other by measure the fractions of shortest paths that pass through a given brain region. Meanwhile, the local efficiency of network or particular brain region measures how efficiently it exchanges information between the other regions.

The higher betweenness (Figure 5.5) was observed at the right central in WSC compared to both other conditions in θ band, likewise at the right superior frontal of patients with spike in α and β1 bands. However, lower betweenness was found at the left occipital junction, left frontal region in α and β1 bands. In comparison of NSC to CON, NSC had higher betweenness at the bilateral occipital junction, and lower at the SMA and parietal regions in θ band. There was lower betweenness at the left prefrontal cortex in NSC compared to controls, left occipital junction in β1 band. Comparison of both epileptic conditions showed higher betweenness at bilateral rolandic regions in δ band and right central region in θ band in WSC. Meanwhile, in β1 band, WSC had higher and lower betweenness at the right and left occipital regions respectively in comparison NSC.

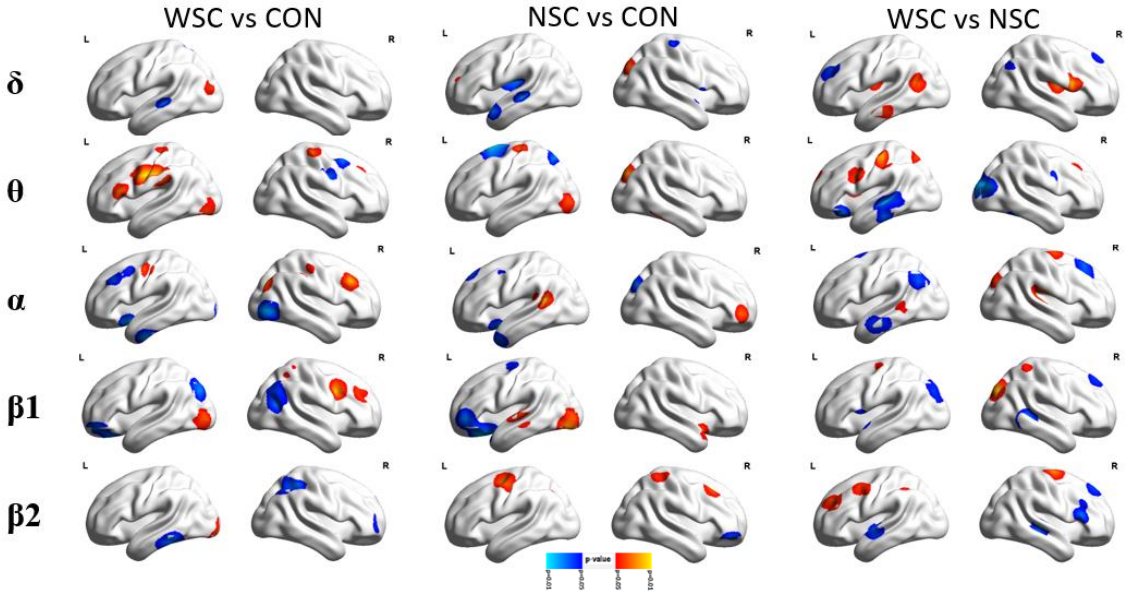

Figure 5.5: Betweeness centrality: comparison between controls (CON), patients group with the spike segments (WSC) and non-spike segments(NSC) (WSC vs CON, NSC vs CON and WSC vs NSC).

Higher local efficiency (Figure 5.6) at occipital regions of WSC compared to CON in δ and β1 bands was observed. Also, WSC had higher local efficiency at the left temporal regions compared to CON in β bands. In the absence of IEDS, there was lower local efficiency at the right superior frontal region in θ bands; higher local efficiency at left centrotemporal region in α and β1 bands. Comparison between epileptic conditions showed decreased local efficiency at the left frontal and parietal in δ bands, left central in θ band; parietal, left and right frontal regions in α band in WSC. In β bands, higher local efficiency at the left occipital region in WSC compared to NSC in β 1 band and right superior frontal region in β2 band were observed.

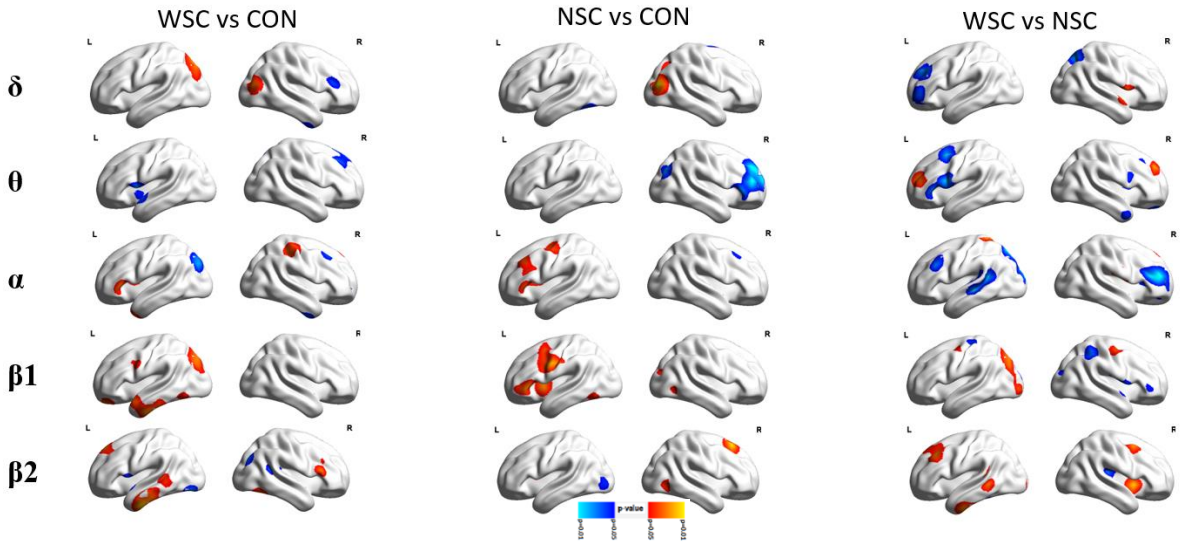

Figure 5.6: Local efficiency: comparison between controls (CON), patients group with the spike segments (WSC) and non-spike segments(NSC) (WSC vs CON, NSC vs CON and WSC vs NSC).

5.2.4 Discussion

In this study we investigated functional connectivity in BCECTS patients in comparison to healthy controls. We presented a clear and robust method for assessing significant functional connectivity differences between patients and healthy subjects. We estimated the imaginary coherence at the source level (Nolte et al., 2004) and we demonstrated alterations in the brain functional network organization of patients. We found that interictal spike activity affected the functional connectivity between the epileptic zone and the ipsilateral frontal, frontocentral, central and temporal areas and the contralateral central, precentral and frontal areas. We also observed a significant increase in IC values between the prefrontal cortex and the epileptic zone in the beta1 band. The sensorimotor regions showed higher betweenness and lower efficiency values in patients in the theta band. Hence, these findings imply that the brain functional networks in BCECTS patients are not only disrupted but also reorganized depending on the frequency band.

Epileptogenic network abnormalities in BCECTS patients

The epileptogenic networks refer to the areas involved in the generation and spread of epileptic activity. These networks may vary across different types of epilepsy. In BCECTS, it covers the sensorimotor networks and central region. The sensorimotor components consist of precentral, central and supplementary motor area (Rosazza and Minati, 2011). In our study, we found that these regions were significantly activated in BCECTS patients in the presence or absence of interictal epileptic spikes especially in the δ and θ bands. In line with previous studies, we found that the patients' central regions, extended to the supplementary motor area, were highly activated (Boor et al., 2007; Tang et al., 2014). The activations of these regions were concomitant with higher betweenness values in the θ band and lower local efficiency values in the frontal superior, fontal mid gyrus and supplementary motor regions. The involvement of these regions could result

in jerking of the mouth, face and hand, kind of semiology of benign childhood epilepsy (Moeller et al., 2013). However, the increased functional connectivity was restricted to the homolateral hemisphere of the epileptic zone in the β band. This observation could be supported by increases in spectral power around the epileptic zone (Adebimpe et al., 2015a; Bourel-Ponchel, 2013). Even in the absence of interictal spikes, we found highly significant changes in IC values at the epileptic zone extending to the frontal regions in higher frequency bands. This might suggest that the abnormal brain function does not only occur during interictal discharges but also exists throughout interictal periods. Meanwhile, increased local efficiency in these patients in the absence of spikes at the left central and frontal region in the α and β1 band can be viewed as the brain functional reorganization due to epileptic activity in the opposite region.

The frontal cortices also showed involvement in the functional reorganization of the brain functional networks in BCECTS patients. This is supported by lower and higher local efficiency at the frontal region in low and high frequency band, respectively. The frontal lobe is known to play a major role in the processing and execution of higher cognitive skills and behaviors (Stuss, 2011). Children with benign epilepsy have been found to be suffering from cognitive deficit and mental activity (Verrotti et al., 2014). One of the distinct features of the benign childhood epilepsy is the absence of large brain structural changes. The structural changes are most common in other types of epilepsy such as temporal lobe epilepsy (Thom, 2014). However, some studies (Kanemura and Aihara, 2009) have reported serial changes in the frontal lobe growth in longitudinal MRI studies and microstructural changes of white matter (S. E. Kim et al., 2014) at the epileptic zones and also in the frontal lobe especially in the superior frontal and right inferior gyrus in BCECTS patients. These little structural changes might be correlated with the cognitive and behavior deficiency in BCECTS patients. Therefore, the changes in functional connectivity patterns between the prefrontal cortex and bilateral central regions might be related to the reported serial growth disturbance and alteration of brain tissues at the frontal region together with experience of motor and cognitive dysfunctions in these patients.

Is DMN impaired in BCECTS patients?

In our study, we found that the pattern of significant functional connectivity did not only depend on the frequency band but also on the seed points (ROIs). Decreased functional connectivity between the prefrontal cortex and the parietal region in BCECTS patients especially in the beta1 band might indicate impairment of the default mode network (DMN) as reported in several fMRI studies (Ibrahim et al., 2014; Xiao et al., 2015) and EEG functional connectivity study (Canuet et al., 2011). This claim is further supported by our results which showed decreased betweenness in the parietal, precuneus, temporal and frontal regions in the β bands. The DMN has been associated to various brain functional activities including cognitive processes and is solicited during attention. The observed decreased functional connectivity and betweenness at these regions may support the idea that epileptic activity might lead to attention and learning deficits in children with epilepsy (E.-H. Kim et al., 2014). In addition, BCECTS children responding to antiepileptic drugs were found to be more attentive, in correlation with the decrease in amplitude of the spike waves (Kaufmann et al., 2009; Schneebaum-Sender et al., 2012). We also found that the presence of

interictal spikes in EEG signals resulted in significant decreases in IC values between the prefrontal cortex to the parietal and precuneus regions and also decreased the flow of information between these regions. The involvement of DMN might be a core neurobiological feature in benign epilepsy and deserves further attention.

Interictal discharges affect temporal connectivity

Interictal discharges in the right centrotemporal area influenced ipsi and contralateral functional connectivity patterns in temporal areas. The functional connectivity analysis using the ROIs seed points at the right central regions indicated increased functional connectivity in the right homolateral temporal region in the delta and theta bands. The increased functional connectivity between the epileptic zone and the ipsilateral temporal region implied that the interictal discharges affected the temporal region. This was also evident from decreased betweenness values in BCECTS patients (especially under WSC) in lower frequency bands. Both the central region and superior temporal gyrus are part of auditory components (Rosazza and Minati, 2011) that are responsible for language and speech processing. Unbalanced auditory processing in both hemisphere could be responsible for phonological and language processing deficits in these patients (Amaral et al., 2015). The reduced IC in the left hemisphere is also supported by several studies (Overvliet et al., 2013) which found reduced cortical thickness predominantly in language mediating brain regions of the left hemisphere in patients compared to controls.

Decreased occipital functional activity in BCECTS patients

With the seed point located at the occipital cortex, the functional connectivity analysis showed significantly decreased connectivity between the occipital regions and postcentral and frontal regions in different frequency bands especially in low frequency bands. The decreased betweenness at the occipital region in the theta and alpha bands in BCECTS patients under WSC and NSC suggest lower functional connectivity in this region. This finding is in agreement with the results of our previous studies(Adebimpe et al., 2015a) which suggest that the functional connectivity pattern in the occipital cortex in BCECTS patients was modified due to interictal epileptic discharges. Several studies (Deltour et al., 2007; Filippini et al., 2015) reported a poor performance in visual assessment and visual spatial coordination in BCECTS children. This is in line with our findings that indicate lower local efficiency in the occipital cortex for these patients in the alpha band.

This study presented a clear and robust method for assessing resting-state EEG source functional connectivity patterns and demonstrated alterations of functional connectivity pattern in BCECTS patients. Although our previous studies have shown the strong impact of interictal epileptic discharges on the brain functional organization in BCECTS patients, dynamic directed interictal connectivity techniques provide important information on the driver-response interactions between the brain regions in BCECTS patients.

5.3 Dynamic directed interictal connectivity

Dynamic directed interictal connectivity in benign childhood epilepsy with centrotemporal spikes: A high density EEG study

This section investigates the dynamic directed interictal functional connectivity pattern associated with interictal epileptic spikes. The EEG source activity was recounsstructed ad reduced to 90 ROIs. The partial directed coherence (PDC) was used to compute the effective connectivity between brain regions. PDC has been shown to be insensitive to volume conduction artifacts. The outflow of the connectivity matrix was then investigated to identify major drivers between the brain regions involved in the propagation and generation of the epileptic activity. Overall, we found that central, rolandic, supplementary motor areas and superior frontal regions of the ipsilateral hemisphere to the epileptic zone were the major drivers among all the brain networks in BCECTS patients.

5.3.1 Introduction

Epilepsy is a neurological disorder characterized by recurrent unprovoked abnormal neuronal discharges. Interictal epileptic discharges (IEDs) involve complex interaction across several brain regions. The dynamics of brain networks during IEDS is the key to understanding pathological mechanism associated with IEDS.

Benign epilepsy with centrotemporal spikes (BCECTS) is the most common idiopathic epileptic syndrome with a prevalence of 8-20% of epileptic children (Holmes, 1993; Panayiotopoulos, 1999; Wirrell, 1998). In BCECTS, the interictal epileptic discharges(IEDS) arise principally from centrotemporal regions, but the functional connectivity analysis has shown that the brain functional networks in BCECTS patients are highly impacted by the IEDS which involve not only the epileptogenic region but also other distant brain regions (Adebimpe et al., 2015b; Kramer and Cash, 2012; Laufs, 2012).

In general, functional connectivity measures are used to investigate non-directional statistical dependency between different brain regions. Effective connectivity is, however, directed and usually used to explore the causal influence from one region to another. Concerning epilepsy, the main question is to understand the mechanism of initiation and propagation of IEDs. There are many measures such as Partial Directed Coherence(PDC) (Baccalá and Sameshima, 2001) and Directed Transfer Function (DTF)(Kamiński et al., 2001) which have been used to study the generation and propagation of IEDS in animal models and human subjects (Gong et al., 2014; Jenssen et al., 2011; van Mierlo et al., 2013; Wilke et al., 2010). The time-varying pattern of the effective connectivity associated with IEDS in scalp EEG remains a critical key to address the initiation and propagation of IEDS in epileptic patients.

In this paper, we used PDC (Baccalá and Sameshima, 2001), an effective connectivity estimator in the frequency domain based on the multivariate autoregressive (MVAR) modeling for investigating causal interactions between EEG source signals. We aimed to investigate the

connectivity patterns associated with IEDs and to explore the brain regions involved in the generation and propagation of epileptic activity. Moreover, we used PDC to investigate the major drivers that draw the brain networks into IEDs.

5.3.2 Materials and methods

Patients

Sixteen BCECTS patients (Table 5.2) were included in this study with right (12) and left (4) epileptic foci. The patients in each group had unilateral epileptic foci with interictal dipolar sources located (Figure 5.7)within centrotemporal regions and oriented from anterior to posterior (Camfield and Camfield, 2002).The study was conducted at the Amiens University Hospital, and approved by the university hospital ethics committee with the reference number: CPP Nord-Ouest No: 2011-A00782-39.

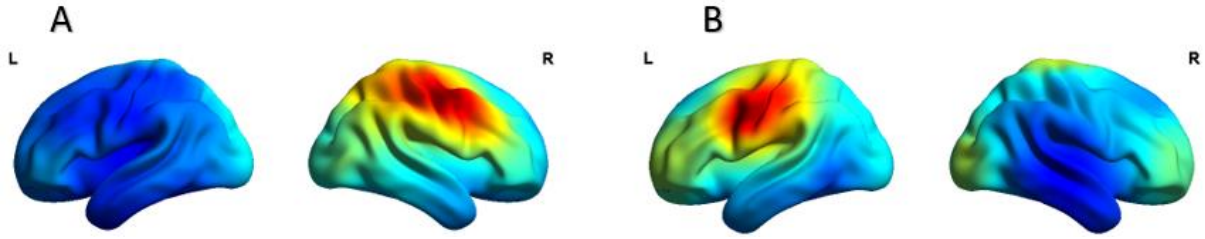

Figure 5.7: EEG source imaging: Average eLORETA source localization of interictal spikes for 12 and 4 BCECTS patients with (A) right and (B) left epileptic focus, respectively

Table 5.2: Patients EEG recordings and clinical characteristics

Patient	Age (years)	Epileptic focus	Neuropsychological assessment	Medication
1	12.63	Right	Normal	Sodium valproate
2	12.64	Right	Normal	Sodium valproate
3	9.25	Right	Attention deficit	Oxcarbezepine
4	6.03	Right	-	Oxcarbezepine
5	10.47	Right	Attention deficit	Sodium valproate
6	7.16	Right	-	Sodium valproate
7	8.51	Right	Attention deficit	-
8	13.16	Right	Normal	Sodium valproate
9	9.67	Right	Language deficit	Lamotrigine
10	7.79	Right	Normal	Micropakine
11	8.91	Right	Normal	Trileptal
12	9.81	Right	Normal	Sodium valproate
13	8.30	Left	Language disabilities	Sodium valproate
14	7.52	Left	Language disabilities	Oxcarbamazepine
15	8.00	Left	Normal	-
16	7.01	Left	Attentional deficit	Sodium valproate

EEG data acquisition and preprocessing

EEG data were recorded from each individual using a high-density EEG recording system (ANT, Netherlands) with a sampling rate of 256 Hz and 64 channels positioned according to the

international 10–10 system. Forehead ground and linked-ear reference electrodes were used for data collection. On average 14 minutes of eyes-closed resting state EEG data were recorded from each patient. During recording, the patients were in a supine position in a quiet dark room. The EEG data were re-referenced to a common average reference and filtered between 0.5 to 40 Hz to remove possible high frequency noise. Two experienced neurophysiologists visually inspected the EEG data to identify centrotemporal spikes. Twenty single spike segments were selected for each patient for connectivity analysis. The selected EEG spikes were free from major artifacts with at least 15 seconds intervals between segments to avoid any spike overlapping. To identify EEG segments with ocular and movement artifacts, the EEG recordings were first normalized by the Z-score transformation and then preprocessed semi-automatically using the thresholding method implemented in the Fieldtrip software (Oostenveld et al., 2011; "tutorial," n.d.). For each segment, EEG channels that exceeded a predefined threshold were marked and visually inspected by the experts. The threshold was set to the mean plus one standard deviation of the z-score amplitude distribution for each channel.

EEG source imaging

We used the Montreal Neurological Institute (MNI) brain MRI template(Fonov et al., 2009) for the construction of a head model required for leadfield calculation using the Boundary Element Method (BEM) (Oostendorp and van Oosterom, 1989). The MNI template was segmented by SPM8 into 3 homogeneous conductive compartments including scalp, skull and brain with conductivity values of 0.33 S/m, 0.0041 S/m and 0.33 S/m, respectively. The lead-fields were calculated using FieldTrip (Oostenveld et al., 2011) with a spatial resolution of 7.5 mm. In total, 4734 source locations were generated inside the brain. The electrodes were aligned to the head geometry using the fiducial points from each subject.

The eLORETA (Pascual-Marqui, 2007) inverse solution was used to calculate three dimensional current density distributions. The inverse solution was first applied to the average interictal spikes of each patient to localize the spike activity. The results were grand averaged (Figure 1) after normalization for each group (with right and left foci). For each spike segment, the inverse solution was used to obtain the source activities which were then projected by the eigen decomposition method (Sekihara et al., 2004). The distributed source activities were reduced to 90 regions of interest (ROIs) by using the automated anatomic labeling (AAL) atlas (Tzourio-Mazoyer et al., 2002). The closest distributed source activity to each ROI centroid was selected as the source activity of the ROI (Figure 5.8).

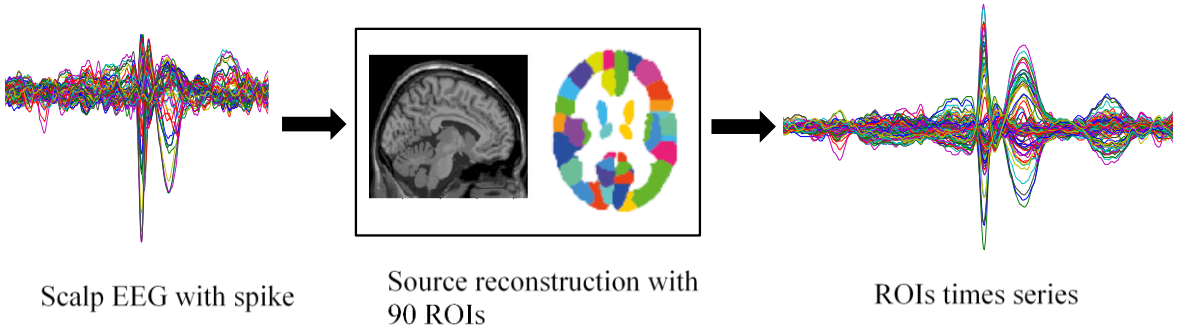

Figure 5.8. Electrical source imaging: EEG source reconstruction using the AAL atlas for 90 regions

Dynamic partial directed coherence

We used the normalized Partial Directed Coherence (PDC) (Baccalá and Sameshima, 2001) to determine the causal inference between the multivariate autoregressive (MVAR) model (Pereda et al., 2005) of the ROIs source activity as implemented in the SIFT toolbox (Delorme et al., 2011). The time-varying normalized PDC estimates directed interactions from the estimated MVAR with an appropriate model order (average of 15 was used for all the patients). This was estimated with sliding window of 500 milliseconds in a time step of 30 millisecodns. The appropriate model order was estimated with the Akaike information criterion (AIC) and estimation theory (Schlögl and Supp, 2006). The estimation theory states that the ratio of $\frac{N*n}{C*p}$ must be of order of 10 or larger where N is the number of data points, n is the number of data segments, C is the number of signals (ROIs) and p is the model order. However, we ran statistical tests to check the stability and consistency in order to validate the model. PDC was estimated in time and frequency domain but only the θ band was considered for analysis. Since the power in this frequency band was maximum (Figure 5.9), therefore, the information transfer was supposed to be most relevant at the maximum power frequency(van Mierlo et al., 2011).

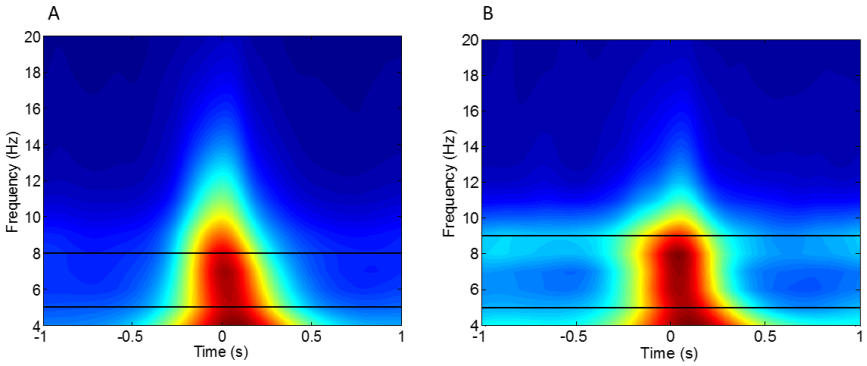

Figure 5.9: Power spectrum. Average power spectrum for patients with (A) right and (B) left epileptic foci in the θ band

Outflow and Laterality

We computed the outflow which is the summed connectivity strengths over outgoing edges. This is computed by summing outflows from each ROI to all other ROIs at a given time instant. The ROI with high summed outflow strongly drives the activity of other regions. The outflow of each region at each time instant was statistically compared to the temporal average of the baseline before the rise of the spike activity with a nonparametric permutation test (Kruskal-Wallis, $p<0.05$) and 1000 permutations.

The laterality was determined from the summed outflow across the rising phase of the spike to represent the network involved in the generation of the spike.

The laterality index, L, was computed to assess the hemispheric or regional dominance as follows:

$$L = \sum \frac{O_R - O_L}{O_R + O_L} \tag{5.9}$$

Where O_R and O_L represent the summed outflow from the right and left brain region to all other regions, respectively.

For the laterality, nonparametric tests (Kruskal-Wallis, $p<0.05$) with 1000 permutations were used for statistical comparison to the baseline. All analyses were performed in Matlab and EEGLAB toolbox(Delorme and Makeig, 2004) and statistics in the BrainNet viewer (Xia et al., 2013) was used for 3D representation and some Figures were plotted with the modified code of the e-connectome software (He et al., 2011).

5.3.3 Results

Electrical source activity

Figure 5.10 shows the electrical source activity reconstructed with the ROIs. In patients with right epileptic foci, we found stronger activities at the ipsilateral hemisphere to the epileptic zone at the right postcentral, inferior parietal and rolandic regions. This was extended to the frontal region at the orbital frontal and superior temporal region. Similarly, in patients with left foci, ROIs with stronger activity were localized at the left precentral and postcentral regions including rolandic regions. Frontal regions, very close to epileptic foci also showed strong activity at the left inferior frontal region.

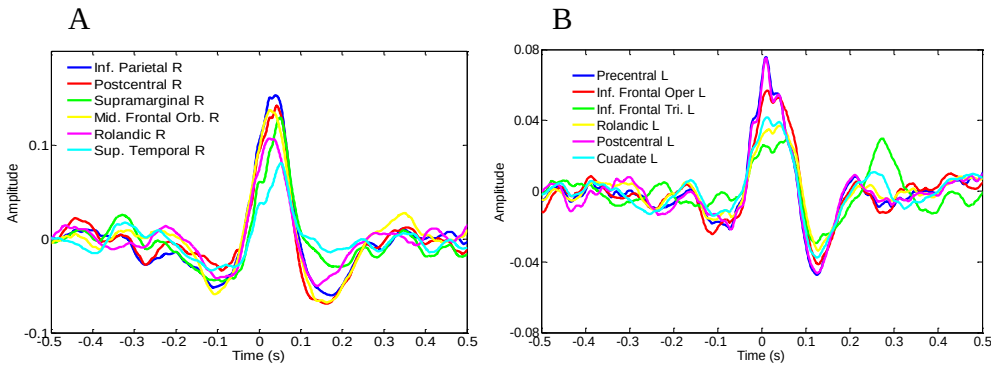

Figure 5.10: EEG source imaging: Average eLORETA source localization of interictal spikes from 12 and 4 BCECTS patients with (A) right and (B) left epileptic foci, respectively.

Outflow density

The summed outflow (Figure 5.11) showed a dominance in the ipsilateral hemisphere to the epileptic focus in both patient groups with right and left epileptic foci. In the patient group with right epileptic focus, the key drivers with highest summed outflow included the right precentral and postcentral regions which were the main spike generation zones. Other regions including the right rolandic and supramarginal regions were also involved, although with lower summed outflow. In the patients with right epileptic foci, the superior and mid frontal regions were also involved and even reached their maximum summed outflow before the central regions. In these patients, the average summed outflow during the rise of flow (surface MRI) showed the right dominance with highest outflow at the central regions.

In the patients with left epileptic focus, just like the other group, the major key drivers included precentral and postcentral regions. It also included the inferior frontal operculum regions. In this group, fewer ROIs showed significant changes compared to the baseline probably due to the low sample size.

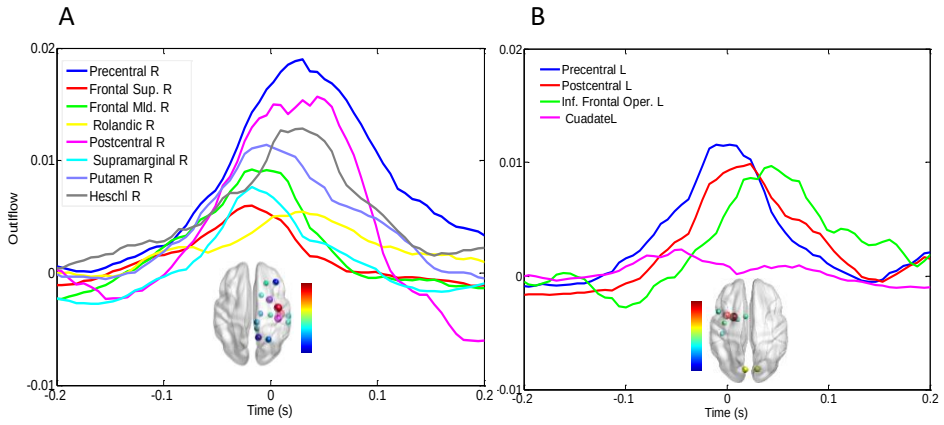

Figure 5.11: Outflow density. Temporal evolution of outflow density compared to the baseline. Only the ROIs in which more than 8 out of 12 patients showed significance differences compared to the baseline were plotted for the group with right epileptic foci (A). The 3D images inside each graph represent the outflow during the rising phase of the spike compared to the baseline.

Network pattern and laterality index

Figure 5.12 shows the network patterns for both groups of patients. The strongest connections were found in the ipsilateral hemisphere to the epileptic focus from pre- and post-central regions and the supplementary area to the frontal regions. There were also functional connections with weaker strength to distant regions in the contralateral hemisphere. In the patient group with left epileptic focus, the major drivers were found at the left rolandic region. Few connections to the other brain region were observed for this group.

Both the patient groups exhibited laterality toward the ipsilateral hemisphere to the epileptic focus (R: 0.38 ± 0.09, L: -0.49±0.20). However, patients with right epileptic foci exhibited more laterality toward the right hemisphere in comparison to the baseline (χ^2=5.47, p=0.019).

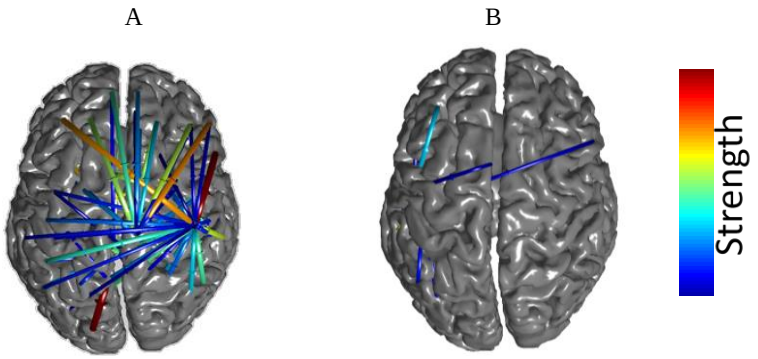

Figure 5.12: Effective connectivity. The connectivity pattern for patients with (A) right and (B) left epileptic foci, respectively, from the ROI to the whole brain region.

5.3.4 Discussion

Our results show the presence of abnormal functional network pattern occurring during the interictal epileptic discharges (IEDs) in BCECTS patients. The causal inference between the brain regions were identified by combining the EEG source imaging and the time-varying effective connectivity method. Both the patient's groups with epileptic foci at the right and left hemisphere showed stronger directional connections to the frontal regions and weaker connectivity to the distant regions in the contralateral hemisphere. We also demonstrated the dynamic changes in interactions between the brain networks before, during and after IEDs. Our results are consistent with the findings reported in our previous studies (Adebimpe et al., 2016, 2015b, 2015c) in which we compared EEG segments with and without IEDs using the source imaging and functional connectivity analysis. The main advantage of PDC as an effective connectivity measure over the phase synchronization or coherence methods is that it allows detecting the direction of interaction between brain regions. All of these analyses provide a meaningful tool to evaluate the epileptic networks, their alteration caused by IEDs, and their possible impact on cognitive deficits reported in the children with BCECTS (Danielsson and Petermann, 2009; Datta et al., 2013).

The EEG source activity analysis revealed stronger activity at the central regions including the rolandic region in the epileptic zone. It also showed that the ipsilateral temporal and frontal regions were also involved in epileptic activity, however, with weaker strength. The stronger activity at the central and frontal regions of the ipsilateral hemisphere to the epileptic zone suggested a fronto-central network activation during the IEDs.

The main driver in the epileptic networks was found in the central regions (post and precentral) including rolandic regions. However, some of other key drivers were also observed outside the epileptic focus with weaker strength especially at the frontal regions, including parietal and temporal regions. We also found the involvement of the frontal regions in spike activity in both the patient groups, especially the frontal superior and mid regions (for patients with right epileptic foci) which reached their maximum summed outflow even before the precentral and postcentral ROIs. This finding suggests that the frontal regions are the secondary driver of the epileptic activity. The involvement of the frontal and central or fronto-central networks in the epileptic activity may suggest that interictal activity might impact the functionality of the attention networks (Kaufmann et al., 2009) in BCECTS patients. The ipsilateral frontal cortex showed increased functional connectivity driven by the right or left (pre and post, including central motor) central gyrus, respectively. The frontal cortex has been known to be involved in monitoring, behavioral adjustments and learning (Rushworth et al., 2007, 2011) all of which are important in complex cognitive tasks such as language. The frontal cortex has been shown to be correlated with the attention and cognitive deficits (Dunn, 2014; Lopes et al., 2013; Riva et al., 2007). The functional involvement of the frontal cortex in epileptic activity may reflect the fontal region growth disturbance (Kanemura and Aihara, 2009) caused by epileptic activity in BCECT patients. This finding is in line with those resulting from several studies performed with fMRI and MEG/EEG indicting the role of frontal cortex in the initiation and propagation of IEDs (Panzica et al., 2013; Rotondi et al., 2016; Wu et al., 2015; Yang et al., 2013). The evidence of involvement of the fronto-central regions may also be in agreement with results reported in other methods concerning clinical diagnosis of BCECTS with the tangential dipole orienting from central to frontal regions or vice versa (Baumgartner et al., 1996; Camfield and Camfield, 2002) and our previous studies (Adebimpe et al., 2016, 2015b, 2015c) reporting high/low activity at the ipsilateral central/frontal regions, respectively.

The existence of other drivers outside the epileptic focus especially at the supramarginal and parietal regions as well as the causal influence from the superior motor and post/pre central regions of the ipsilateral hemisphere to the epileptic foci to the contralateral hemisphere and extra-temporal regions support the evidence that the impairment of BCECTS brain networks might not be restricted to the epileptogenic focus. We also observed connections with weaker strength from the epileptic foci to the contralateral hemisphere compared to the ipsilateral frontal regions. This could represent the reorganization of the brain network during IEDs serving as the compensatory mechanism (Bettus et al., 2009; Datta et al., 2013). Laterality toward the epileptic foci also confirmed the reorganization of functional network organization due to epileptic discharges. The laterality toward the epileptic foci might have influence on the cognitive ability, language processing and verbal memory in BCECTS patients(Li et al., 2015; Piccirilli et al., 1988; Sveller et al., 2006). The causal influence from the ipsilateral supplementary motor areas to the

bilateral frontal regions indicates the involvement of motor region as well. This might explain the high prevalence of language impairment in children with rolandic epilepsy as previously reported (Overvliet et al., 2011; Wolff et al., 2005). Interestingly, many of the patients with BCECTS have a language-related learning disorder and not a general learning disorder. It is also reported that there is correlations (Besseling et al., 2013; Overvliet et al., 2011) between problems with motor development and language impairment in children with BCECTS, probably due to the casual influence from the motor region to other brain regions.

In this study, the PDC was only estimated in the θ band, the frequency range with maximum spectral power, mainly because it is generally believed that frequency with higher spectral power has potential for driving brain networks. Higher frequencies above 80Hz regarded as high frequencies oscillation (HFO) (Kobayashi et al., 2011) might be involved in the generation and propagation of spike. This is subjected for future study because HFO is needed to be recorded with higher sampling rates than the one used in the current study. Our study is limited with small sample size especially for the patient group with left epileptic foci (4 subjects), though, the group was almost homogenous in terms of age range and source localization of IEDs.

In conclusion, we identified the causal connectivity patterns in BCECTS patients and the major drivers of the epileptic activity. The post and precentral regions with the supplementary motor areas were the major drivers in the ipsilateral hemisphere to the epileptic foci. The causal influence from the central to the ipsilateral frontal region and the contralateral hemisphere suggest that the BCECTS brain networks are functionally altered during IEDs. This could explain the negative impact of epileptic activity on the cognitive ability of the children with BCECTS.

Chapter 6

Functional Development in Neonates

6.1 Introduction

The adult brain is composed of networks with complex interactions. Several studies with the graph theory or network science have expanded our knowledge on the brain functional connectome in adults (Bassett and Bullmore, 2006; Bassett and Gazzaniga, 2011; Sporns et al., 2000). In turn, little is known about the brain functional connectome in neonates. There have been predictions that the human brain functional connectivity evolves from birth (with local connections) to adulthood (with distributed topology) (Fair et al., 2009). Several fMRI studies in neonates have shown the presence of cortical hubs in the posterior, frontal and sensorimotor regions (Ball et al., 2014; Fransson et al., 2007). The early brain activity especially in preterm is quite different from the mature brain. Neonatal brain activity is characterized with the occurrence of specific electrophysiological features such as theta temporal bursts in preterm and frontal transients in full-term neonates with relative period of discontinuity which serve as a biomarker for brain maturation and development (André et al., 2010; Wallois, 2010). All these features can be observed only with EEG in neonates. Recent studies (González et al., 2011; Meijer et al., 2014; Omidvarnia et al., 2014; Tokariev et al., 2015) with EEG in neonates have attempted to explore functional connectivity in neonates. All of these studies were done using sparse electrodes. However, functional studies in neonates require a high number of electrodes due to the spatial specificity of EEG (Odabaee et al., 2013). In addition, most of the specific neonatal features including sleep stages have not been taken into consideration in functional studies. These features might have impact on the brain development.

In this chapter, functional brain connectivity patterns in preterm and full-term neonates were studied using high density EEG data (64 channels). The specific features of neonates such as the theta temporal burst activity and both quiet and active sleep stages were taken into considerations.

6.2 EEG functional connectivity in preterm neonates

EEG functional connectivity in preterm neonates modulated by endogenous activity

6.2.1 Introduction

Early preterm birth can highly affect the brain development at later infancy. Preterm babies are at high risk of neurodevelopmental disabilities and health impairments (Drassinower et al., 2015; Karolis et al., 2016; Périvier et al., 2015; Rose et al., 2014) due to the immaturity of the brain

neural networks at birth. The development of the immature brain is concomitant with rapid alterations in functional connectivity patterns of the brain networks after birth (Grieve et al., 2008). The appearance or disappearance of specific cerebral transient events in neonates is related to the temporary involvement of the cerebral neural networks. There is increasing interest in understanding the neurodevelopmental dynamic of the preterm brain networks and their functional connectome. (Doria et al., 2010; Fransson et al., 2011, 2007; Omidvarnia et al., 2015)

The brain neuronal activities in preterm infants is strongly different from those observed in full-term neonates, young children and adults (André et al., 2010). The preterm EEG is characterized by its discontinuity with the occurrence of short burst of activity of high amplitude with dominant low frequencies (André et al., 2010; Vecchierini et al., 2007). During the maturation process, the dynamics of preterm brain networks is characterized by the occurrence of specific features considered as biomarkers. The absence or a delay in the occurrence of these biomarkers during the neurodevelopmental process suggests a poor functional prognosis (Vecchierini et al., 2003; Wallois, 2010). The appearance of cortical bursts in early preterm has been found to be correlated with the mental development (Iyer et al., 2015; Vecchierini et al., 2003). Other biomarkers include frontal sharp waves [24-28 wGA], Theta Temporal Activities in coalescence with Slow Waves (TTA-SW) [25-30wGA], delta brushes [30-36wGA] and frontal transients [36-42wGA] (André et al., 2010; Selton et al., 2000; Vanhatalo and Kaila, 2006; Wallois, 2010). The inter-hemispheric synchronization also evolves in the course of neurodevelopment. The functional interactions in premature infants follow a temporally variable complex pattern. In the very premature babies before 32wGA, short bursts of activity are highly synchronized across hemispheres. For a short period of time between 32 to 36wGA, the two hemispheres are out synchronization then they become resynchronized after 36 wGA.

The TTA-SWs are one of the earliest neurodevelopmental biomarkers of the brain maturation process in preterm babies. It has been shown that the TTA-SW is not sensory driven and that their generators are located bilaterally along the Superior Temporal Sulci (STS) (Routier et al., 2016). The generators of the TTA-SW are located in deeper structures at 26wGA than at 30 wGA probably within the subplate (Routier et al., 2016). Because of the small parcellation of the brain in preterm babies, the EEG patterns are region specific (Odabaee et al., 2013).

Few studies have been conducted to investigate functional connectivity patterns in premature infants. A resting-state functional connectivity study with fMRI (Fransson et al., 2011; Omidvarnia et al., 2014) has shown cortical hubs and their associated cortical networks largely confined to primary sensory and motor brain regions in the infant brain. Due to its poor temporal resolution, fMRI cannot be used to investigate the dynamic of the functional connectivity in the immature neonatal brain especially during short bursts of activities. Using low density EEG data, Omidvarnia et al., (Omidvarnia et al., 2014) have investigated EEG functional connectivity patterns at the frontal and posterior regions in full term neonates and during EEG bursts of activity in preterm neonates.

In this study, we aimed to investigate the functional organization of the brain networks and the impact of the TTA-SW on the functional connectivity organization in the very preterm neonates during the quite sleep. To investigate the brain functional connectivity topology, we used

graph metrics to characterized the functional connectivity using high density EEG data in this age group. To specifically characterize the connectivity pattern of TTA-SW and its impact on overall functional connectivity, we compared the graph metrics during bursts of activity with and without TTA-SW.

6.2.2 Materials and Methods

Figure 6.1 shows the block diagram of the processing pipeline.

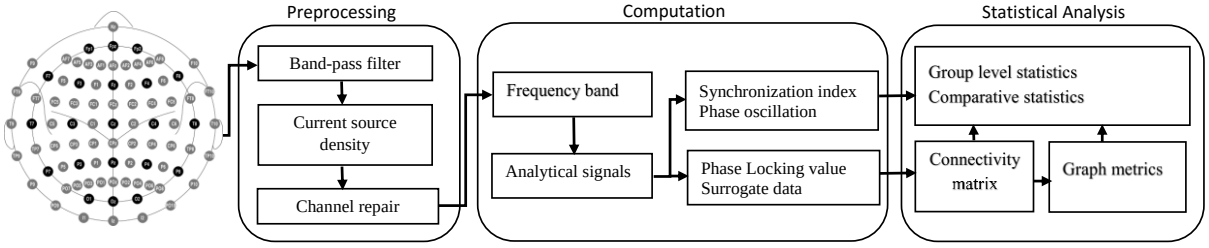

Figure 6.1: Schematic illustration of the processing pipeline.

Subjects and EEG recordings

High density EEG (HD-EEG) data recorded from 12 healthy preterm neonates (31.26 ± 0.18weeks, Gestational age, GA) were included in this study from the clinical database of the pediatric functional exploration of the nervous system service in Amiens University Hospital, France. The inclusion criteria were the absence of neurological disorders and illness. The HD-EEG data were recorded in the neonatal intensive care unit of the university hospital of Amiens, France. The data had been recorded for clinical routine use during quite sleep (QS) using *ANT's EEG* acquisition system (ANT, Netherlands) with a sampling rate of 1024Hz and a high density EEG cap (Medelopt™, France) adapted for preterm neonates with 64 channels positioned according to the international 10-10 standard system. EEG data of premature neonates are characterized by a discontinuous pattern alternating with short-lasting periods of cerebral activities mostly consisting of irregular intermingled θ-δ activities (Figure 6.2 (A)). Based on these characteristics, two electrophysiology experts selected twelve six-second artifact free EEG segments with theta temporal activity (TTA) followed by a slow wave (Figure 6.2 (B)) separately for each subject.

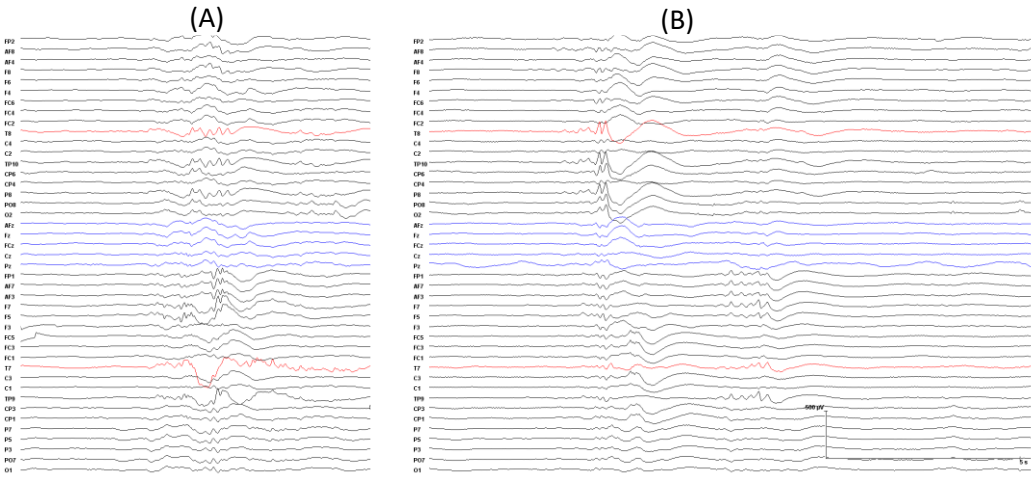

Figure 6.2: Examples of EEG in preterm babies. (A) discontinuous EEG pattern with short burst activity, and (B) EEG signals with TTA at the temporal channels.

Table 6.1. Overview of the characteristics of the preterm babies included in the study.

Preterm babies	12 (6F)
Gestational age at birth (weeks)	29.11 ± 1.39
Gestational age at recording (weeks)	31.26 ± 0.63
Weight at Birth (gram)	1145 ± 297
Weight at recording (gram)	1295 ± 262

EEG data preprocessing

EEG data were first band-pass filtered between 0.5 and 40 Hz to exclude very low frequency activities as well as high frequency noise. The EEG trials were then re-referenced using a Laplacian montage *(* current source density, CSD) (Perrin et al., 1989) to effectively minimize volume conduction effects. CSD has been shown to have optimal source separation and performance required for functional connectivity analysis (Srinivasan et al., 2007). Considering missing or bad channels, 59 electrodes were considered for all the neonates for further analysis.

Frequency-domain signal

The frequency-domain signal was computed using the Morlet wavelet, which is localized in both time and frequency and useful for processing nonstationary signals. However, Morlet wavelet, w (*t*,*f*) is defined as:

$$w(t,f) = \left(\sigma_t\sqrt{\pi}\right)^{-\frac{1}{2}}\ e^{-\frac{t^2}{2\sigma_t^2}}\ e^{-i2\pi ft} \qquad (6.\ 1)$$

Here, f is the center frequency and σ_t is the temporal standard deviation. The time-frequency complex signal Z (*t*,*f*) of a signal *z*(*t*) was computed by convolving it with *w*(*t*,*f*):

$$Z(t,f) = z(t) * w(t,f) \qquad (6.2)$$

We choose the spectral bandwidth for each frequency band by controlling the center frequency f and its ratio to the standard deviation (σ_f). Two frequency bands δ(1 - 4 Hz) with f= 2.5Hz and f/σ_f =3 and θ(4.17 – 7.83 Hz) with f=6Hz and f/σ_f=6 were selected for connectivity analysis.

Synchronization index

The synchronization index was used to evaluate coupling between pairs of EEG channels over time. This was applied to 6-second EEG of 12 segments for each patient in order to investigates the dynamic synchronization within and between temporal regions only. Synchronization index computation is based on the statistical phase locking of the distribution of phase differences between pairs of EEG channels based on the normalized Shannon entropy (Hurtado et al., 2004). The phase of the signal was obtained from the complex signal as obtained from equation 6.2. Therefore, the synchronization index, e(t) is defined as:

$$e(t) = -\sum_{i=1}^{N} p_j\ \log p_j \qquad (6.3)$$

Where p_j is the relative frequency of phase difference within the ith bin. e varies between 0 and E=logN where N is the number of bins and this was obtained with sliding windows of 200 milliseconds in a step of 20 milliseconds. In this study, we used 72 bins (5^o spaced). The synchronization index was normalized at each time point:

$$q(t) = \frac{E - e(t)}{E} \tag{6.4}$$

Functional connectivity analysis

To investigate the functional connectivity patterns for each condition, Phase Locking Value (PLV) was computed between all pairs of EEG channels (Lachaux et al., 1999; Mormann et al., 2000). The PLV was computed for 3-second EEG data of 12 segments for both TTA-WS segment and normal activity (NAT). The PLV between electrodes X and Y is computed as:

$$PLV(x,y) = \frac{1}{N}\left|\sum_{t=1}^{N} e^{i(\varphi_x(t) - \varphi_y(t))}\right| \tag{6.5}$$

Where φ_x and φ_y are the instantaneous phases computed from the frequency-domain signals of X and Y. The PLV ranged from 0 to 1, with 0 and 1 indicating no connection and maximum connection between any given pair of signals, respectively. The end-result of computing the PLV for all pairs of channels was a square connectivity matrix of size 59 (number of EEG channels). In the connectivity matrices, each entry $N_{x,y}$(= $N_{y,x}$) contained the PLV for channels X and Y.

Single- and group-level statistical analysis

To evaluate the significance in PLV, we generated 200 time-shifted surrogate signals sharing statistical characteristics of the original data (Theiler et al., 1992). The PLV between the first signal and all the time-shifted versions of the second signal yielded a null distribution for statistical testing. The significance was defined by the difference between the original and the mean of the surrogate values of statistics, divided by the standard deviation of the surrogate values:

$$Z = \frac{PLV - \mu_{surrogate}}{\sigma_{surrogate}} \tag{6.6}$$

We used a criterion of 5%, which implies that the proportion of surrogate values higher than the original PLV (between x and y) must be less than 5% (95% significance level). This procedure was performed for each individual connectivity matrix (Figure 1). The error rate in multiple comparisons was also corrected by controlling the false discovery rate (Nichols, 2012) at 5% significance level for the grand averaging over individual connectivity matrices. Statistical comparisons between the TTA and normal activity (NAT) segments were done using the pair-wise nonparametric permutation test with correction for multiple comparisons(Maris and

Oostenveld, 2007) with 1000 permutations and the false discovery rate controlled at 5% significance level.

Graph theoretical measures

To compute graph metrics, the functional connectivity matrices were first thresholded and binarized the functional connectivity matrices. The matrices were thresholded by applying false discovery rate, q=0.01which controls the expected proportion of false positives among suprathreshold correlations. This was done to prune out the weaker correlation between the EEG channels.

The following graph metrics (Rubinov and Sporns, 2010) were computed after the thresholding:

Degree: Degree is the most common measures of centrality with straight forward neurobiological interpretation. A node with high degree implies more interaction with many nodes in the network.

Global Efficiency: Global efficiency measures the functional integration by computing the path between two vertices as the inverse of the shortest distance between the vertices.

Clustering coefficient: Clustering coefficient computes the functional segregation by measuring the presence of clusters or modules in functional networks.

Local Efficiency: The local efficiency of a particular node is similar to clustering coefficient. This was added in order to estimate the efficiency of local connectivity within neighbors.

The details of the mathematical descriptions of these metrics are provided in the appendix.

The above graph metrics were selected in order to characterized the distribution of connection density (degree) in preterm neonates, global connectivity processing (global efficiency) and local connectivity and efficiency (clustering coefficient and local efficiency) of neighbor's nodes.

Nonparametric permutation testing was used for all graph metrics with correction for multiple comparisons including *post hoc* tests. A total of 1,000 permutations were used to determine the significance level for each test.

All computations and statistical analyses were performed in Matlab with custom scripts and open source toolboxes: EEGLAB (for 3D topological plots, http://sccn.ucsd.edu/eeglab/), and the brain connectivity toolbox (for graph parameter computations, https://sites.google.com/site/bctnet/).

6.2.3 Results

Synchronization between channels

As shown in Figure 6.3, the synchronization results indicated that the synchronizations level between the bilateral temporal regions (T7-T8 and P7-P8) were very weak compared to the

synchronization within each temporal region (P8-T8 and P7-TP7). Though slightly increased due to the occurrence of TTA, the synchronization level still remained weak between and within the right and left temporal regions (around 2000 ms). The increase (started around 2000 ms as shown in Figure 3B) in the synchronization index within each temporal region (P8-T8 and P7-TP7) highlighted the impact of TTA on the synchronization level which lasted longer over the right hemisphere (P8-T8) compared to left hemisphere (P7-TP7).

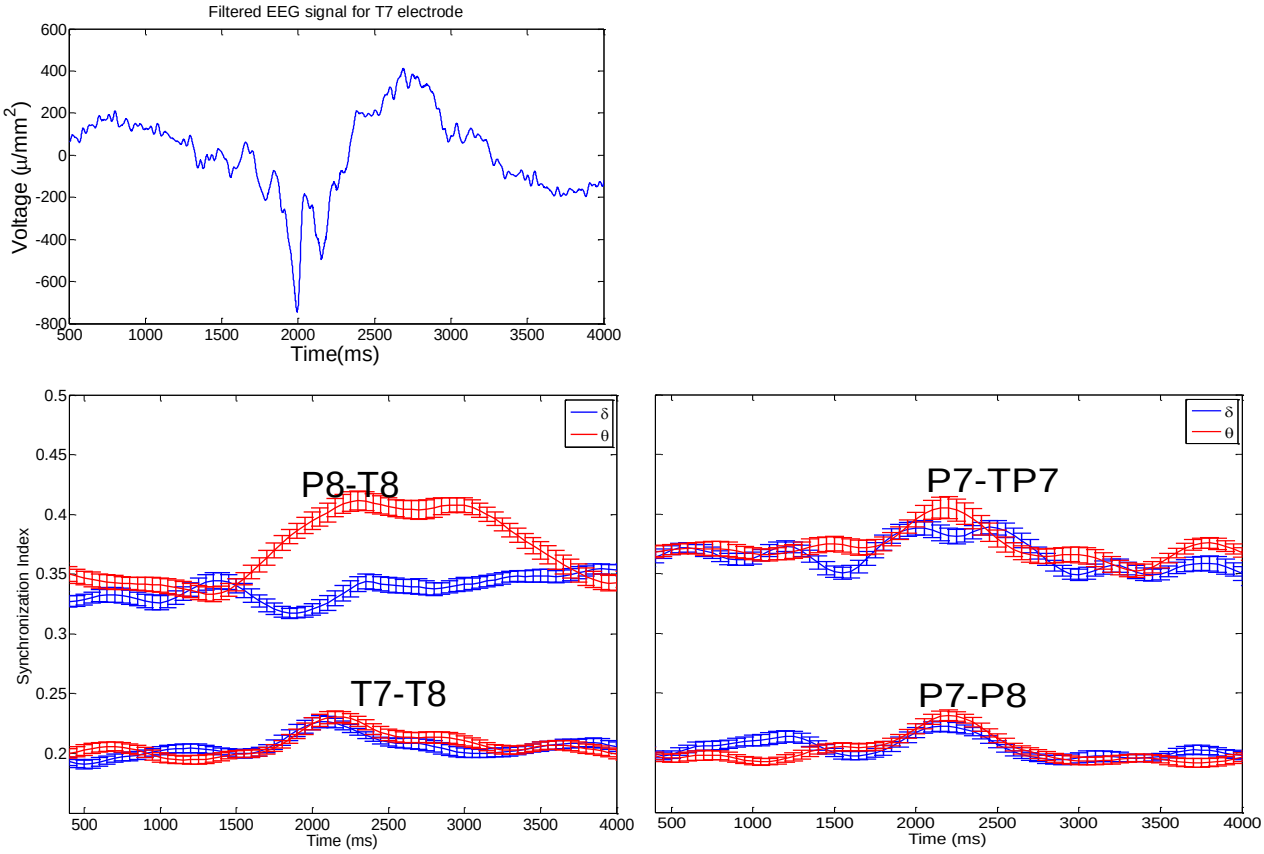

Figure 6.3: Synchronization index: (A) Filtered EEG segment with TTA on T7, (B), the dynamic synchronization index between EEG channels for the delta (blue) and theta (red) frequency bands.

Topological organization of functional connectome

Figures 6.4 and 6.5 show the spatial topology of the pair-wire functional connectivity patterns for NAT and TTA. As shown, the functional connections were only densely packed at bilateral frontal and posterior regions. No long-distance functional connections with significant strength were observed between the both hemispheres as well as between anterior and posterior regions in the preterm brain networks. Regardless of the presence of TTA (TTA vs NAT) the spatial topology of the functional connections remained densely local at the bilateral frontal and posterior regions. In order to better investigate the impact of TTA on the brain functional organization, we compared the spatial distribution of degree between the TTA and NTA segments. The connection density

was higher due to the presence of TTA in the θ band, though functional connections were restricted to the temporal regions. In the δ band, the occurrence of TTA spuriously lowered ($p<0.01$) the functional connectivity level between the temporal and parietal regions in the left hemisphere.

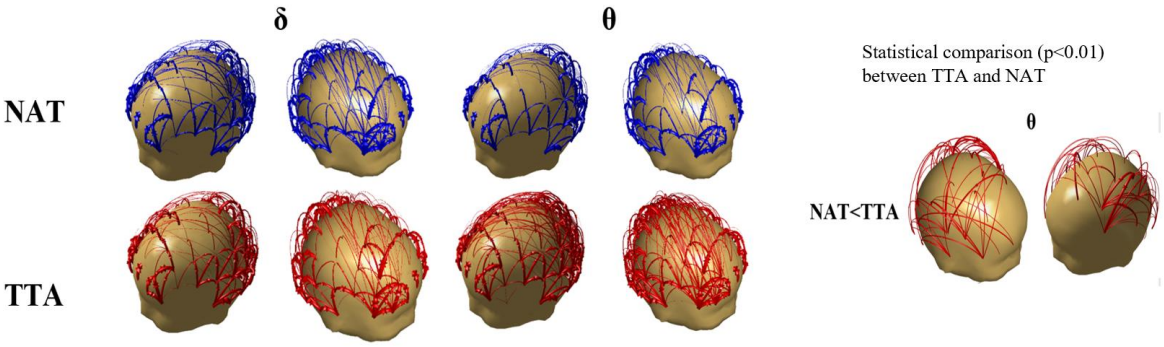

Figure 6.4: Spatial topology of functional connectivity. The group average is for normal activity (NAT) and theta temporal activity (TTA) shows the prominent functional connectivity in frontal and posterior regions and statistical difference between the two activities reveals increased functional connectivity at each of the temporal region due to TTA in θ band.

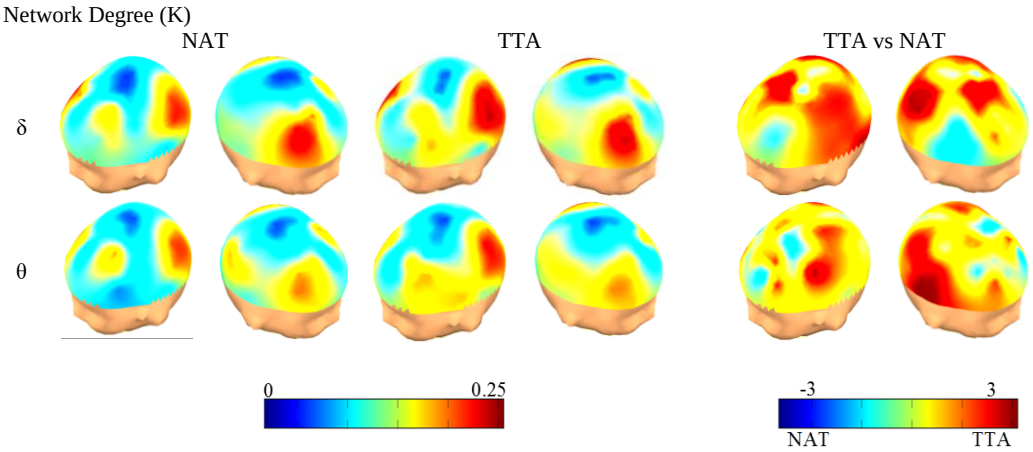

Figure 6.5: Spatial topology of functional connectivity pattern. The degree for normal activity (NAT) and theta temporal activity (TTA) indicated prominent functional connections in the frontal and posterior regions. The statistical differences between the two activities revealed stronger functional connections at each of the temporal regions due to the occurrence of TTA.

Spatial topology and network metrics

The spatial topology of the functional connectivity pattern indicated dense functional connections at the frontal and posterior regions. We further characterized the functional connectivity pattern to investigation the spatial distribution of local connectivity (Figure 6.6). The clustering coefficient (C) in δ band was higher at the bilateral frontal and posterior regions but lower (mainly in θ band) at central region for both NAT and TTA. Compared to NAT, the presence of TTA also resulted in increased C values over the temporal regions in θ band, and decreased C values over the frontal regions in δ band. The local efficiency (LE) presented topological patterns similar to the one that was found for the clustering coefficient with higher LE at the frontal and posterior regions and lower LE at the central region, especially in θ band, for both NAT and TTA.

The global network metrics (Figure 6.7) were higher for TTA compared to NAT except for the clustering coefficient in the δ band where TTA was significantly lower.

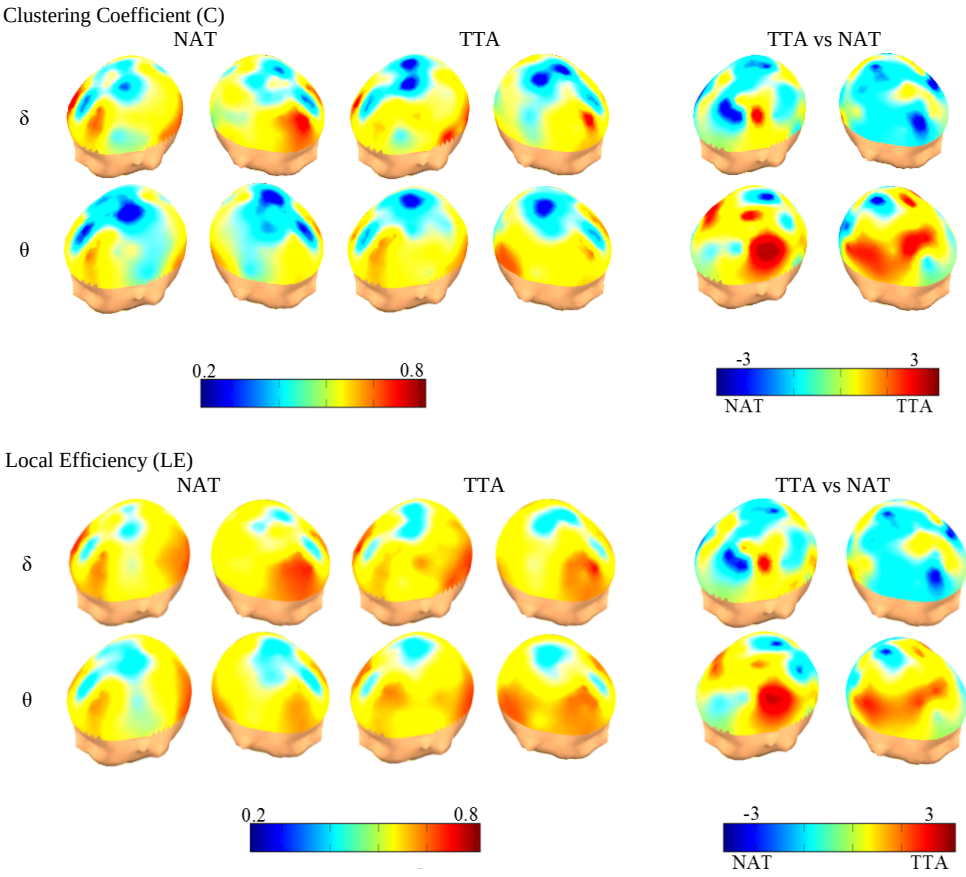

Figure 6.6: Spatial topology of the network metrics, clustering coefficient C, and local efficiency LE for TTA and NAT and their statistical differences. The first column is the group average with the bar indicating the range on changes. The second column shows the statistical differences between TTA and NAT with the bar indicating t-values.

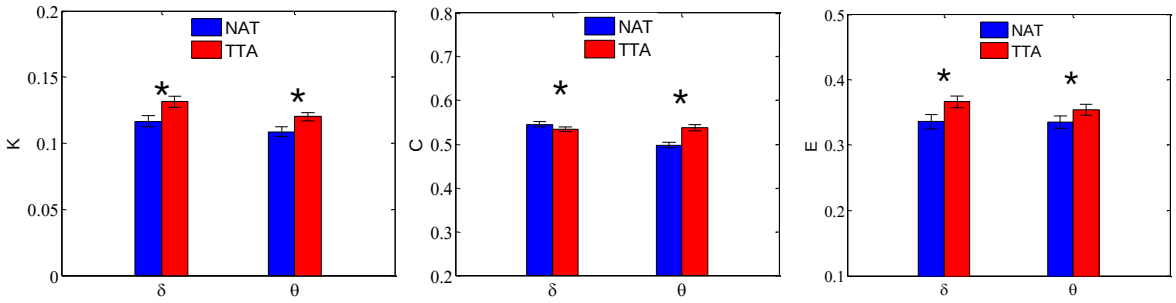

Figure 6.7: Global network metrics. Global network degree (K), clustering coefficient (C) and global efficiency (E) for both TTA and NAT. The asterisks indicate statistical significance with $p<0.05$.

Brain symmetry index

The functional brain symmetry index was computed from the relative differences in network metrics between the right and left hemispheres in both frequency bands. We divided the brain regions as shown in Table 6.2. The Brain Symmetry Index (BSI) was computed for the frontal (F), temporal (T), central (C) and posterior (P) regions. The BSI was defined as:

$$BSI = \sum_{i=1}^{M} \frac{R_i - L_i}{R_i + L_i} \tag{6.7}$$

Where R and L for the right and left hemisphere, respectively, and M indicates the number of channels in each region. A positive value refers to the rightward asymmetry.

Table 6.1: EEG Channels in each region

Regions		EEG channels
Frontal (F)	Right frontal (RF)	FP2, AF4, AF8, F2, F4, F6, F8
	Left frontal (LF)	FP1, AF3, AF7, F1, F3, F5, F7
Temporal (T)	Right temporal (RT)	FC6, C6, CP6, T8, TP8
	Left temporal (LT)	FC5, C5, CP5, T7, TP7
Central (C)	Right central (RC)	FC2, FC4, C2, C4, CP2, CP4
	Left central (LC)	FC1, FC3, C1, C3, CP1, CP3
Posterior (P)	Right posterior (RP)	P2, P4, P6, P8, PO4, PO8, O2
	Left posterior (LP)	P1, P3, P5, P7, PO3, PO7, O1

The BSI result is shown in Figure 6.8 for all the graph metrics. Generally, there was a rightward asymmetry in the frontal region and a leftward asymmetry in the posterior region for all the network metrics and frequency bands. In θ band, there was a rightward asymmetry in the temporal region under both conditions, with and without TTA. The asymmetry was more pronounced for the TTA segments.

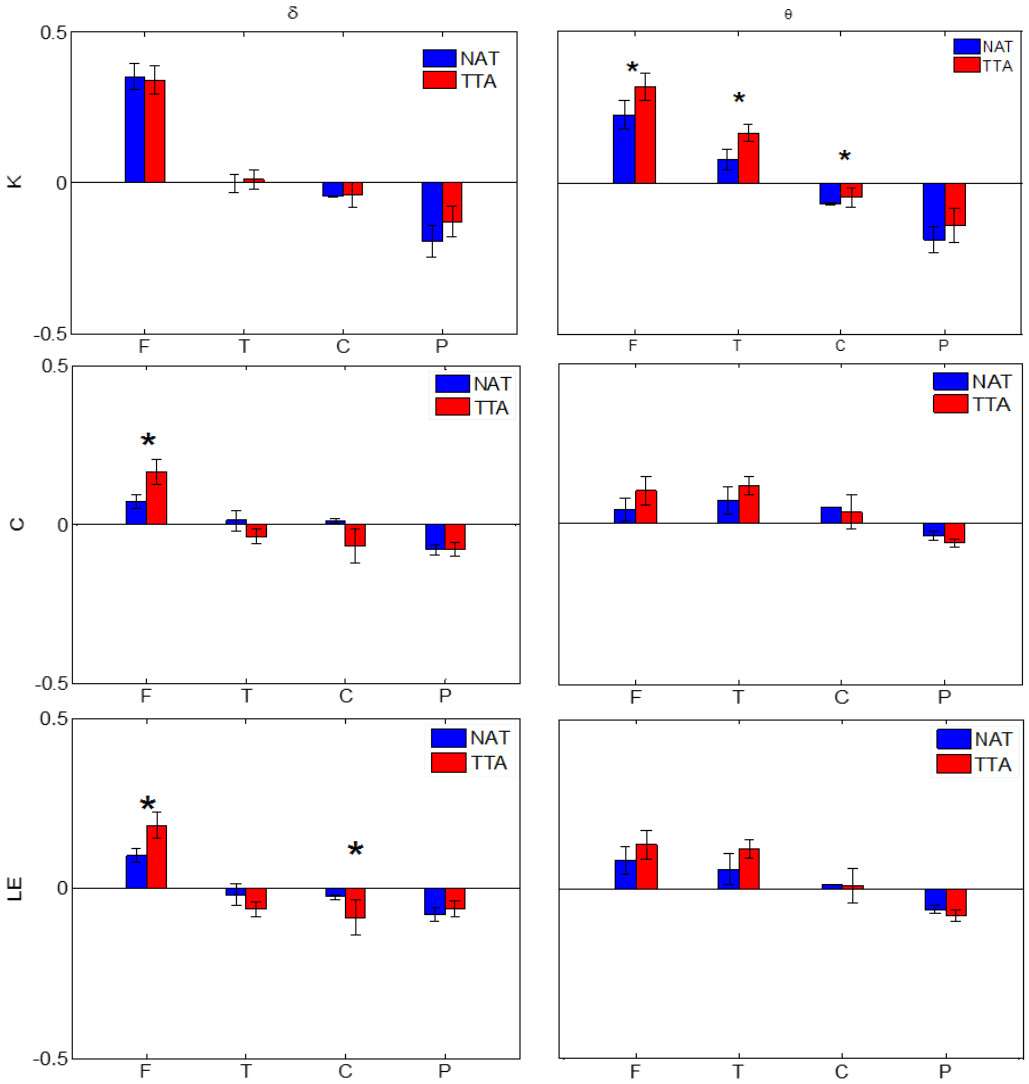

Figure 6.8: Brain Symmetry Index (BSI) results for Network degree (K), Clustering coefficient (C) and Local efficiency (LE). F, T, C, and P represent frontal, temporal, central and posterior regions, respectively, as shown in Table 6.2.

6.2.4 Discussion

In order to assess the spatial functional organization of the premature's brain we analyzed the synchronization and functional connectivity of the brain networks using high density EEG in preterm neonates. The synchronization level between brain regions during TTA were assessed by the synchronization index in two frequency bands (δ and θ). The pairwise correlation between all the channels was also computed by the phase locking value (PLV). We further computed three graph metrics- degree, clustering coefficient and efficiency to characterize the functional connectivity pattern of the preterm brain networks. Our results showed that functional connectivity in the healthy preterm infants were local with very weak direct long-range functional connections between the hemispheres and between anterior to posterior areas. Moreover, the functional connectivity analysis of the theta temporal activity (TTA), as a specific biomarker at this period of

neurodevelopment, showed restricted high connectivity density within the left and right temporal regions.

The functional connectivity analysis of resting state fMRI data has shown dense functional connectivity patterns at the frontal and posterior regions in preterm neonates (Ball et al., 2014; Fransson et al., 2011; Heuvel et al., 2015; Smyser et al., 2011). Using high-density EEG, we found locally dense functional connectivity in the bilateral frontal and posterior regions with very weak long-range functional connectivity between the hemispheres. Our findings support the hypothesis that the frontal and the posterior regions are at least partly functionally developed before the term birth (Pandit et al., 2014; Teffer et al., 2013). The existence of the rich-club structural connectivity predominantly in frontal and parietal regions has been reported in preterm neonates between 30 and 40 week using the diffusion magnetic resonance imaging (Ball et al., 2014). The absence of inter-hemispheric asynchrony of EEG burst activity has also been reported in preterms of 28- 32 wGA (Wallois, 2010). This is likely due to the immaturity of transcallosal connection at this early stage of development (Anderson et al., 2006, 2005; Rose et al., 2014). In line with the findings reported for fullterm neonates, we found weaker long range functional connections between anterior and posterior cortical regions in preterm infants (Fransson et al., 2007; Kwon et al., 2014; Smyser et al., 2011).

We also found that the increase in functional connectivity due to theta temporal activity was restricted to the temporal regions only. The TTA is not stimulus driven and appear as local endogenous generators most likely located in the subplate (Kostović and Judas, 2010)). They occur from 24wGA on, before the connection of thalamic afferents with the cortical plate (28wGA). The very dense functional connectivity pattern associated with the occurrence of TTA at the temporal region might be related to the development of the language/communication regions (Judaš et al., 2013; Kostović and Judas, 2010). In contrast to the idea that the brain can establish long range connectivity during brief events of endogenous network activity" (Omidvarnia et al., 2014), we did not find strong long range connectivity between the hemispheres or between anterior and posterior regions during TTA.

(Omidvarnia et al., 2014) have reported a random global functional network organization in preterm neonates (Omidvarnia et al., 2014). We found the small-world properties in the preterm brain networks with locally dense and sparse and weak long distance functional connectivity within and between the two hemispheres. Our finding is in agreement with the results of other studies (Heuvel et al., 2015). The small-world functional organization of the brain networks seems to be topologically optimal for information segregation and integration in adults and neonates(Fair et al., 2009); (Bassett and Bullmore, 2006; Ratnarajah et al., 2013). Our finding confirms the idea that most functional networks present in neonates are subject to functional reorganization and development (Dosenbach et al., 2010; Fair et al., 2009) from functionally local segregated network to distributed networks.

One significant feature of the mature human brain lies in its asymmetry structurally and functionally (Dehaene-Lambertz and Spelke, 2015). The rightward asymmetry in spectral power

in the frontal and temporal regions has been reported in preterm neonates (Field and Diego, 2008; Mento et al., 2010) . The rightward asymmetry suggests more activity in the right hemisphere than the left hemisphere. We found higher values of clustering coefficient and efficiency in the right hemisphere compared to the left side. This finding, however, suggests the information processing is likely to be done more efficiently within the local regions of the right hemisphere. In preterm neonates, compared to the left side, the right hemisphere has shown higher cerebral blood flow at rest (Roche-Labarbe et al., 2012) and higher hemodynamic responses in the superior temporal sulcus to auditory stimulation in preterm (Mahmoudzadeh et al., 2013). These findings may confirm that the right hemisphere in the preterm brain is relatively more developed in preterm infants (Dehaene-Lambertz and Spelke, 2015). Conversely, the leftward asymmetry in parieto-occipital areas, with or without TTA, might be partly explained by the stronger functional hemodynamic activity observed in the same regions during the phonemes stimulation in preterm (Mahmoudzadeh et al., 2013).

Conclusion

The present findings provide more information on the functional organization of the brain networks in preterm neonates. We showed that the activity of the preterm brain networks is densely localized in bilateral frontal and posterior regions with the weaker direct long-range functional connectivity between hemispheres and between anterior/posterior regions. Endogenous activity such as TTA may play an important role in the neurodevelopment with dense functional connections and high degree of clustering coefficient and local efficiency within each temporal region. However, further studies are required to confirm the role of the TTA generators in the maturation process of the brain in preterm neonates.

6.3 Full-term EEG functional connectivity

Functional organization of full-term neonates during natural quiet and active sleep

6.3.1 Introduction

The early infancy is a crucial period concomitant with rapid neurodevelopment in human life. Though relatively small at birth, the brain structure develops quickly in the first few weeks after birth. Despite the tremendous advances in neonatal healthcare, neonates are highly at high risk of poor neurodevelopment (Back and Miller, 2014). The period between 37 and 42-week gestational age is a critical transitional period and constitutes a break in the maturation process between utero and ex-utero. This period is also considered as the beginning of a more linear progression of cerebral activities with a gradual increase in the frequency of brain activities and specialization (Wallois, 2010).

So far, there has been little attempt to investigate the functional neonatal connectome using the functional Magnetic Resonance Imagining (fMRI) (Ball et al., 2014; Doria et al., 2010; Fransson et al., 2009, 2007). Fransson et al. (2011 and 2007) have revealed the existence of cortical hubs at primary sensory and motor brain regions in infant brain. In adults, the majority of cortical hubs and hub-related networks are located in the heteromodal association cortex. These findings provide some evidence on how brain connectivity evolves quickly from the immature neonatal

brain to the mature brain in adults due to mainly the process of myelination and tangential connectivity which speed up the transfer of information (Kostović and Judas, 2010; Stiles and Jernigan, 2010). In neonates, brain electrical activity is characterized by some endogenous bursts of activity such as the frontal transients, and period of discontinuity in quiet sleep (André et al., 2010). Compared to fMRI, due to its high temporal resolution, EEG is well suited to investigate the functional connectivity associated with these transient activities in full-term neonates. There have been efforts to assess the functional connectivity of neonatal brain activity with low density EEG (Grieve et al., 2008). To characterize the spatial specificity of the EEG data as well as the functional connectivity patterns in neonates, the acquisition of high density EEG data is required (Odabaee et al., 2013). Recent EEG studies (Grieve et al., 2008; Omidvarnia et al., 2015, 2014; Tokariev et al., 2015) have shown the benefit of high-density EEG for studying the functional neuronal activity at the early stage of neurodevelopment in preterm and full-term babies.

The neonatal sleep architecture consists of active and quite sleep with intermixed transitional or intermediate sleep segments (André et al., 2010). The differentiation between quiet and active periods with amplitude correlation (Tokariev et al., 2015) has revealed intra and interhemispheric connectivity during the active sleep in higher frequencies compared to the quite sleep. This observation suggests that functional brain networks are rapidly evolving from in-utero to ex-utero situations.

In the present study we investigated the brain functional connectivity patterns in full term neonates during both the quiet and active sleep stages using the spectral power and functional connectivity analyses. We also used different graph metrics to characterize the brain functional connectivity. We further searched for biomarkers of the brain functional maturation in neonates by exploring their brain functional topology for short- or long-range connections during the quiet and active sleep stages.

6.3.2 Material and methods

Subjects and EEG recordings

High Density EEG (HD-EEG) data recorded from 14 healthy full-term neonates (35.81 ± 2.71 weeks, Gestational age, GA) were included in this study from the clinical database of the pediatric functional exploration of the nervous system service in Amiens University Hospital, France. The inclusion criteria were the absence of neurological disorders and illness. The HD-EEG data were recorded in the neonatal intensive care unit of the university hospital of Amiens, France. The data had been recorded for clinical routine use during both quite sleep (QS) and active sleep (AS) using the ANT's EEG acquisition system (ANT, Netherlands) with a sampling rate of 1024Hz and a high density EEG cap (Medelopt™, France) adapted for full term neonates with 64 channels positioned according to the international 10-10 standard system. Two electrophysiology experts selected 3 seconds of 25 segments during the QS and AS conditions separately for each subject.

EEG data preprocessing

EEG data were first band-pass filtered between 0.5 and 40 Hz to exclude very low frequency activities as well as high frequency noise. The EEG trials were then re-referenced using a Laplacian

montage (current source density, CSD) (Perrin et al., 1989) to effectively minimized volume conduction artifacts. CSD has been shown to have optimal source separation and performance required for the connectivityanalysis (Srinivasan et al., 2007). Considering missing or bad channels, 59 electrodes were used for all the neonates for further analysis.

Power spectral analysis and EEG source analysis

We performed the spectral power analysis in four frequency bands (δ, θ, α and β) in both sensor and source spaces. The scalp spectral power was divided into different brain regions based on their anatomical locations as shown in Table 6.3.

Table 6.3: EEG Channels in each region. R and L denote right and left hemisphere, respectively.

Regions		EEG channels
Frontal (F)	Right frontal (RF)	FP2, AF4, AF8, F2, F4, F6, F8
	Left frontal (LF)	FP1, AF3, AF7, F1, F3, F5, F7
Temporal (T)	Right temporal (RT)	FC6, C6, CP6, T8, TP8
	Left temporal (LT)	FC5, C5, CP5, T7, TP7
Central (C)	Right central (RC)	FC2, FC4, C2, C4, CP2, CP4
	Left central (LC)	FC1, FC3, C1, C3, CP1, CP3
Posterior (P)	Right posterior (RP)	P2, P4, P6, P8, PO4, PO8, O2
	Left posterior (LP)	P1, P3, P5, P7, PO3, PO7, O1

We used the neonatal MRI template (Fonov et al., 2011) for the construction of the head model. The template was segmented by SPM8 (Ashburner et al., 2012) into scalp, skull and brain compartments defining 3 homogeneous conductive mediums. The lead field was calculated using FieldTrip (Oostenveld et al., 2011) with 6 mm spatial resolution. In total, 4744 source locations were generated inside the brain. The leadfield wa calculated using the Boundary Element Method (BEM) (Oostendorp and van Oosterom, 1989) The eLORETA (Pascual-Marqui, 2007b) inverse solution was used to calculate three dimensional current density distributions in the four frequency bands. We used eigen decomposition method (Sekihara et al., 2004) to determine the dominant dipole orientation and to obtain high SNR for reconstructed current density.

Frequency-domain signal

The frequency-domain signal was computed using the Morlet wavelet, which is localized in both time and frequency and useful for processing nonstationary signals. However, Morlet wavelet, w (t,f) is defined as:

$$w(t,f) = \left(\sigma_t\sqrt{\pi}\right)^{-\frac{1}{2}}\ e^{-\frac{t^2}{2\sigma_t^2}}\ e^{-i2\pi ft} \quad (6.\ 8)$$

Here, f is the center frequency and σ_t is the temporal standard deviation. The time-frequency complex signal Z (t,f) of a signal $z(t)$ was computed by convolving it with $w(t,f)$:

$$Z(t,f) = z(t) * w(t,f) \quad (6.9)$$

We choose the spectral bandwidth for each frequency band by controlling the center frequency, f and its ratio to the standard deviation (σ_f). The following center frequencies 2.5, 6, 10 and 15

were used for the these frequency bands δ(1 - 4 Hz), θ(4.17 – 7.83 Hz), α(7.5 – 12.5 Hz) and β (12 – 18 Hz).

Functional connectivity analysis

To investigate the functional connectivity patterns for each condition, Phase Locking Value (PLV) was computed between all pairs of EEG channels ((Lachaux et al., 1999; Mormann et al., 2000). The PLV between electrodes X and Y is computed as:

$$PLV(x,y) = \frac{1}{N}\left|\sum_{t=1}^{N} e^{i(\varphi_x(t)-\varphi_y(t))}\right| \quad (6.10)$$

Where φ_x and φ_y are the instantaneous phases computed using the complex signals of X and Y. The PLV ranged from 0 to 1, with 0 and 1 indicating no connection and maximum connection between any given pair of signals, respectively. The end-result of computing the PLV for all pairs of channels was a square connectivity matrix of size 59 (number of EEG channels), in which each entry $N_{x,y}$(= $N_{y,x}$) contained the PLV for channels X and Y.

Single- and group-level statistical analysis

To evaluate the significance of PLV, we generated 200 time-shifted surrogate signals sharing statistical characteristics of the original data (Theiler et al., 1992). The PLV between the first signal and all the time-shifted versions of the second signal yielded a null distribution for statistical testing. The significance was defined by the difference between the original and the mean of the surrogate values of statistics, divided by the standard deviation of the surrogate values:

$$Z = \frac{PLV - \mu_{surrogate}}{\sigma_{surrogate}} \tag{6.11}$$

We used a criterion of 1%, which implies that the proportion of surrogate values higher than the original PLV (between x and y) must be less than 1% (99% significance level). This procedure was performed for each individual connectivity matrix (Figure 6.9). The error rate in multiple comparisons was also corrected by controlling the false discovery rate (Nichols, 2012) at 0.1% significance level for the grand average of individual connectivity matrices (Figure 6.9).

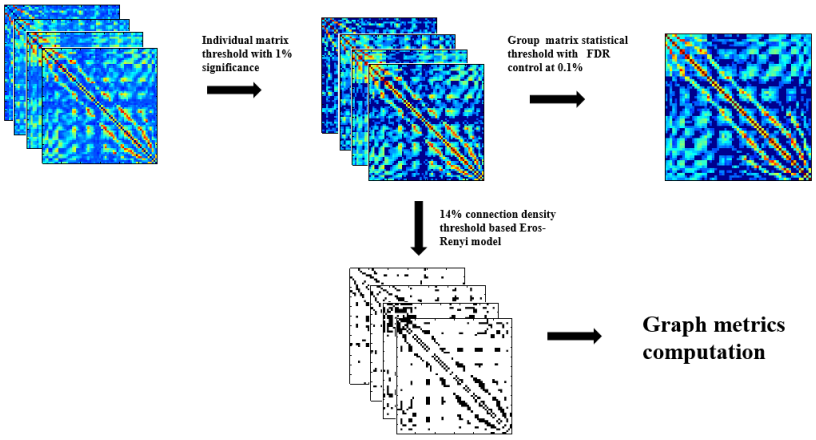

Figure 6.9: Statistical procedures: The single-level significance was tested using distributions derived from time shifted surrogates, while the group-level testing was done with the FDR control at 0.1% significance level. The individual significance matrix was thresholded at 14% connection density based on the Eros-Renyi model before computing the graph metrics.

Graph theoretical measures

To compute graph metrics, the functional connectivity matrices were first thresholded and binarized using the Erdos-Renyi model (Erdős and Rényi, 2013), in which the threshold is determined in a way that most of the nodes remain fully connected at a connection density of 2ln(N)/N, where N is the number of nodes. In our study with 59 EEG channels, the connection density was approximately 14% using the Erdos-Renyi model. We then computed the following graph metrics (Rubinov and Sporns, 2010):

Degree: the most common measure of centrality with a straight forward neurobiological interpretation. A node with high degree implies more interaction with many nodes in the network.

Betweeness centrality: a very sensitive measure of centrality that measures the fraction of all shortest paths that pass through a given node. Like the network degree, it is used to detect the important functional connection.

Clustering coefficient: computes the functional segregation by measuring the presence of clusters or modules in functional networks.

Characteristics path length: estimates the potential functional integration in the network and is computed by the average shortest path length between all pairs of the nodes in the network.

Small-worldness: a metric that measures the ability of the functional network to combine functionally segregated modules with robust integration links. This metric is measured by computing the ratio of the normalized clustering coefficient to the normalized path length. A network with a small-worldness greater than 1 is said to exhibit small-world property.

The details of the mathematical descriptions of these metrics are provided in the Appendix.

The degree measures the presence of cortical hubs and the bewteeness centrality was computed on order to investigate the region that are involved in the transfer of information from one region to the other. The functional segregation was estimated by clustering coefficient, and the global connectivity processing by characteristic path length. There is general idea that neonatal brain also estimated small-world features and this investigate by computing small-worldness which measures the ratio of normalized clustering coefficient to characteristic path length.

All computations and statistical analyses were performed in Matlab with custom scripts and open source toolboxes: EEGLAB (for 3D topological plots, http://sccn.ucsd.edu/eeglab/), and the brain connectivity toolbox (for graph parameter computations, https://sites.google.com/site/bctnet/).

6.3.3 Results

EEG power spectral and Source analysis

The results of the EEG power spectral and source analyses in all frequency bands are shown in Figures 6.10 and 6.11, respectively. As shown in Fig. 6.10, the power spectra decreased as the frequency increased (Figure 6.10). There was no difference between both sleep conditions in each region and in all the frequency bands. As shown in Fig. 6.11, the QS condition, significant increases in CSD were observed at the posterior region in the δ and θ bands and at the right temporal region in the α and β bands. In the AS condition, we found increased CSD at the frontal region in all the frequency bands. The AS condition also exhibited higher CSD at the posterior region compared to other regions in the δ and θ bands similar to that observed in QS.

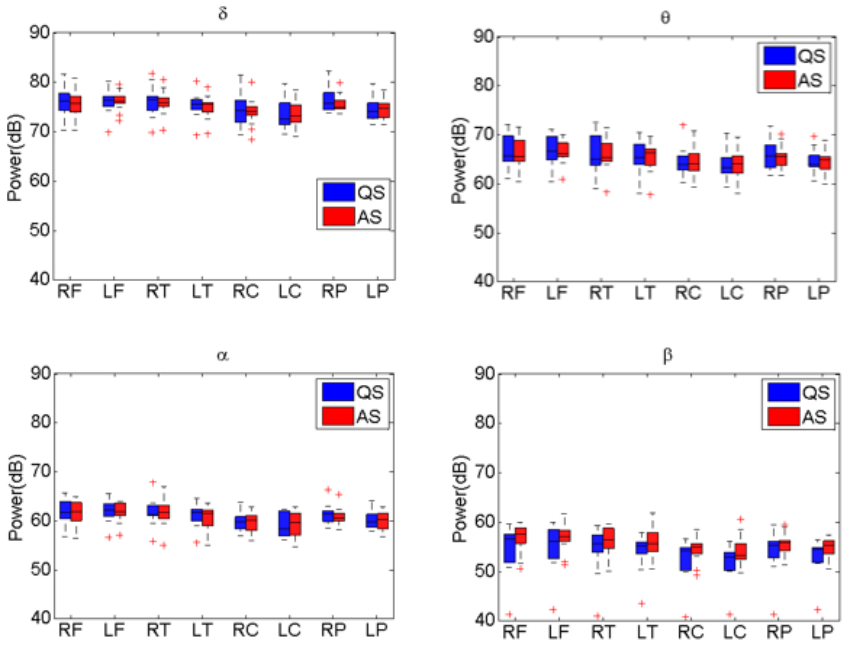

Figure 6.10: EEG spectral power results. Average power for the four frequency bands and each region (see Table 6.3) for both conditions (QS and AS)

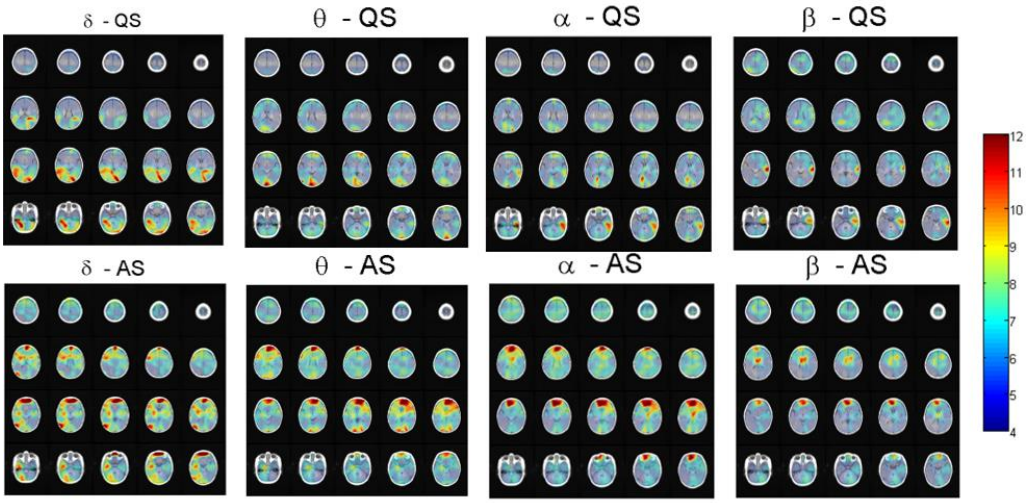

Figure 6.11. Results of the Statistical analysis of eLORETA current source density for both conditions (QS and AS) in all the frequency bands. The color bar indicates t-values.

Whole brain connectivity

Figure 6.12 shows the average PLV matrices for both conditions and all the frequency bands. In both conditions, functional connectivity matrices look similar in each frequency band. However, the connectivity density (number of significance elements) increased with increasing frequency with weaker strengths in the α and β bands. No difference was observed between the two sleep

conditions for all the frequency bands with p<0.10. However, the mean PLV as shown in Figure 6.13 shows higher mean PLVs in the δ and θ bands than in the α and β bands.

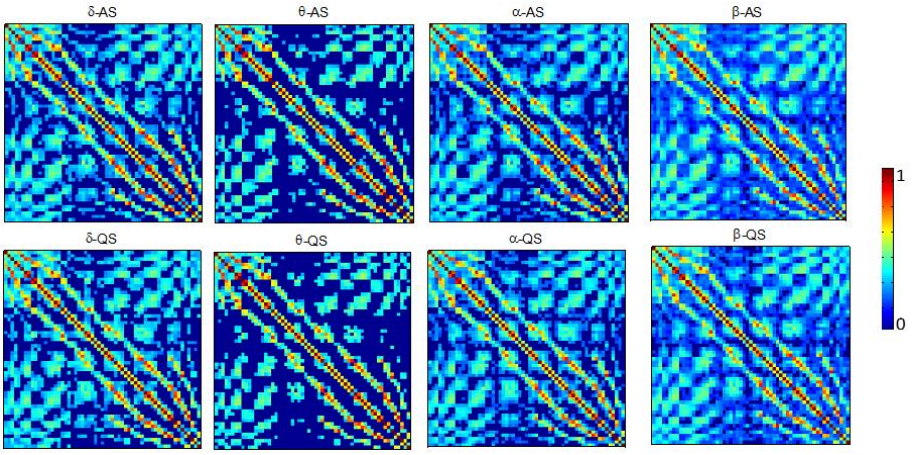

Figure 7.12: Mean PLV connectivity matrices for both conditions (QS and AS) with 59 EEG channels. Each matrix is the result of the group average with a FDR value of 0.1 for all the frequency bands. The colorbar indicates the strength of the elements in the matrix.

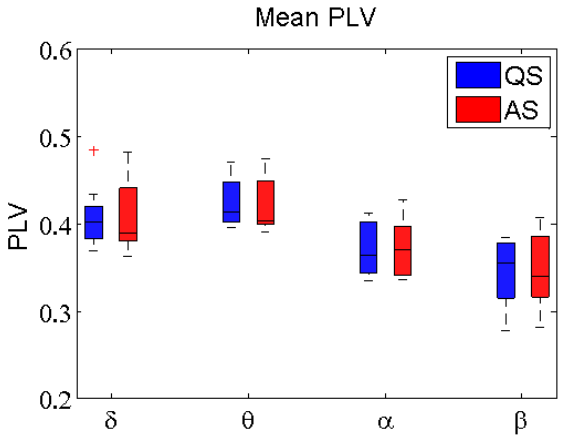

Figure 6.13: Mean PLV for both conditions (QS and AS) in all the frequency bands

Global networks properties

Figure 6.14 shows the global network properties; mean betweenness centrality, clustering coefficient, characteristics path length and small-worldness, in both sleep conditions and all the frequency bands. All the network metrics were calculated with a connection density of 14% determined based on the Erdos-Renyi model (Erdős and Rényi, 2013) to make sure all the nodes are fully connected. There was no significant difference in all the graph metrics between both the sleep conditions within all the frequency bands. The graph metrics for both the conditions showed

similar values for QS and AS with a betweenness centrality around 0.015, a relatively average path length around 2.7 and a clustering coefficient around 0.35.

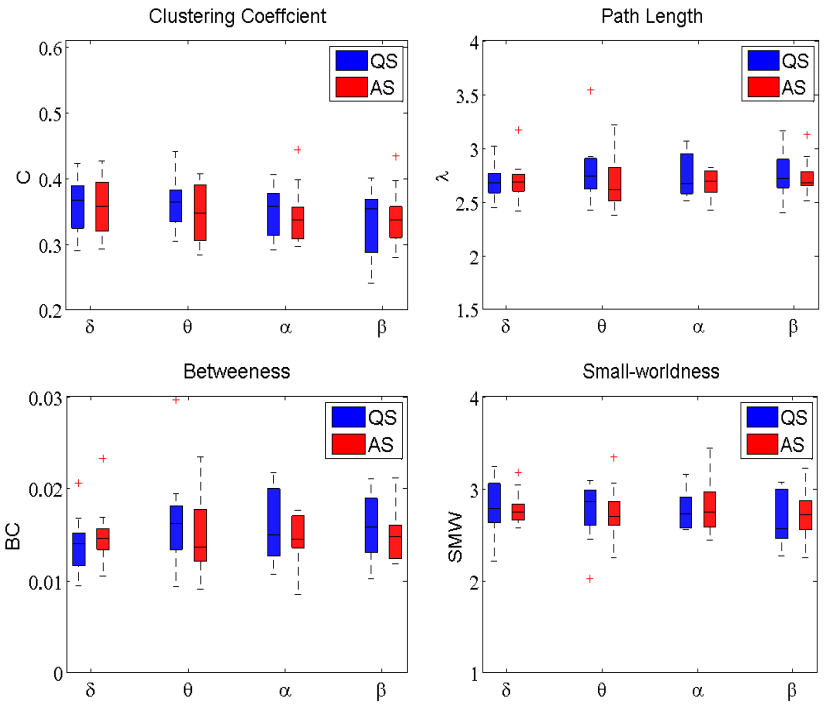

Figure 6.14:Global network metrics: Betweenness, Clustering coefficient, Characteristics Path length and Small-worldness for both conditions and all the frequency bands. All the graph metrics were calculated from the thresholded connectivity matrix with a connection density of 14% determined using the Erdos-Renyi model.

Local network properties

The spatial topology of the degree (K), betweenness centrality (BC), and clustering coefficient (C) for QS and AS are shown in Figures 6.15 and 6.16, respectively.

High degree (K) were found in the frontal and the posterior regions in all the frequency bands in both the sleep conditions. The degree was lower at the central region of the brain especially in the β band with no statistical differences between the two sleep conditions.

The betweenness centrality (BC) was lower in lower frequency bands. It increased significantly bilaterally in anterior temporal regions in the θ, α and β bands especially in the QS conditions. In both conditions, bilateral frontal-temporal regions showed increased betweenness centrality notably in the β band.

In both conditions, the spatial distribution of the clustering coefficient was similar in all the frequency bands. The average clustering coefficient (C) was about 0.35 over all the brain regions excluding the central areas

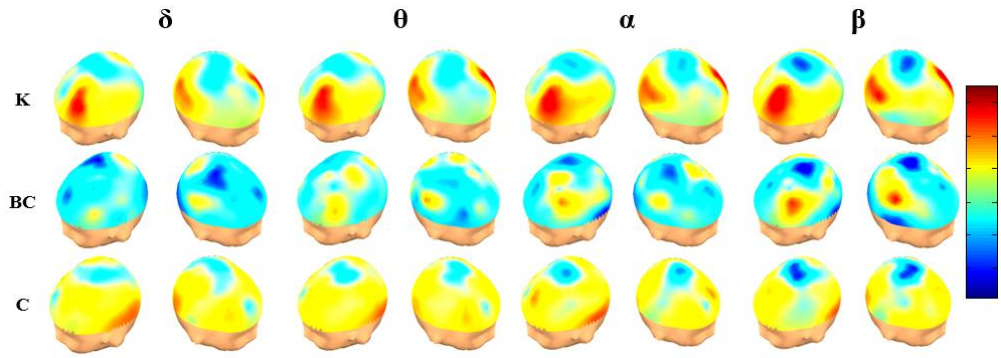

Figure 6.15: Spatial topology of the network degree (K), betweenness (BC) and clustering coefficient (C) during QS. The colorbar indicates the strength of the metrics from zero (blue) to highest value (red) corresponding to 0.25, 0.03 and 0.6 for K, BC and C, respectively. All the graph metrics were calculated from the thresholded connectivity matrix with a connection density of 14% determined using the Erdos-Renyi model.

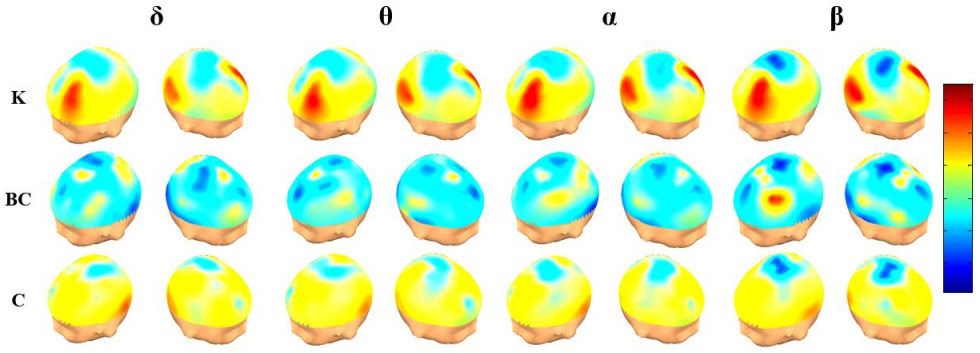

Figure 6.16 Spatial topology of the network degree (K), betweenness (BC) and clustering coefficient (C) during AS The colorbar indicates the strength of the metrics from zero (blue) to highest value (red) corresponding to 0.25, 0.03 and 0.6 for K, BC and C, respectively All the graph metrics were calculated from the thresholded connectivity matrix with a connection density of 14% determined using the Erdos-Renyi model.

6.3.4 Discussion

The results of our functional connectivity analysis strongly suggest that the functional organization of the brain networks in full term neonates is dominated by the short-range functional connections at the frontal, temporal and posterior regions. In contrast to previous results (Omidvarnia et al., 2014; Tokariev et al., 2015), our results indicate that long range functional connections in neonates are sparse and limited during both active and quiet sleeps. This discrepancy might be related to the higher EEG spatial resolution used in our study for functional connectivity analysis. Statistically, we did not find any differences in functional connectivity between the quite sleep (QS) and active sleep (AS). However, our results show some overlap with the structural and functional MRI studies in neonates (Ball et al., 2014; Fransson et al., 2009) with the exception of lower activity at the central regions.

We found higher power in lower frequency bands and lower power in high frequency bands. This can be directly deduced from the finding that EEG activity in neonate has high amplitude and low frequency (André et al., 2010). In other word, EEG activity with higher frequency has lower power and vice versa in the mature brain. The higher current source density at the frontal region during active sleep is likely to be related to the occurrence of frontal transients and the slow anterior dysrhythmia that are well characterized during AS from 37wGA (André et al., 2010). Although, we cannot rule out with certainty the effect of rapid eye movement artifacts on the results of the spectral analysis during AS. In both AS and QS, higher source activity were observed at the posterior regions in lower frequency bands most likely due to the predominant slow delta waves at the occipital region (André et al., 2010; de Weerd and van den Bossche, 2003). The occurrence of slow delta waves at the temporal and occipital regions can be considered as one of the biomarkers used for studying the brain maturation in full-term neonates. In the lower frequency band, relatively higher source activity values were observed over rolandic areas in AS and to a lesser extent in QS. This increase in source activity might be partly explained by the presence of temporal specific activity such as theta temporal bursts which predominantly occur in the rolandic/temporal regions during AS (André et al., 2010). During QS, we observed an increase in high frequency source activity at the temporal lobe which is highly involved in communication, hearing and language skills. The temporal region as well as the amygdala and the hippocampus are highly involved in learning, memory, emotional responses, visual recognition memory and attention (Bachevalier and Mishkin, 1994; Málková et al., 1995).

In our study, the graph-based network characterization demonstrated the small-world properties of the brain functional networks in full-term neonates, including high clustering coefficient and high centrality and betweenness (Fransson et al., 2011). We further found nodes with high degrees and high betweenness centrality at the frontal, temporal and posterior regions that correspond to brain regions functionally classified as "polysensory", or "multimodal association areas". These regions might be related to the parietal and prefrontal cortical regions in which the presence of cortical hubs has been demonstrated (Ball et al., 2014; Heuvel et al., 2015). These regions are thought to provide a foundation for coherent neuronal activation across distal cortical regions (Judaš et al., 2013; Kostović and Judas, 2010). This supports the evidence that the frontal, and the posterior regions are functionally developing during the infancy period (Dehaene-Lambertz and Spelke, 2015; Dubois et al., 2008; Pandit et al., 2014). These regions are established by the third trimester (Judaš et al., 2013) and have been reported to start to develop earlier than other brain regions with early functional and structural development of neuronal networks (Stiles and Jernigan, 2010; Teffer et al., 2013). The spatial location of these regions (frontal and parietal regions) tend to show large overlaps with structural and functional hub regions in the adult brain (van den Heuvel and Sporns, 2013). Although the functional spatial topology of the brain is very complex in neonates but it is generally believed that the brain networks evolve from a local architecture dominated by frontal, temporal and parietal regions to a more diffuse topology in adults (Dosenbach et al., 2010; Fair et al., 2009).

The neonatal functional networks exhibiting small-world properties may suggest that the neonatal brain support primary as well as higher cognitive functions (Bullmore and Sporns, 2009; Collin and van den Heuvel, 2013). The presence of small-word features (high clustering

coefficient and global efficiency/path length) in neonates and adults has been previously demonstrated (Fair et al., 2009; Fransson et al., 2011) though small-world connectivity properties are likely to increase as functional connectivity spatial patterns evolve from local connectivity in neonates to long-distance connectivity in adult (Cao et al., 2014; Gao et al., 2015; Supekar et al., 2009). The small-world features of EEG functional brain networks present in different frequency bands are highly heritable (Smit et al., 2008; Stam and van Straaten, 2012). The clustering coefficient and characteristic path lengths were found to be increasing by age (Betzel et al., 2014; Smit et al., 2012) with a maximum value during the youth period. This means that as the brain matures, distant brain regions communicate through strong long distance connectivity. This finding is in contrast with those reported in the fMRI studies (Fransson et al., 2011, 2007) which showed that neonates have distributed brain networks at some regions throughout the childhood and adolescence. This might be due to the differences between these modalities (for instance voxel/hemodynamic activity in fMRI and sensors/electrical activity in EEG). In general, the temporal dynamics of the brain neuronal signal (André et al., 2010) cannot be captured by the fMRI. Previous comparisons between EEG and fMRI signals in adult (Mantini et al., 2007) have shown the consistency and discrepancy between them in different frequency bands. There is, however, very little information available on the relationships between underlying neuronal and hemodynamic mechanisms in neonates.

In conclusion, our findings indicate that only local connectivity is present in neonates with higher activity and connection density at the frontal, posterior and temporal regions. This study indicated that the long range functional connectivity is limited and healthy full-term neonatal brain network exhibit small word properties. Our study supports the hypothesis that the neonatal brain network developed from local networks in neonates toward more integrated networks in adults.

These studies show that early brain activity of preterm is densely localized at the frontal and the occipital regions and long-range functional connectivity is limited. The presence of endogenous activity such as theta temporal activity plays an important role in the neurodevelopmental period with increased connection density at the temporal regions. Full-term neonates exhibited high connection density at the frontal, posterior and temporal regions during both quiet and active sleeps. The small world network properties were present in neonates, suggesting the presence of both information segregation and integration at local networks.

Chapter 7

General conclusions

7.1 Introduction

This chapter summarizes all the studies carried out in this thesis. The directions for future are also discussed. The purpose of this thesis was to investigate changes in the resting-state EEG functional connectivity topology in BCECTS patients in comparison to healthy controls as well as to investigate functional organization of brain networks in preterm and full-term neonates during the resting state.

7.2 Benign childhood epilepsy with centrotemporal spikes

In the first part of this thesis, we investigated whether the resting-state brain functional connectivity patterns in BCECTS patients in comparison to healthy controls were disrupted. In the first study, the EEG spectral power analysis in both the sensor and source spaces revealed that BCECTS patients had significantly higher θ power in all the brain regions and lower α power at the occipital region. The individual alpha frequency (IAF) was significantly lower in patients in all cortical regions compared to the healthy controls especially due to the presence of IEDs in EEG segments. The resting state EEG cortical source analysis also revealed stronger activity at the centrotemporal regions involved in the generation and propagation of the epileptic activity. Bilateral temporal regions displayed higher cortical activity in patients in all frequency bands and weaker activity at the frontal and occipital lobes in comparison to healthy controls.

We also found that the presence of IEDs impacted the global and local functional connectivity (FC) in comparison to healthy controls. For patients, the FC analysis using EEG segments with IEDs revealed significantly higher global θ phase synchronization and lower global connection density in the δ band in comparison to healthy controls. The topological distribution of the network degree revealed higher connection density at the epileptic zone (centrotemporal region) due to the presence of IEDs in all the frequency bands. A higher connection density was observed at the same zone in the absence of IEDs in higher frequency bands. Under both the epileptic conditions (with and without IEDs) patients exhibited lower connection density at the frontal and occipital regions especially in the α band in comparison to the healthy controls. Without IEDs, patients displayed higher lagged phase synchronization values (LPS) in the θ and α bands and lower LPS in the β band. The changes in the FC pattern support the idea that the disruption in the functional connectivity topology in BCECTS patients may not be restricted to the epileptic zone.

The characterization of the brain functional connectivity networks by the graph metrics revealed that the BCECTS brain networks was functionally more ordered in low frequency bands compared to the healthy controls. However, patients under both conditions (with and without IEDs) were characterized with less global information processing and stronger integration in higher frequency bands. In the absence of IEDs, patients exhibited less ordered brain networks compared to the healthy controls, a pathological network presented for rapid transition to the onset of epileptic discharges.

The seed-based functional connectivity analysis confirmed the functional reorganization of the brain in BCECTS patients compared to healthy subjects. It was shown that the epileptogenic networks were always activated. The existence of functional connections between the epileptic zone and the ipsilateral frontal and temporal regions suggested the involvement of distant cerebral regions in the generation and propagation of IEDs. We further found higher local efficiency in the contralateral hemisphere of the epileptic zone and the frontal region and weaker functional connections between the prefrontal cortex and the regions that were correlated with the default mode network (DMN). This may imply that DMN in BCECTS patients might be impaired.

The last study on the BCECTS functional connectivity was the identification of major drivers (brain regions) that were involved in the generation and propagation of IEDs, and the connectivity pattern with the aid of time-varying effective connectivity. Major drivers identified with higher outflow were the epileptic zone (pre and post central regions), ipsilateral parietal, rolandic, supramarginal and supplementary motor areas (SMA) and superior frontal regions. There was stronger causal influence from these regions to the frontal regions, indicating the involvement of frontal regions in the propagation of IEDs. The BCECTS brain networks also exhibited laterality toward the epileptic focus.

Clinical relevance

Higher source activity and functional connection density at the epileptic zone with the presence of IEDs is expected due to high amplitude of IEDs. However, higher functional connection density in high frequency bands in the absence of IEDs at the epileptic zone revealed that functional connectivity can detect transient activity of IEDs in EEG segment without IEDs. Lower activity at the frontal (especially prefrontal), parietal and posterior regions indicate the primary effect of IEDs. These regions correlated with the default mode network (DMN) and consistent with fMRI studies (Archer et al., 2003; Ibrahim et al., 2014) that reported the deactivation of the epileptic zone. The lower activity at these regions might related to the cognitive impairment and learning problems (Datta et al., 2013; Jambaqué et al., 1993; Verrotti et al., 2014) in these patients. In addition, lower activity and functional connection density at the frontal region at the ipsilateral of epileptic zone might be related to growth disturbance at the frontal region of the patients(Kanemura et al., 2011; Kanemura and Aihara, 2009).

Higher θ spectral power and synchronization with and without IEDs is a common feature of epilepsy and other neurological disorders most especially in young children. However, lower α activity especially at the posterior of the patients might relate to their cognitive and mental skills

deficits (Holmes and Lenck-Santini, 2006; Klimesch, 1999; Metz-Lutz et al., 1999). The lower beta β synchronization in patients shows that brain network of patients is frequency dependent.

The presence of IEDs increase source activity and functional connectivity at the epileptogenic networks. Epileptogenic networks in this group of patients is similar to the sensorimotor network which include central regions and supplementary motor areas. Higher activity and functional connectivity at these regions might related to the movement disturbance and jerking of mouth and throat(Boor et al., 2007; Tang et al., 2014) in patients during IEDs. Also, in the presence of IEDs the ipsilateral temporal region always had higher source activity which might have impact on the imbalanced auditory processing in patients as well as language and phonologic deficits(Amaral et al., 2015; Overvliet et al., 2011). The dynamic of directed interictal connectivity showed that the central regions drove frontal regions during IEDs which might be related clinical diagnosis of this type of epilepsy with the dipole pointing from from posterior to anterior position and vice versa. The occurrence of frontal-central connectivity during IEDs might also related to attention deficits and transient cognitive deficits in patients as some of these patients were diagnosed with attention deficit hyperactive disorder(ADHD) (Dunn, 2014; Dunn et al., 2003).

7.3 Brain functional connectivity in neonates

In the second part of the thesis, we assessed the brain functional connectivity in preterm and full-term neonates using high density EEG. The brain neuronal activity in neonates is different from that in adults. The neonatal EEG is characterized with different features such as theta temporal activity (TTA) in preterm and slow delta waves at the occipital region in full-term neonates. In preterm neonates, the results of functional connectivity analysis showed high connection density at the bilateral frontal and posterior regions. We further found that the direct long-range functional connections between the two hemispheres and between the anterior and posterior regions were limited. However, the presence of TTA burst at the bilateral temporal regions increased the connection density at the temporal region especially in the θ band and decreased the connection density at the left parietal regions in the δ band. The presence of TTA at the temporal region increased also the global network degree, global clustering coefficient and global efficiency in comparison to the normal EEG activity. Meanwhile, the preterm brain network exhibited the small-worldness features with local dense short-range and sparse long-range functional connectivity within and between the brain regions. The preterm brain also showed functional rightward asymmetry in the frontal and temporal regions and leftward asymmetry in the posterior region in terms of the network degree, global efficiency and clustering coefficient.

In full-term neonates, we investigated changes in the brain functional connectivity pattern during the quiet (QS) and active (AS) sleep. The spectral power analysis showed decreases in power with increasing frequency during both the quiet and active sleep periods. We also found higher source activity at frontal regions during AS and higher source activity at posterior region during QS especially in lower frequency bands (δ and θ bands). The right temporal regions displayed higher source activity during QS in higher frequency band. The functional connectivity

analysis revealed increased phase synchronization in lower frequency bands. The local functional connectivity topology was similar to that of preterm neonates. However, full term babies exhibited higher degree at the frontal and posterior regions and lower network degrees at the central region in all frequency bands under both conditions. We further found higher betweenness centrality at the bilateral temporal regions. Similarly, the full-term neonates showed distributed clustering coefficient throughout the brain excluding the central brain region. The global network metrics were also similar in all frequency bands. The full-term neonates exhibited small-worldness properties with an average small-worldness index of 2.7.

7.4 Methodological considerations and limitations

The thesis developed and implemented different techniques and analyses. Both EEG data of BCECTS patients and neonates were filtered within 0.5 to 40 Hz in order to remove high frequency noise. The laplacian Current Source Density (CSD) (Perrin et al., 1989) was applied to neonate EEG data to obtained distinct topography, effectively reducing the negative impact of volume conduction, which widely blurs the EEG signal. The CSD wasn't applied to the study of BCECTS because the IEDs is at the cortical surface (not deeper structure) and application of CSD can reduced the strength and intensity of IEDs.

Phase synchronization is the common functional connectivity measure used in this thesis. Phase synchronization is a nonlinear functional connectivity that measure relative phase difference between two nodes or brain regions. The phase locking value (PLV) (Lachaux et al., 1999; Schmidt et al., 2014) is zero-lag phase synchronization techniques that are developed based on scalp sensors and sensitive to volume conduction. The PLV was applied to all functional connectivity studies with scalp EEG data. For neonate EEG data, we created surrogate data to test for the significance of functional connectivity because neonatal EEG is different from mature adult EEG. In source space, the lagged phase synchronization (LPS) (Pascual-Marqui, 2007) was used to estimate the functional connectivity between brain regions. LPS is non-zero lag phase synchronization that is resistant to artifact of volume conduction by excluding instantaneous zero-lag contribution. However, LPS is also sensitive to uncorrelated perturbation especially strong noise which can turn phase lags into leads which could be a problem in sensor space. In addition, LPS was motivated due to its implementation in the eLORETA toolbox that was used for functional connectivity study in source space. We further used a ROI-based approached to reduced volume conduction as it is shown that spatial correlation between sources decays with increasing distance between them (Mehrkanoon et al., 2014). The imaginary coherence was used to estimated voxel-wise whole brain functional connectivity in source space. The imaginary coherence is based on the imaginary part of spectral coherence between two signals and has been shown to be less sensitive to volume conduction (Nolte et al., 2004) and measure true brain interaction. Imaginary coherence is one of the promising techniques have been proposed that are aimed at tackling the effects of field spread (Nunez et al., 1997; Schoffelen and Gross, 2009) which is common effect of source connectivity. In the dynamic interictal connectivity, the effective connectivity was estimated by the partial directed coherence (PDC), that measure the directed functional connectivity unlike PLV, LPS and imaginary coherence that measure non-directed functional connectivity.

Before the computation of graph metrics, the connectivity matrices were thresholded. However, the thresholding of the graph metrics were different for each study. This was motivated by the group of patients involved. Generally, threshold was applied in such a way all the groups and the conditions in the same study have the similar brain topology with similar connection density. However, in BCECTS studies compare to healthy control, both patients and control had similar topology and graph metrics were computed as a function of range of threshold values. In preterm neonates, the threshold was based on the first discovery rate (FDR) due to the nature of functional connectivity of the group.

The functional connectivity matrices in all the studies by the graph metrics most especially in term of functional integration and segregation. However, the degree was also computed which is the basic and the most important graph metric. For the second and third studies of BCECTS, the functional segregation was computed by clustering coefficient and functional integration by characteristics path length (or global efficiency). In the fourth study of BCECTS, the whole brain functional connectivity was characterized by the betweeness centrality and local efficiency. These graph metrics were employed in order to characterized the presence of regions involve in transfer of information between other regions and efficiency of local connectivity. Similarly, in preterm neonate, in addition to degree, the functional connectivity was characterized by the clustering coefficient and local efficiency both measured functional segregation. This was motivated by general idea that neonatal brain network consists of local connectivity in preterm neonate. However, in full-term neonate which is the starting period of linear brain progression, the functional connectivity was characterized by the betweeness centrality in order to detect the regions that involve in transfer of information between cortical regions; by functional segregation (by clustering coefficient) and functional segregation (by characteristic path length) and the small-world index to investigate the presence of small-world features in full-term neonates.

Before the computation of graph metrics, the connectivity matrices were thresholded. However, the thresholding of the graph metrics were different for each study. This was motivated by the group of patients involved. Generally, threshold was applied in such a way all the groups and the conditions in the same study have the similar brain topology with similar connection density. However, in BCECTS studies compare to healthy control, both patients and control had similar topology and graph metrics were computed as a function of range of threshold values. In preterm neonates, the threshold was based on the first discovery rate (FDR) due to the nature of functional connectivity of the group.

7.5 Directions for future research

In this thesis, the majority of the studies conducted on BCECTS patients was conducted on a homogeneous group of patients with right centrotemporal spikes with the same age and epileptic zone. Only in one study, we included whose epileptic zone was located in the left centro-temporal regions. This helped us to study patients with similar epileptic characteristics. However, due to low sample size, statistical comparisons between the patient groups with right and left epileptic foci were not possible. It would be interesting to compare patients with right centro-temporal

spikes with those with left hemispheric focus in terms of brain functional reorganization mainly because the left brain hemisphere is dominant in understanding and processing language, memory while the right brain hemisphere tends to be more dominant in creative activities such as decision making and non-verbal processing. Both of these studies will help us to investigate the impact of epileptic activity of the brain functional organization. In addition, we only used EEG signals to investigate the functional connectivity patterns in these patients. Combination of EEG and fMRI or Near-infrared spectroscopy (NIRS) would help to better investigate the topology of functional connections with high temporal and spatial resolutions.

Concerning neonates, our findings open new avenues to better understanding of brain functions during the early periods of neurodevelopment. However, there are still some features to be investigated in neonates such as frontal transients and slow delta waves superimposed with rapid activity (Delta Brushs) at the temporal/occipital region. Longitudinal studies would be very important to establish links between the brain functional organizations in preterm and full-term neonates. This could provide an opportunity for identifying functional biomarkers at early stages of the brain maturation process. However, it could be interesting to see how the brain networks are organized in the presence of neurological conditions such as neonatal seizures, hypoxic-ischemic, periventricular leukomalacia with Positive Rolandic Spikes (PRS), intracranial hemorrhage, cerebrovascular malformations, hydrocephalus and as well as newborn EEG abnormal patterns such as synchrony/asynchrony or symmetry/asymmetry. Further exploration of the EEG features and understanding of the brain functional organization in the outcome prediction of these abnormalities is needed to determine the urgent aids required in neonatal intensive care unit (NICU). Developing an integrated neonatal EEG assessment system with high density could assist not only for monitoring brain development but also for identification of neurological problems at earliest possible time after birth.

Résumé en Français de la problématique et des principaux résultats de la Thèse

Chapitre 1 : Introduction

Problématique

Des progrès importants ont été réalisés pour améliorer la compréhension de l'épilepsie notamment chez les jeunes enfants, portant par exemple sur la reconnaissance de nouveaux syndromes et l'utilisation de nouveaux traitements antiépileptiques. Il y a de nombreuses caractéristiques de l'épilepsie qui sont liées à l'âge, la clinique ou l'électroencéphalographiques (EEG). Les conséquences de l'épilepsie sur le développement cérébral en relation avec les fonctions cognitives n'est toujours pas totalement élucidés. Toutefois, le chemin à parcourir est encore long concernant la compréhension des différents mécanismes impliqués. La compréhension du développement cérébral fonctionnelle chez les jeunes enfants et en particulier chez les nouveau-nés est nécessaire pour guider la prise en charge clinique. Il est ainsi opportun de tirer profit des connaissances acquises dans le domaine de la science des réseaux pour étudier le réseau cérébral. Cette approche peut apporter des connaissances fondamentales sur les relations complexes des réseaux cérébraux et éclairer sur la dynamique de l'organisation fonctionnelle cérébrale. Cette thèse se concentre sur deux études portant (i) sur la connectivité fonctionnelle à l'état de repos chez les enfants atteints d'épilepsie bénigne avec pointes Centro-temporales (EPCT) et (ii) sur l'évaluation des réseaux cérébraux au cours du développement chez le nouveau-né à terme et prématuré.

L'EPCT est le syndrome épileptique idiopathique le plus commun avec 8 à 20 % des épilepsies de l'enfant (Holmes, 1993 ; Panayiotopoulos, 1999). Les décharges épileptiques intercritiques (IEDs) proviennent de régions centrales autour des zones sensorimotrices. L'EPCT et souvent appelé épilepsie rolandique en raison de l'implication des régions autour du sillon de Rolando. L'EPCT est une épilepsie focale sans changements structurels cérébraux majeurs (Camfield and Camfield, 2014) à l'inverse d'autres épilepsies temporales par exemple (Taylor et al., 2015). Toutefois, des déficiences cognitives ont été rapportées (Datta et al., 2013) chez les enfants avec EPCT. Les altérations cognitives concernent entre autre l'attention, la mémoire auditive et visuelle. Toutefois, l'influence directe des pointes intercritiques sur les déficiences cognitives reste peu explorée. Plusieurs études (Clemens, 2004 ; Fonseca et al., 2007) ont rapporté des altérations fonctionnelles de l'activité cérébrale dans les EPCT. Toutefois, certaines de ces études souffraient de l'hétérogénéité des patients, des approches méthodologiques et du nombre de patients évalués.

Chez les nouveau-nés, l'activité neuronale cérébrale précoce du cerveau néonatal immature est différente de l'activité observée dans le cerveau adulte mature. Particulièrement, l'électroencéphalographie (EEG) du prématuré est caractérisée par l'occurrence de courtes bouffées activités intriquées à des périodes de discontinuité (André et al., 2010). Il existe plusieurs neurobiomarqueurs (activités théta temporales, Delta brushs, Encoches Frontales) de l'activité cérébrale du prématuré qui sont utilisés en clinique pour

caractériser l'activité fonctionnelle néonatale et la dynamique de la maturation cérébrale à cette période du développement (André et al., 2010 ; Wallois, 2010). L'organisation fonctionnelle du réseau cérébrale néonatale reste encore à préciser. Cependant, différentes études ont tentées de préciser la connectivité cérébrale chez le nouveau-né avec l'imagerie par résonance magnétique (IRM) (Doria et al., 2010 ; Fransson et al., 2011, 2007). Cependant la faible résolution temporelle de l'IRM ne permet pas de rendre compte les caractéristiques dynamiques spécifiques de l'EEG du prématuré (asynchronie, discontinuité, neurobiomarqueurs spécifiques….). Plusieurs études (González et al., 2011 ; Meijer et coll., 2014) ont tentées d'évaluer la connectivité fonctionnelle chez les nouveau-nés à partir de l'EEG, mais l'interprétation des résultats est limitée par la faible résolution spatiale des EEG classiques utilisant 8 électrodes. (Lamblin et de Villepin-Touzery, 2015). Des études récentes en EEG (Grieve et al., 2008 ; Omidvarnia et coll., 2014) avec une augmentation significative du nombre d'électrodes, ont permis de montrer qu'il était possible de préciser l'organisation fonctionnelle de l'activité électrique des nouveau-nés en prenant en considération l'impact de certains des biomarqueurs. En attendant, Il est généralement admis que les réseaux cérébraux évoluent à partir d'une connectivité essentiellement locale vers une connectivité plus distribuée chez l'adulte. (Foire et coll., 2009). Comprendre l'organisation fonctionnelle du réseau cérébrale chez les nouveau-nés élargira notre compréhension des étapes de la maturation cérébrale et pourrait permettre une meilleure prise en charge clinique.

Objectif de la thèse

La première partie de la thèse porte sur l'étude des modifications de la connectivité cérébrale à l'état de repos des patients présentant une EPCT en comparant des périodes avec et sans pointes intercritiques chez les patients avec EPCT et des périodes similaires chez des sujets sains sans EPCT. Les étapes de cette étude sont les suivantes :

- Étude à partir des données EEG à l'état de repos des modifications de la puissance spectrale et de la distribution spatiale des sources corticales dans différentes bandes de fréquence selon la présence ou non de pointes interictales en comparaison avec le sujet sains.
- Étudier la connectivité fonctionnelle cérébrale dans les espaces capteur et source chez les patients EPCT vs témoins sains afin d'identifier plus particulièrement le pattern de connectivité cérébrale dans les EPCT.
- Caractériser la connectivité fonctionnelle des patients EPCT en utilisant les outils de la théorie des graphs pour préciser la topologie locale et globale tels que la centralité, l'intégration et la ségrégation fonctionnelle des réseaux.
- Evaluer les profils de connectivité en fonction de la présence ou non de pointes interictales dans les EPCT.
- Identifier les profils de connectivité en étudiant la connectivité dynamique et les régions cérébrale impliquées dans la production et la propagation de l'activité épileptique.

La deuxième partie de la thèse porte sur l'évaluation fonctionnelle du réseau cérébral des prématurés et des nouveau-nés nés à terme à partir d'enregistrements EEG en haute densité pendant les périodes de sommeil calme et agité. Les étapes de cette étude sont les suivantes :

- Étudier l'organisation fonctionnelle cérébrale précoce chez les nouveau-nés prématurés et les nouveau-nés nés à terme. L'objectif est de mieux comprendre la fonctionnalité du réseau cérébrale et son organisation au cours du développement.
- Etudier l'impact d'une activité endogène (Activité Theta Temporale, delta brush, Encoche frontal,) sur la connectivité cérébrale chez les nouveau-nés.
- Caractérisation de la connectivité fonctionnelle en utilisant les outils de théorie des graphs comme la centralité, l'intégration fonctionnelle et la ségrégation des réseaux pour une meilleure compréhension de la topologie cérébrale néonatal et la distribution spatiale de cette connectivité.
- Étudier l'organisation fonctionnelle du cerveau chez les nouveau-nés nés à terme pendant les périodes de sommeil calme et agité qui pourrait donner un aperçu de la maturation cérébrale néonatale.

Les contours de la Thèse

Ce chapitre présente la vue d'ensemble et l'objectif principal de la thèse. Le reste de la thèse est organisé comme suit.

Le chapitre 2 présente le contexte lié à cette thèse. Le chapitre décrit brièvement l'évolution de l'anatomie du cerveau et de la maturation fonctionnelle du nouveau-né à l'adulte. Un rappel est réalisé du principe et de la méthodologie de l'enregistrement de l'EEG chez le nouveau-né et l'adulte. La dynamique de l'évolution de l'EEG néonatal est décrite. Une brève description de plusieurs fonctionnalités est réalisée. La dernière partie du chapitre 2 présente une vue d'ensemble de l'activité épileptique en EEG avec une attention particulière portée sur l'épilepsie bénigne à pointe centro-temporale (EPCT)

Le chapitre 3 porte sur l'analyse de la connectivité cérébrale. Les trois types ou modes de connectivité cérébrale, notamment la connectivité structurelle, fonctionnelle et effective sont examinées. Une attention particulière est portée sur l'analyse de la connectivité fonctionnelle Différents concepts tels que la connectivité fonctionnelle axée sur la puissance, sur la phase et sur la théorie de l'information sont présentés dans des applications en neuro-imagerie. Quelques exemples sont donnés sur certaines mesures de connectivité fonctionnelle. De même, la connectivité effective est expliquée en détail avec certains aspects tels que la fonction de transfert direct et la cohérence partielle dirigée. Par la suite, la théorie des graphs est introduite avec une description des étapes requises pour la caractérisation des matrices de connectivité. Certains aspects de la théorie des graphs comme la centralité, la ségrégation et l'intégration fonctionnelle ainsi que la notion de « small world network » sont également abordés.

Dans le chapitre 4, l'impact des EPCT sur l'activité cérébrale est étudié en comparaison avec des sujets sains. Cette étude porte sur un groupe homogène de patients avec les mêmes sources épileptiques focales afin d'éliminer une éventuelle hétérogénéité et d'améliorer la comparaison méthodologique par rapport aux témoins sains. Les différences par rapport aux témoins sains de l'activité cérébrale à l'état de repos des patients EPCT sont étudiées par des mesures de puissance spectrale et de sources corticales dans différentes bandes de fréquence. La connectivité fonctionnelle dans l'espace capteur et l'espace source est évaluée pour étudier l'effet de la présence et de l'absence de pointes épileptiques intericales sur la dynamique de la connectivité des réseaux cérébraux. Les différentes mesures utilisant la théorie des graphs servent à caractériser la connectivité fonctionnelle en mesurant les caractéristiques d'intégration fonctionnelle globale et locale et de ségrégation des réseaux cérébraux des patients EPCT par rapport aux témoins sains.

De même, le chapitre 5 est centré sur l'analyse des patients EPCT. Certaines régions cérébrales sont initialement choisies en fonction des études antérieures et la connectivité est mesurée à partir des « seeds » points placés dans ces régions d'intérêts. Cela s'applique aux patients épileptiques avec ou sans pointes épileptiques intericales en comparaison aux sujets sains. La seconde étude porte sur la dynamique de la connectivité effective intercritique pour étudier la génération et la propagation et des pointes épileptiques intericales. Les principales sources et régions impliquées dans les EPCT sont identifiées à partir des patterns de connectivité.

Le chapitre 6 porte sur la connectivité des réseaux neuronaux chez le nouveau-né prématuré et le nouveau-né à terme. Les rythmes corticaux et la connectivité cérébrale fonctionnelle sont étudiés à partir des données EEG haute densité obtenus chez les nouveau-nés prématurés et les nouveau-nés à terme. Ils sont étudiés dans différentes gammes de fréquences. Les caractéristiques spécifiques de l'EEG des nouveau-nés prématurés comme les activités thêta temporales (TTA) sont prises en considérations dans les deux phases de sommeil calme et agité. Les mesures issues de la théorie des Graphs sont appliqués (centralité, ségrégation, intégration) à la connectivité fonctionnelle afin de mieux quantifier et caractériser l'organisation du réseau cérébral immature.

Le chapitré 7 constitue le résumé de la thèse. Il contient les principales conclusions de la thèse sur les patients EPCT et les caractéristiques des réseaux fonctionnelles chez les nouveau-nés. Il ouvre vers de nouvelles perspectives.

Chapitre 2 : EEG et Epilepsie

Introduction

La dynamique temporelle des réseaux neuronaux est déterminée par des successions spatio-temporelles de modèles transitoires d'activités cérébrales qui sont intégrées au niveau de la structure cérébrale et qui sont sous tendues par des connections dont l'une des caractéristiques est leur importante adaptabilité. La cohérence temporelle est obtenue par la synchronisation des réseaux neuronaux fonctionnant en harmonie dans des bandes de fréquences distinctes. Le fonctionnement cérébral peut s'expliquer au niveau des réseaux neuronaux interconnectés par un modèle complexe. Dans cette perspective, le cerveau peut être considéré comme un ensemble de systèmes dynamiques connectés reliant les entrées et les sorties de ces différents constituants. Ce chapitre décrit brièvement l'anatomie cérébrale et ses principales fonctions, les caractéristiques de l'EEG, les rythmes de base de l'EEG à l'état de repos chez les adultes, les jeunes enfants et les nouveau-nés. Un bref aperçu des grands principes de l'épilepsie est également proposé avec une attention particulière portée aux EPCT.

Structure et fonction cérébrale

Le tissu cérébral est constitué de milliards de neurones qui sont protégés par le crâne, la dure mère, l'arachnoïde et la pie mère. L'espace entre la pie mère et l'arachnoïde est rempli de liquide céphalo-rachidien (LCR) (Silverthorn, 2007). La structure du cerveau humain mature rapidement dès le début de la période fœtale durant laquelle le cerveau est relativement lisse. Il développe progressivement un aspect mature plus caractéristique avec notamment une gyrification qui se met en place. La formation de circonvolutions et de sillons suit une séquence ordonnée, en fonction de l'âge (Stiles et Jernigan, 2010). Certaines structures cérébrales sont identifiées plus rapidement tels que le cortex cingulaire, le cortex pariétal et le cortex occipital (14-16 semaines). Les régions centrales temporales supérieures, puis le cortex frontal supérieur, precentral, frontal inférieur et les régions postcentrales apparaissent entre 20 et 26 semaines. Les sillons secondaires apparaissent plus tardivement entre 30 et 35 semaines.

La maturation cérébrale néonatale est fonctionnellement caractérisée par des graphoéléments EEG spécifiques qui servent de marqueurs biologiques pour le développement fonctionnel du cerveau (André et al., 2010). La plupart des systèmes sensoriels primaires sont déjà établis à la naissance mais la connectivité fonctionnelle est limitée chez les nourrissons âgés de moins de 2 ans (Stiles et Jernigan, 2010). Le développement fonctionnel cérébral chez les nouveau-nés est concomitant de la maturation fonctionnelle séquentielle des différentes régions corticales. Le cortex cérébral constitue un centre d'intégration des informations sensorielles et participe à la prise de décision. Le cortex cérébral est divisé en plusieurs régions (Silverthorn, 2007).

Origine et Enregistrement de l'EEG

L'EEG représente l'activité électrique du cerveau enregistré à distance au moyen délectrodes dispsoées sur le scalp. Plus précisément, cela représente la somme des flux extracellulaires de grand groupe de neurones (Holmes et Khazipov, 2007). L'EEG découle de l'activité synaptique synchronisée dans de populations de neurones corticaux, appelées cellules pyramidales. Les neurones pyramidaux sont organisés de telle sorte que les arbres dendritiques voisins sont parallèles les uns aux autres et presque orthogonaux à la surface corticale. Ces neurones pyramidaux sont censés être le principal générateur de l'EEG. Pour plus

d'informations sur la génération de l'EEG, les lecteurs peuvent consulter les commentaires suivants (Holmes et Khazipov, 2007). La haute résolution temporelle de l'EEG représente un excellent outil de l'analyse de l'activité neuronale des différentes régions cérébrales.

Les enregistrements EEG sont effectués en plaçant des électrodes dans des positions standard prédéfinies sur la tête. La position des électrodes est basée sur des repères anatomiques. Dans la pratique clinique, généralement 20 à 32 électrodes sont utilisés chez l'adulte en routine. À des fins de recherche, il faut habituellement, pour augmenter la résolution spatiale, augmenter le nombre d'électrodes (Sohrabpour et al., 2015).

Activité à l'état de repos

L'état de repos est le substrat dynamique de l'état actuel au repos du cerveau tout en considérant l'intégration des informations entrantes. Au repos, le cerveau englobe tous les modes de fonctionnement tels que la sensorialité, l'attention, le contrôle exécutif et le contrôle de certaines fonctions telles que le langage. Certaines régions du cerveau sont activées ou désactivées au repos, l'état de repos peut aussi être abordé avec l'imagerie par résonance magnétique fonctionnelle (IRMf).

L'EEG à l'état de repos est utilisé pour caractériser l'activité cérébrale en l'absence de stimulation ou de tâche. Il peut être utilisé pour identifier certains dysfonctionnements en analysant les capacités d'intégration à partir des potentiels évoqués visuels ou autres dans différentes situations pathologiques à l'état de repos. La manière la plus courante utilisée pour caractériser l'EEG au repos est la séparation des patterns oscillatoires en différentes bandes de fréquence. L'analyse de la puissance spectrale est la méthode le plus couramment utilisée pour quantifier l'EEG à l'état de repos dans les différentes bandes de fréquence.

L'EEG chez le nouveau-né est très différent de celui de l'enfant plus âgé et de l'adulte. Il nécessite une expérience spécifique pour l'interprétation. Cela est dû aux changements de maturation rapides des réseaux neuronaux chez le nouveau-né et notamment le prématuré entre 26 et 40 semaines de gestation (André et al., 2010). L'EEG s'est avéré indispensable pour l'évaluation clinique des pathologies cérébrales telles que l'épilepsie, Il permet par ailleurs le monitoring en réanimation néonatale (Vecchierini et coll., 2003).

Activité épileptique et EEG

L'épilepsie est un trouble cérébral qui affecte environ 0,5 à 1 % de la population mondiale. Elle est caractérisée par une activité cérébrale récurrente, excessive et incontrôlée. L'épilepsie peut commencer à tous les âges, mais est plus fréquente chez les enfants par rapport aux adultes. La crise d'épilepsie est caractérisée par une décharge anormale hypersynchrone d'une large population neuronale. Les manifestations cliniques sont présentes sous de nombreuses formes selon les régions cérébrales impliquées dans l'activité épileptique. Les mécanismes sous-jacents à l'épilepsie sont encore mal connus. Il existe de

nombreuses classifications de l'épilepsie. Selon l'étiologie de l'épilepsie ou selon le caractère focal ou distribué. Ainsi, elle peut être classée en épilepsie partielle ou généralisée. Les épilepsies partielles ont une origine focale. Elles peuvent être simple (sans perte de conscience) ou complexe (avec perte de conscience). L'épilepsie partielle peut évoluer vers une épilepsie généralisée. L'épilepsie généralisée implique de nombreuses régions cérébrales.

Une des applications importantes de l'EEG est l'étude de l'épilepsie. L'apparition des ondes d'amplitude supérieures (pointes) et de plusieurs autres paroxysmes sont des points de repère permettant de caractériser l'activité épileptique. Ces graphoéléments participent à l'identification, le classement et la localisation des phénomènes épileptiques (crises ou pointes intericales). Les graphoéléments épileptiques varient en termes de fréquence, de durée, et de topographie. Quand ils apparaissent entre les crises sous forme de pointes, pointes ondes ou polypointes ondes ils sont considérés comme des éléments épileptiques intercritiques et constituent des biomarqueurs de l'activité épileptique entre les crises.

Épilepsie bénigne de l'enfance

L'épilepsie bénigne de l'enfant représente 10 à 20 % des épilepsies de l'enfant (Camfield and Camfield, 2014). Le risque de déficit cognitif est plus élevé chez les enfants avec épilepsie bénigne que chez les enfants sains du même âge (Datta et al., 2013). L'épilepsie bénigne la plus courante est l'EPCT (Panayiotopoulos, 1999). Typiquement, la crise débute dans le sommeil ou à l'endormissement et correspond à une crise partielle. La généralisation secondaire n'est pas systématique. L'outil diagnostic le plus utile est certainement l'EEG dans les épilepsies bénignes, il permet de caractériser les pointes intericales qui ont un aspect bi ou triphasiques qui sont localisées dans les zones rolandiques ou périroloandiques et qui sont très évocatrices de l'EPCT. Elles apparaissent tantôt à droite, tantôt à gauche, le plus souvent asynchrones et de localisation variable d'un examen à l'autre entre les deux hémisphères.

Chapitre 3 : Analyse de la connectivité cérébrale

Le cerveau est un système complexe, distribué, à grande échelle, dans lequel un très grand nombre de processus sont traités simultanément, en parallèle. La complexité du cerveau peut être définie à partir de ses populations neuronales, qui, à l'échelle macroscopique ont un fonctionnement en modes aléatoires et/ou réguliers. L'architecture complexe du cerveau implique des réseaux neuronaux qui sont hautement spécialisés dans plusieurs opérations en parallèles fonctionnant en interaction pour permettre des perceptions et des actions cohérentes. La connectivité anatomique et fonctionnelle entre les réseaux de neurones peut se mettre en place entre des structures proches et/ou distantes. Les connections entre structures proches ayant une plus grande probabilité d'occurrence. Les connectivités fonctionnelles entre les réseaux cérébraux sont organisées de telle manière à permettre un traitement effectif de l'information incluant les capacités de ségrégation et d'intégration des informations. Plus particulièrement, la ségrégation et l'intégration des informations doivent pouvoir être traitées dans une architecture unique de réseaux cérébraux. À l'échelle microscopique, le cerveau est constitué de circuits électriques constitués par l'interconnexion de milliards d'unités élémentaires de traitement de l'information (neurones et cellules gliales) (Bear et coll., 2001).

Le cerveau adulte a été décrit comme correspondant à un maillage de type Web avec de nombreuses interconnections impliquant l'ensemble des réseaux neuronaux. Chez l'adulte certaines régions montrent un haut niveau, disproportionné, de connectivité anatomique appelée « cortical hubs » ou centres corticaux qui pourraient contrôler le flux d'information.

Les réseaux de hubs ou de centres corticaux recouvrent dans une large mesure le réseau en mode par défaut et le réseau attentionnel fronto-pariétal (Buckner et al., 2009). Ainsi, l'organisation des réseaux adultes basée sur cette notion de hubs sous-tend complexité de la fonctionnalité cérébrale chez l'adulte (Heuvel et Sporns, 2011).

Le cerveau de l'enfant contient des réseaux moins complexes avec des connexions relativement plus labiles et moins fonctionnelles. La connectivité fonctionnelle associée à des hubs corticaux recouvre chez l'enfant en grande partie les régions sensorimotrices, auditives et visuelles primaires (Fransson et al., 2009, 2007). Au cours du processus de maturation, se produit une réorganisation progressive de la connectivité des réseaux qui passent d'une organisation " local et ségrégée " à une organisation " distribuée et intégrée " (Fair et al., 2009).

Ce chapitre décrit les méthodes d'analyse de connectivité utilisées avec une attention particulière pour les mesures de connectivité fonctionnelle et effective. Les mesures utilisant la théorie de graphs sont également décrites. Le chapitre commence par un bref examen des signaux analytiques qui sont nécessaires au calcul de la connectivité fonctionnelle et imagerie de source EEG**.**

Connectivité cérébrale

La connectivité cérébrale révèle les voies par lesquelles, où la façon dont les informations sont échangées entre les régions du cerveau (Breakspear et Jirsa, 2007). Les mesures de connectivité cérébrales sont bivariées, c'est-à-dire, qu'elles concernent les interactions entre deux régions cérébrales ou les électrodes du cuir chevelu.

Il existe trois modes de connectivité cérébrale structurelle, fonctionnelle et effective (Friston, 2005 ; Horwitz, 2003). La connectivité structurelle ou anatomique se réfère à un réseau de connexions (synaptiques) structurales, reliant des ensembles de neurones ou éléments neuronaux. Fondamentalement, la connectivité fonctionnelle est une notion statistique qui permet d'estimer la corrélation temporelle entre deux signaux au fil du temps. En général, la connectivité fonctionnelle capture les écarts par rapport à l'indépendance statistique entre les unités neuronales distribuées et souvent distantes. La connectivité effective examine la directionnalité du flux d'informations d'un élément neural par rapport à un autre.

Connectivité fonctionnelle

La connectivité fonctionnelle est définie en tant que dépendances statistiques entre deux régions cérébrales (Friston, 1994). La connectivité fonctionnelle en neuro-imagerie peut être estimée à partir de l'IRMf et /ou de séries chronologiques EEG/MEG. Il y a beaucoup de mesures de la connectivité fonctionnelle. Dans

cette thèse nous nous limiterons aux mesures de la connectivité fonctionnelle basées sur la puissance, sur la phase et sur l'information.

La connectivité fonctionnelle basée sur la puissance du signal

La connectivité fonctionnelle basée sur la puissance du signal est une mesure linéaire, dépendante, entre deux signaux dans le domaine temporel, évaluée par le coefficient de corrélation ou dans le domaine fréquentiel par la cohérence. Le coefficient de corrélation de Pearson est une méthode courante de corrélation utilisée et est définie comme la covariance de deux signaux x et y. La cohérence spectrale est semblable au coefficient de corrélation, mais dans le domaine fréquentiel. La cohérence spectrale inclut des informations sur la puissance (amplitude et phase).

La connectivité fonctionnelle basée sur la phase

Ce type de connectivité fonctionnelle est une mesure non linéaire. Elle repose sur l'hypothèse que les séries chronologiques neuronales ont des caractéristiques non linéaires. Une méthode commune pour obtenir la force de la synchronisation de phase entre les différentes régions du cerveau est la valeur de la phase de verrouillage (Phase Locking value, PLV) (Lachaux et coll., 1999). D'autres méthodes incluent le délai de phase (phase lag, PLI) (Stam et coll., 2007), ou l'indice de délai de phase pondéré (Weighted phase lag indice, wPLI) (Vinck et al., 2011).

La connectivité fonctionnelle basée sur l'information

la connectivité fonctionnelle basée sur l'information capture les dépendance statistiques linéaires et non linéaires entre deux séries temporelles (Hurtado et al., 2004 ; Jeong et al., 2001). Cette technique est basée sur le concept d'entropie qui mesure la probabilité de la variable.

Connectivité effective

La connectivité effective correspond aux dépendances asymétriques ou causales entre les régions cérébrales. Elle identifie quelle région du cerveau, dans un réseau fonctionnel, influence d'autres régions cérébrales (Friston, 1994). Contrairement à la connectivité fonctionnelle, la connectivité effective indique la direction du flux d'informations entre les différentes régions (Friston, 1994). L'interaction directionnelle peut être définie comme une technique basée sur des modèles tels que la modélisation dynamique causale (Friston et coll., 2003), la modélisation par équation structurelle (Ullman et Bentler, 2003), ou le modèle libre avec la causalité de Granger (Hesse et al., 2003).

La connectivité effective nécessite un model autorégressif et une estimation des paramètres du modèle avant l'estimation de la connectivité. Les mesures les plus courantes de connectivité incluent la cohérence partielle dirigée (partial directed coherence, PDC) (Baccalá et Sameshima, 2001) et la fonction de transfert direct (direct transfer function , DTF) (Kamiński et coll., 2001).

Analyse des réseaux par la théorie des Graph

La théorie des graphs est un cadre mathématique mis au point pour étudier les systèmes physiques, biologiques et d'informations. Il y a une augmentation des applications de la théorie des graphs en neuro-imagerie pour étudier les réseaux cérébraux fonctionnels et structurels. La théorie des Graphs est aussi utilisé pour caractériser la connectivité des réseaux dans les études expérimentales cognitives (il et Evans, 2010 ; Sporns, 2011) Cela permet d'élargir nos connaissances sur les maladies cérébrales, le vieillissement et les fonctions cognitives supérieures (Bullmore et Bassett, 2011 ; Deuker et al., 2009 ; Netoff et al., 2004 ; Stam, 2014).

Tous les réseaux sont constitués de deux éléments de base : les nœuds et les bords appariées (liens) entre les nœuds (Bullmore et Sporns, 2009). Les nœuds dans les réseaux cérébraux sont généralement représentés par les régions cérébrales ou les positions des électrodes EEG. Les nœuds sont parfois déterminés par l'activité fonctionnelle et la parcellisation de la surface du cortex ou de l'ensemble du cortex (Figure 3.3). La parcellisation se fait parfois à l'aide d'atlas de cerveau (Stanley et al., 2013). Les bords et les liens sont généralement des mesures de la connectivité fonctionnelle et effective. Le choix des mesures de connectivité dépend des questions de recherche et des expériences menées. Tous les réseaux sont représentés par leurs matrices de connectivité (contiguïté). Lignes et colonnes dans ces matrices correspondent aux nœuds, tandis que les entrées désignent les bords.

Les mesures dans la théorie des Graphs

Il y a de nombreux paramètres qui peuvent être utilisés pour étudier la connectivité des réseaux à l'aide de la théorie des graphs (Roubinov et Sporns, 2010). Avant de réalise le calcul des paramètres de réseaux, le graph est parfois seuillé. Le seuil est très important parce que les liens faibles et non significatifs peuvent représenter des connexions fallacieuses, qui pourraient augmenter le rapport signal / bruit. La méthode courante consiste à choisir une valeur arbitraire commune pour tous les sujets où une condition dans une expérience. Une autre option consiste à spécifier le nombre de connexions (densité de connexion) et garder les connexions les plus fortes tout en définissant le reste à zéro. Les autres méthodes de seuillage consistent à générer des données de remplacement pour l'évaluation statistique des mesures fonctionnelles, en particulier pour des signaux brefs (Drakesmith et al., 2015 ; Langer et al., 2013). Les mesures de connectivité des réseaux cérébraux sont toujours classifiées selon les interprétations neurobiologiques comme la centralité des réseaux, la ségrégation fonctionnelle, l'intégration fonctionnelle, les réseaux de type petit monde (small word network), les patterns des réseaux et bien d'autres.

La centralité des réseaux est la propriété la plus importante de n'importe quel réseau. Elle évalue l'importance des nœuds individuels ou des régions du cerveau en mesurant combien de fois un nœud particulier interagit avec plusieurs autres nœuds du réseau. La mesure la plus commune de centralité est le degré qui correspond au nombre de connexions d'un des nœuds rattaché au reste du réseau. D'autres mesures incluent la betweenness centrality (BC) (Freeman, 1979) qui mesure la fraction de tous les chemins

les plus courts dans le réseau qui passent par un nœud donné. La centralité de la proximité est une autre mesure.

La ségrégation fonctionnelle du réseau cérébrale est caractérisée par l'existence de régions cérébrales spécialisées comme des modules organisés en populations distinctes (Tononi et al., 1994). Des mesures de ségrégation fonctionnelle calculent la présence de clusters ou de modules au sein du réseau qui suggèrent une organisation de dépendances statistiques. La commune mesure de ségrégations fonctionnelle est le « clustering coefficient » qui mesure la fraction des triangles autour des nœuds individuels (Watts et Strogatz, 1998). Une alternative est la mesure de l'efficacité locale d'un nœud ou d'une région particulière du cerveau.

L'intégration fonctionnelle mesure la facilité de transfert d'information ou de communication entre les régions du cerveau (Tononi et al., 1994). La communication entre les réseaux neuronaux est mesurée par les chemins qui les relient. La longueur du trajet caractéristique (Characteristic path length, L) est le plus couramment utilisée pour mesurer l'intégration fonctionnelle. L est le plus court chemin entre les régions cérébrales (Watts et Strogatz, 1998).

L'inverse de la moyenne de la longueur du plus court chemin est connu comme l'efficacité globale (E).

Le cerveau est un réseau complexe supportant le traitement d'informations spatio-temporelles. Un réseau cérébral normal combine la présence de modules fonctionnels distincts et de liens fonctionnels robustes. Ce type de réseau est appelé un réseau en petit monde (SWN) soutenant l'intégration fonctionnelle optimale et la ségrégation (Bassett et Bullmore, 2006 ; Sporns et Zwi, 2004). Cette structure en réseau SWN est ordonné avec un coefficient de clusters élevé (clustering coefficient élevé) et une longueur du plus court chemin courte (ou haute effectivité) entre les régions du cerveau qui est un intermédiaire entre un réseau ordonnée (C élevé et L long) et un réseau aléatoire (faible C et L court) (Watts et Strogatz, 1998).

Chapitres 4 et 5 : Analyse de la connectivité à l'état de repos chez les enfants atteints d'épilepsie bénigne à pointes centrotemporales

La relation entre l'épilepsie et les incapacités cognitives et neuropsychologiques chez les enfants a été largement étudiée (Datta et al., 2013). Malgré le grand nombre d'études sur ce sujet, les effets propres de l'activité épileptique sur le fonctionnement cognitif et le développement ne sont pas encore clairement définis. De nombreuses études sont réalisées sur des patients avec différentes sources focales d'épilepsie, différents âges, selon la fréquence des crises et selon les syndromes épileptiques. Les déficits cognitifs et comportementaux observés chez des enfants épileptiques sont parfois considérés comme le résultat d'interactions complexes entre des facteurs biologiques, psychologiques et sociaux (Ay et al., 2009 ; Boucliers et Snead, 2009).

L’épilepsie bénigne de l’enfant représente 10 à 20 % des épilepsies de l’enfant (Camfield and Camfield, 2014). Le risque de déficit cognitif est plus élevé chez les enfants avec épilepsie bénigne que chez les enfants sains du même âge (Datta et al., 2013). L’épilepsie bénigne la plus courante est l'EPCT (Panayiotopoulos, 1999). La plupart des crises surviennent pendant le sommeil ou à l'endormissement (Camfield et Camfield, 2014). Contrairement aux autre types d’épilepsie tels que l'épilepsie du lobe temporal (Taylor et al., 2015), l’EPCT est connu pour ne pas être liée à des anomalies structurales (Hughes, 2010). Toutefois, l'activité épileptique peut provoquer différents dysfonctionnements entre les régions sous-corticales et corticales qui peuvent entraîner des changements dans l'activité EEG à l’état de repos.

Dans ce chapitre, nous examinons des différences d'activité cérébrale à l'état de repos les yeux fermés entre les patients EPCT et les témoins sains dans 2 conditions en présence et en absence de pointes épileptiques intercritiques (EEI). À cette fin, nous avons étudié les variations de la puissance spectrale de l'EEG et la connectivité fonctionnelle dans l’espace capteur et l’espace source. Les outils de la théorie de graphs ont aussi servis à caractériser la connectivité fonctionnelle entre réseaux cérébraux des patients EPCT par rapport aux témoins sains.

Analyse spectrale et source de puissance EEG

L’analyse de la puissance spectrale est l'une des méthodes standards utilisées pour la quantification de l'EEG. La puissance de la densité spectrale (spectre de puissance) reflète la distribution de la puissance du signal en fonction de la fréquence. L’analyse de la puissance spectrale dans les différentes bandes de fréquence mélange les différentes propriétés physiologiques (Clément et al., 2013 ; Klimesch et coll., 2007).

Il existe plusieurs études de l'analyse de la puissance spectrale de l’EEG et de l’analyse des sources dans les épilepsie bénignes de l'enfant (Clemens et al., 2010 ; Kikumoto et al., 2006). Toutes montrent une puissance spectrale élevée notamment autour de la région épileptique. La plupart de ces études ont été effectuée sur divers groupes de patients avec différentes sortes de foyers épileptiques, différents groupes d'âge et une hétérogénéité syndromique.

Dans la première étude, nous avons recruté vingt et un patients avec EPCT avec une moyenne d'âge de 9,84 ± 1,75 ans et onze témoins sains dans la même tranche d'âge pour analyser l'état de repos. Les données EEG en haute densité ont été enregistrées sous la condition yeux fermés pendant au moins 14 minutes pour chaque sujet. Un groupe homogène de douze patients a été sélectionné à partir de la localisation des sources des décharges épileptiques intercritiques (IEDs). Les données EEG Haute densité ont été prétraitées pour supprimer les artefacts. Les segments sans artéfact ont été ensuite segmentés par époques de 2s sans overlap pour chaque sujet. Deux conditions ont été utilisées pour les patients épileptiques, les segments avec ou sans pointe épileptiques intercritiques. Les puissances spectrales absolue et relative ont été calculées pour ces conditions dans cinq bandes de fréquences différentes (δ, θ, α, $\beta 1$ et $\beta 2$) dans l'espace capteur. Statistiquement, les trois conditions ont été comparées avec des tests statistiques non paramétriques.

Nos résultats ont montré que les réseaux à l'état de repos des patients EPCT étaient fonctionnellement perturbés en présence et en absence de pointes épileptiques. Les principales conclusions ont été de mettre en évidence un dysfonctionnement dans la région centrotemporale, le désengagement corticale dans les régions frontales et occipitales chez les patients, indiquant une dysfonction du réseau de repos chez les patients EPCT. On retrouve la puissance élevée dans la bande θ par rapport aux autres les régions cérébrales et une puissance spectrale significativement plus faible dans la bande α plus particulièrement dans les régions occipitales en présence de pointes épileptiques intercritiques.

L'interaction entre les régions du cerveau peut être analysée par des analyses bivariées et multivariées telles que de la connectivité cérébrale. La connectivité fonctionnelle se réfère à la relation fonctionnellement intégrée entre les régions cérébrales spatialement séparées. Ceci a été appliqué à plusieurs études, y compris l'épilepsie (Centeno et Carmichael, 2014). La caractérisation de la dynamique des réseaux corticaux en EEG et ECoG chez des patients épileptiques à l'état de repos a démontré des perturbations globales et régionales des réseaux neuronaux qui pouvaient être estimées par la connectivité fonctionnelle (Douw et al., 2010 a, 2010 b ; Coran et coll., 2013). La connectivité fonctionnelle des réseaux neuronaux est souvent caractérisée par la théorie des graphs (Roubinov et Sporns, 2010) qui est une application courante dans le domaine des neurosciences dont l'épilepsie (Netoff et al., 2004). Un grand nombre de paramètres de la théorie des graphs a été proposé et le plus commun est le degré qui mesure la centralité du réseau.

La théorie des graphs et la connectivité fonctionnelle

Dans cette étude, la théorie des graphs et la connectivité fonctionnelle ont été appliquées pour explorer l'altération fonctionnelle des réseaux cérébraux chez les patients EPCT en comparaison avec les sujets sains. Cela a été fait en présence et en l'absence de décharges intercritiques dans le groupe patient. Cela a été réalisé dans l'espace capteur et l'espace source pour étudier l'impact des décharges épileptiques intercritiques sur les interactions fonctionnelles entre réseaux cérébraux. Il existe différentes mesures de connectivité fonctionnelle et toutes ont leurs propres avantages et inconvénients. Dans la première étude, la valeur de verrouillage de phase (PLV) (Lachaux et al., 1999) a été appliquée pour estimer la connectivité fonctionnelle et caractériser la connectivité avec les différents paramètres issus de la théorie des graphs. La connectivité fonctionnelle dans la seconde étude a été estimée par le délai de synchronisation de phase (LPS) (Pascual-Marqui, 2007) dans l'espace source avec 84 régions cérébrales définies selon l'atlas de Brodmann (Brodmann, 1909). La mesure de LPS est moins sensible aux signaux non physiologiques, y compris les artefacts et l'effet de volume de conduction (Pascual-Marqui et al., 2011).

Dans l'espace capteur, les patients présentent une densité de connexion plus élevée autour de la zone épileptique dans toutes les bandes de fréquences. Le réseau cérébral des patients EPCT a été dévié du mode small word par rapport aux témoins sains selon la fréquence analysée. Le réseau cérébral des patients EPCT était plus ordonné en présence de pointes interictales quand il était comparé au réseau des sujets sains. Toutefois, en l'absence de pointes interictales, le réseau cérébral des patients EPCT était moins ordonné par rapport aux contrôles sains dans toutes les bandes de fréquence.

La connectivité fonctionnelle peut perturber les résultats du fait du volume de conduction dans la mesure où l'EEG de surface détecte une moyenne spatiale de signaux se chevauchant provenant de plusieurs sources cérébrales. Ceci a motivée la troisième étude dans l'espace source et l'analyse du délai de la synchronisation de phase (LPS) qui est généralement considéré comme insensible au volume de conduction par rapport aux autres métriques de connectivité fonctionnelle tel que le zéro délai ou la mesure de cohérence classique. Dans cette étude, 84 région d'intérêts (ROIs) ont été définis par l'atlas de Brodmann afin de réduire la variabilité de la taille du cerveau pour l'ensemble des sujets et de minimiser l'effet de volume de conduction par rapport à l'approche voxel-par-voxel. Par rapport aux témoins, les patients (sans pointes intericales) ont montré plus de LPS dans la bande θ et α mais moins de LPS dans la bande β. Les patients affichent aussi des valeurs d'intégration supérieures et de ségrégations inférieures dans les bandes θ et α par rapport aux témoins sains. Ils montrent également une connectivité fonctionnelle locale plus élevée au niveau du réseau épileptogène comprenant les aires motrices, la région centrale et la région temporale ipsilatérale à la zone épileptique. La connectivité locale est aussi plus faible dans la région frontale controlatérale chez les patients. Toutes ces résultats sont en faveur d'une altération de la connectivité fonctionnelle à l'état de repos chez les patients EPCT et ce dans différentes bandes de fréquence.

Ces deux études montrent que la connectivité fonctionnelle à l'état de repos chez les patients EPCT avec et sans pointes intericales a été modifiée selon la fréquence des activités cérébrales. Toutefois, dans ce chapitre, nous avons utilisé la connectivité fonctionnelle non dirigé. Dans le chapitre suivant, nous nous concentrons sur le sens de circulation de l'information entre les différentes régions cérébrales chez les patients EPCT.

Connectivité fonctionnelle à l'état de repos dans l'espace Source

Dans cette étude, nous avons étudié l'impact des pointes intericales sur la connectivité fonctionnelle (FC) dans l'espace source à l'état de repos chez les patients EPCT par rapport aux témoins sains. Le FC dans l'espace source a été calculé par la cohérence imaginaire (IC), qui a été démontrée pour être insensible au volume de conduction (Nolte et al., 2004) et donc qui permet de refléter plus exactement la mesure de la connectivité cérébrale à partir des données EEG à l'état de repos. Certaines régions d'intérêts (ROIs) ont été choisies comme « seed points » incluant la zone épileptique (centrale droite), le cortex central gauche, le cortex préfrontal et les régions occipitales. Ces régions se sont révélées être activées/désactivées dans nos études précédentes. Les patterns de FC issus de ces régions vers d'autres régions ont été étudiés sous trois conditions (contrôles, avec ou sans pointes intercritique chez les patients). La topologie de la connectivité fonctionnelle était caractérisée en utilisant deux types de mesures : la betweenness et l'effectivité locale.

Grâce à l'analyse de connectivité fonctionnelle dans l'espace source à l'état de repos, nous avons constaté que les régions centrales, y compris les aires motrices supplémentaires ont montré une activation en présence de pointes intericales. Des patterns de FC plus élevée ont été également observés dans la région frontale supérieure homolatérale à la zone épileptique chez ces patients

Cette étude présente une méthode claire et robuste permettant d'évaluer les patterns de connectivité fonctionnelle à l'état de repos dans l'espace source et de démontrer leurs perturbations chez les patients EPCT. Bien que nos études antérieures aient montré la forte incidence des pointes épileptique intercritiques sur l'organisation fonctionnelle cérébrale des patients EPCT, les techniques dynamiques de connectivité intercritique apportent des informations importantes sur la directionnalité des interactions entre les régions cérébrales chez les patients EPCT.

Directionnalité et dynamique de la connectivité intericale

Dans cette étude, le modèle de directionnalité de la connectivité intercritique associé aux pointes intercritiques a été étudié tout d'abord en reconstruisant la source de l'EEG pour 90 ROIs à l'aide de l'EEG haute densité pour chaque patient épileptique. Nous avons ensuite utilisé la cohérence partielle dirigée (PDC) en guise de mesure de la connectivité effective entre les régions cérébrales. La sortie de la matrice de connectivité a été étudiée afin d'identifier les principaux triggers dans les différentes régions cérébrales impliqués dans la génération et la propagation de l'activité épileptique. Nous avons constaté que les régions centrales rolandiques, les aires motrices supplémentaires et les régions frontales supérieures toutes ipsilatérales aux zones épileptiques étaient les principaux triggers chez les patients EPCT. La PDC nous a permis d'étudier le sens de circulation de l'information entre les régions du cerveau de manière causale. En outre, la PDC est insensible à l'artefact de volume de conduction.

Chapitre 6 : Connectivité fonctionnelle chez les nouveau-nés

Le réseau cérébral adulte est le résultat d'interactions complexes entre les différentes régions du cerveau. Plusieurs études utilisant la science des réseaux ou la théorie des graphs ont élargi notre connaissance sur la connectome fonctionnelle du cerveau adulte (Bassett et Bullmore, 2006 ; Bassett et Gazzaniga, 2011 ; Sporns et coll., 2000). Néanmoins, on connaît mal la connectome fonctionnelle du cerveau chez les nouveau-nés. Il y a eu des hypothèses selon lesquelles la connectivité fonctionnelle du cerveau humain évolue à partir d'un réseau organisé de manière locale à la naissance, vers un réseau distribué chez l'adulte (Foire et coll., 2009). Plusieurs études en IRMf chez les nouveau-nés ont montré la présence de centres corticaux dans les régions postérieures, frontales et sensorimotrices (Ball et al., 2014 ; Fransson et coll., 2007). Cependant, l'activité cérébrale précoce en particulier chez les nouveau-nés prématurés est très différente de celle du cerveau mature. L'activité neuronale cérébrale néonatale est caractérisée par la présence de graphoéléments caractéristiques comme les activités thêta temporales chez les grands prématurés ou les encoches frontales chez le nouveau-né à terme. L'EEG chez le prématuré est aussi caractérisé par des périodes de discontinuité. Toutes ces caractéristiques spécifiques servent de

biomarqueurs utilisés en clinique pour préciser les stades de maturation cérébrales (André et al., 2010 ; Wallois, 2010). Les études récentes (González et al., 2011 ; Meijer et coll., 2014 ; Omidvarnia et coll., 2014 ; Tokariev et coll., 2016) ont tenté d'introduire la notion de connectivité fonctionnelle chez le nouveau-né. Toutes ces études ont été réalisées à l'aide d'un nombre restreint d'électrodes. Cependant, les études de connectivité fonctionnelle chez les nouveau-nés nécessitent un grand nombre d'électrodes en raison de la spécificité spatiale de l'EEG chez le prématuré (Odabaee et coll., 2013). En outre, la plupart des spécificités néonatales y compris les stades du sommeil n'ont pas été prise en considération dans ces études de connectivité fonctionnelle.

Dans ce chapitre, les patterns de connectivité fonctionnelle cérébrale chez les nouveau-nés prématurés et nouveau-nés à terme ont été étudiés en utilisant des données EEG haute densité. Les spécificités de l'EEG du prématuré comme les activités thêta temporales et les phases de sommeil ont été prises en considération.

Ces études montrent que l'activité cérébrale précoce des nouveau-nés prématurés est densément localisée aux régions frontales et occipitales et surtout que la connectivité fonctionnelle à longue distance est limitée. La présence d'une activité endogène comme l'activité thêta temporale joue un rôle important dans cette période de développement avec une densité de connexion accrue dans les régions temporales. Les nouveau-nés à terme montrent une haute densité de connexion dans les régions frontales, postérieures et temporales durant le sommeil calme et agité. Les propriétés de « small world network » présents chez les nouveau-nés, suggèrent que les principes de ségrégation et d'intégration de l'information sont présents à cette période du développement.

Chapitre 7 : Conclusions générales

Ce chapitre résume toutes les études menées dans cette thèse. Les différentes perspectives sont explorées

Appendix: Supplementary information

Supporting information for section 4.2

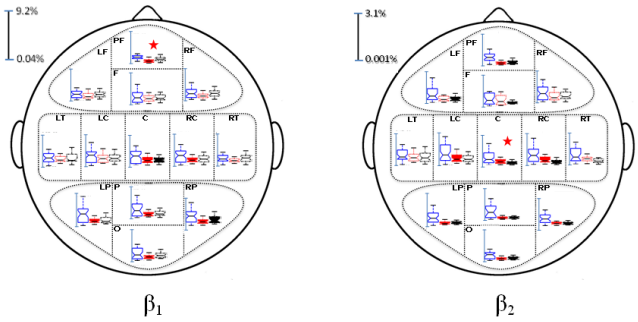

Figure S1. Average normalized spectral power maps (± standard deviation) in the sensor space under the eyes-closed condition for the control group (EC_{CT}, left boxplots), patient group (EC_{NS}, no spike condition, middle boxplots) and patient group (EC_{WS}, with spike condition, right boxplots) in β_1 and β_2 bands. Significant differences between EC_{CT} and EC_{NS}/EC_{WS} are shown in solid boxplots. Asterisks indicate statistically significant differences ($p<0.01$) between EC_{NS} and EC_{WS}.

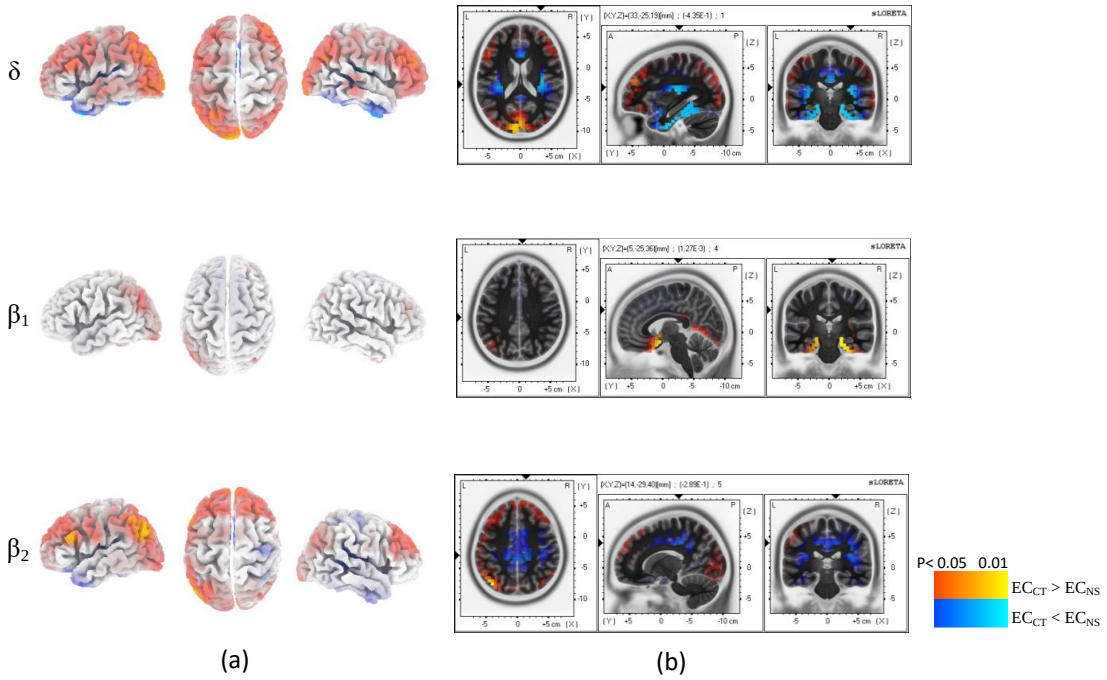

Figure S2. Statistical maps of differences between cortical sources computed under the eyes-closed condition for the control group (EC_{CT}, left boxplots) and patient group (EC_{NS}, no spike condition, right boxplots) in δ, β_1 and β_2 bands. The results have been projected onto the cortical layer of the realistic head model (a) and the MNI152 MRI (b). Color bars indicate significant differences between EC_{CT} and EC_{NS}, red ($EC_{CT} > EC_{NS}$) and blue ($EC_{CT} < EC_{NS}$).

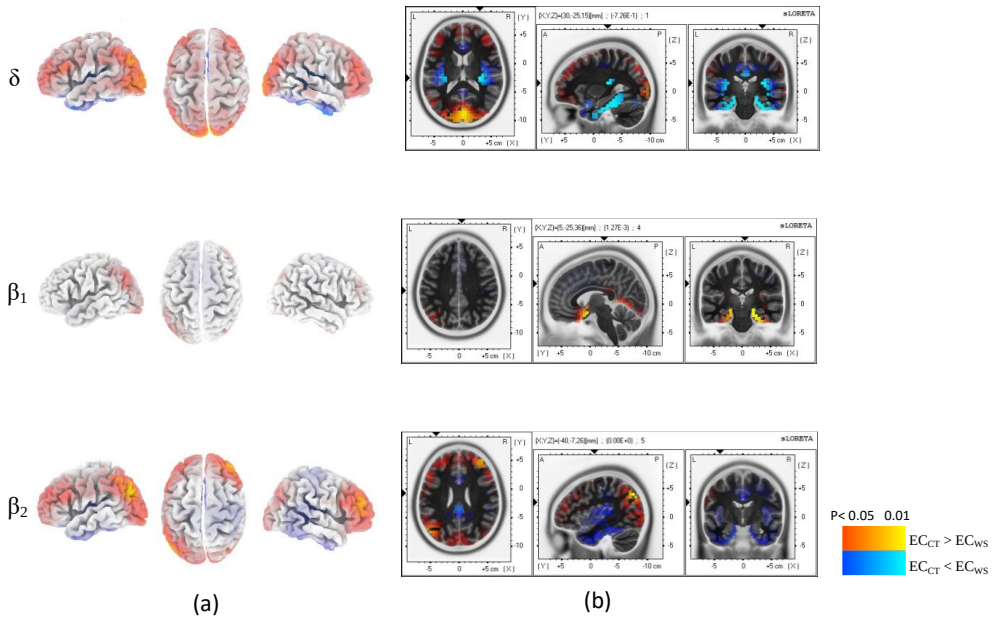

Figure S3. Statistical maps of differences between cortical sources computed under the eyes-closed condition for the control group (EC_{CT}, left boxplots) and patient group (EC_{WS}, with spike condition, right boxplots) in δ, β_1 and β_2. The results have been projected onto the cortical layer of the realistic head model (a) and the MNI152 MRI (b). Color bars indicate significant differences between EC_{CT} and EC_{WS}, red ($EC_{CT} > EC_{WS}$) and blue ($EC_{CT} < EC_{WS}$).

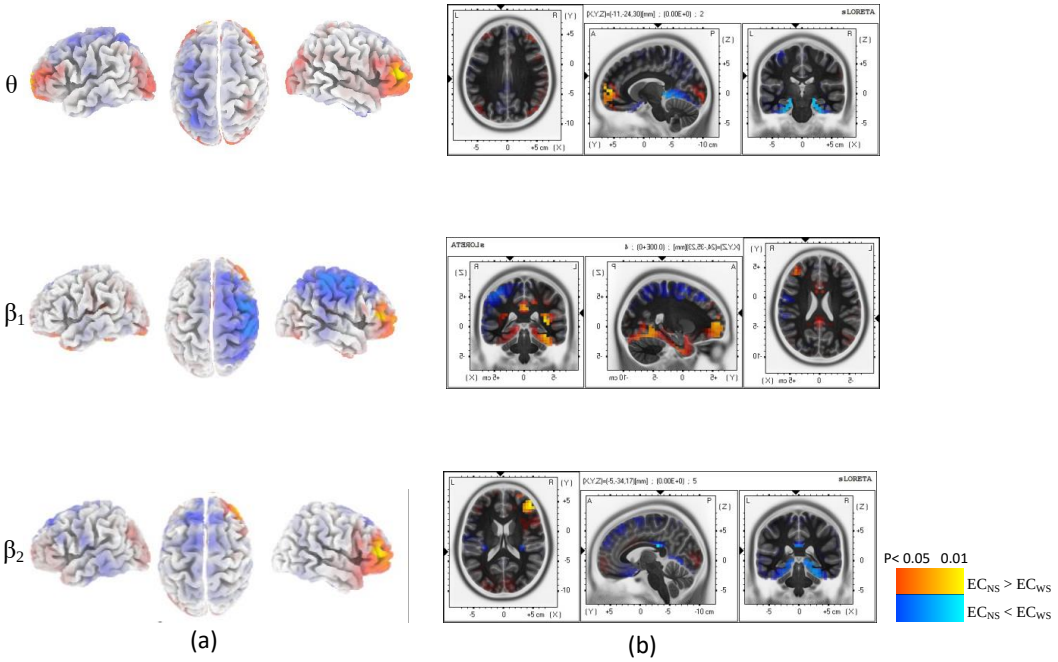

Figure S4. Statistical maps of differences between cortical sources computed under the no-spike (EC_{NS}, left boxplots) and with-spike (EC_{WS}, right boxplots) eyes-closed conditions in θ, β_1 and β_2 bands for the epileptic group. The results have been projected onto the cortical layer of the realistic head model (a) and the MNI152 MRI (b). Color bars indicate significant differences between EC_{NS} and EC_{WS}, red ($EC_{NS} > EC_{WS}$) and blue ($EC_{NS} > EC_{WS}$).

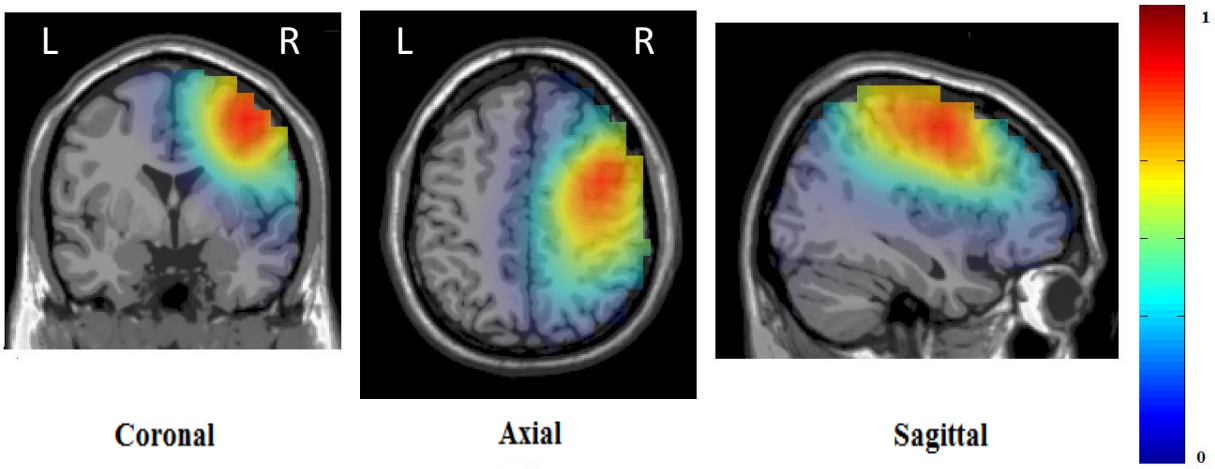

Figure S5. Average eLORETA localization of interictal spikes from the patients' scalp EEG.

Supporting information for section 4.3

Epileptic subjects

Dipole source analysis of the centrotemporal spikes region of the patients was performed with Advanced Source Analysis (ASA) software (http://www.ant-neuro.com). The location of interictal epileptic spikes (IES) was identified for each patient using the spatiotemporal dipole modeling method [1] (S2 Fig) . All dipoles were oriented in the anterior to posterior direction or *vice versa* and were located in the right precentral and postcentral regions, confirming the homogeneity of the patient population. The C4/C6/CP2/CP6 always recorded IES in BCECTS patients as shown in S2 Fig.

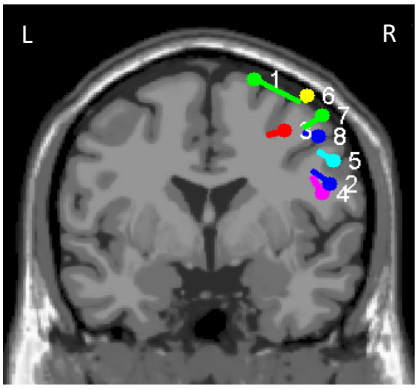

S1 Fig. Dipole locations of the averaged spikes for patients.

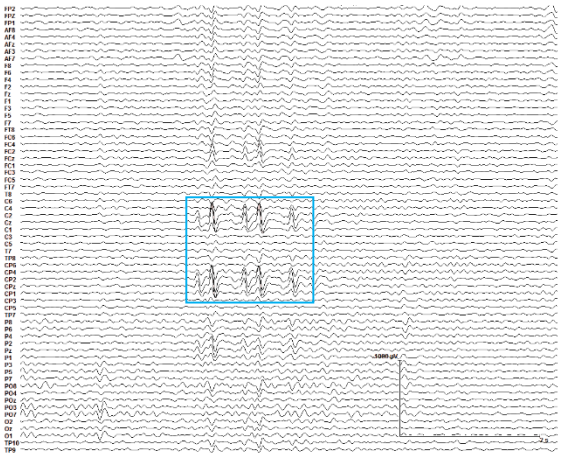

S2 Fig. A sample interictal EEG recording from patient 1. The spikes have been outlined in blue.

Functional connectivity

The phase locking value (PLV) was computed from the analytical signals obtained from Hilbert transformation of the band-pass filtered signals, filtered by a linear-phase FIR (finite impulse response) filter. The analytical signals (x (t, f)) were first computed by:

$$\check{x}(t,f) = x(t,f) + ix_H(t,f)$$

Where x_H (t, f) is the Hilbert transform of the input signals x (t,f).

The phases of the analytical signals were then extracted:

$$\varphi_x(t,f) = \arctan\left(\frac{x_H(t,f)}{x(t,f)}\right)$$

The relative phase between each channel pair x and y was obtained by:

$$\emptyset(t) = \varphi_x(t,f) - \varphi_y(t,f)$$

The PLV was finally computed by calculating the exponential of the relative phase:

$$PLV(x,y) = \frac{1}{N}\left|\sum_{n=1}^{N} e^{i(\emptyset(t))}\right|$$

Where N is the time point.

Computation of graph theory parameters

Degree

The degree of a node is the number of links connected to that node. The degree (K) is mathematically defined as:

$$K_i = \sum_{J \in N} A_{ij}$$

Where K_i is the degree for the ith node, and A_{ij} is the connection status between nodes i and j. The degree is a characteristic measure of the functional interactions between brain regions.

Clustering coefficient

The clustering coefficient C and characteristic path length L were computed as described in [2,3]. The clustering coefficient C_i of the node *i* is defined as:

$$C_i = \frac{1}{n}\sum_{i \in N} \frac{2t_i}{k_i(k_i - 1)}$$

Where n is the number of nodes, t_i is the number of existing connections among the neighbours of node *i*, and k_i is the actual number of neighbours of node *i* (i.e. degree). The mean clustering coefficient (C) of a network is defined as the mean clustering coefficient over all nodes in the network:

$$C = \frac{1}{N}\sum_{i=1}^{N} C_i$$

Characteristic path length

The characteristic path length L_i of a node *i* is defined as

$$L_i = \frac{\sum_{j=1, j\neq i}^{N} d_{ij}}{N-1}$$

Where is d_{ij} is the absolute distance between the nodes *i* and *j* and the mean characteristic path length L over a network is defined as:

$$L = \frac{1}{N}\sum_{i=1}^{N} L_i$$

Threshold optimization procedure for computation of degree

Before computing the graph parameters, we applied the threshold (τ) based on the three constraints described in Methods. The first method consists of obtaining one standard deviation above the median connectivity value as shown in S3 Fig. The connectivity matrix before thresholding has shown in Figure A of S3Fig. The distribution of the PLV values has been plotted in Figure B of S3 Fig. In this plot, the vertical pink line represents τ (one standard deviation above the median connectivity value) for a particular subject and frequency band. The optimal threshold was applied to the connectivity matrix (Figure A of S3 Fig) to obtain the binary matrix, as shown in Figure C of S3 Fig.

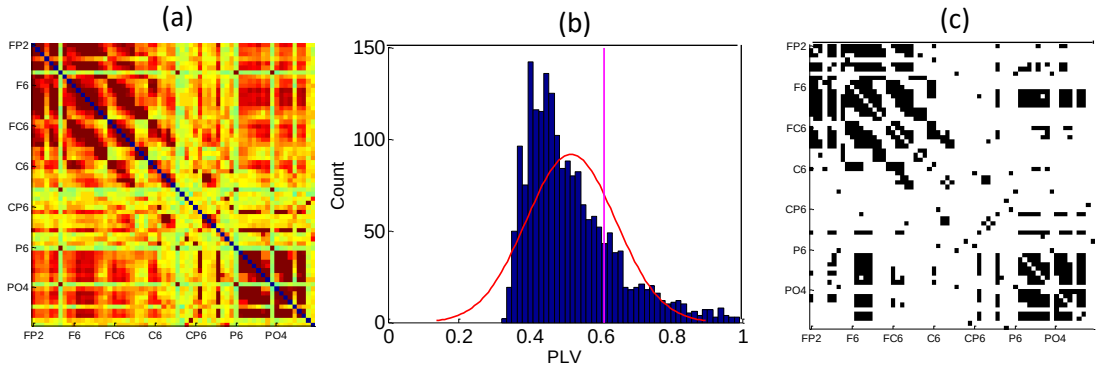

S3 Fig. (a) Example of the functional connectivity matrix obtained for Subject 1, (b) the distribution of the PLV values of the functional connectivity matrix; the vertical line shows the optimal threshold, (c) the binarized functional connectivity matrix obtained after applying the optimal threshold.

References

Addis, D.R., Wong, A.T., Schacter, D.L., 2007. Remembering the past and imagining the future: common and distinct neural substrates during event construction and elaboration. Neuropsychologia 45, 1363–1377. doi:10.1016/j.neuropsychologia.2006.10.016

Adebimpe, A., Aarabi, A., Bourel-Ponchel, E., Mahmoudzadeh, M., Wallois, F., 2016. EEG Resting State Functional Connectivity Analysis in Children with Benign Epilepsy with Centrotemporal Spikes. Brain Imaging Methods 143. doi:10.3389/fnins.2016.00143

Adebimpe, A., Aarabi, A., Bourel-Ponchel, E., Mahmoudzadeh, M., Wallois, F., 2015a. EEG resting state analysis of cortical sources in patients with benign epilepsy with centrotemporal spikes. NeuroImage Clin. 9, 275–282. doi:10.1016/j.nicl.2015.08.014

Adebimpe, A., Aarabi, A., Bourel-Ponchel, E., Mahmoudzadeh, M., Wallois, F., 2015b. Functional Brain Dysfunction in Patients with Benign Childhood Epilepsy as Revealed by Graph Theory. PLoS ONE 10, e0139228. doi:10.1371/journal.pone.0139228

Adebimpe, A., Aarabi, A., Bourel-Ponchel, E., Mahmoudzadeh, M., Wallois, F., 2015c. EEG resting state analysis of cortical sources in patients with benign epilepsy with centrotemporal spikes. NeuroImage Clin. 9, 275–282. doi:10.1016/j.nicl.2015.08.014

Akin, M., 2002. Comparison of Wavelet Transform and FFT Methods in the Analysis of EEG Signals. J. Med. Syst. 26, 241–247. doi:10.1023/A:1015075101937

Amaral, M.I.R., Casali, R.L., Boscariol, M., Lunardi, L.L., Guerreiro, M.M., Colella-Santos, M.F., 2015. Temporal auditory processing and phonological awareness in children with benign epilepsy with centrotemporal spikes. BioMed Res. Int. 2015, 256340. doi:10.1155/2015/256340

Anderson, N.G., Laurent, I., Cook, N., Woodward, L., Inder, T.E., 2005. Growth rate of corpus callosum in very premature infants. AJNR Am. J. Neuroradiol. 26, 2685–2690.

Anderson, N.G., Laurent, I., Woodward, L.J., Inder, T.E., 2006. Detection of impaired growth of the corpus callosum in premature infants. Pediatrics 118, 951–960. doi:10.1542/peds.2006-0553

André, M., Lamblin, M.-D., d'Allest, A.M., Curzi-Dascalova, L., Moussalli-Salefranque, F., S Nguyen The, T., Vecchierini-Blineau, M.-F., Wallois, F., Walls-Esquivel, E., Plouin, P., 2010. Electroencephalography in premature and full-term infants. Developmental features and glossary. Neurophysiol. Clin. Clin. Neurophysiol. 40, 59–124. doi:10.1016/j.neucli.2010.02.002

Archer, J.S., Abbott, D.F., Waites, A.B., Jackson, G.D., 2003. fMRI "deactivation" of the posterior cingulate during generalized spike and wave. NeuroImage 20, 1915–1922.

Ashburner, J., Barnes, G., Chen, C., Daunizeau, J., Flandin, G., Friston, K., Gitelman, D., Kiebel, S., Kilner, J., Litvak, V., others, 2012. SPM8 manual. Funct. Imaging Lab. Inst. Neurol.

Ay, Y., Gokben, S., Serdaroglu, G., Polat, M., Tosun, A., Tekgul, H., Solak, U., Kesikci, H., 2009. Neuropsychologic impairment in children with rolandic epilepsy. Pediatr. Neurol. 41, 359–363. doi:10.1016/j.pediatrneurol.2009.05.013

Baccalá, L.A., Sameshima, K., 2001. Partial directed coherence: a new concept in neural structure determination. Biol. Cybern. 84, 463–474. doi:10.1007/PL00007990

Bachevalier, J., Mishkin, M., 1994. Effects of selective neonatal temporal lobe lesions on visual recognition memory in rhesus monkeys. J. Neurosci. 14, 2128–2139.

Back, S.A., Miller, S.P., 2014. Brain injury in premature neonates: A primary cerebral dysmaturation disorder? Ann. Neurol. 75, 469–486. doi:10.1002/ana.24132
Ball, G., Aljabar, P., Zebari, S., Tusor, N., Arichi, T., Merchant, N., Robinson, E.C., Ogundipe, E., Rueckert, D., Edwards, A.D., Counsell, S.J., 2014. Rich-club organization of the newborn human brain. Proc. Natl. Acad. Sci. 111, 7456–7461. doi:10.1073/pnas.1324118111
Banerjee, P.N., Filippi, D., Allen Hauser, W., 2009. The descriptive epidemiology of epilepsy—A review. Epilepsy Res. 85, 31–45. doi:10.1016/j.eplepsyres.2009.03.003
Başar, E., Başar-Eroğlu, C., Güntekin, B., Yener, G.G., 2013. Brain's alpha, beta, gamma, delta, and theta oscillations in neuropsychiatric diseases: proposal for biomarker strategies. Suppl. Clin. Neurophysiol. 62, 19–54.
Başar, E., Güntekin, B., 2013. Review of delta, theta, alpha, beta, and gamma response oscillations in neuropsychiatric disorders. Suppl. Clin. Neurophysiol. 62, 303–341.
Bassett, D.S., Bullmore, E., 2006. Small-world brain networks. Neurosci. Rev. J. Bringing Neurobiol. Neurol. Psychiatry 12, 512–523. doi:10.1177/1073858406293182
Bassett, D.S., Gazzaniga, M.S., 2011. Understanding complexity in the human brain. Trends Cogn. Sci. 15, 200–209. doi:10.1016/j.tics.2011.03.006
Baumgartner, C., Graf, M., Doppelbauer, A., Serles, W., Lindinger, G., Olbrich, A., Bacher, J., Pataraia, E., Almer, G., Lischka, A., 1996. The Functional Organization of the Interictal Spike Complex in Benign Rolandic Epilepsy. Epilepsia 37, 1164–1174. doi:10.1111/j.1528-1157.1996.tb00548.x
Bear, M.F., Connors, B.W., Paradiso, M.A., 2001. Neuroscience: Exploring the Brain, 2nd edition. ed. Lippincott Williams & Wilkins, Baltimore, Md.
Béla, C., Mónika, B., Márton, T., István, K., 2007. Valproate selectively reduces EEG activity in anterior parts of the cortex in patients with idiopathic generalized epilepsy. A low resolution electromagnetic tomography (LORETA) study. Epilepsy Res. 75, 186–191. doi:10.1016/j.eplepsyres.2007.06.009
Besenyei, M., Varga, E., Fekete, I., Puskás, S., Hollódy, K., Fogarasi, A., Emri, M., Opposits, G., Kis, S.A., Clemens, B., 2012. EEG background activity is abnormal in the temporal and inferior parietal cortex in benign rolandic epilepsy of childhood: a LORETA study. Epilepsy Res. 98, 44–49. doi:10.1016/j.eplepsyres.2011.08.013
Besseling, R.M.H., Overvliet, G.M., Jansen, J.F.A., van der Kruijs, S.J.M., Vles, J.S.H., Ebus, S.C.M., Hofman, P.A.M., de Louw, A.J.A., Aldenkamp, A.P., Backes, W.H., 2013. Aberrant functional connectivity between motor and language networks in rolandic epilepsy. Epilepsy Res. 107, 253–262. doi:10.1016/j.eplepsyres.2013.10.008
Bettus, G., Guedj, E., Joyeux, F., Confort-Gouny, S., Soulier, E., Laguitton, V., Cozzone, P.J., Chauvel, P., Ranjeva, J.-P., Bartolomei, F., Guye, M., 2009. Decreased basal fMRI functional connectivity in epileptogenic networks and contralateral compensatory mechanisms. Hum. Brain Mapp. 30, 1580–1591. doi:10.1002/hbm.20625
Betzel, R.F., Byrge, L., He, Y., Goñi, J., Zuo, X.-N., Sporns, O., 2014. Changes in structural and functional connectivity among resting-state networks across the human lifespan. NeuroImage 102, 345–357. doi:10.1016/j.neuroimage.2014.07.067
Biswal, B.B., 2012. Resting state fMRI: A personal history. NeuroImage, 20 YEARS OF fMRI20 YEARS OF fMRI 62, 938–944. doi:10.1016/j.neuroimage.2012.01.090
Bonney, P.A., Boettcher, L.B., Conner, A.K., Glenn, C.A., Briggs, R.G., Santucci, J.A., Bellew, M.R., Battiste, J.D., Sughrue, M.E., 2015. Review of seizure outcomes after surgical

resection of dysembryoplastic neuroepithelial tumors. J. Neurooncol. 126, 1–10. doi:10.1007/s11060-015-1961-4
Boor, R., Jacobs, J., Hinzmann, A., Bauermann, T., Scherg, M., Boor, S., Vucurevic, G., Pfleiderer, C., Kutschke, G., Stoeter, P., 2007. Combined spike-related functional MRI and multiple source analysis in the non-invasive spike localization of benign rolandic epilepsy. Clin. Neurophysiol. 118, 901–909. doi:10.1016/j.clinph.2006.11.272
Bourel-Ponchel, E., 2013. Exploration de l'unité neurovasculaire dans l'épilepsie de l'enfant : approche multimodale haute densité couplant l'EEG à l'imagerie optique fonctionnelle. Amiens.
Breakspear, M., Jirsa, V.K., 2007. Neuronal Dynamics and Brain Connectivity, in: Jirsa, V.K., McIntosh, A.R. (Eds.), Handbook of Brain Connectivity, Understanding Complex Systems. Springer Berlin Heidelberg, pp. 3–64.
Brillinger, D., 2001. Time Series, Classics in Applied Mathematics. Society for Industrial and Applied Mathematics.
Brodmann, K., 1909. Vergleichende Lokalisationslehre der Großhirnrinde. Barth, Leipzig.
Bronez, T.P., 1992. On the performance advantage of multitaper spectral analysis. IEEE Trans. Signal Process. 40, 2941–2946. doi:10.1109/78.175738
Buckner, R.L., Sepulcre, J., Talukdar, T., Krienen, F.M., Liu, H., Hedden, T., Andrews-Hanna, J.R., Sperling, R.A., Johnson, K.A., 2009. Cortical Hubs Revealed by Intrinsic Functional Connectivity: Mapping, Assessment of Stability, and Relation to Alzheimer's Disease. J. Neurosci. 29, 1860–1873. doi:10.1523/JNEUROSCI.5062-08.2009
Bullmore, E., Sporns, O., 2009. Complex brain networks: graph theoretical analysis of structural and functional systems. Nat. Rev. Neurosci. 10, 186–198. doi:10.1038/nrn2575
Bullmore, E.T., Bassett, D.S., 2011. Brain Graphs: Graphical Models of the Human Brain Connectome. Annu. Rev. Clin. Psychol. 7, 113–140. doi:10.1146/annurev-clinpsy-040510-143934
Camfield, C.S., Berg, A., Stephani, U., Wirrell, E.C., 2014. Transition issues for benign epilepsy with centrotemporal spikes, nonlesional focal epilepsy in otherwise normal children, childhood absence epilepsy, and juvenile myoclonic epilepsy. Epilepsia 55 Suppl 3, 16–20. doi:10.1111/epi.12706
Camfield, C.S., Camfield, P.R., 2014. Rolandic epilepsy has little effect on adult life 30 years later: a population-based study. Neurology 82, 1162–1166. doi:10.1212/WNL.0000000000000267
Camfield, P., Camfield, C., 2002. Epileptic Syndromes in Childhood: Clinical Features, Outcomes, and Treatment. Epilepsia 43, 27–32. doi:10.1046/j.1528-1157.43.s.3.3.x
Canuet, L., Ishii, R., Pascual-Marqui, R.D., Iwase, M., Kurimoto, R., Aoki, Y., Ikeda, S., Takahashi, H., Nakahachi, T., Takeda, M., 2011. Resting-State EEG Source Localization and Functional Connectivity in Schizophrenia-Like Psychosis of Epilepsy. PLoS ONE 6, e27863. doi:10.1371/journal.pone.0027863
Cao, M., Wang, J.-H., Dai, Z.-J., Cao, X.-Y., Jiang, L.-L., Fan, F.-M., Song, X.-W., Xia, M.-R., Shu, N., Dong, Q., Milham, M.P., Castellanos, F.X., Zuo, X.-N., He, Y., 2014. Topological organization of the human brain functional connectome across the lifespan. Dev. Cogn. Neurosci. 7, 76–93. doi:10.1016/j.dcn.2013.11.004
Centeno, M., Carmichael, D.W., 2014. Network connectivity in epilepsy: resting state fMRI and EEG–fMRI contributions. Epilepsy 5, 93. doi:10.3389/fneur.2014.00093

Ciumas, C., Saignavongs, M., Ilski, F., Herbillon, V., Laurent, A., Lothe, A., Heckemann, R.A., de Bellescize, J., Panagiotakaki, E., Hannoun, S., Marinier, D.S., Montavont, A., Ostrowsky-Coste, K., Bedoin, N., Ryvlin, P., 2014. White matter development in children with benign childhood epilepsy with centro-temporal spikes. Brain J. Neurol. 137, 1095–1106. doi:10.1093/brain/awu039

Clemens, B., 2004. Pathological theta oscillations in idiopathic generalised epilepsy. Clin. Neurophysiol. 115, 1436–1441. doi:10.1016/j.clinph.2004.01.018

Clemens, B., Bessenyei, M., Fekete, I., Puskás, S., Kondákor, I., Tóth, M., Hollódy, K., 2010. Theta EEG source localization using LORETA in partial epilepsy patients with and without medication. Clin. Neurophysiol. Off. J. Int. Fed. Clin. Neurophysiol. 121, 848–858. doi:10.1016/j.clinph.2010.01.020

Coben, R., Clarke, A.R., Hudspeth, W., Barry, R.J., 2008. EEG power and coherence in autistic spectrum disorder. Clin. Neurophysiol. 119, 1002–1009. doi:10.1016/j.clinph.2008.01.013

Cohen, M.X., 2014. Analyzing Neural Time Series Data: Theory and Practice. MIT Press.

Collin, G., van den Heuvel, M.P., 2013. The ontogeny of the human connectome: development and dynamic changes of brain connectivity across the life span. Neurosci. Rev. J. Bringing Neurobiol. Neurol. Psychiatry 19, 616–628. doi:10.1177/1073858413503712

Corbetta, M., Shulman, G.L., 2002. Control of goal-directed and stimulus-driven attention in the brain. Nat. Rev. Neurosci. 3, 201–215. doi:10.1038/nrn755

Danielsson, J., Petermann, F., 2009. Cognitive deficits in children with benign rolandic epilepsy of childhood or rolandic discharges: a study of children between 4 and 7 years of age with and without seizures compared with healthy controls. Epilepsy Behav. EB 16, 646–651. doi:10.1016/j.yebeh.2009.08.012

Datta, A.N., Oser, N., Bauder, F., Maier, O., Martin, F., Ramelli, G.P., Steinlin, M., Weber, P., Penner, I.-K., 2013. Cognitive impairment and cortical reorganization in children with benign epilepsy with centrotemporal spikes. Epilepsia 54, 487–494. doi:10.1111/epi.12067

Deco, G., Kringelbach, M.L., 2014. Great Expectations: Using Whole-Brain Computational Connectomics for Understanding Neuropsychiatric Disorders. Neuron 84, 892–905. doi:10.1016/j.neuron.2014.08.034

Dehaene-Lambertz, G., Spelke, E.S., 2015. The Infancy of the Human Brain. Neuron 88, 93–109. doi:10.1016/j.neuron.2015.09.026

Delorme, A., Makeig, S., 2004. EEGLAB: an open source toolbox for analysis of single-trial EEG dynamics including independent component analysis. J. Neurosci. Methods 134, 9–21. doi:10.1016/j.jneumeth.2003.10.009

Delorme, A., Mullen, T., Kothe, C., Akalin Acar, Z., Bigdely-Shamlo, N., Vankov, A., Makeig, S., Delorme, A., Mullen, T., Kothe, C., Akalin Acar, Z., Bigdely-Shamlo, N., Vankov, A., Makeig, S., 2011. EEGLAB, SIFT, NFT, BCILAB, and ERICA: New Tools for Advanced EEG Processing, EEGLAB, SIFT, NFT, BCILAB, and ERICA: New Tools for Advanced EEG Processing. Comput. Intell. Neurosci. Comput. Intell. Neurosci. 2011, 2011, e130714. doi:10.1155/2011/130714, 10.1155/2011/130714

Deltour, L., Barathon, M., Quaglino, V., Vernier, M.-P., Despretz, P., Boucart, M., Berquin, P., 2007. Children with benign epilepsy with centrotemporal spikes (BECTS) show impaired attentional control: evidence from an attentional capture paradigm. Epileptic Disord. Int. Epilepsy J. Videotape 9, 32–38. doi:10.1684/epd.2007.0066

Deuker, L., Bullmore, E.T., Smith, M., Christensen, S., Nathan, P.J., Rockstroh, B., Bassett, D.S., 2009. Reproducibility of graph metrics of human brain functional networks. NeuroImage 47, 1460–1468. doi:10.1016/j.neuroimage.2009.05.035

de Weerd, A.W., van den Bossche, R.A.S., 2003. The development of sleep during the first months of life. Sleep Med. Rev. 7, 179–191.

Ding, M., Bressler, S.L., Yang, W., Liang, H., 2000. Short-window spectral analysis of cortical event-related potentials by adaptive multivariate autoregressive modeling: data preprocessing, model validation, and variability assessment. Biol. Cybern. 83, 35–45.

Doria, V., Beckmann, C.F., Arichi, T., Merchant, N., Groppo, M., Turkheimer, F.E., Counsell, S.J., Murgasova, M., Aljabar, P., Nunes, R.G., Larkman, D.J., Rees, G., Edwards, A.D., 2010. Emergence of resting state networks in the preterm human brain. Proc. Natl. Acad. Sci. 107, 20015–20020. doi:10.1073/pnas.1007921107

Dosenbach, N.U.F., Nardos, B., Cohen, A.L., Fair, D.A., Power, J.D., Church, J.A., Nelson, S.M., Wig, G.S., Vogel, A.C., Lessov-Schlaggar, C.N., Barnes, K.A., Dubis, J.W., Feczko, E., Coalson, R.S., Pruett, J.R., Barch, D.M., Petersen, S.E., Schlaggar, B.L., 2010. Prediction of individual brain maturity using fMRI. Science 329, 1358–1361. doi:10.1126/science.1194144

Douw, L., de Groot, M., van Dellen, E., Heimans, J.J., Ronner, H.E., Stam, C.J., Reijneveld, J.C., 2010a. "Functional connectivity" is a sensitive predictor of epilepsy diagnosis after the first seizure. PloS One 5, e10839. doi:10.1371/journal.pone.0010839

Douw, L., Dellen, E. van, Groot, M. de, Heimans, J.J., Klein, M., Stam, C.J., Reijneveld, J.C., 2010b. Epilepsy is related to theta band brain connectivity and network topology in brain tumor patients. BMC Neurosci. 11, 103. doi:10.1186/1471-2202-11-103

Drakesmith, M., Caeyenberghs, K., Dutt, A., Lewis, G., David, A.S., Jones, D.K., 2015. Overcoming the effects of false positives and threshold bias in graph theoretical analyses of neuroimaging data. NeuroImage 118, 313–333. doi:10.1016/j.neuroimage.2015.05.011

Drassinower, D., Friedman, A.M., Običan, S.G., Levin, H., Gyamfi-Bannerman, C., 2015. Prolonged latency of preterm premature rupture of membranes and risk of cerebral palsy. J. Matern. Fetal Neonatal Med. 0, 1–5. doi:10.3109/14767058.2015.1107539

Drongelen, D.W. van, Yuchtman, M., Veen, B.D.V., Huffelen, A.C. van, 1996. A spatial filtering technique to detect and localize multiple sources in the brain. Brain Topogr. 9, 39–49. doi:10.1007/BF01191641

Dubois, J., Benders, M., Cachia, A., Lazeyras, F., Ha-Vinh Leuchter, R., Sizonenko, S.V., Borradori-Tolsa, C., Mangin, J.F., Hüppi, P.S., 2008. Mapping the early cortical folding process in the preterm newborn brain. Cereb. Cortex N. Y. N 1991 18, 1444–1454. doi:10.1093/cercor/bhm180

Dunn, D.W., 2014. Focusing on ADHD and attention in children with epilepsy. Epilepsy Behav. 37, 308–309. doi:10.1016/j.yebeh.2014.06.022

Dunn, D.W., Austin, J.K., Harezlak, J., Ambrosius, W.T., 2003. ADHD and epilepsy in childhood. Dev. Med. Child Neurol. 45, 50–54.

Erdős, P., Rényi, A., 2013. On the strength of connectedness of a random graph. Acta Math. Acad. Sci. Hung. 12, 261–267. doi:10.1007/BF02066689

Fair, D.A., Cohen, A.L., Power, J.D., Dosenbach, N.U.F., Church, J.A., Miezin, F.M., Schlaggar, B.L., Petersen, S.E., 2009. Functional brain networks develop from a "local to distributed" organization. PLoS Comput. Biol. 5, e1000381. doi:10.1371/journal.pcbi.1000381

Fallani, F.D.V., Richiardi, J., Chavez, M., Achard, S., 2014. Graph analysis of functional brain networks: practical issues in translational neuroscience. Philos. Trans. R. Soc. B Biol. Sci. 369, 20130521–20130521. doi:10.1098/rstb.2013.0521

Field, T., Diego, M., 2008. Maternal Depression Effects on Infant Frontal Eeg Asymmetry. Int. J. Neurosci. 118, 1081–1108. doi:10.1080/00207450701769067

Filippini, M., Boni, A., Giannotta, M., Pini, A., Russo, A., Musti, M.A., Guerra, A., Lassonde, M., Gobbi, G., 2015. Comparing cortical auditory processing in children with typical and atypical benign epilepsy with centrotemporal spikes: Electrophysiologic evidence of the role of non–rapid eye movement sleep abnormalities. Epilepsia 56, 726–734. doi:10.1111/epi.12959

Fonov, V., Evans, A.C., Botteron, K., Almli, C.R., McKinstry, R.C., Collins, D.L., 2011. Unbiased average age-appropriate atlases for pediatric studies. NeuroImage 54, 313–327. doi:10.1016/j.neuroimage.2010.07.033

Fonov, V., Evans, A., McKinstry, R., Almli, C., Collins, D., 2009. Unbiased nonlinear average age-appropriate brain templates from birth to adulthood. NeuroImage 47, S102. doi:10.1016/S1053-8119(09)70884-5

Fonseca, L.C., Tedrus, G.M.A.S., Pacheco, E.M.C., 2007. Epileptiform EEG discharges in benign childhood epilepsy with centrotemporal spikes: reactivity and transitory cognitive impairment. Epilepsy Behav. EB 11, 65–70. doi:10.1016/j.yebeh.2007.04.001

Forsgren, L., Beghi, E., Õun, A., Sillanpää, M., 2005. The epidemiology of epilepsy in Europe – a systematic review. Eur. J. Neurol. 12, 245–253. doi:10.1111/j.1468-1331.2004.00992.x

Forsgren, L., Hauser, W.A., Olafsson, E., Sander, J.W. a. S., Sillanpää, M., Tomson, T., 2005. Mortality of epilepsy in developed countries: a review. Epilepsia 46 Suppl 11, 18–27. doi:10.1111/j.1528-1167.2005.00403.x

Fountain, N.B., 2008. Evidence for Functional Impairment But Not Structural Disease in Benign Rolandic Epilepsy. Epilepsy Curr. 8, 14–16. doi:10.1111/j.1535-7511.2007.00220.x

Fransson, P., Aden, U., Blennow, M., Lagercrantz, H., 2011. The functional architecture of the infant brain as revealed by resting-state fMRI. Cereb. Cortex N. Y. N 1991 21, 145–154. doi:10.1093/cercor/bhq071

Fransson, P., Skiöld, B., Engström, M., Hallberg, B., Mosskin, M., Åden, U., Lagercrantz, H., Blennow, M., 2009. Spontaneous Brain Activity in the Newborn Brain During Natural Sleep—An fMRI Study in Infants Born at Full Term. Pediatr. Res. 66, 301–305. doi:10.1203/PDR.0b013e3181b1bd84

Fransson, P., Skiöld, B., Horsch, S., Nordell, A., Blennow, M., Lagercrantz, H., Aden, U., 2007. Resting-state networks in the infant brain. Proc. Natl. Acad. Sci. U. S. A. 104, 15531–15536. doi:10.1073/pnas.0704380104

Freeman, L.C., 1979. Centrality in social networks conceptual clarification. Soc. Netw. 1, 215–239.

Freeman, W., 2007. Hilbert transform for brain waves. Scholarpedia 2, 1338. doi:10.4249/scholarpedia.1338

Freeman, W.J., 2006. Origin, structure, and role of background EEG activity. Part 4: Neural frame simulation. Clin. Neurophysiol. 117, 572–589. doi:10.1016/j.clinph.2005.10.025

Friston, K.J., 2005. Models of Brain Function in Neuroimaging. Annu. Rev. Psychol. 56, 57–87. doi:10.1146/annurev.psych.56.091103.070311

Friston, K.J., 1994. Functional and effective connectivity in neuroimaging: A synthesis. Hum. Brain Mapp. 2, 56–78. doi:10.1002/hbm.460020107

Friston, K.J., Harrison, L., Penny, W., 2003. Dynamic causal modelling. NeuroImage 19, 1273–1302. doi:10.1016/S1053-8119(03)00202-7

Fuchs, M., Kastner, J., Wagner, M., Hawes, S., Ebersole, J.S., 2002. A standardized boundary element method volume conductor model. Clin. Neurophysiol. Off. J. Int. Fed. Clin. Neurophysiol. 113, 702–712.

Gao, W., Alcauter, S., Smith, J.K., Gilmore, J.H., Lin, W., 2015. Development of human brain cortical network architecture during infancy. Brain Struct. Funct. 220, 1173–1186. doi:10.1007/s00429-014-0710-3

Gong, W., Ji, M., Cao, Z., Wang, L., Qian, Y., Hu, M., Qian, L., Pan, X., 2008. Establishment and characterization of a cell based artificial antigen-presenting cell for expansion and activation of CD8+ T cells ex vivo. Cell. Mol. Immunol. 5, 47–53. doi:10.1038/cmi.2008.6

Gong, X.-W., Li, J.-B., Lu, Q.-C., Liang, P.-J., Zhang, P.-M., 2014. Effective Connectivity of Hippocampal Neural Network and Its Alteration in Mg2+-Free Epilepsy Model. PLoS ONE 9, e92961. doi:10.1371/journal.pone.0092961

González, J.J., Mañas, S., De Vera, L., Méndez, L.D., López, S., Garrido, J.M., Pereda, E., 2011. Assessment of electroencephalographic functional connectivity in term and preterm neonates. Clin. Neurophysiol. Off. J. Int. Fed. Clin. Neurophysiol. 122, 696–702. doi:10.1016/j.clinph.2010.08.025

Gramfort, A., Kowalski, M., Hämäläinen, M., 2012. Mixed-norm estimates for the M/EEG inverse problem using accelerated gradient methods. Phys. Med. Biol. 57, 1937–1961. doi:10.1088/0031-9155/57/7/1937

Grech, R., Cassar, T., Muscat, J., Camilleri, K.P., Fabri, S.G., Zervakis, M., Xanthopoulos, P., Sakkalis, V., Vanrumste, B., 2008. Review on solving the inverse problem in EEG source analysis. J. NeuroEngineering Rehabil. 5, 25. doi:10.1186/1743-0003-5-25

Grieve, P.G., Isler, J.R., Izraelit, A., Peterson, B.S., Fifer, W.P., Myers, M.M., Stark, R.I., 2008. EEG functional connectivity in term age extremely low birth weight infants. Clin. Neurophysiol. Off. J. Int. Fed. Clin. Neurophysiol. 119, 2712–2720. doi:10.1016/j.clinph.2008.09.020

Gross, J., Kujala, J., Hamalainen, M., Timmermann, L., Schnitzler, A., Salmelin, R., 2001. Dynamic imaging of coherent sources: Studying neural interactions in the human brain. Proc. Natl. Acad. Sci. U. S. A. 98, 694–699. doi:10.1073/pnas.98.2.694

Gusnard, D.A., Akbudak, E., Shulman, G.L., Raichle, M.E., 2001. Medial prefrontal cortex and self-referential mental activity: relation to a default mode of brain function. Proc. Natl. Acad. Sci. U. S. A. 98, 4259–4264. doi:10.1073/pnas.071043098

Hagmann, P., Cammoun, L., Gigandet, X., Meuli, R., Honey, C.J., Wedeen, V.J., Sporns, O., 2008. Mapping the Structural Core of Human Cerebral Cortex. PLOS Biol 6, e159. doi:10.1371/journal.pbio.0060159

Hallez, H., 2008. Incorporation of anisotropic conductivities in EEG source analysis. Ghent University.

Hallez, H., Vanrumste, B., Grech, R., Muscat, J., De Clercq, W., Vergult, A., D'Asseler, Y., Camilleri, K.P., Fabri, S.G., Van Huffel, S., Lemahieu, I., 2007. Review on solving the forward problem in EEG source analysis. J. NeuroEngineering Rehabil. 4, 46. doi:10.1186/1743-0003-4-46

Hallez, H., Vanrumste, B., Van Hese, P., D'Asseler, Y., Lemahieu, I., Van de Walle, R., 2005. A finite difference method with reciprocity used to incorporate anisotropy in electroencephalogram dipole source localization. Phys. Med. Biol. 50, 3787.
He, B., Dai, Y., Astolfi, L., Babiloni, F., Yuan, H., Yang, L., 2011a. eConnectome: A MATLAB Toolbox for Mapping and Imaging of Brain Functional Connectivity. J. Neurosci. Methods 195, 261–269. doi:10.1016/j.jneumeth.2010.11.015
He, B., Yang, L., Wilke, C., Yuan, H., 2011b. Electrophysiological imaging of brain activity and connectivity-challenges and opportunities. IEEE Trans. Biomed. Eng. 58, 1918–1931. doi:10.1109/TBME.2011.2139210
Hesse, W., Möller, E., Arnold, M., Schack, B., 2003. The use of time-variant EEG Granger causality for inspecting directed interdependencies of neural assemblies. J. Neurosci. Methods 124, 27–44. doi:10.1016/S0165-0270(02)00366-7
Heuvel, M.P. van den, Kersbergen, K.J., Reus, M.A. de, Keunen, K., Kahn, R.S., Groenendaal, F., Vries, L.S. de, Benders, M.J.N.L., 2015. The Neonatal Connectome During Preterm Brain Development. Cereb. Cortex 25, 3000–3013. doi:10.1093/cercor/bhu095
Heuvel, M.P. van den, Sporns, O., 2011. Rich-Club Organization of the Human Connectome. J. Neurosci. 31, 15775–15786. doi:10.1523/JNEUROSCI.3539-11.2011
He, Y., Evans, A., 2010. Graph theoretical modeling of brain connectivity. Curr. Opin. Neurol. 23, 341–350. doi:10.1097/WCO.0b013e32833aa567
Holmes, G.L., 1993. Benign focal epilepsies of childhood. Epilepsia 34, S49–S61.
Holmes, G.L., Khazipov, R., 2007. Basic Neurophysiology and the Cortical Basis of EEG, in: PHD, A.S.B.M., MD, S.B.R. (Eds.), The Clinical Neurophysiology Primer. Humana Press, pp. 19–33.
Holmes, G.L., Lenck-Santini, P.-P., 2006. Role of interictal epileptiform abnormalities in cognitive impairment. Epilepsy Behav. EB 8, 504–515. doi:10.1016/j.yebeh.2005.11.014
Horwitz, B., 2003. The elusive concept of brain connectivity. NeuroImage 19, 466–470. doi:10.1016/S1053-8119(03)00112-5
Hughes, J.R., 2010. Benign epilepsy of childhood with centrotemporal spikes (BECTS): to treat or not to treat, that is the question. Epilepsy Behav. EB 19, 197–203. doi:10.1016/j.yebeh.2010.07.018
Hurtado, J.M., Rubchinsky, L.L., Sigvardt, K.A., 2004. Statistical Method for Detection of Phase-Locking Episodes in Neural Oscillations. J. Neurophysiol. 91, 1883–1898. doi:10.1152/jn.00853.2003
Ibrahim, G.M., Morgan, B.R., Lee, W., Smith, M.L., Donner, E.J., Wang, F., Beers, C.A., Federico, P., Taylor, M.J., Doesburg, S.M., Rutka, J.T., Carter Snead, O., 2014. Impaired development of intrinsic connectivity networks in children with medically intractable localization-related epilepsy. Hum. Brain Mapp. 35, 5686–5700. doi:10.1002/hbm.22580
Iyer, K.K., Roberts, J.A., Hellström-Westas, L., Wikström, S., Hansen Pupp, I., Ley, D., Vanhatalo, S., Breakspear, M., 2015. Cortical burst dynamics predict clinical outcome early in extremely preterm infants. Brain J. Neurol. 138, 2206–2218. doi:10.1093/brain/awv129
Jackson, A.F., Bolger, D.J., 2014. The neurophysiological bases of EEG and EEG measurement: A review for the rest of us. Psychophysiology 51, 1061–1071. doi:10.1111/psyp.12283
Jambaqué, I., Dellatolas, G., Dulac, O., Ponsot, G., Signoret, J.-L., 1993. Verbal and visual memory impairment in childrem with epilepsy. Neuropsychologia 31, 1321–1337. doi:10.1016/0028-3932(93)90101-5

Jenssen, S., Roberts, C.M., Gracely, E.J., Dlugos, D.J., Sperling, M.R., 2011. Focal seizure propagation in the intracranial EEG. Epilepsy Res. 93, 25–32. doi:10.1016/j.eplepsyres.2010.10.008

Jeong, J., Gore, J.C., Peterson, B.S., 2001. Mutual information analysis of the EEG in patients with Alzheimer's disease. Clin. Neurophysiol. 112, 827–835. doi:10.1016/S1388-2457(01)00513-2

Johansen-Berg, H., Rushworth, M.F.S., 2009. Using Diffusion Imaging to Study Human Connectional Anatomy. Annu. Rev. Neurosci. 32, 75–94. doi:10.1146/annurev.neuro.051508.135735

Johnson, M.H., 2001. Functional brain development in humans. Nat. Rev. Neurosci. 2, 475–483. doi:10.1038/35081509

Judaš, M., Sedmak, G., Kostović, I., 2013. The significance of the subplate for evolution and developmental plasticity of the human brain. Front. Hum. Neurosci. 7, 423. doi:10.3389/fnhum.2013.00423

Kamiński, M., Ding, M., Truccolo, W.A., Bressler, S.L., 2001. Evaluating causal relations in neural systems: Granger causality, directed transfer function and statistical assessment of significance. Biol. Cybern. 85, 145–157. doi:10.1007/s004220000235

Kanemura, H., Aihara, M., 2009. Growth disturbance of frontal lobe in BCECTS presenting with frontal dysfunction. Brain Dev. 31, 771–774. doi:10.1016/j.braindev.2008.12.007

Kanemura, H., Hata, S., Aoyagi, K., Sugita, K., Aihara, M., 2011. Serial changes of prefrontal lobe growth in the patients with benign childhood epilepsy with centrotemporal spikes presenting with cognitive impairments/behavioral problems. Brain Dev. 33, 106–113. doi:10.1016/j.braindev.2010.03.005

Karolis, V.R., Froudist-Walsh, S., Brittain, P.J., Kroll, J., Ball, G., Edwards, A.D., Dell'Acqua, F., Williams, S.C., Murray, R.M., Nosarti, C., 2016. Reinforcement of the Brain's Rich-Club Architecture Following Early Neurodevelopmental Disruption Caused by Very Preterm Birth. Cereb. Cortex bhv305. doi:10.1093/cercor/bhv305

Kaufmann, R., Goldberg-Stern, H., Shuper, A., 2009. Attention-deficit disorders and epilepsy in childhood: incidence, causative relations and treatment possibilities. J. Child Neurol. 24, 727–733. doi:10.1177/0883073808330165

Kiebel, S.J., Tallon-Baudry, C., Friston, K.J., 2005. Parametric analysis of oscillatory activity as measured with EEG/MEG. Hum. Brain Mapp. 26, 170–177.

Kikumoto, K., Yoshinaga, H., Oka, M., Ito, M., Endoh, F., Akiyama, T., Ohtsuka, Y., 2006. EEG and seizure exacerbation induced by carbamazepine in Panayiotopoulos syndrome. Epileptic Disord. Int. Epilepsy J. Videotape 8, 53–56.

Kim, E.-H., Yum, M.-S., Kim, H.-W., Ko, T.-S., 2014. Attention-deficit/hyperactivity disorder and attention impairment in children with benign childhood epilepsy with centrotemporal spikes. Epilepsy Behav. 37, 54–58. doi:10.1016/j.yebeh.2014.05.030

Kim, S.E., Lee, J.H., Chung, H.K., Lim, S.M., Lee, H.W., 2014. Alterations in white matter microstructures and cognitive dysfunctions in benign childhood epilepsy with centrotemporal spikes. Eur. J. Neurol. 21, 708–717. doi:10.1111/ene.12301

Kim, T.-K., Hemberg, M., Gray, J.M., Costa, A.M., Bear, D.M., Wu, J., Harmin, D.A., Laptewicz, M., Barbara-Haley, K., Kuersten, S., Markenscoff-Papadimitriou, E., Kuhl, D., Bito, H., Worley, P.F., Kreiman, G., Greenberg, M.E., 2010. Widespread transcription at neuronal activity-regulated enhancers. Nature 465, 182–187. doi:10.1038/nature09033

Klimesch, W., 1999. EEG alpha and theta oscillations reflect cognitive and memory performance: a review and analysis. Brain Res. Rev. 29, 169–195. doi:10.1016/S0165-0173(98)00056-3

Klimesch, W., Sauseng, P., Hanslmayr, S., 2007. EEG alpha oscillations: the inhibition-timing hypothesis. Brain Res. Rev. 53, 63–88. doi:10.1016/j.brainresrev.2006.06.003

Knecht, S., Dräger, B., Deppe, M., Bobe, L., Lohmann, H., Flöel, A., Ringelstein, E.-B., Henningsen, H., 2000. Handedness and hemispheric language dominance in healthy humans. Brain 123, 2512–2518. doi:10.1093/brain/123.12.2512

Kobayashi, K., Yoshinaga, H., Toda, Y., Inoue, T., Oka, M., Ohtsuka, Y., 2011. High-frequency oscillations in idiopathic partial epilepsy of childhood. Epilepsia 52, 1812–1819. doi:10.1111/j.1528-1167.2011.03169.x

Kostović, I., Judas, M., 2010. The development of the subplate and thalamocortical connections in the human foetal brain. Acta Paediatr. Oslo Nor. 1992 99, 1119–1127. doi:10.1111/j.1651-2227.2010.01811.x

Kramer, M.A., Cash, S.S., 2012. Epilepsy as a disorder of cortical network organization. Neurosci. Rev. J. Bringing Neurobiol. Neurol. Psychiatry 18, 360–372. doi:10.1177/1073858411422754

Kwon, S.H., Vasung, L., Ment, L.R., Huppi, P.S., 2014. The role of neuroimaging in predicting neurodevelopmental outcomes of preterm neonates. Clin. Perinatol. 41, 257–283. doi:10.1016/j.clp.2013.10.003

Lachaux, J.-P., Rodriguez, E., Le Van Quyen, M., Lutz, A., Martinerie, J., Varela, F.J., 2000. Studying single-trials of phase synchronous activity in the brain. Int. J. Bifurc. Chaos 10, 2429–2439. doi:10.1142/S0218127400001560

Lachaux, J.P., Rodriguez, E., Martinerie, J., Varela, F.J., 1999. Measuring phase synchrony in brain signals. Hum. Brain Mapp. 8, 194–208.

Lamblin, M.D., André, M., Challamel, M.J., Curzi-Dascalova, L., d'Allest, A.M., De Giovanni, E., Moussalli-Salefranque, F., Navelet, Y., Plouin, P., Radvanyi-Bouvet, M.F., Samson-Dollfus, D., Vecchierini-Blineau, M.F., 1999. [Electroencephalography of the premature and term newborn. Maturational aspects and glossary]. Neurophysiol. Clin. Clin. Neurophysiol. 29, 123–219.

Lamblin, M.D., de Villepin-Touzery, A., 2015. EEG in the neonatal unit. Neurophysiol. Clin. Clin. Neurophysiol. 45, 87–95. doi:10.1016/j.neucli.2014.11.007

Langer, N., Pedroni, A., Jäncke, L., 2013. The problem of thresholding in small-world network analysis. PloS One 8, e53199. doi:10.1371/journal.pone.0053199

Lantz, G., Grave de Peralta, R., Spinelli, L., Seeck, M., Michel, C.M., 2003. Epileptic source localization with high density EEG: how many electrodes are needed? Clin. Neurophysiol. Off. J. Int. Fed. Clin. Neurophysiol. 114, 63–69.

Latora, V., Marchiori, M., 2001. Efficient Behavior of Small-World Networks. Phys. Rev. Lett. 87. doi:10.1103/PhysRevLett.87.198701

Laufs, H., 2012. Functional imaging of seizures and epilepsy: evolution from zones to networks. Curr. Opin. Neurol. 25, 194–200. doi:10.1097/WCO.0b013e3283515db9

Le Van Quyen, M., Foucher, J., Lachaux, J.-P., Rodriguez, E., Lutz, A., Martinerie, J., Varela, F.J., 2001. Comparison of Hilbert transform and wavelet methods for the analysis of neuronal synchrony. J. Neurosci. Methods 111, 83–98. doi:10.1016/S0165-0270(01)00372-7

Li, W., Wu, N., Hou, W., Zhang, J., Xu, W., Wu, G., Zheng, X., Feng, H., 2015. Lateralization of epileptic foci through causal analysis of scalp-EEG interictal spike activity. J. Clin. Neurophysiol. Off. Publ. Am. Electroencephalogr. Soc. 32, 57–65. doi:10.1097/WNP.0000000000000120

Loiseau, P., 2001. Benign Childhood Partial Seizures and Related Epileptic Syndromes. J. R. Soc. Med. 94, 651.

Lopes, A.F., Simões, M.R., Monteiro, J.P., Fonseca, M.J., Martins, C., Ventosa, L., Lourenço, L., Robalo, C., 2013. Intellectual functioning in children with epilepsy: Frontal lobe epilepsy, childhood absence epilepsy and benign epilepsy with centro-temporal spikes. Seizure 22, 886–892. doi:10.1016/j.seizure.2013.08.002

Lütkepohl, H., 2005. New Introduction to Multiple Time Series Analysis. Springer Berlin Heidelberg, Berlin, Heidelberg.

Mahmoudzadeh, M., Dehaene-Lambertz, G., Fournier, M., Kongolo, G., Goudjil, S., Dubois, J., Grebe, R., Wallois, F., 2013. Syllabic discrimination in premature human infants prior to complete formation of cortical layers. Proc. Natl. Acad. Sci. 110, 4846–4851. doi:10.1073/pnas.1212220110

Málková, L., Mishkin, M., Bachevalier, J., 1995. Long-term effects of selective neonatal temporal lobe lesions on learning and memory in monkeys. Behav. Neurosci. 109, 212–226. doi:10.1037/0735-7044.109.2.212

Mantini, D., Perrucci, M.G., Del Gratta, C., Romani, G.L., Corbetta, M., 2007. Electrophysiological signatures of resting state networks in the human brain. Proc. Natl. Acad. Sci. U. S. A. 104, 13170–13175. doi:10.1073/pnas.0700668104

Maris, E., Oostenveld, R., 2007. Nonparametric statistical testing of EEG- and MEG-data. J. Neurosci. Methods 164, 177–190. doi:10.1016/j.jneumeth.2007.03.024

Marlow, N., Wolke, D., Bracewell, M.A., Samara, M., 2005. Neurologic and Developmental Disability at Six Years of Age after Extremely Preterm Birth. N. Engl. J. Med. 352, 9–19. doi:10.1056/NEJMoa041367

Mehrkanoon, S., Breakspear, M., Britz, J., Boonstra, T.W., 2014. Intrinsic Coupling Modes in Source-Reconstructed Electroencephalography. Brain Connect. 4, 812–825. doi:10.1089/brain.2014.0280

Meijer, E.J., Hermans, K.H.M., Zwanenburg, A., Jennekens, W., Niemarkt, H.J., Cluitmans, P.J.M., van Pul, C., Wijn, P.F.F., Andriessen, P., 2014. Functional connectivity in preterm infants derived from EEG coherence analysis. Eur. J. Paediatr. Neurol. 18, 780–789. doi:10.1016/j.ejpn.2014.08.003

Mento, G., Suppiej, A., Altoè, G., Bisiacchi, P.S., 2010. Functional hemispheric asymmetries in humans: electrophysiological evidence from preterm infants. Eur. J. Neurosci. 31, 565–574. doi:10.1111/j.1460-9568.2010.07076.x

Metz-Lutz, M.N., Kleitz, C., de Saint Martin, A., Massa, R., Hirsch, E., Marescaux, C., 1999. Cognitive development in benign focal epilepsies of childhood. Dev. Neurosci. 21, 182–190. doi:17397

Michel, C.M., 2009. Electrical Neuroimaging. Cambridge University Press.

Michel, C.M., Lehmann, D., Henggeler, B., Brandeis, D., 1992. Localization of the sources of EEG delta, theta, alpha and beta frequency bands using the FFT dipole approximation. Electroencephalogr. Clin. Neurophysiol. 82, 38–44. doi:10.1016/0013-4694(92)90180-P

Michel, C.M., Murray, M.M., Lantz, G., Gonzalez, S., Spinelli, L., Grave de Peralta, R., 2004. EEG source imaging. Clin. Neurophysiol. Off. J. Int. Fed. Clin. Neurophysiol. 115, 2195–2222. doi:10.1016/j.clinph.2004.06.001

Mitra, P.P., Pesaran, B., 1999. Analysis of dynamic brain imaging data. Biophys. J. 76, 691–708.

Mizrahi, E.M., 2004. Atlas of neonatal electroencephalography. Lippincott Williams & Wilkins.

Moeller, F., Moehring, J., Ick, I., Steinmann, E., Wolff, S., Jansen, O., Boor, R., Stephani, U., Siniatchkin, M., 2013. EEG-fMRI in atypical benign partial epilepsy. Epilepsia 54, e103–108. doi:10.1111/epi.12243

Monset-Couchard, M., de Bethmann, O., 2000. Catch-Up Growth in 166 Small-for- Gestational Age Premature Infants Weighing Less than 1,000 g at Birth. Biol. Neonate 78, 161–167. doi:10.1159/000014265

Mormann, F., Lehnertz, K., David, P., E. Elger, C., 2000. Mean phase coherence as a measure for phase synchronization and its application to the EEG of epilepsy patients. Phys. Nonlinear Phenom. 144, 358–369. doi:10.1016/S0167-2789(00)00087-7

Mosher, J.C., Baillet, S., Leahy, R.M., 1999. EEG source localization and imaging using multiple signal classification approaches. J. Clin. Neurophysiol. Off. Publ. Am. Electroencephalogr. Soc. 16, 225–238.

Mosher, J.C., Lewis, P.S., Leahy, R.M., 1992. Multiple dipole modeling and localization from spatio-temporal MEG data. IEEE Trans. Biomed. Eng. 39, 541–557. doi:10.1109/10.141192

Murias, M., Webb, S.J., Greenson, J., Dawson, G., 2007. Resting State Cortical Connectivity Reflected in EEG Coherence in Individuals With Autism. Biol. Psychiatry, Mechanisms of Circuit Dysfunction in Neurodevelopmental Disorders 62, 270–273. doi:10.1016/j.biopsych.2006.11.012

Netoff, T.I., Clewley, R., Arno, S., Keck, T., White, J.A., 2004. Epilepsy in small-world networks. J. Neurosci. Off. J. Soc. Neurosci. 24, 8075–8083. doi:10.1523/JNEUROSCI.1509-04.2004

Nichols, T.E., 2012. Multiple testing corrections, nonparametric methods, and random field theory. NeuroImage 62, 811–815. doi:10.1016/j.neuroimage.2012.04.014

Nolte, G., Bai, O., Wheaton, L., Mari, Z., Vorbach, S., Hallett, M., 2004. Identifying true brain interaction from EEG data using the imaginary part of coherency. Clin. Neurophysiol. Off. J. Int. Fed. Clin. Neurophysiol. 115, 2292–2307. doi:10.1016/j.clinph.2004.04.029

Nunez, P.L., Srinivasan, R., Westdorp, A.F., Wijesinghe, R.S., Tucker, D.M., Silberstein, R.B., Cadusch, P.J., 1997. EEG coherency: I: statistics, reference electrode, volume conduction, Laplacians, cortical imaging, and interpretation at multiple scales. Electroencephalogr. Clin. Neurophysiol. 103, 499–515. doi:10.1016/S0013-4694(97)00066-7

Odabaee, M., Freeman, W.J., Colditz, P.B., Ramon, C., Vanhatalo, S., 2013. Spatial patterning of the neonatal EEG suggests a need for a high number of electrodes. NeuroImage 68, 229–235. doi:10.1016/j.neuroimage.2012.11.062

O'Leary, D.D.M., Chou, S.-J., Sahara, S., 2007. Area patterning of the mammalian cortex. Neuron 56, 252–269. doi:10.1016/j.neuron.2007.10.010

Olejniczak, P., 2006. Neurophysiologic basis of EEG. J. Clin. Neurophysiol. Off. Publ. Am. Electroencephalogr. Soc. 23, 186–189. doi:10.1097/01.wnp.0000220079.61973.6c

Omidvarnia, A., Fransson, P., Metsäranta, M., Vanhatalo, S., 2014. Functional bimodality in the brain networks of preterm and term human newborns. Cereb. Cortex N. Y. N 1991 24, 2657–2668. doi:10.1093/cercor/bht120

Omidvarnia, A., Metsäranta, M., Lano, A., Vanhatalo, S., 2015. Structural damage in early preterm brain changes the electric resting state networks. NeuroImage 120, 266–273. doi:10.1016/j.neuroimage.2015.06.091

Oostendorp, T.F., van Oosterom, A., 1989. Source parameter estimation in inhomogeneous volume conductors of arbitrary shape. IEEE Trans. Biomed. Eng. 36, 382–391. doi:10.1109/10.19859

Oostenveld, R., Fries, P., Maris, E., Schoffelen, J.-M., 2011. FieldTrip: Open Source Software for Advanced Analysis of MEG, EEG, and Invasive Electrophysiological Data. Comput. Intell. Neurosci. 2011, e156869. doi:10.1155/2011/156869

Overvliet, G.M., Aldenkamp, A.P., Klinkenberg, S., Nicolai, J., Vles, J.S.H., Besseling, R.M.H., Backes, W., Jansen, J.F.A., Hofman, P.A., Hendriksen, J., 2011. Correlation between language impairment and problems in motor development in children with rolandic epilepsy. Epilepsy Behav. 22, 527–531. doi:10.1016/j.yebeh.2011.08.012

Overvliet, G.M., Besseling, R.M.H., Jansen, J.F.A., van der Kruijs, S.J.M., Vles, J.S.H., Hofman, P.A.M., Ebus, S.C.M., de Louw, A., Aldenkamp, A.P., Backes, W.H., 2013. Early onset of cortical thinning in children with rolandic epilepsy. NeuroImage Clin. 2, 434–439. doi:10.1016/j.nicl.2013.03.008

Panayiotopoulos, C.P., 2005. The Epilepsies: Seizures, Syndromes and Management. Bladon Medical Publishing, Oxfordshire (UK).

Panayiotopoulos, C.P., 1999. Benign Childhood Partial Seizures and Related Epileptic Syndromes. John Libbey Eurotext.

Panayiotopoulos, C.P., 1999. Early-onset benign childhood occipital seizure susceptibility syndrome: a syndrome to recognize. Epilepsia 40, 621–630.

Panayiotopoulos, C.P., Michael, M., Sanders, S., Valeta, T., Koutroumanidis, M., 2008. Benign childhood focal epilepsies: assessment of established and newly recognized syndromes. Brain 131, 2264–2286. doi:10.1093/brain/awn162

Pandit, A.S., Robinson, E., Aljabar, P., Ball, G., Gousias, I.S., Wang, Z., Hajnal, J.V., Rueckert, D., Counsell, S.J., Montana, G., Edwards, A.D., 2014. Whole-brain mapping of structural connectivity in infants reveals altered connection strength associated with growth and preterm birth. Cereb. Cortex N. Y. N 1991 24, 2324–2333. doi:10.1093/cercor/bht086

Panzica, F., Varotto, G., Rotondi, F., Spreafico, R., Franceschetti, S., 2013. Identification of the Epileptogenic Zone from Stereo-EEG Signals: A Connectivity-Graph Theory Approach. Front. Neurol. 4, 175. doi:10.3389/fneur.2013.00175

Pascual-Marqui, R.D., 2007a. Instantaneous and lagged measurements of linear and nonlinear dependence between groups of multivariate time series: frequency decomposition. ArXiv07111455 Stat.

Pascual-Marqui, R.D., 2007b. Discrete, 3D distributed, linear imaging methods of electric neuronal activity. Part 1: exact, zero error localization. ArXiv07103341 Math-Ph Physicsphysics Q-Bio.

Pascual-Marqui, R.D., 2002. Standardized low-resolution brain electromagnetic tomography (sLORETA): technical details. Methods Find. Exp. Clin. Pharmacol. 24 Suppl D, 5–12.

Pascual-Marqui, R.D., Lehmann, D., Koukkou, M., Kochi, K., Anderer, P., Saletu, B., Tanaka, H., Hirata, K., John, E.R., Prichep, L., Biscay-Lirio, R., Kinoshita, T., 2011. Assessing

interactions in the brain with exact low-resolution electromagnetic tomography. Philos. Transact. A Math. Phys. Eng. Sci. 369, 3768–3784. doi:10.1098/rsta.2011.0081
Pereda, E., Quiroga, R.Q., Bhattacharya, J., 2005. Nonlinear multivariate analysis of neurophysiological signals. Prog. Neurobiol. 77, 1–37. doi:10.1016/j.pneurobio.2005.10.003
Périvier, M., Rozé, J.-C., Gascoin, G., Hanf, M., Branger, B., Rouger, V., Berlie, I., Montcho, Y., Péréon, Y., Flamant, C., Tich, S.N.T., 2015. Neonatal EEG and neurodevelopmental outcome in preterm infants born before 32 weeks. Arch. Dis. Child. - Fetal Neonatal Ed. fetalneonatal–2015–308664. doi:10.1136/archdischild-2015-308664
Perrin, F., Pernier, J., Bertrand, O., Echallier, J.F., 1989. Spherical splines for scalp potential and current density mapping. Electroencephalogr. Clin. Neurophysiol. 72, 184–187. doi:10.1016/0013-4694(89)90180-6
Piccirilli, M., D'Alessandro, P., Tiacci, C., Ferroni, A., 1988. Language lateralization in children with benign partial epilepsy. Epilepsia 29, 19–25.
Power, J.D., Fair, D.A., Schlaggar, B.L., Petersen, S.E., 2010. The Development of Human Functional Brain Networks. Neuron 67, 735–748. doi:10.1016/j.neuron.2010.08.017
Prinz, A.A., 2008. Understanding epilepsy through network modeling. Proc. Natl. Acad. Sci. 105, 5953–5954. doi:10.1073/pnas.0802299105
Quraan, M.A., McCormick, C., Cohn, M., Valiante, T.A., McAndrews, M.P., 2013. Altered Resting State Brain Dynamics in Temporal Lobe Epilepsy Can Be Observed in Spectral Power, Functional Connectivity and Graph Theory Metrics. PLoS ONE 8, e68609. doi:10.1371/journal.pone.0068609
Ratnarajah, N., Rifkin-Graboi, A., Fortier, M.V., Chong, Y.S., Kwek, K., Saw, S.-M., Godfrey, K.M., Gluckman, P.D., Meaney, M.J., Qiu, A., 2013. Structural connectivity asymmetry in the neonatal brain. NeuroImage 75, 187–194. doi:10.1016/j.neuroimage.2013.02.052
Rheims, S., Cucherat, M., Arzimanoglou, A., Ryvlin, P., 2008. Greater Response to Placebo in Children Than in Adults: A Systematic Review and Meta-Analysis in Drug-Resistant Partial Epilepsy. PLoS Med 5, e166. doi:10.1371/journal.pmed.0050166
Riva, D., Vago, C., Franceschetti, S., Pantaleoni, C., D'Arrigo, S., Granata, T., Bulgheroni, S., 2007. Intellectual and language findings and their relationship to EEG characteristics in benign childhood epilepsy with centrotemporal spikes. Epilepsy Behav. 10, 278–285. doi:10.1016/j.yebeh.2006.12.003
Roche-Labarbe, N., Fenoglio, A., Aggarwal, A., Dehaes, M., Carp, S.A., Franceschini, M.A., Grant, P.E., 2012. Near-infrared spectroscopy assessment of cerebral oxygen metabolism in the developing premature brain. J. Cereb. Blood Flow Metab. Off. J. Int. Soc. Cereb. Blood Flow Metab. 32, 481–488. doi:10.1038/jcbfm.2011.145
Rosazza, C., Minati, L., 2011. Resting-state brain networks: literature review and clinical applications. Neurol. Sci. Off. J. Ital. Neurol. Soc. Ital. Soc. Clin. Neurophysiol. 32, 773–785. doi:10.1007/s10072-011-0636-y
Rose, J., Vassar, R., Cahill-Rowley, K., Guzman, X.S., Stevenson, D.K., Barnea-Goraly, N., 2014. Brain microstructural development at near-term age in very-low-birth-weight preterm infants: an atlas-based diffusion imaging study. NeuroImage 86, 244–256. doi:10.1016/j.neuroimage.2013.09.053
Rotondi, F., Franceschetti, S., Avanzini, G., Panzica, F., 2016. Altered EEG resting-state effective connectivity in drug-naïve childhood absence epilepsy. Clin. Neurophysiol. 127, 1130–1137. doi:10.1016/j.clinph.2015.09.003

Rubinov, M., Sporns, O., 2010. Complex network measures of brain connectivity: uses and interpretations. NeuroImage 52, 1059–1069. doi:10.1016/j.neuroimage.2009.10.003
Rushworth, M.F., Buckley, M.J., Behrens, T.E., Walton, M.E., Bannerman, D.M., 2007. Functional organization of the medial frontal cortex. Curr. Opin. Neurobiol., Cognitive neuroscience 17, 220–227. doi:10.1016/j.conb.2007.03.001
Rushworth, M.F.S., Noonan, M.P., Boorman, E.D., Walton, M.E., Behrens, T.E., 2011. Frontal Cortex and Reward-Guided Learning and Decision-Making. Neuron 70, 1054–1069. doi:10.1016/j.neuron.2011.05.014
Scheffer, I.E., Berkovic, S.F., 1997. Generalized epilepsy with febrile seizures plus. A genetic disorder with heterogeneous clinical phenotypes. Brain J. Neurol. 120 (Pt 3), 479–490.
Scherg, M., Von Cramon, D., 1985. Two bilateral sources of the late AEP as identified by a spatio-temporal dipole model. Electroencephalogr. Clin. Neurophysiol. Potentials Sect. 62, 32–44. doi:10.1016/0168-5597(85)90033-4
Scher, M.S., Loparo, K.A., 2009. Neonatal EEG/sleep state analyses: a complex phenotype of developmental neural plasticity. Dev. Neurosci. 31, 259–275. doi:10.1159/000216537
Schlögl, A., Supp, G., 2006. Analyzing event-related EEG data with multivariate autoregressive parameters. Prog. Brain Res. 159, 135–147. doi:10.1016/S0079-6123(06)59009-0
Schmidt, B.T., Ghuman, A.S., Huppert, T.J., 2014. Whole brain functional connectivity using phase locking measures of resting state magnetoencephalography. Front. Neurosci. 8. doi:10.3389/fnins.2014.00141
Schneebaum-Sender, N., Goldberg-Stern, H., Fattal-Valevski, A., Kramer, U., 2012. Does a normalizing electroencephalogram in benign childhood epilepsy with centrotemporal spikes abort attention deficit hyperactivity disorder? Pediatr. Neurol. 47, 279–283. doi:10.1016/j.pediatrneurol.2012.06.009
Schoffelen, J.-M., Gross, J., 2009. Source connectivity analysis with MEG and EEG. Hum. Brain Mapp. 30, 1857–1865. doi:10.1002/hbm.20745
Sekihara, K., Nagarajan, S.S., Poeppel, D., Marantz, A., 2004. Asymptotic SNR of scalar and vector minimum-variance beamformers for neuromagnetic source reconstruction. IEEE Trans. Biomed. Eng. 51, 1726–1734. doi:10.1109/TBME.2004.827926
Selton, D., Andre, M., Hascoët, J.M., 2000. Normal EEG in very premature infants: reference criteria. Clin. Neurophysiol. Off. J. Int. Fed. Clin. Neurophysiol. 111, 2116–2124.
Semah, F., Picot, M.-C., Adam, C., Broglin, D., Arzimanoglou, A., Bazin, B., Cavalcanti, D., Baulac, M., 1998. Is the underlying cause of epilepsy a major prognostic factor for recurrence? Neurology 51, 1256–1262. doi:10.1212/WNL.51.5.1256
Shenton, M.E., Hamoda, H.M., Schneiderman, J.S., Bouix, S., Pasternak, O., Rathi, Y., Vu, M.-A., Purohit, M.P., Helmer, K., Koerte, I., Lin, A.P., Westin, C.-F., Kikinis, R., Kubicki, M., Stern, R.A., Zafonte, R., 2012. A review of magnetic resonance imaging and diffusion tensor imaging findings in mild traumatic brain injury. Brain Imaging Behav. 6, 137–192. doi:10.1007/s11682-012-9156-5
Shields, W.D., Snead, O.C., 2009. Benign epilepsy with centrotemporal spikes. Epilepsia 50 Suppl 8, 10–15. doi:10.1111/j.1528-1167.2009.02229.x
Silva, F.L. da, 2009. EEG: Origin and Measurement, in: Mulert, C., Lemieux, L. (Eds.), EEG - fMRI. Springer Berlin Heidelberg, pp. 19–38.
Silverthorn, D.U., 2007. Human Physiology: An Integrated Approach. Pearson/Benjamin Cummings.

Singh, R., Scheffer, I.E., Crossland, K., Berkovic, S.F., 1999. Generalized epilepsy with febrile seizures plus: A common childhood-onset genetic epilepsy syndrome. Ann. Neurol. 45, 75–81. doi:10.1002/1531-8249(199901)45:1<75::AID-ART13>3.0.CO;2-W

Smit, D.J.A., Boersma, M., Schnack, H.G., Micheloyannis, S., Boomsma, D.I., Pol, H.E.H., Stam, C.J., Geus, E.J.C. de, 2012. The Brain Matures with Stronger Functional Connectivity and Decreased Randomness of Its Network. PLOS ONE 7, e36896. doi:10.1371/journal.pone.0036896

Smit, D.J.A., Stam, C.J., Posthuma, D., Boomsma, D.I., de Geus, E.J.C., 2008. Heritability of "small-world" networks in the brain: a graph theoretical analysis of resting-state EEG functional connectivity. Hum. Brain Mapp. 29, 1368–1378. doi:10.1002/hbm.20468

Smyser, C.D., Snyder, A.Z., Neil, J.J., 2011. Functional connectivity MRI in infants: exploration of the functional organization of the developing brain. NeuroImage 56, 1437–1452. doi:10.1016/j.neuroimage.2011.02.073

Sohrabpour, A., Lu, Y., Kankirawatana, P., Blount, J., Kim, H., He, B., 2015. Effect of EEG electrode number on epileptic source localization in pediatric patients. Clin. Neurophysiol. Off. J. Int. Fed. Clin. Neurophysiol. 126, 472–480. doi:10.1016/j.clinph.2014.05.038

Song, J., Davey, C., Poulsen, C., Luu, P., Turovets, S., Anderson, E., Li, K., Tucker, D., 2015. EEG source localization: Sensor density and head surface coverage. J. Neurosci. Methods 256, 9–21. doi:10.1016/j.jneumeth.2015.08.015

Sponheim, S.R., Clementz, B.A., Iacono, W.G., Beiser, M., 2000. Clinical and biological concomitants of resting state EEG power abnormalities in schizophrenia. Biol. Psychiatry 48, 1088–1097. doi:10.1016/S0006-3223(00)00907-0

Sporns, O., 2011. Networks of the Brain. MIT press.

Sporns, O., Tononi, G., Edelman, G.M., 2000. Connectivity and complexity: the relationship between neuroanatomy and brain dynamics. Neural Netw. Off. J. Int. Neural Netw. Soc. 13, 909–922.

Sporns, O., Zwi, J.D., 2004. The small world of the cerebral cortex. Neuroinformatics 2, 145–162. doi:10.1385/NI:2:2:145

Springer, S.P., Deutsch, G., 1998. Left brain, right brain: Perspectives from cognitive neuroscience (5th ed.), A series of books in psychology. W H Freeman/Times Books/ Henry Holt & Co, New York, NY, US.

Srinivasan, R., Winter, W.R., Ding, J., Nunez, P.L., 2007. EEG and MEG coherence: measures of functional connectivity at distinct spatial scales of neocortical dynamics. J. Neurosci. Methods 166, 41–52. doi:10.1016/j.jneumeth.2007.06.026

Stam, C.J., 2014. Modern network science of neurological disorders. Nat. Rev. Neurosci. 15, 683–695. doi:10.1038/nrn3801

Stam, C.J., Haan, W. de, Daffertshofer, A., Jones, B.F., Manshanden, I., Walsum, A.M. van C. van, Montez, T., Verbunt, J.P.A., Munck, J.C. de, Dijk, B.W. van, Berendse, H.W., Scheltens, P., 2009. Graph theoretical analysis of magnetoencephalographic functional connectivity in Alzheimer's disease. Brain 132, 213–224. doi:10.1093/brain/awn262

Stam, C.J., Nolte, G., Daffertshofer, A., 2007. Phase lag index: Assessment of functional connectivity from multi channel EEG and MEG with diminished bias from common sources. Hum. Brain Mapp. 28, 1178–1193. doi:10.1002/hbm.20346

Stam, C.J., van Straaten, E.C.W., 2012. The organization of physiological brain networks. Clin. Neurophysiol. Off. J. Int. Fed. Clin. Neurophysiol. 123, 1067–1087. doi:10.1016/j.clinph.2012.01.011
Stanley, M.L., Moussa, M.N., Paolini, B.M., Lyday, R.G., Burdette, J.H., Laurienti, P.J., 2013. Defining nodes in complex brain networks. Front. Comput. Neurosci. 7, 169. doi:10.3389/fncom.2013.00169
Stiles, J., Jernigan, T.L., 2010. The Basics of Brain Development. Neuropsychol. Rev. 20, 327–348. doi:10.1007/s11065-010-9148-4
Stuss, D.T., 2011. Functions of the frontal lobes: relation to executive functions. J. Int. Neuropsychol. Soc. JINS 17, 759–765. doi:10.1017/S1355617711000695
Supekar, K., Musen, M., Menon, V., 2009. Development of Large-Scale Functional Brain Networks in Children. PLOS Biol 7, e1000157. doi:10.1371/journal.pbio.1000157
Sveller, C., Briellmann, R.S., Saling, M.M., Lillywhite, L., Abbott, D.F., Masterton, R. a. J., Jackson, G.D., 2006. Relationship between language lateralization and handedness in left-hemispheric partial epilepsy. Neurology 67, 1813–1817. doi:10.1212/01.wnl.0000244465.74707.42
Tallon-Baudry, C., Bertrand, O., Delpuech, C., Pernier, J., 1996. Stimulus specificity of phase-locked and non-phase-locked 40 Hz visual responses in human. J. Neurosci. Off. J. Soc. Neurosci. 16, 4240–4249.
Tang, Y.-L., Ji, G.-J., Yu, Y., Wang, J., Wang, Z.-J., Zang, Y.-F., Liao, W., Ding, M.-P., 2014. Altered Regional Homogeneity in Rolandic Epilepsy: A Resting-State fMRI Study. BioMed Res. Int. 2014, e960395. doi:10.1155/2014/960395
Taylor, P.N., Han, C.E., Schoene-Bake, J.-C., Weber, B., Kaiser, M., 2015. Structural connectivity changes in temporal lobe epilepsy: Spatial features contribute more than topological measures. NeuroImage Clin. 8, 322–328. doi:10.1016/j.nicl.2015.02.004
Teffer, K., Buxhoeveden, D.P., Stimpson, C.D., Fobbs, A.J., Schapiro, S.J., Baze, W.B., McArthur, M.J., Hopkins, W.D., Hof, P.R., Sherwood, C.C., Semendeferi, K., 2013. Developmental changes in the spatial organization of neurons in the neocortex of humans and common chimpanzees. J. Comp. Neurol. 521, 4249–4259. doi:10.1002/cne.23412
Telesford, Q.K., Simpson, S.L., Burdette, J.H., Hayasaka, S., Laurienti, P.J., 2011. The brain as a complex system: using network science as a tool for understanding the brain. Brain Connect. 1, 295–308. doi:10.1089/brain.2011.0055
Theiler, J., Eubank, S., Longtin, A., Galdrikian, B., Doyne Farmer, J., 1992. Testing for nonlinearity in time series: the method of surrogate data. Phys. Nonlinear Phenom. 58, 77–94. doi:10.1016/0167-2789(92)90102-S
Thom, M., 2014. Review: Hippocampal sclerosis in epilepsy: a neuropathology review. Neuropathol. Appl. Neurobiol. 40, 520–543. doi:10.1111/nan.12150
Tokariev, A., Videman, M., Palva, J.M., Vanhatalo, S., 2015. Functional Brain Connectivity Develops Rapidly Around Term Age and Changes Between Vigilance States in the Human Newborn. Cereb. Cortex bhv219. doi:10.1093/cercor/bhv219
Tononi, G., Sporns, O., Edelman, G.M., 1994. A measure for brain complexity: relating functional segregation and integration in the nervous system. Proc. Natl. Acad. Sci. U. S. A. 91, 5033–5037.
Torres, F., Anderson, C., 1985. The normal EEG of the human newborn. J. Clin. Neurophysiol. Off. Publ. Am. Electroencephalogr. Soc. 2, 89–103.

Tracy, J.I., Doucet, G.E., 2015. Resting-state functional connectivity in epilepsy: growing relevance for clinical decision making. Curr. Opin. Neurol. 28, 158–165. doi:10.1097/WCO.0000000000000178

Travis, F., Haaga, D.A.F., Hagelin, J., Tanner, M., Arenander, A., Nidich, S., Gaylord-King, C., Grosswald, S., Rainforth, M., Schneider, R.H., 2010. A self-referential default brain state: patterns of coherence, power, and eLORETA sources during eyes-closed rest and Transcendental Meditation practice. Cogn. Process. 11, 21–30. doi:10.1007/s10339-009-0343-2

tutorial:visual_artifact_rejection – FieldTrip [WWW Document], n.d. URL http://www.fieldtriptoolbox.org/tutorial/visual_artifact_rejection (accessed 5.15.15).

Tzourio-Mazoyer, N., Landeau, B., Papathanassiou, D., Crivello, F., Etard, O., Delcroix, N., Mazoyer, B., Joliot, M., 2002. Automated anatomical labeling of activations in SPM using a macroscopic anatomical parcellation of the MNI MRI single-subject brain. NeuroImage 15, 273–289. doi:10.1006/nimg.2001.0978

Ullman, J.B., Bentler, P.M., 2003. Structural Equation Modeling, in: Handbook of Psychology. John Wiley & Sons, Inc.

van den Broek, S.P., Reinders, F., Donderwinkel, M., Peters, M.J., 1998. Volume conduction effects in EEG and MEG. Electroencephalogr. Clin. Neurophysiol. 106, 522–534. doi:10.1016/S0013-4694(97)00147-8

van den Heuvel, M.P., Sporns, O., 2013. Network hubs in the human brain. Trends Cogn. Sci. 17, 683–696. doi:10.1016/j.tics.2013.09.012

Van Essen, D.C., Dierker, D.L., 2007. Surface-Based and Probabilistic Atlases of Primate Cerebral Cortex. Neuron 56, 209–225. doi:10.1016/j.neuron.2007.10.015

Vanhatalo, S., Kaila, K., 2006. Development of neonatal EEG activity: from phenomenology to physiology. Semin. Fetal. Neonatal Med. 11, 471–478. doi:10.1016/j.siny.2006.07.008

van Mierlo, P., Carrette, E., Hallez, H., Raedt, R., Meurs, A., Vandenberghe, S., Van Roost, D., Boon, P., Staelens, S., Vonck, K., 2013. Ictal-onset localization through connectivity analysis of intracranial EEG signals in patients with refractory epilepsy. Epilepsia 54, 1409–1418. doi:10.1111/epi.12206

van Mierlo, P., Carrette, E., Hallez, H., Vonck, K., Van Roost, D., Boon, P., Staelens, S., 2011. Accurate epileptogenic focus localization through time-variant functional connectivity analysis of intracranial electroencephalographic signals. NeuroImage 56, 1122–1133. doi:10.1016/j.neuroimage.2011.02.009

van Vugt, M.K., Sederberg, P.B., Kahana, M.J., 2007. Comparison of spectral analysis methods for characterizing brain oscillations. J. Neurosci. Methods 162, 49–63. doi:10.1016/j.jneumeth.2006.12.004

Vecchierini, M.-F., André, M., d'Allest, A.M., 2007. Normal EEG of premature infants born between 24 and 30 weeks gestational age: terminology, definitions and maturation aspects. Neurophysiol. Clin. Clin. Neurophysiol. 37, 311–323. doi:10.1016/j.neucli.2007.10.008

Vecchierini, M.-F., d'Allest, A.-M., Verpillat, P., 2003. EEG patterns in 10 extreme premature neonates with normal neurological outcome: qualitative and quantitative data. Brain Dev. 25, 330–337. doi:10.1016/S0387-7604(03)00007-X

Verrotti, A., Filippini, M., Matricardi, S., Agostinelli, M.F., Gobbi, G., 2014. Memory impairment and Benign Epilepsy with centrotemporal spike (BECTS): a growing suspicion. Brain Cogn. 84, 123–131. doi:10.1016/j.bandc.2013.11.014

Vinck, M., Oostenveld, R., van Wingerden, M., Battaglia, F., Pennartz, C.M.A., 2011. An improved index of phase-synchronization for electrophysiological data in the presence of volume-conduction, noise and sample-size bias. NeuroImage 55, 1548–1565. doi:10.1016/j.neuroimage.2011.01.055

Wallois, F., 2010. Synopsis of maturation of specific features in EEG of premature neonates. Neurophysiol. Clin. Clin. Neurophysiol. 40, 125–126. doi:10.1016/j.neucli.2010.02.001

Walls-Esquivel, E., Vecchierini, M.F., Héberlé, C., Wallois, F., 2007. Electroencephalography (EEG) recording techniques and artefact detection in early premature babies. Neurophysiol. Clin. Neurophysiol. 37, 299–309.

Watts, D.J., Strogatz, S.H., 1998. Collective dynamics of "small-world" networks. Nature 393, 440–442. doi:10.1038/30918

Wilke, C., van Drongelen, W., Kohrman, M., He, B., 2010. Neocortical seizure foci localization by means of a directed transfer function method. Epilepsia 51, 564–572. doi:10.1111/j.1528-1167.2009.02329.x

Wirrell, E.C., 1998. Benign epilepsy of childhood with centrotemporal spikes. Epilepsia 39, S32–S41.

Wolff, M., Weiskopf, N., Serra, E., Preissl, H., Birbaumer, N., Kraegeloh-Mann, I., 2005. Benign Partial Epilepsy in Childhood: Selective Cognitive Deficits Are Related to the Location of Focal Spikes Determined by Combined EEG/MEG. Epilepsia 46, 1661–1667. doi:10.1111/j.1528-1167.2005.00255.x

Wolters, C.H., Anwander, A., Tricoche, X., Weinstein, D., Koch, M.A., MacLeod, R.S., 2006. Influence of tissue conductivity anisotropy on EEG/MEG field and return current computation in a realistic head model: a simulation and visualization study using high-resolution finite element modeling. NeuroImage 30, 813–826. doi:10.1016/j.neuroimage.2005.10.014

Wolters, C.H., Kuhn, M., Anwander, A., Reitzinger, S., 2002. A parallel algebraic multigrid solver for finite element method based source localization in the human brain. Comput. Vis. Sci. 5, 165–177. doi:10.1007/s00791-002-0098-0

Wu, Y., Ji, G.-J., Zang, Y.-F., Liao, W., Jin, Z., Liu, Y.-L., Li, K., Zeng, Y.-W., Fang, F., 2015. Local Activity and Causal Connectivity in Children with Benign Epilepsy with Centrotemporal Spikes. PLoS ONE 10. doi:10.1371/journal.pone.0134361

Xia, M., Wang, J., He, Y., 2013. BrainNet Viewer: A Network Visualization Tool for Human Brain Connectomics. PLoS ONE 8, e68910. doi:10.1371/journal.pone.0068910

Xiao, F., Li, L., An, D., Lei, D., Tang, Y., Yang, T., Ren, J., Chen, S., Huang, X., Gong, Q., Zhou, D., 2015. Altered attention networks in benign childhood epilepsy with centrotemporal spikes (BECTS): A resting-state fMRI study. Epilepsy Behav. 45, 234–241. doi:10.1016/j.yebeh.2015.01.016

Yang, T., Luo, C., Li, Q., Guo, Z., Liu, L., Gong, Q., Yao, D., Zhou, D., 2013. Altered resting-state connectivity during interictal generalized spike-wave discharges in drug-naïve childhood absence epilepsy. Hum. Brain Mapp. 34, 1761–1767. doi:10.1002/hbm.22025

Yeom, J.S., Kim, Y.-S., Jung, S., Kwon, O.-Y., 2014. Changes in current-source density of interictal spikes in benign epilepsy of childhood with centrotemporal spikes following treatment with oxcarbazepine. Seizure 23, 560–566. doi:10.1016/j.seizure.2014.04.007

Zhang, Y.S., Huang, C.X., Wen, J.G., Sheng, G.Y., Cheng, X.Y., Zhang, Q., 2015. Relationship between brain activity and voiding patterns in healthy preterm neonates. J. Pediatr. Urol. doi:10.1016/j.jpurol.2015.10.004

Zhang, Z., Liao, W., Wang, Z., Xu, Q., Yang, F., Mantini, D., Jiao, Q., Tian, L., Liu, Y., Lu, G., 2014. Epileptic discharges specifically affect intrinsic connectivity networks during absence seizures. J. Neurol. Sci. 336, 138–145. doi:10.1016/j.jns.2013.10.024

Resting-state EEG functional connectivity analysis in benign childhood epilepsy and neonates

Abstract

The thesis investigated the functional connectivity in children with benign childhood epilepsy with centrotemporal spike and functional brain network organization in preterm and full-term neonates. The patients with the epilepsy had functional brain disruption and the alterations of resting state functional connectivity is frequency dependent in comparison to the healthy controls. The epileptic brain network is disrupted in the presence and absence of interictal epileptic discharges. The regions involved in the generation and propagation of epilepsy were identified including epileptic zone (central region), rolandic region and the supplementary motor areas. In the neonates, preterm neonates were characterized with the high functional connectivity at the frontal and posterior regions. The presence of endogenous activity in preterm such as theta temporal activity revealed high functional connectivity at the temporal region. Similar functional brain network organization was observed in full-term neonates with the high functional activity at the frontal, temporal and posterior regions in both active and quite sleep periods.

Analyse de connectivité EEG régime reposant dans l'épilepsie bénigne de l'enfance et des nouveau-nés

Résumé

Le travail réalisé au cours de cette thèse a porté sur l'étude de la connectivité cérébrale fonctionnelle des réseaux épileptiques chez des enfants présentant des épilepsies avec pointes centro temporales (EPCT), et sur l'organisation fonctionnelle des réseaux de repos chez des nouveau-né sains et des prématurés. Les patients épileptiques présentent une désorganisation fonctionnelle cérébrale qui participe à une altération des réseaux de repos selon la gamme de fréquence des activités cérébrales. Cette désorganisation fonctionnelle bien que plus importante durant les périodes de pointes épileptiques intercritiques est aussi observée dans les périodes sans pointes intercritiques. Les régions impliquées dans la genèse et la propagation des pointes intercritiques englobent la région centrale (zone épileptiques), la région rolandique et l'aire prémotrice. Chez le nouveau-né et le prématuré la connectivité fonctionnelle est majeure dans les régions frontales et postérieures. Les activités endogènes thêta temporales du prématuré présentent une connectivité restreinte aux seules régions temporales. Chez le nouveau-né à terme l'organisation fonctionnelle est similaire avec une forte connectivité dans les régions frontales temporales et postérieures dans le sommeil calme et le sommeil agité.